

# MOLECULAR CHARACTERISATION OF THE PERIPHERAL BENZODIAZEPINE RECEPTOR IN VARIOUS HUMAN CANCER TISSUES

**Nimisha H. Bhoola**

A dissertation submitted to the Faculty of Science, University of the Witwatersrand, Johannesburg, South Africa, in fulfilment of the requirements for the degree of Masters of Science.

Johannesburg, South Africa, 2007

# DECLARATION

I Nimisha H. Bhoola, declare that the dissertation **Molecular Characterisation of the Peripheral Benzodiazepine Receptor in Various Human Cancer Tissues** is my own original work and that all the sources that I have used have been indicated by complete references. This dissertation is being submitted in fulfilment for the degree of Masters of Science at the University of the Witwatersrand, Johannesburg, South Africa.

_____

Nimisha H. Bhoola

Date: _____

# DEDICATION

In dedication to my parents:

In loving memory of my father (1947-1997), who had such dreams and hopes for me and my mother, who has continuously supported me through the years allowing me to fulfil each one.

# ABSTRACT

**Background:** The Peripheral Benzodiazepine Receptor (PBR) can be classified as a distinct receptor from the central benzodiazepine receptor. The *PBR* gene has been located to chromosome 22q13.31 in humans and has been found to consist of four exons, with the first and half of the fourth exon being untranslated to form the PBR protein. PBR is involved in numerous biological conditions including the regulation of cellular proliferation and apoptosis, steroidogenesis, heme biosynthesis, anion and porphyrin transport and mitochondrial functions such as oxidative phosphorylation and translocation of cholesterol from the outer to the inner mitochondrial membrane. Recent studies showed that the expression of PBR correlated with tumour malignancy and patient survival.

**Aim:** The objectives of this research were to determine the expression pattern and level of PBR mRNA in various types of human normal and cancer tissues and to isolate the PBR protein.

**Materials and Methods:** Tissue arrays of multiple organs containing normal and diseased tumour tissues that were formalin-fixed were purchased from Cybrdi Inc. (Frederick, Maryland, USA). Sense and anti-sense RNA probes were synthesised by *in vitro* transcription and labelled with digoxigenin (DIG). Anti-sense RNA probe complimentary to the PBR mRNA was used to localise the PBR mRNA transcript in tissue sections during colorimetric and fluorescent *in situ* hybridisation (ISH and FISH). Human normal and various human cancerous cell lines purchased from Highveld Biological (Pty) Ltd (Johannesburg, South Africa) were used for relative quantitative real-time PCR in order to determine the expression levels of PBR mRNA in the various cell lines. PBR was ligated into the pGEX-6P-2

expression vector, which formed a gluthathione-*S*-transferase (GST) fusion protein when induced with isopropyl-β-D-thiogalactopyranoside (IPTG).

**Results:** Increase levels of PBR mRNA were seen in Grade II and Grade III liver hepatocellular carcinoma, Grade I colonic adenocarcinoma, Grade III stomach squamous cell carcinoma, Grade II and Grade III prostate adenocarcinoma of the peripheral duct and acini, Grade III breast invasive ductal carcinoma (NST), Grade III lung squamous cell carcinoma, kidney chromophobe renal cell carcinoma, kidney clear cell carcinoma, Grade II brain diffuse fibrillary astrocytoma, brain primary central nervous system lymphoma and brain ependymoma while the expression of PBR mRNA decreased in Grade II and Grade III colonic adenocarcinoma, Grade III lung adenocarcinoma and lung small cell carcinoma when compared to their normal counterparts. In liver hepatocellular carcinoma, it was found that PBR mRNA expression levels decreased as tumours became more invasive while in prostate adenocarcinoma of the peripheral duct and acini PBR mRNA expression increased as tumour invasion increased. Relative quantitative real-time PCR showed that the expression of PBR mRNA decreased in lung adenocarcinoma when compared to lung normal and in the cancerous cell lines the concentration of PBR mRNA increases as follows: liver hepatocellular carcinoma > cervical carcinoma ≥ lung adenocarcinoma.

**Conclusion:** PBR mRNA is expressed in most types of human cancer tissues. It is highly expressed in most cancerous tissues when compared to its normal counterparts. Expression of PBR mRNA varies with tumour malignancy grade. In most cells PBR mRNA is expressed cytoplasmically, however, nuclear localisation has been seen in some cells. Determination of PBR mRNA expression in the various types of cancer tissues serves as the preliminary step to future studies that will elucidate the role of PBR in the development of cancer.

# AKNOWLEDGEMENTS


- My sincere gratitude goes to my supervisor Dr. Zodwa Dlamini, who even when I thought that the objectives of my project was beyond my reach encouraged me to strive and achieve them. Thus, thanks to her for the advice, encouragement and support that she has given me over the past two years.

- To Dr. Monde Ntwasa from the School of Molecular and Cell Biology for the use of the AxioCam (MRm/MRc) camera and AxioVision software (Carl Zeiss AG, Oberkochen, Germany), without whom this project would not have been possible. I would also like to thank Rodney Hull for all his assistance in showing me how to use the microscope.

- To Dr. Etienne Hurter from the School of Anatomical Sciences for the use of his laboratory, which allowed me to conduct my protein synthesis work.

- To the Red Cell Membrane Unit from the School of Physiology for the use of their JA-20 rotor and J2-21 Beckman centrifuge (Beckman Coulter, Inc., Fullerton, California, USA) and 37 ˚C shaker used for my protein synthesis work.

- To my colleagues in the laboratory, who encouraged, supported and provided me with advice throughout these two years. My sincere gratitude goes out especially to Michelle McCabe, who provided me with encouragement, support as well as taking out her own time to help me with my project so that I could gain confidence in the new techniques that I learnt. I would also like to thank Thokozile Ledwaba for all the assistance she provided

for *in situ* hybridisation. Last, but not least I would like to thank Zukile Mbita for all his help with protein synthesis.

- To my family and friends for all their love, support and encouragement. I am especially grateful to my mother, who has always provided me with the support and encouragement that I needed even when I thought that goals were beyond my reach.

- I would like to acknowledge the University of the Witwatersrand, National Research Foundation (NRF), Medical Research Council (MRC) and the University Research Council (URC) for the funding and scholarships that they provided enabling me to complete and conduct my research and degree.

# PUBLICATIONS

**Journal Articles:**

- Bhoola NH, Dlamini Z, (2006), Expression Pattern of the Peripheral Benzodiazepine mRNA in Various Human Normal and Cancer Tissues, *(in preparation)*

- Bhoola NH, Dlamini Z, (2006), Characterisation of the Peripheral Benzodiazepine Receptor and its Role in the Development of Cancer, *(in preparation)*

**Meetings:**

- 97th Annual American Association of Cancer Research International Meeting

  Bhoola NH, Dlamini Z, Expression Levels of the Peripheral Benzodiazepine Receptor (PBR) mRNA in Various Human Normal and Cancer Cell Lines, Proceedings of the American Association for Cancer Research, 2006, Volume 47, Abstract Number LB-66

- SASBMB XXth Conference

  Bhoola NH, Dlamini Z, Expression Levels of the Peripheral Benzodiazepine Receptor (PBR) mRNA in Various Human Normal and Cancer Cell Lines, 2006, University of KwaZulu-Natal, P110

- 96th Annual American Association of Cancer Research International Meeting

  Bhoola NH, Dlamini Z, Expression of Peripheral Benzodiazepine Receptor (mRNA) in Various Cancer Tissues, Proceedings of the American Association for Cancer Research, 2005, Volume 46, Abstract Number 821, Page 193

- SASBMB XIXth Conference

  Bhoola NH, Dlamini Z, Expression of Peripheral Benzodiazepine Receptor (mRNA) in Various Cancer Tissues, 2005, Stellenbosch University, P90, 210

# TABLE OF CONTENTS

DECLARATION ..... i

DEDICATION ..... ii

ABSTRACTiii

AKNOWLEDGEMENTS ..... v

PUBLICATIONS ..... vii

TABLE OF CONTENTS ..... ix

LIST OF FIGURES ..... xxi

LIST OF TABLES ..... xxviii

ABBREVIATIONS ..... xxxi

1. INTRODUCTION ..... 1

1.1. Cancer ..... 1

1.1.1. Introduction ..... 1

1.1.2. Carcinogenesis ..... 3

1.1.2.1. Evasion of Apoptosis ..... 4

1.1.2.2. Limitless Replicative Potential ..... 4

1.2. Cell Proliferation and the Cell Cycle ..... 5

1.2.1. Cell Proliferation ..... 5

1.2.2. The Cell Cycle ..... 6

1.2.2.1. Phases of the Cell Cycle ..... 6

1.2.2.2. Cell Cycle Control Mechanisms ..... 8
1.2.2.2.1. Cascade of Protein Phosphorylations ..... 8
1.2.2.2.2. Cell Cycle Checkpoints ..... 11
1.2.2.2.2.1. The $G_1$ and $G_2$ Checkpoints ..... 12
1.2.2.2.2.1.1. The $G_1$ Checkpoint ..... 13
1.2.2.2.2.1.2. The $G_2$ Checkpoint ..... 13
1.3. Apoptosis ..... 14
1.3.1. Pathways of Apoptosis ..... 16
1.3.1.1. Caspases ..... 16
1.3.1.2. Extrinsic or Death Receptor Pathway of Apoptosis ..... 18
1.3.1.2.1. The Influence of Mitogen-Activated Protein Kinase Pathways in Extrinsic Apoptosis Pathway ..... 20
1.3.1.2.1.1. The Extracellular-Signal-Related Kinase Pathway ..... 21
1.3.1.2.1.2. The p38 Mitogen-Activated Protein Kinase Pathway ..... 23
1.3.1.3. Intrinsic or Mitochondrial Pathway of Apoptosis ..... 24
1.3.1.3.1. The Mitochondrial Permeability Transition Pore ..... 24
1.3.1.3.2. The Mitochondrial Permeability Transition Pore and the Intrinsic Pathway of Apoptosis ..... 27
1.3.1.3.2.1. Caspase-Dependent Pathway of Apoptosis ..... 27
1.3.1.3.2.2. Caspase-Independent Pathway of Apoptosis ..... 30
1.3.1.3.3. Regulatory Mechanisms Involved in Intrinsic Pathway of Apoptosis ..... 31
1.3.1.3.3.1. The Bcl-2 Family of Proteins ..... 31

1.4. The Peripheral Benzodiazepine Receptor ..... 32
1.4.1. Introduction ..... 32
1.4.2. Molecular Identity of the Peripheral Benzodiazepine Receptor ..... 34
1.4.3. Proteins Associated with the Peripheral Benzodiazepine Receptor ..... 36
1.4.4. Evolutionary Conservation of the Peripheral Benzodiazepine Receptor ..... 38
1.4.5. Expression and Subcellular Localisation of the Peripheral Benzodiazepine Receptor ..... 40
1.4.6. Ligands of the Peripheral Benzodiazepine Receptor ..... 42
1.4.6.1. Endogenous Ligands ..... 42
1.4.6.2. Synthetic Ligands ..... 43
1.4.7. Functions of the Peripheral Benzodiazepine Receptor ..... 45
1.5. The Peripheral Benzodiazepine Receptor and Cell Proliferation ..... 47
1.5.1. The Effect of the Peripheral Benzodiazepine Receptor in the Induction of Cell Proliferation ..... 48
1.5.2. The Effect of the Peripheral Benzodiazepine Receptor in the Suppression of Cell Proliferation ..... 49
1.6. The Peripheral Benzodiazepine Receptor and Apoptosis ..... 50
1.6.1. The Effect of the Peripheral Benzodiazepine Receptor in the Induction of Apoptosis ..... 51
1.6.2. The Effect of the Peripheral Benzodiazepine Receptor in the Suppression of Apoptosis ..... 53
1.7. The Peripheral Benzodiazepine Receptor and Cancer ..... 54
1.8. Rationale ..... 57
1.9. Objectives ..... 58

2. MATERIALS AND METHODS ..... 59
2.1. Materials ..... 59
2.1.1. Cell Lines ..... 59
2.1.2. Human Tissue Array ..... 59
2.2. Methodology ..... 60
2.2.1. Preparation of Competent Cells ..... 60
2.2.2. Expression of the Peripheral Benzodiazepine Receptor mRNA in Various Human Cancer Tissues ..... 61
2.2.2.1. Molecular Cloning ..... 61
2.2.2.1.1. RNA Extraction ..... 61
2.2.2.1.2. Reverse Transcription/Complementary DNA Synthesis ..... 63
2.2.2.1.3. Polymerase Chain Reaction ..... 64
2.2.2.1.4. Cloning ..... 65
2.2.2.1.4.1. Ligation ..... 65
2.2.2.1.4.2. Transformation ..... 66
2.2.2.1.5. Colony Polymerase Chain Reaction ..... 67
2.2.2.1.6. Miniprep Analysis/Plasmid DNA Extraction ..... 67
2.2.2.1.7. Restriction Digestion ..... 69
2.2.2.1.8. Sequencing ..... 70
2.2.2.1.9. Linearisation of Recombinant DNA Molecules ..... 71
2.2.2.1.10. Purification of Linearised Recombinant DNA Molecules ..... 72
2.2.2.2. Sense and Anti-Sense Probe Synthesis ..... 73
2.2.2.2.1. *In Vitro* Transcription of Digoxigenin Labelled Sense and Anti-Sense Transcripts ..... 73
2.2.2.2.2. Estimation of Minimal Concentration of Probes ..... 75

2.2.2.3. *In S*itu Hybridisation ..... 76
2.2.2.3.1. Pre-Hybridisation ..... 77
2.2.2.3.2. Hybridisation ..... 78
2.2.2.3.3. Post-Hybridisation ..... 78
2.2.2.3.3.1. Colorimetric Detection ..... 79
2.2.2.3.3.2. Fluorescent Detection ..... 80
2.2.3. Expression Levels of the Peripheral Benzodiazepine Receptor mRNA in Various Human Cancer Tissues ..... 81
2.2.3.1. RNA Isolation ..... 81
2.2.3.2. Relative Quantitative Reverse Transcriptase- Real-Time Polymerase Chain Reaction ..... 82
2.2.3.2.1. Reverse Transcription/Complementary DNA Synthesis ..... 83
2.2.3.2.2. Real-Time Polymerase Chain Reaction ..... 83
2.2.4. Peripheral Benzodiazepine Receptor Protein Expression ..... 84
2.2.4.1. Restriction Digestion of the Peripheral Benzodiazepine Receptor Insert and pGEX-6P-2 Expression Vector ..... 84
2.2.4.2. Purification of the Peripheral Benzodiazepine Receptor Insert and pGEX-6P-2 Expression Vector ..... 85
2.2.4.3. Cloning… ..... 85
2.2.4.4. Colony Polymerase Chain Reaction ..... 85
2.2.4.5. Miniprep Analysis/Plasmid DNA Extraction ..... 85
2.2.4.6. Restriction Digestion ..... 86
2.2.4.7. Sequencing ..... 86
2.2.4.8. Optimisation of the Gluthathione-*S*-Transferase Fusion Protein using Isopropyl-β-D-Thiogalactopyranoside ..... 86

2.2.5. Electrophoresis ..... 88
2.2.5.1. Formaldehyde Agarose Gel Electrophoresis ..... 88
2.2.5.2. Agarose Gel Electrophoresis ..... 89
2.2.5.3. Sodium Dodecyl Sulphate-Polyacrylamide Gel Electrophoresis ..... 90
APPENDIX 1: Information of Tissue Array Panel ..... 93
APPENDIX 2: Composition of Reagents and Solutions ..... 98
APPENDIX 3: Composition of Reactions and Procedures ..... 111
APPENDIX 4: Sequence ..... 119
APPENDIX 5: Vectors ..... 120
APPENDIX 6: DNA and Protein Ladders ..... 122

3. RESULTS ..... 124
3.1. Confirmation of the Histology and Histopathology of Normal Tissues and Histopathology of Cancer Tissues ..... 124
3.1.1. Introduction ..... 124
3.1.2. Histology of Normal Tissue and Histopathology of Tumour Disease in Liver 125
3.1.2.1. Normal Tissue ..... 125
3.1.2.2. Hepatocellular Carcinoma ..... 126
3.1.3. Histology of Normal Tissue and Histopathology of Tumour Disease in Colon 127
3.1.3.1. Normal Tissue ..... 127
3.1.3.2. Colonic Adenocarcinoma ..... 128

3.1.4. Histology of Normal Tissue and Histopathology of Tumour Disease in Epiploon and Stomach ..... 128
3.1.4.1. Normal Tissue ..... 128
3.1.4.1.1. Epiploon Normal Tissue ..... 128
3.1.4.1.2. Stomach Normal Tissue ..... 129
3.1.4.2. Squamous Cell Carcinoma of the Stomach ..... 130
3.1.5. Histology of Normal Tissue and Histopathology of Tumour Disease in Prostate… ..... 131
3.1.5.1. Hyperplastic Tissue ..... 131
3.1.4.2. Adenocarcinoma of the Peripheral Ducts and Acini ..... 132
3.1.6. Histology of Normal Tissue and Histopathology of Tumour Disease in Breast…. ..... 133
3.1.6.1. Normal Tissue ..... 133
3.1.6.2. Invasive Carcinoma (No Special Type) ..... 134
3.1.7. Histology of Normal Tissue and Histopathology of Tumour Diseases in Lung 135
3.1.7.1. Normal Tissue ..... 135
3.1.7.2. Bronchogenic Carcinomas ..... 136
3.1.7.2.1. Adenocarcinoma ..... 136
3.1.7.2.2. Squamous Cell Carcinoma ..... 136
3.1.7.2.3. Classic Small Cell Carcinoma ..... 137
3.1.8. Histology of Normal Tissue and Histopathology of Tumour Diseases in Kidney… ..... 138
3.1.8.1. Normal Tissue ..... 138

3.1.8.2. Renal Cell Carcinomas ..... 139
3.1.8.2.1. Chromophobe Renal Cell Carcinoma ..... 139
3.1.8.2.2. Clear Cell Carcinoma ..... 140
3.1.9. Histopathology of Normal Tissue and Tumour Diseases in Brain ..... 141
3.1.9.1. Normal Tissue ..... 141
3.1.9.2. Brain Cancer ..... 142
3.1.9.2.1. Diffuse Fibrillary Astrocytoma ..... 142
3.1.9.2.2. Ependymoma ..... 143
3.1.9.2.3. Peripheral Central Nervous System Lymphoma ..... 144
3.1.10. Summary ..... 144
3.2. Expression of the Peripheral Benzodiazepine Receptor mRNA in Various Human Cancer Tissues ..... 145
3.2.1. Introduction ..... 145
3.2.2. Molecular Cloning ..... 145
3.2.2.1. RNA Extraction ..... 145
3.2.2.2. Polymerase Chain Reaction ..... 146
3.2.2.3. Cloning… ..... 147
3.2.2.4. Colony Polymerase Chain Reaction ..... 148
3.2.2.5. Miniprep Analysis/Plasmid DNA Extraction ..... 149
3.2.2.6. Restriction Digestion ..... 151
3.2.2.7. Sequencing ..... 153
3.2.2.8. Linearisation of Clones ..... 153
3.2.2.9. Purification of Linearised Clones ..... 155
3.2.3. Sense and Anti-Sense Probe Synthesis ..... 157
3.2.3.1. Estimation of Minimal Concentration of Probes ..... 158

3.2.4. *In Situ* Hybridisation ..... 159
3.2.4.1. Expression of the Peripheral Benzodiazepine Receptor mRNA in Liver Normal and Tumour Tissues ..... 160
3.2.4.2. Expression of the Peripheral Benzodiazepine Receptor mRNA in Colon Normal and Tumour Tissues ..... 162
3.2.4.3. Expression of the Peripheral Benzodiazepine Receptor mRNA in Epiploon Normal and Tumour Tissues ..... 166
3.2.4.4. Expression of the Peripheral Benzodiazepine Receptor mRNA in Prostate Normal and Tumour Tissues ..... 171
3.2.4.5. Expression of the Peripheral Benzodiazepine Receptor mRNA in Breast Normal and Tumour Tissues ..... 174
3.2.4.6. Expression of the Peripheral Benzodiazepine Receptor mRNA in Lung Normal and Tumour Tissues ..... 177
3.2.4.7. Expression of the Peripheral Benzodiazepine Receptor mRNA in Kidney Normal and Tumour Tissues ..... 182
3.2.4.8. Expression of the Peripheral Benzodiazepine Receptor mRNA in Brain Normal and Tumour Tissues ..... 186
3.2.5. Summary ..... 191
3.3. Expression Levels of Peripheral Benzodiazepine Receptor mRNA in Various Human Cancer Tissues ..... 193
3.3.1. Introduction ..... 193
3.3.2. Relative Quantitative Real-Time Polymerase Chain Reaction ..... 194
3.3.2.1. Optimisation of the Concentration of Template DNA Required for Real-Time Polymerase Chain Reaction ..... 194

3.3.2.2. Determination of Expression of Peripheral Benzodiazepine Receptor mRNA in Various Cell Lines using Optimal Concentration of Template DNA…… 198
3.3.3. Summary 207
3.4. Peripheral Benzodiazepine Receptor Protein Expression 208
3.4.1. Introduction 208
3.4.2. Restriction Digestion of the Peripheral Benzodiazepine Receptor Insert and pGEX-6P-2 Expression Vector 208
3.4.3. Purification of the Peripheral Benzodiazepine Receptor Insert and pGEX-6P-2 Expression Vector 210
3.4.4. Cloning 211
3.4.5. Colony Polymerase Chain Reaction 213
3.4.6. Miniprep Analysis/Plasmid DNA Extraction 214
3.4.7. Restriction Digestion 215
3.4.8. Sequencing 217
3.4.9. Optimisation of Glutathione-*S*-Transferase Fusion Protein using Isopropyl-β-D-Thiogalactopyranoside 219
3.4.10. Summary 223
APPENDIX 7: Calculations 224
APPENDIX 8: Summary of PBR mRNA Localisation Studies 231

4. DISCUSSION 240
4.1. Cancer 240
4.1.1. Liver Cancer 241
4.1.2. Colon Cancer 241

4.1.3. Stomach Cancer ..... 242
4.1.4. Prostate Cancer ..... 243
4.1.5. Breast Cancer ..... 244
4.1.6. Lung Cancer ..... 245
4.1.7. Kidney Cancer ..... 246
4.1.8. Brain Cancer ..... 246
4.1.9. Cervical Cancer ..... 247
4.2. Expression of the Peripheral Benzodiazepine Receptor mRNA in Various Normal and Cancer Tissues ..... 248
4.2.1. Tissue Microarrays ..... 248
4.2.2. *In Situ* Hybridisation ..... 249
4.2.2.1. Localisation of the Peripheral Benzodiazepine Receptor mRNA in Various Normal Tissues ..... 251
4.2.2.2. Localisation of the Peripheral Benzodiazepine Receptor mRNA in Various Human Cancer Tissues ..... 252
4.2.3. Expression Levels of Peripheral Benzodiazepine Receptor mRNA in Human Normal and Various Cancer Cell Lines ..... 255
4.2.3.1. Quantitative Real-Time Reverse-Transcriptase Polymerase Chain Reaction. ..... 255
4.2.3.2. Relative Expression Levels of the Peripheral Benzodiazepine Receptor mRNA in Normal and Various Cancer Cell Lines ..... 255
4.2.3.2.1. Quantitative Real RT-PCR Versus Conventional PCR ..... 256
4.2.3.2.2. Expression Levels of Peripheral Benzodiazepine Receptor mRNA…….. ..... 257

4.2.4. *In Situ* Hybridisation Versus Quantitative Reverse Transcriptase Real-Time Polymerase Chain Reaction ..... 258

4.3. Peripheral Benzodiazepine Receptor Protein Expression ..... 259

5. CONCLUSION ..... 262

6. REFERENCES ..... 266

# LIST OF FIGURES

## 1. INTRODUCTION

Figure 1-1: The Cell Cycle ..... 7

Figure 1-2: Morphological Features of Apoptosis ..... 15

Figure 1-3: Extrinsic or Death Receptor Pathway of Apoptosis ..... 19

Figure 1-4: The Extracellular Signal-Related Pathway ..... 22

Figure 1-5: The p38 Mitogen-Activated Protein Kinase Pathway ..... 26

Figure 1-6: Schematic Structure of the Mitochondrial Permeability Transition Pore ..... 27

Figure 1-7: Intrinsic or Mitochondrial Pathway of Apoptosis ..... 29

Figure 1-8: Regulatory Mechanisms of the Bcl-2 Family of Proteins in the Control of Apoptosis ..... 33

Figure 1-9: Molecular Identity of the Peripheral Benzodiazepine Receptor ..... 35

Figure 1-10: Chemical Structures of Synthetic Ligands that bind to the Peripheral Benzodiazepine Receptor ..... 44

## APPENDIX 4

Figure 1: Sequence of the *Peripheral Benzodiazepine Receptor* (*PBR*) Gene ..... 119

## APPENDIX 5

Figure 1: Schematic Diagram of the pGEM-T Easy Vector ..... 120

Figure 2: Schematic Diagram of pGEX-6P-2 Expression Vector ..... 121

## APPENDIX 6

Figure 1: DNA Molecular Weight Ladders ..... 122

Figure 2: Protein Molecular Weight Ladder ..... 123

## 3. RESULTS

Figure 3-1: H&E of Normal Liver Tissue ..... 125

Figure 3-2: H&E of Hepatocellular Carcinoma ..... 126

Figure 3-3: H&E of Normal Colon Tissue ..... 127

Figure 3-4: H&E of Colonic Adenocarcinoma ..... 128

Figure 3-5: H&E of Normal Epiploon Tissue ..... 128

Figure 3-6: H&E of Normal Stomach Tissue ..... 129

Figure 3-7: H&E of Stomach Squamous Cell Carcinoma ..... 130

Figure 3-8: H&E of Hyperplastic Prostate Tissue ..... 131

Figure 3-9: H&E of Adenocarcinoma of the Peripheral Ducts and Acini in the Prostate ..... 132

Figure 3-10: H&E of Inactive Mammary Gland Normal Tissue ..... 133

Figure 3-11: H&E of Invasive Carcinoma (No Specific Type) ..... 134

Figure 3-12: H&E of Lung Normal Tissue ..... 135

Figure 3-13: H&E of Lung Adenocarcinoma ..... 136

Figure 3-14: H&E of Lung Squamous Cell Carcinoma ..... 136

Figure 3-15: H&E of Lung Classic Small Cell Carcinoma ..... 137

Figure 3-16: H&E of Normal Kidney Tissue ..... 138

Figure 3-17: H&E of Chromophobe Renal Carcinoma ..... 139

Figure 3-18: H&E of Clear Cell Carcinoma ..... 140

Figure 3-19: H&E of Normal Brain Tissue ..... 141

Figure 3-20: H&E of Diffuse Fibrillary Astrocytoma ..... 142

Figure 3-21: H&E of Ependymoma ..... 143

Figure 3-22: H&E of Primary Central Nervous System Lymphoma ..... 144

Figure 3-23: Isolation of Total RNA ..... 146

Figure 3-24: Amplification of the *Peripheral Benzodiazepine Receptor* Gene Region of Interest ..... 147
Figure 3-25: Cloning of the Peripheral Benzodiazepine Receptor Insert into pGEM-T Easy Vector ..... 148
Figure 3-26: Amplification of the Peripheral Benzodiazepine Receptor Insert via Colony PCR ..... 149
Figure 3-27: Isolation of Plasmid DNA ..... 150
Figure 3-28: Restriction of Plasmid DNA containing Insert ..... 152
Figure 3-29: Amplification of Peripheral Benzodiazepine Receptor Insert via Polymerase Chain Reaction ..... 152
Figure 3-30: Sequence Alignment of the *Peripheral Benzodiazepine Receptor* Gene ..... 154
Figure 3-31: Linearisation of Recombinant Plasmid DNA ..... 155
Figure 3-32: Purification of Linearised Clones ..... 156
Figure 3-33: Blot showing Minimal Concentration of DIG-Labelled Sense and Anti-Sense Probes ..... 158
Figure 3-34: Schematic Diagram of *In Situ* Hybridisation ..... 159
Figure 3-35: Expression of the Peripheral Benzodiazepine Receptor mRNA in Liver ..... 161
Figure 3-36: Subcellular Localisation of the Peripheral Benzodiazepine Receptor mRNA in Normal Liver Tissue ..... 162
Figure 3-37: Subcellular Localisation of the Peripheral Benzodiazepine Receptor mRNA in Hepatocellular Carcinoma ..... 163
Figure 3-38: Expression of the Peripheral Benzodiazepine Receptor mRNA in Colon ..... 164
Figure 3-39: Subcellular Localisation of the Peripheral Benzodiazepine Receptor mRNA in Normal Colon Tissue ..... 165

Figure 3-40: Subcellular Localisation of Peripheral Benzodiazepine Receptor mRNA in Colonic Adenocarcinoma ..... 167
Figure 3-41: Expression of the Peripheral Benzodiazepine Receptor mRNA in Normal Epiploon and Stomach ..... 168
Figure 3-42: Subcellular Localisation of the Peripheral Benzodiazepine Receptor mRNA in Normal Epiploon Tissue ..... 169
Figure 3-43: Subcellular Localisation of the Peripheral Benzodiazepine Receptor mRNA in Normal Stomach Tissue ..... 170
Figure 3-44: Subcellular Localisation of the Peripheral Benzodiazepine Receptor mRNA in Stomach Squamous Cell Carcinoma ..... 171
Figure 3-45: Expression of the Peripheral Benzodiazepine Receptor mRNA in Prostate .... 172
Figure 3-46: Subcellular Localisation of the Peripheral Benzodiazepine Receptor mRNA in Hyperplastic Prostate Tissue ..... 173
Figure 3-47: Subcellular Localisation of the Peripheral Benzodiazepine Receptor mRNA in Prostate Adenocarcinoma of the Peripheral Duct and Acini ..... 174
Figure 3-48: Expression of the Peripheral Benzodiazepine Receptor mRNA in Breast ..... 175
Figure 3-49: Subcellular Localisation of the Peripheral Benzodiazepine Receptor mRNA in Normal Breast Tissue ..... 176
Figure 3-50: Subcellular Localisation of the Peripheral Benzodiazepine Receptor mRNA in Breast Invasive Carcinoma (No Specific Type) ..... 177
Figure 3-51: Expression of the Peripheral Benzodiazepine Receptor mRNA in Lung ..... 178
Figure 3-52: Subcellular Localisation of the Peripheral Benzodiazepine Receptor mRNA in Lung Adenocarcinoma ..... 179
Figure 3-53: Subcellular Localisation of the Peripheral Benzodiazepine Receptor mRNA in Normal Lung Tissue ..... 180

Figure 3-54: Subcellular Localisation of the Peripheral Benzodiazepine Receptor mRNA in Lung Squamous Cell Carcinoma ..... 181
Figure 3-55: Subcellular Localisation of the Peripheral Benzodiazepine Receptor mRNA in Lung Small Cell Carcinoma ..... 181
Figure 3-56: Expression of the Peripheral Benzodiazepine Receptor mRNA in Kidney ..... 183
Figure 3-57: Subcellular Localisation of the Peripheral Benzodiazepine Receptor mRNA in Normal Kidney Tissue ..... 184
Figure 3-58: Subcellular Localisation of the Peripheral Benzodiazepine Receptor mRNA in Chromophobe Renal Cell Carcinoma ..... 185
Figure 3-59: Subcellular Localisation of the Peripheral Benzodiazepine Receptor mRNA in Renal Clear Cell Carcinoma ..... 185
Figure 3-60: Expression of the Peripheral Benzodiazepine Receptor mRNA in Brain ..... 187
Figure 3-61: Subcellular Localisation of the Peripheral Benzodiazepine Receptor mRNA in Normal Brain Tissue ..... 188
Figure 3-62: Subcellular Localisation of the Peripheral Benzodiazepine Receptor mRNA in Diffuse Fibrillary Astrocytoma ..... 189
Figure 3-63: Subcellular Localisation of the Peripheral Benzodiazepine Receptor mRNA in Primary Central Nervous System Lymphoma ..... 190
Figure 3-64: Subcellular Localisation of the Peripheral Benzodiazepine Receptor mRNA in Ependymoma ..... 191
Figure 3-65: Quantitative Curve of the *Peripheral Benzodiazepine Receptor* Gene in the Serial Dilutions of the MRC5 Cell Line..... 196
Figure 3-66: Melting Curve of the Real-Time PCR Products Synthesised..... 198
Figure 3-67: Quantitative Curve of the *Peripheral Benzodiazepine Receptor* Gene in Various Cell Lines ..... 201

Figure 3-68: Relative Expression Level of Lung Adenocarcinoma When Compared to its Normal Counterpart ..... 203
Figure 3-69: Relative Expression Levels of Peripheral Benzodiazepine Receptor mRNA in Various Cancers ..... 204
Figure 3-70: Melting Curve of the Real-Time PCR Products Synthesised ..... 205
Figure 3-71: Amplification of Real-Time Polymerase Chain Reaction Product ..... 207
Figure 3-72: Virtual Results for Peripheral Benzodiazepine Receptor Digested with *Bam*HI and *Xho*I ..... 209
Figure 3-73: Double Digestion of pGEM-T Easy Containing Peripheral Benzodiazepine Receptor Insert and pGEX-6P-2 Expression Vector ..... 211
Figure 3-74: Purification of the Peripheral Benzodiazepine Receptor Insert and pGEX-6P-2 Expression Vector ..... 212
Figure 3-75: Cloning of the Peripheral Benzodiazepine Receptor Insert into pGEX-6P-2 Expression Vector ..... 213
Figure 3-76: Amplification of the Peripheral Benzodiazepine Receptor via Colony Polymerase Chain Reaction ..... 214
Figure 3-77: Isolation of Plasmid DNA via Miniprep Analysis ..... 215
Figure 3-78: Restriction Digestion of Plasmid DNA containing Peripheral Benzodiazepine Receptor Insert ..... 216
Figure 3-79: Alignment of the *Peripheral Benzodiazepine Receptor* (*PBR*) Gene ..... 218
Figure 3-80: Schematic Representation of the Reading Frames of the Peripheral Benzodiazepine Receptor Protein ..... 219
Figure 3-81: Translation of Peripheral Benzodiazepine Receptor (PBR) Insert ..... 220
Figure 3-82: Transformation of the pGEX-6P-2 Expression Vector Containing the Peripheral Benzodiazepine Receptor Insert ..... 222

Figure 3-83: SDS-PAGE of Optimising the Concentration of IPTG Required to Induce Gluthathione-*S*-Transferase Fusion Protein ..... 222

# LIST OF TABLES

## APPENDIX 1

Table 1: Tissue Array Panel Display..... 93

Table 2: Summary of the Number of Patients with Cancer on the Tissue Array Panel..... 96

Table 3: Summary of the Number of Normal Patients on the Tissue Array Panel..... 97

## APPENDIX 3

Table 1: Composition of Reverse Transcription Reaction..... 111

Table 2: Reverse Transcription Conditions used to Synthesise Complementary DNA..... 111

Table 3: Composition of Polymerase Chain Reaction (PCR) Reaction..... 112

Table 4: PCR Conditions used to amplify the Region of Interest..... 112

Table 5: Composition of Ligation Reaction..... 113

Table 6: Composition Restriction Digestion Reaction..... 113

Table 7: Composition of *In Vitro* Transcription Reactions..... 114

Table 8: Serial Dilutions of Probes to Estimate Minimal Concentrations of Probes..... 115

Table 9: Composition of Reverse Transcription Reaction..... 116

Table 10: Reverse Transcription Conditions used to Synthesise Complementary DNA..... 116

Table 11: Composition of Relative Quantitative Polymerase Chain Reaction (PCR)..... 117

Table 12: Relative Quantitative PCR Conditions used to Amplify Region of Interest..... 117

Table 13: Reagents used in Preparation of SDS-PAGE..... 118

## 3. RESULTS

Table 3-1: Absorbance, Purity and Concentration of Sense and Anti-Sense Probes Measured at 260 nm and 280 nm ..... 157

Table 3-2: Efficiency and Threshold Cycle Values of PCR Product Synthesised..... 197

Table 3-3: Calculation of Melting Temperatures for the PCR Product Synthesised in Serial Dilution of the MRC5 Cell Line ..... 199

Table 3-4: Absorbance, Purity and Concentration of Sense and Anti-Sense Probes Measured at 260 nm and 280 nm ..... 200

Table 3-5: Efficiency and Threshold Cycle Values of PCR Product Synthesised..... 202

Table 3-6: Relative Expression Level of the Peripheral Benzodiazepine Receptor mRNA in Lung Adenocarcinoma when Compared Lung Normal in Absolute Terms ..... 203

Table 3-7: Relative Expression Level of the Peripheral Benzodiazepine Receptor mRNA in Various Cancers in Absolute Terms..... 204

Table 3-8: Calculation of Melting Temperatures for the PCR Product Synthesised in each Cell Line..... 206

Table 3-9: Molecular Composition of the Peripheral Benzodiazepine Receptor Insert ..... 219

## APPENDIX 8

Table 1: Expression of the Peripheral Benzodiazepine mRNA in Various Normal Human Tissues..... 231

Table 2: Expression of the Peripheral Benzodiazepine Receptor mRNA in Various Human Cancer Tissues..... 234

Table 3: Variation in Expression Levels of PBR mRNA in the Various Normal Tissues of the Human Body……236

Table 4: Variation in Expression Levels of PBR mRNA in the Various Cancer Tissues…..237

Table 5: Summary of Expression Pattern of Peripheral Benzodiazepine Receptor mRNA in Various Cancerous Tissues when Compared to its Normal Counterpart……238

# ABBREVIATIONS

| | | |
|---|---|---|
| α | - | Alpha |
| ± | - | Approximately |
| A | - | Adenosine/Adenine |
| A | - | Alanine |
| $A_{260/280}$ | - | Absorbance at 260 nm or 280 nm |
| A549 | - | Human Epithelial Cell Lung Carcinoma Cell Line |
| ACBP | - | Acyl CoA Binding Protein |
| Acinus | - | Apoptotic Chromatin Condensation Inducer in the Nucleus |
| ADP | - | Adenosine Diphosphate |
| AIF | - | Apoptotic Inducing Factor |
| ANC | - | Adenine Nucleotide Carrier |
| AP | - | Alkaline Phosphatase |
| APO | - | Apoptosis-Mediating Surface Antigen Fas |
| Apaf | - | Apoptosis Activating Factor |
| Arg | - | Arginine |
| ASK | - | Apoptosis Signal-Regulating Kinase |
| ATF | - | Activating Transcription Factor |
| ATM | - | Ataxia Telengiectasia Mutated |
| ATP | - | Adenosine Triphosphate |
| ATPases | - | Adenosine Triphosphatases |
| ATR | - | ATM and Rad3-Related |
| β | - | Beta |
| Bad | - | Bcl-2-Antagonist of Cell Death Protein |

| | | |
|---|---|---|
| Bax | - | Bcl-Associated X Protein |
| BCIP | - | 5-Bromo-4-Chloro-3-Indolyl Phosphate |
| Bcl | - | B-Cell Lymphoma/Leukaemia |
| BH | - | Bcl-2 Homologue |
| Bid | - | Bcl-2-Interacting Domain Death Agonist |
| Bim | - | Bcl-2-Interacting Mediator of Cell Death |
| bp | - | Base Pair |
| BSA | - | Bovine Serum Albumin |
| c | - | Concentration |
| C | - | Cysteine |
| C | - | Cytosines |
| $CaCl_2$ | - | Calcium Chloride |
| CAD | - | Caspase-Activated DNase Poly (ADP-Ribose) |
| CARD | - | Caspase Recruitment Domain |
| Caspases | - | Cysteinyl Aspartate-Specific Proteases |
| CBR | - | Central Benzodiazepine Receptor |
| CD | - | Cell Determinant |
| Cdc | - | Cell Division Cycle |
| CDK | - | Cyclin-Dependent Kinases |
| CDKI | - | CDK Inhibitors |
| cDNA | - | Complementary DNA |
| C/EBP | - | CCAAT/Enhancer Binding Protein |
| Chk | - | Checkpoint Kinase |
| CHOP | - | C/EBP Homologous Protein |
| CIP/KIP | - | Cyclin-Dependent Kinase Inhibitor Protein |

CNS - Central Nervous System

CoA - Coenzyme A

CREB - Cyclic Adenosine Monophosphate Responsive Element Binding Protein

$C_t$ - Threshold Cycle

CTP - Cytosine Triphosphate

$cm^3$ - Cubic Centimetre

˚C - Degrees Celsius

D - Aspartic Acid

dATP - Deoxyadenine Triphosphate

DAX - Dishevelled Anadaxin Domain

DBI - Diazepam Binding Inhibitor

DCT - Distal Convoluted Tubule

dCTP - Deoxycytosine Triphosphate

DEPC - Diethyl Pyrocarbonate

DF - Dilution Factor

dGTP - Deoxyguanine Triphosphate

Diablo - Direct IAP Binding Protein with Low pI

$-dI/dT_{max}$ - Relative Fluorescence Units Over Time

DIG - Digoxigenin

DISCs - Death-Inducing Signalling Complexes

DNA - Deoxyribonucleic acid

DNase - Deoxyribonuclease

DMEM - Dulbecco's Modified Eagle Media

dNTP - Deoxyribonucleotide Triphosphate

ds - Double-Stranded

dT - Deoxythymidines

DTT - Dithiothreitol

dTTP - dT Triphosphate

dUTP - Deoxyuridine Triphosphate

E - Glutamic Acid

EDTA - Ethylenediamine Tetra Acetic Acid

EGFR - Epidermal Growth Factor Receptor

Ena - Enabled

ERK - Extracellular-Signal Related Kinase

EVH - Ena/VASP Homology Domain

F - Phenylalanine

FADD - Fas-Associated Death Domain

Fas - Fibroblast-Associated

FBS - Foetal Bovine Serum

FGIN-1-27 - *N*, *N*-Di-*n*-Hexyl-2-(4-Fluotophenyl)Indole-3-Acetamide

FITC - Fluorescein Isothiocyanate

FLIP - FADD-Like Interleukin-1β Converting Enzyme Inhibitory Protein

FWHM - Full Width Half Maximum

γ - Gamma

g - Grams

G - Glycine

G - Guanines

$G_0$ - Quiescence Phase

$G_1$ - First Growth Gap Phase

$G_2$ - Second Growth Gap Phase

GABA - γ-Aminobutyric Acid

gadd - Growth Arrest and DNA Damage-Inducible

GDP - Guanosine Diphosphate

Glu - Glutamic Acid

Graham 293 - Normal Human Embryonic Kidney Cell Line

GST - Gluthathione-*S*-Transferase

GTP - Guanidine Triphosphate/Guanosine Triphosphate

GTPases - Guanosine Triphosphatases

H - Histidine

HCl - Hydrochloric Acid

H&E - Haematoxylin and Eosin

HeLa - Human Epithelial Cell Cervical Carcinoma Cell Line

HepG - Human Liver Hepatocellular Carcinoma Cell Line

HMG-CoAR - 3-Hydroxy-3-Methylglutaryl Coenzyme A Reductase

hnRNP - Heterogeneous Nuclear Ribonuclear Protein

Htr - High Temperature Requirement Protein

$H_2O$ - Water

I - Isoleucine

I - One

IAP - Inhibitors of Apoptosis Protein

ICAD - Inhibitor of Caspase-Activated Deoxyribonuclease

Ig - Immunoglobulin

II - Two

III - Three

INK - Inhibitors of CDKs

IPTG - Isopropyl-β-D-Thiogalactopyranoside

IV - Four

JNK - c-Jun Amino-Terminal Kinase

κ - Kappa

KAc - Potassium Acetate

kb - Kilobase

KCl - Potassium Chloride

kDa - Kilodalton

KDS - Potassium Dodecyl Sulphate

l - Litre

L - Leucine

LB - Luria Bertani

LiCl - Lithium Chloride

Lys - Lysine

$\Delta\psi_m$ - Mitochondrial Transmembrane Potential

M - Methionine

M - Mitosis Phase

M - Molar

µl - Microlitre

µm - Micrometer

µM - Micromolar

MA-10 - Mouse Leydig Tumour Cell Line

MAPK - Mitogen-Activated Protein Kinase

MAPKAP - MAPK-Activated Protein

MAPKAPK - MAPKAP Kinase

MAPKK - MAPK Kinase

MEF - Myocyte Enhancer Factor

MEK - MAPK/ERK Kinase

MEKK - MEK Kinase

MSK - Mitogen and Stress-Activated Kinase

mg - Milligram

$MgCl_2$ - Magnesium Chloride

min - Minutes

ml - Millilitre

mm - Millimetre

mM - Millimolar

$MnCl_2$ - Manganese Chloride

MnSOD - Manganese-dependent Dismutase

MOPS - 3-[N-Morpholino] Propane Sulfonic Acid

MPTP - Mitochondrial Permeability Transition Pore

MRC5 - Normal Human Embryonic Fibroblast-Like Lung Cell Line

mRNA - Messenger RNA

N - Asparagine

NaCl - Sodium Chloride

NADH - Nicotinamide Adenine Dinucleotide Hydrogenase

NaOH - Sodium Hydroxide

NBT - Nitroblue Tetrazolium

NCBI - National Centre for Biomedical Information

NF - Nuclear Factor

nm - Nanometre

| | | |
|---|---|---|
| Noxa | - | NADH Oxidase |
| NST | - | No Specific Type |
| ω | - | Omega |
| δ | - | Psi |
| % | - | Percent |
| p | - | Polypeptide |
| P | - | Proline |
| P-450$_{scc}$ | - | Side Chain Cleavage Cytochrome P-450 |
| PAGE | - | Polyacrylamide Gel Electrophoresis |
| PAPs | - | PBR-Associated Proteins |
| PARP | - | Poly (ADP-Ribose) Polymerase |
| PBR | - | Peripheral Benzodiazepine Receptor |
| PBS | - | Phosphate Buffered Saline |
| PCNSL | - | Primary Central Nervous System Lymphoma |
| PCR | - | Polymerase Chain Reaction |
| PCT | - | Proximal Convoluted Tubule |
| PEG | - | Polyethylene Glycol |
| PFA | - | Paraformaldehyde |
| pg | - | Picogram |
| pH | - | Hydrogen Ion Concentration |
| pI | - | Isoelectric Point |
| PI-3K | - | Phosphotidylinositol-3 Kinase |
| PK | - | Protein Kinase |
| PK11195 | - | 1-(2-Chlorophenyl)-*N*-Methyl-*N*-(1-Methylpropyl)-3-Isoquinoline Carboxamide |

| | | |
|---|---|---|
| PRAX-1 | - | PBR-Associated Protein-1 |
| Q | - | Glutamine |
| R | - | Arginine |
| Raf | - | Riboflavin-Aldehyde Forming Enzyme |
| Ran | - | Ras-Related Protein |
| Rb | - | Retinoblastoma |
| Rho | - | Renin Angiotensin System Homology |
| RIP | - | Receptor-Integrating Protein |
| RNA | - | Ribonucleic Acid |
| RNase | - | Ribonuclease |
| Ro5-4864 | - | 7-Chloro-1, 3-Dihydro-1-Methyl-5 (4'-Cholorphenyl) 2H-1, 4-Benzodiazepine |
| ROS | - | Reactive Oxygen Species |
| rpm | - | Revolutions Per Minute |
| rRNA | - | Ribosomal RNA |
| s | - | Second |
| S | - | Serine |
| S | - | DNA Synthesis Phase |
| SCID | - | Severe Combined Immunodeficiency |
| $sdH_2O$ | - | Sterile Distilled $H_2O$ |
| SDS | - | Sodium Dodecyl Sulphate |
| Site II | - | Succinate-Cytochrome *c* Oxidoreductase |
| Smac | - | Second Mitochondrial Activator of Caspases |
| Sp | - | Stimulatory Protein |
| Spred | - | Sprout-Related Protein with EVH-1 Domain |

SSC - NaCl and Sodium Citrate

STAT - Signal Transducer and Activator of Transcription

T - Threonine

T - Thymidines/Thymines

TAE - Tris-Acetate/EDTA

TBE - Tris-Borate/EDTA

TBS - Tris Buffer Saline

TCA - Tricarboxylic Acid Cycle

TE - Tris-HCl/EDTA

TEMED - N, N, N', N'-Tetramethylenediamine

TGF - Transforming Growth Factor

$T_m$ - Melting Temperature

TNB - Tri-Sodium Blocking

TNF - Tumour Necrosis Factor

TNFR - TNF Receptor

TRADD - TNFR-I-Associated Death Domain

TRAIL - TNF-Related Apoptosis Inducing Ligand

Tris - Tris (Hydroxymethyl) Aminomethane

TspO - Tryptophan-Rich Sensory Protein

Tween 20 - Polyethylene Sorbitan Monolaurat

TYM - Tryptone Yeast Extract $MgCl_2$

U937 - Human Pleural Effusion Histiocytic Lymphoma Cell Line

UTP - Uridine Triphosphate

UV - Ultraviolet

V - Valine

| | | |
|---|---|---|
| V | - | Volts |
| VASP | - | Vasodilator-Stimulated Phosphoprotein |
| VDAC | - | Voltage-Dependent Anion Channel |
| v/v | - | Volume/Volume |
| W | - | Tryptophan |
| WHO | - | World Health Organisation |
| w/v | - | Weight/Volume |
| XIAP | - | X-Linked IAP |
| Y | - | Tyrosine |

# 1. INTRODUCTION

## 1.1. Cancer

### *1.1.1. Introduction*

Cancer is one of the most important medico-biological problems that still remain unsolved (Lokitnov, 2004) and can be seen as a disease involving dynamic changes at multiple sites in the genome, which include the discovery of mutations that produce oncogenes that have a dominant gain of function and tumour suppressor genes that have a recessive loss of function (Hanahan, *et al.*, 2000, Karpinets, *et al.*, 2004). Furthermore, these mutations can be as subtle as point mutations and obvious as changes in chromosome complement (Hanahan, *et al.*, 2000). Thus, it is thought that cancer progression can be seen as analogous to Darwinian evolution where a succession of genetic changes that confer some form of growth advantage to environmental stresses result in cell survival and genomic instability leading to the progressive conversion of normal human cells into cancer cells (Hanahan, *et al.*, 2000, Karpinets, *et al.*, 2004, Vineis, 2003). Thus, this conversion of normal cells to cancer cells occurs where natural selection occurs through several sequential steps to direct mutations to adaptation (Karpinets, *et al.*, 2004, Vineis, 2003).

Normal cells have exquisite machinery that governs cellular fates in response to external stimuli (Huang, *et al.*, 2004). The tumour tissue grows as an abnormal analogue of the tissue of origin as it is influenced and often governed by the interplay of multiple basically normal physiological processes and corresponding regulatory mechanisms, which are not necessarily damaged but deregulated or taken out of their physiological context in such a manner that the beneficial role in normal cells is now distorted (Lokitnov, 2004). Normal cells are transformed into immortal and malignant when there is a loss of control of cell proliferation,

differentiation and cell death (Decaudin, *et al.*, 2002, Huang, *et al.*, 2004). Deregulated cell proliferation is caused by a loss of balance between cell proliferation and apoptosis at certain stages during tumour development (Hsu, *et al.*, 2004).

Numerous genetic factors involved in the pathogenesis of neoplastic growth have been identified but the complex mechanism by which it occurs is still not completely understood (Lokitnov, 2004). Neoplastic growth should not be regarded as a cell-autonomous process intrinsic to the cancer cell because cancer development depends on the changes in interactions between malignant cells and their normal neighbours (Lokitnov, 2004). It is usually triggered by genetic damage, which causes chromosomal aberrations and somatic mutations and the accumulation of these mutations in many genes encoding crucial proteins or oncoproteins that control cell growth and apoptosis leads to malignant transformation that occurs as a result of loss of cell multiplication and death control (Hsu, *et al.*, 2004, Lokitnov, 2004). These genes include those coding for cell cycle regulators such as cyclins, cyclin-dependent kinases (CDKs), CDK inhibitors (CDKIs), mainly from the first growth gap ($G_1$) phase of the cell cycle and Retinoblastoma (Rb) (Deane, *et al.*, 2005, Reynolds, *et al.*, 1995, Sutter, *et al.*, 2003), pro-survival genes encoding telomerase, growth factors or their receptors, inhibitors of apoptotic proteins such as nuclear factor (NF)-kappa (κ) B, B-cell lymphoma/leukaemia (Bcl)-2 and Bcl-$X_L$, the pro-apoptosis genes encoding caspases, Bcl-associated X protein (Bax), Bak, Bcl-2-interacting domain death agonist (Bid), fibroblast-associated (Fas), receptors for tumour necrosis factor (TNF) alpha (α) and genes encoding key transcription factors or elements for signal transduction lead to apoptosis/survival (Hsu, *et al.*, 2004).

Hallmarks to the development of cancer include evasion of apoptosis and uncontrolled cell proliferation (Hanahan, *et al.*, 2000, Huang, *et al.*, 2005, Lokitnov, 2004). It is now believed that most types of cancers even though they have different manifestations, etiology and clinical features share a relatively small number of molecular, biochemical and cellular traits, also known as acquired capabilities at the level of development and progression and at the level of function of an individual cancer cell since nearly all mammalian cells carry similar molecular machinery that regulates cell proliferation, differentiation and cell death (Hanahan, *et al.*, 2000, Karpinets, *et al.*, 2004, Lokitnov, 2004).

### *1.1.2. Carcinogenesis*

Tumorigenesis is characterised by the outgrowth of abnormal cells that is controlled at the cellular level (Huang, *et al.*, 2000, Lokitnov, 2004) and can be defined as a multistep process that reflect the genetic alterations that drives the progressive transformation of normal human cells into a highly malignant derivative (Hanahan, *et al.*, 2000). This progression of the cell evolves from normal to malignant to invasive to metastatic cancers (Lokitnov, 2004, Hanahan, *et al.*, 2000). Hanahan and Weinberg have suggested that the factors relevant for malignancy include: self-sufficiency in growth signals, insensitivity to growth-inhibitory signals, evasion of apoptosis, limitless replicative potential, sustained angiogenesis, tissue invasion and metastasis (Hanahan, *et al.*, 2004, Lokitnov, 2004). Each of these physiological factors are acquired during tumour development and can be seen as a successful breaching of anticancer defence mechanisms that is hardwired into cells (Hanahan, *et al.*, 2000). Advanced stages of neoplasia are characterised by the progressive failure of protective mechanisms against tumour growth and spread (Lokitnov, 2004).

*1.1.2.1. Evasion of Apoptosis*

Tumour cell growth is determined by the rate of cell proliferation and the rate of cell death, principally by apoptosis (Hanahan, *et al.*, 2000). Cancer cells have acquired the ability to resist apoptosis through a variety of strategies with the most common been the loss of a proapoptotic regulator through mutation of the *p53* tumour suppressor gene, which results in the inactivation of its product that results in the loss of a checkpoint control, which results in cells with damaged genomes not undergoing apoptosis and thus allows for defective genomes to persist and replicate in daughter cells (Hanahan, *et al.*, 2000, Hsu, *et al.*, 2004). In addition, apoptosis can be evaded by tumour cells expressing a non-signalling decoy receptor in order to sequester the death factor or by stimulation of survival signal pathways (Herzig, *et al.*, 2002).

*1.1.2.2. Limitless Replicative Potential*

In addition to acquired disruption in cell-to-cell signalling through growth signal autonomy, insensitivity to antigrowth signals and resistance to apoptosis, the cell autonomous program found in all mammalian cells, which limits multiplication, must also be disrupted (Hanahan, *et al.*, 2000). Thus, in order to disrupt any process that places cells in senescence, the Rb and p53 tumour suppressor proteins must be disabled, which allows cells to continue to replicate without limit known as immortalisation (Hanahan, *et al.*, 2000). Rb and p53 are two regulatory proteins that control two major interconnected signalling pathways and when they undergo genetic alterations play a role as tumour suppressors in cancer (Deane, *et al.*, 2005, Lokitnov, 2004). These two proteins function in the early stage of cancer progression (Lokitnov, 2004).

Genomic instability that is observed in many types of cancers may occur through chromosome missegregation during mitosis. Normally, if this occurs, a checkpoint that monitors the proper separation of chromosomes during mitosis results in cell cycle arrest. However, a loss of this checkpoint results in accumulation of chromosome missegregation (Herzig, *et al.*, 2002).

## 1.2. Cell Proliferation and the Cell Cycle

### *1.2.1. Cell Proliferation*

Cell proliferation can be defined as the expansion of cell populations that is driven by stem cell replication that is a major characteristic of developing embryos and young organisms (Deane, *et al.*, 2005). In adult organisms, cells are in quiescence but a few exceptions do occur such as the epithelia of the gastrointestinal system, which is a continuously renewing organ system, and the hepatobillary system, which is a senescent organ system (Deane, *et al.*, 2005).

During the early phases of cell growth, cells are uncommitted having the capacity to either continue their proliferative cycle or to exit the cell cycle and enter differentiation, which is dependent on tissue-specific gene expression and extracellular signals derived from the microenvironment such as growth factors and cell-cell or cell-matrix contact interactions (Deane, *et al.*, 2005, Reynolds, *et al.*, 1995). These extracellular signals include epidermal growth factor ligands such as epidermal growth factor (EGF), transforming growth factor alpha (TGFα), amphiregulin, the "wingless" (Wnt) protein, TGF beta (TGFβ), platelet derived growth factor, fibroblast growth factor, erythropoietin, insulin-like growth factor and large families of integrins, interleukins, tumour necrosis factors, interferons, and colon-stimulating growth factors (Deane, *et al.*, 2005). Extracellular ligands function in the induction or

repression of gene transcription, stabilisation of mRNA transcripts, rate of protein translation and posttranslational modification of proteins that includes protein degradation. Furthermore, the overall result of all the signalling pathways activated by extracellular growth factors and ligands results in either the activation or cessation of the regulatory machinery of the cell cycle and thus subsequently controls development and homeostasis (Deane, *et al.*, 2005).

An imbalance of growth inhibitory and growth-promoting effects of factors influencing cell cycle, coupled with the lack of accurate positional information can have dire consequences for the organism in the form of cancer (Deane, *et al.*, 2005, Reynolds, *et al.*, 1995).

### *1.2.2. The Cell Cycle*

#### *1.2.2.1. Phases of the Cell Cycle*

The cell cycle or the cell division cycle is the process by which DNA is replicated and a cell divided in a series of coordinated events (Collins, *et al.*, 1997). It can be divided into five different stages including $G_0$, $G_1$, the S phase, $G_2$ and the M phase (Figure 1-1) (Deane, *et al.*, 2005). In the $G_0$ phase the cell is in quiescence or in the resting state where it is uncommitted having the capacity to enter the cell cycle and undergo proliferation or enter the differentiation process (Deane, *et al.*, 2005, Reynolds, *et al.*, 1995). During this state, the cell cycle machinery may be partially dismantled (Reynolds, *et al.*, 1995). $G_1$ is the first growth gap phase where newly generated cells will typically spend most of their lives (Deane, *et al.*, 2005, Reynolds, *et al.*, 1995). An additional point located in this phase is known as the restriction point. Prior to the restriction point, the cell remains sensitive to a variety of negative regulatory signals that counter the effect of mitogenic signals allowing the cell to enter and remain in the $G_0$ phase. However, once the cell passes this restriction point, it becomes committed to continuing through the rest of the cell cycle (Reynolds, *et al.*, 1995).

The S phase is the DNA synthesis phase where DNA replication occurs resulting in the entire genome been duplicated (Deane, *et al.*, 2005, Reynolds, *et al.*, 1995). $G_2$ is the second growth gap phase where the cell continues to grow in preparation for the M phase (Deane, *et al.*, 2005, Reynolds, *et al.*, 1995). The M phase is the phase at which mitosis occurs, that is the phase at which the duplicated chromosomes split into single chromosomes and nuclear and cell division occurs (Deane, *et al.*, 2005, Reynolds, *et al.*, 1995).

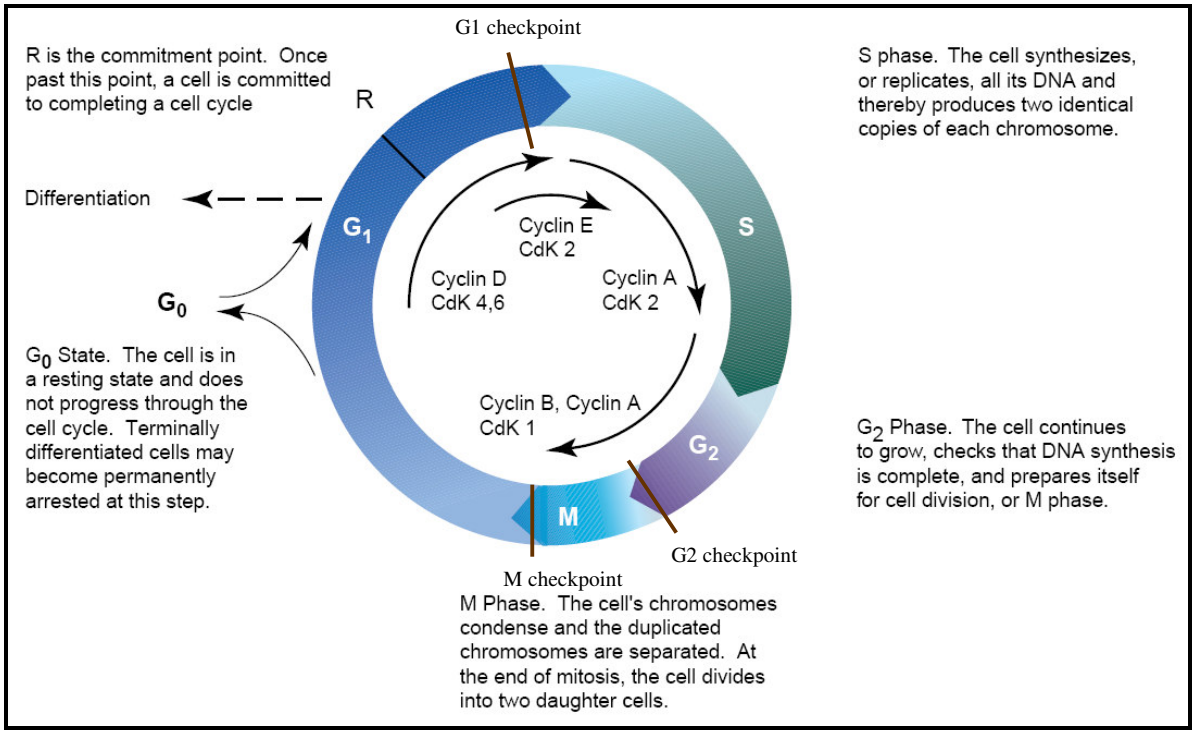



**Figure 1-1: The Cell Cycle**

(Reference: Reynolds, *et al.*, 1995)

#### *1.2.2.2. Cell Cycle Control Mechanisms*

Eukaryotic cells have evolved signalling pathways to coordinate cell-cycle transitions and ensure faithful replication of the genome before cell division (Stewart, *et al.*, 2003). There are at least two types of cell cycle control mechanisms that are recognised: (i) a cascade of protein phosphorylations that coveys a cell from one stage to the next and (ii) a set of checkpoints that monitor completion of critical events if necessary (Collins, *et al.*, 1997).

Proteins involved in the cell cycle include cyclin proteins, cyclin-dependent kinases (CDKs), CDK inhibitors (CDKIs), master regulatory proteins Rb and p53 and the E2F transcription factor that are usually activated by extracellular signals (Deane, *et al.*, 2005). They function in guiding the cell through the different distinct and sequential replicative stages of the cell cycle (Deane, *et al.*, 2005, Reynolds, *et al.*, 1995).

##### *1.2.2.2.1. Cascade of Protein Phosphorylations*

This control mechanism involves a highly regulated protein kinase family known as cyclins, whose expression is restricted by transcriptional regulation of cyclin-encoding genes and by ubiquitin-mediated degradation. Cyclins are a family of proteins that are highly conserved in evolution and are so named because their expression levels are cyclic, that is each cyclin is synthesised at a unique and discrete point in the cell cycle and degraded at a second relatively discrete point, which is coincidental with the different stages of the cell cycle (Deane, *et al.*, 2005, Reynolds, *et al.*, 1995).

Activation of this kinase family requires association with a second subunit of catalytic proteins that is expressed constitutively at the appropriate period of the cell cycle and is known as the cyclin-dependent kinases (CDKs) resulting in the formation of an active complex with an unique substrate specificity (Collins, *et al.*, 1997, Deane, *et al.*, 2005, Stewart, *et al.*, 2003). Regulation by phosphorylation and dephosphorylation perfects the activity of the CDK-cyclin complexes, thus ensuring well-delineated transitions between cell cycle stages (Collins, *et al.*, 1997, Stewart, *et al.*, 2003). These activated complexes then trigger the activation of the downstream phases of the cell cycle (Deane, *et al.*, 2005).

The complexes cyclin D-CDK4, cyclin D-CDK6 and cyclin E-CDK2 regulates the progression of the cell from the $G_1$ phase to the S phase (Figure 1-1). Activation of cyclin D-CDK4/6 results in the progression of the cell through the $G_1$ checkpoint after which it is degraded and cyclin E-CDK2 is activated resulting in the transition of the cell from the $G_1$ to S phase of the cell cycle (Deane, *et al.*, 2005, Reynolds, *et al.*, 1995, Stewart, *et al.*, 2003).

Rb is a crucial substrate of activated cyclin-CDK complexes in $G_1$ phase. It is sequentially phosphorylated by cyclin D-CDK4/6 and cyclin E-CDK2 during $G_1$ phase progression and either represses or activates transcription depending on its phosphorylation state and associated proteins. Hypophosphorylated Rb and Rb-related “pocket” proteins such as p107 and p130 binds to and inactivates members of the E2F family of transcription factors and arrests cells in the $G_1$ phase (Deane, *et al.*, 1995, Stewart, *et al.*, 2003). E2F family members mediate transcription of genes required for DNA synthesis. (Stewart, *et al.*, 2003). During $G_1$ phase progression, CDK-mediated hyperphosphorylation of Rb and its cousins results in the dissociation of Rb and E2F, which enters into the nucleus where it acts as a transcription factor functioning in the expression of genes whose products are required for and results in

the entry of the cell into the S phase (Deane, *et al.*, 2005, Reynolds, *et al.*, 1995, Stewart, *et al.*, 2003).

The rest of the phases of the cell cycle consists of a sequential activation of proteins such as the cyclin/CDK complexes that are exquisitely sensitive to cellular integrity and is essentially protected from extracellular influences (Deane, *et al.*, 2005, Reynolds, *et al.*, 1995). Thus, the late phases of the cell cycle have been described as a cell autonomous process (Deane, *et al.*, 2005). In the S phase, cyclin D-CDK4/6 and cyclin-E-CDK2 is degraded prior to DNA synthesis and replication and cyclin A-CDK2 forms resulting in the progression of the cell through the S phase and in the initiation of DNA and histone biosynthesis (Deane, *et al.*, 2005, Reynolds, *et al.*, 1995). Once successful DNA replication has occurred, cyclin A-CDK2 levels are decreased and the cell enters into the $G_2$ phase where the cyclin B-CDK1 complex, also known as the mitosis promoting factor accumulates and functions in regulating the progression of the cell from $G_2$ to the M phase (Deane, *et al.*, 2005, Stewart, *et al.*, 2003). After mitosis, cyclin B is degraded rapidly to prevent a second round of division. (Deane, *et al.*, 2005).

During the $G_2$ phase, inactive cyclin B-CDK1 complexes accumulate through the phosphorylation of CDK1 by Wee1 and Myt1 resulting in its inhibition. In order for the cell to enter the M phase, the cyclin B-CDK1 complexes are activated by cell division cycle (Cdc) 25C phosphatase, which functions in the dephosphorylation of CDK1 while termination of the M phase occurs after ubiquitination and proteolytic degradation of cyclin B by the anaphase-promoting complex (APC), which results in the inactivation of CDK1 (Stewart, *et al.*, 2003). Cyclin B-CDK1 is a complex that is regulated at many levels especially through p53 activity,

which blocks M phase entry when DNA is damaged, causing the cell to undergo apoptosis (Deane, *et al.*, 2005).

*1.2.2.2.2.* *Cell Cycle Checkpoints*

The cell cycle is regulated by a checkpoint control that has a more supervisory role and does not form an essential part of the cycle progression machinery (Collins, *et al.*, 1997). These cell cycle checkpoints are control mechanisms developed by eukaryotic cells that function in sensing flaws during critical events such as DNA replication and chromosome segregation and in response to stress (Collins, *et al.*, 1997, Stewart, *et al.*, 2003). The checkpoint control consists of three elements; (i) stimuli such as under replicated or damaged DNA that activate the checkpoints, (ii) signal transduction machinery are relayed to (iii) the cell-cycle progression machinery, that is the different basal cell cycle regulators forming the targets (Samuel, *et al.*, 2002). These signals cause a delay in cycle progression, until the danger of mutation has been averted, thus resulting in the repair of cellular damage (Collins, *et al.*, 1997, Stewart, *et al.*, 2003). Thus, a DNA damage checkpoint can be regarded as a coherent signal transduction system that allows for the transfer of information from a DNA lesion to the cell cycle (Samuel, *et al.*, 2002). However, if the damage is irreparable, the checkpoint signalling can activate pathways that result in apoptosis (Stewart, *et al.*, 2003). Thus, it should be noted that a loss of checkpoint integrity allows for the accumulation of DNA lesions that results in permanent genomic alteration (Stewart, *et al.*, 2003).

CDKs are negatively regulated by a group of functionally related proteins called CDKIs, which can be divided into two families: (i) the inhibitor of CDKs (INK) 4 family, which consists of four members including the $p16^{INK4a}$, $p15^{INK4b}$, $p18^{INK4c}$ and $p19^{INK4d}$ and (ii) the cyclin-dependent kinase inhibitor protein (CIP/KIP) family, which consists of three members

including the $p21^{Waf1/Cip1}$, $p27^{Kip1}$ and $p57^{Kip2}$ (Deane, *et al.*, 2005, Stewart, *et al.*, 2003). The INK4 family of inhibitors inhibit CDK4 and CDK6 during the $G_1$ phase of the cell cycle while the CIP/KIP family of inhibitors inhibit CDK activity during all phases of the cell cycle (Deane, *et al.*, 2005, Stewart, *et al.*, 2003). The presence of CDKI in the cell is regulated at several levels including imprinting programs for $p57^{Kip2}$, transcriptional activation through Rb for $p16^{INK4a}$ or p53 for $p21^{Waf1}$, TGFβ signalling for $p15^{INK4b}$, $p21^{Waf1}$ and $p27^{Kip1}$ and posttranslational mechanisms such as ubiquitin-mediated proteolysis for $p27^{Kip1}$ (Deane, *et al.*, 2005). Interaction of CDKIs with cyclin/CDK complexes is stochastic and dose dependent having implications in both cell cycle activation and apoptosis, thus the cellular processes that trigger the production and degradation of the cyclins or CDKIs regulate cell proliferation (Deane, *et al.*, 2005).

Different types of checkpoints exist throughout the cell cycle monitoring different aspects of DNA replication and chromosome segregation and regulation of different phases of the cell cycle. These include the: (i) $G_1$ checkpoint that controls entry into S phases and protects against DNA damage, (ii) the $G_2$ checkpoint that monitors the completion of DNA replication, chromosomal damage and entry into the M phase and (iii) the M checkpoint, which arrests mitosis if chromosomes are not properly aligned along the mitotic spindle (Figure 1-1) (Reynolds, *et al.*, 1995).

1.2.2.2.2.1. <u>The $G_1$ and $G_2$ Checkpoints</u>

The $G_1$ checkpoint and the $G_2$ checkpoint are sensory states that are controlled by the Rb and p53 respectively (Deane, *et al.*, 2005). These checkpoints function in surveying the cell for deviations from the normal proliferation program. These deviations include imbalances of cellular proteins and/or the coincident activation of conflicting signalling cascades (Deane, *et*

*al.*, 2005, Reynolds, *et al.*, 1995). However, when these deviations do occur Rb and p53 mediate the cessation of proliferation and the induction of apoptosis or it slows down the progression of the cell through the cell cycle allowing the damaged DNA to be repaired and thus prevents the propagation of genetic mutations and aberrant, unregulated growth (Deane, *et al.*, 2005, Reynolds, *et al.*, 1995).

1.2.2.2.2.1.1. The $G_1$ Checkpoint

The $G_1$ checkpoint functions in the inhibition of cyclin-CDK complexes activated during the $G_1$ phase (Stewart, *et al.*, 2003). Exposure of normal cells to genotoxic agents results in the activation of p53, which in turn results in the transcription of $p21^{Waf1/Cip1}$. This protein binds to and inactivates cyclin D-CDK4/6 and cyclin E-CDK2 complexes resulting in Rb hypophosphorylation and cell cycle arrest during the $G_1$ phase (Stewart, *et al.*, 2003).

1.2.2.2.2.1.2. The $G_2$ Checkpoint

The $G_2$ checkpoint, which is also known as the $G_2$/M checkpoint functions in preventing the initiation of mitosis when the cell has been exposed to DNA damage during $G_2$ or when the cell has progressed into $G_2$ with unrepaired damage acquired during the previous phases of the cell cycle (Kastan, *et al.*, 2004). Cell cycle arrest is initiated in the $G_2$ phase via checkpoint pathways that are triggered by genotoxic stress (Stewart, *et al.*, 2003). For example, DNA damage triggers the activation of two phosphatidylinositol-3-kinase (PI-3K)-related proteins ataxia telengiectasia mutated (ATM)- and ATM and Rad3-related (ATR)-dependent signalling, which induces $G_2$ cell cycle arrest via the inhibition of CDK1 (Samuel, *et al.*, 2002, Stewart, *et al.*, 2003). Cells that are exposed to ionising radiation result in the activation of the ATM pathway, which in turn activates human checkpoint kinase (Chk)2 while cells that are exposed to ultraviolet radiation results in the activation of the ATR

pathway, which in turn activates Chk1. Thereafter, both Chk1 and Chk2 trigger the phosphorylation of Cdc25C, which results in the consensus binding site for 14-3-3 protein. The binding of 14-3-3 proteins to Cdc25C results in the nuclear export and cytoplasmic sequestration of the phosphatase, with subsequent $G_2$ arrest through the inhibition of CDK1 (Stewart, *et al.*, 2003).

### 1.3. Apoptosis

Cell death can occur via apoptosis, necrosis, autophagic cell death or other forms of cell death that cannot be easily classified (Debatin, 2004, Hsu, *et al.*, 2004). Apoptosis or programmed cell death, which was originally defined in 1972, can be defined as a distinct physiological mode of cellular suicide that occurs under various physiological and pathological conditions (Debatin, 2004, Hsu, *et al.*, 2004, Scoltock, *et al.*, 2004). It is a tightly controlled process where cell death is executed through the activation of specific signalling pathways functioning as an important mechanism to regulate cell death signalling (Huang, *et al.*, 2004, Pulido, *et al.*, 2003). Apoptosis plays a pivotal role in embryogenesis, development, immune response, morphogenesis, pathophysiology and normal tissue homeostasis thus any disruption in this process can have severe consequences (Pulido, *et al.*, 2003, Scoltock, *et al.*, 2004). The discovery of apoptosis has stimulated contemporary concepts in the development of cancer and other diseases (Hsu, *et al.*, 2004). There are positive and negative regulatory pathways of apoptosis and a balance between these pathways determines cell fate (Pulido, *et al.*, 2003).

The morphological and biochemical features of apoptosis are distinct (Debatin, *et al.*, 2004, Huang, *et al.*, 2004) and include depolarisation of the plasma membrane, phosphotidylserine translocation, membrane blebbing, cell shrinking, alterations in intracellular ion concentrations, mitochondrial membrane depolarisation and disruption in mitochondrial

membrane integrity, nuclear condensation, chromatin aggregation, degradation of DNA and apoptotic body formation prior to cell lysis (Figure 1-2) (Debatin, *et al.*, 2004, Decaudin, *et al.*, 2002, Hsu, *et al.*, 2004, Pulido, *et al.*, 2003, Scoltock, *et al.*, 2004). Neighbouring cells and macrophages then rapidly digest cellular fragments or apoptotic bodies without inducing inflammation or damage (Pulido, *et al.*, 2003).

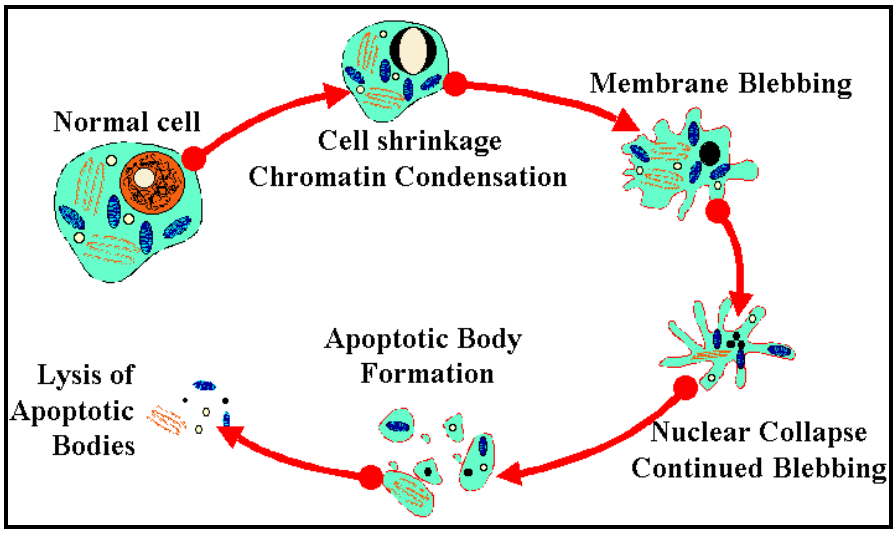



**Figure 1-2: Morphological Features of Apoptosis**

(Reference: URL: http://www-micro.msb.le.ac.uk/3035/kalmakoff/baculo/pics/Apoptosis.gif)

Apoptosis occurs in many organelles including the mitochondria, endoplasmic reticulum, Golgi apparatus and lysosomes (Pulido, *et al.*, 2003). However, most research has focused on the role of mitochondria in apoptosis, which is considered to be the regulatory centre of the apoptotic process and plays an important role in cellular homeostasis (Pulido, *et al.*, 2003, Strohmeier, *et al.*, 2002).

The biochemical and molecular factors regulating apoptosis are complex and not completely defined. However, some regulatory mechanisms that have been identified include death receptors, cysteinyl aspartate-specific proteases (caspases), mitochondria, Bcl-2 family of proteins and tumour suppressor genes (Pulido, *et al.*, 2003).

### *1.3.1. Pathways of Apoptosis*

Diverse internal and external stimuli including damage of DNA or other critical molecules or subcellular structures propagate the cellular stress response that initiates apoptosis through complex signal transduction pathways that eventually lead to a central cascade of effectors that mediate the final stages of cell death (Debatin, *et al.*, 2004, Scoltock, *et al.*, 2004). Distinct pathways are activated depending on both the cell type and the initiating factor (Pulido, *et al.*, 2003). Two primary modes of apoptosis have been identified: (i) the extrinsic pathway or receptor pathway, which is mediated via Fas or TNF receptors at the plasma membrane and (ii) the intrinsic pathway or mitochondrial pathway, which is mediated by the disruption of cellular homeostasis and is initiated intracellularly at the mitochondria (Debatin, 2004, Huang, *et al.*, 2004, Pulido, *et al.*, 2003). However, even though these two pathways are divergent with respect to induction, they tend to converge at later stages and may be interconnected at different levels (Debatin, 2004, Pulido, *et al.*, 2003).

#### *1.3.1.1. Caspases*

Caspases are aspartate-specific cysteine proteases that function as cytoplasmic proenzymes that play an important role in the initiation and effector phases of apoptosis (Debatin, 2004, Pulido, *et al.*, 2003). These proteins are synthesised as inactive zymogens that are activated by proteolytic cleavage, that is cleavage takes place between the large subunit and the small subunit of caspases (Debatin, 2004). Once activated, they target important cellular proteins

that are important in both the extrinsic and intrinsic pathway of apoptosis (Pulido, *et al.*, 2003).

Depending on their substrate specificity, two types of caspases have been identified. These include the initiator caspases that function in the initiation and amplification of the death signal and thus functions as a direct link to death-inducing signalling complexes (DISCs) and the effector caspases that function in the degradation of vital cellular components that may be cytoplasmic or nuclear marking the morphological features of cell death (Debatin, 2004, Pulido, *et al.*, 2003). Examples of initiator caspases include caspase-8, caspase-9 and caspase-10 and examples of effector caspases include caspase-2, caspase-3, caspase-4, caspase-6 and caspase-7 (Pulido, *et al.*, 2003).

Furthermore caspases are capable of activating other caspases, thus resulting in the activation of the caspase cascade. For example, caspase-8 activates caspase-3, caspase-4, caspase-7 and caspase-9 while caspase-9 activates caspase-3 and caspase-7 (Pulido, *et al.*, 2003). Caspase-3 is the most potent effector caspase having many substrates that results in the amplification of the c-Jun amino-terminal kinase (JNK) pathway by cleaving MAPK/extracellular-signal related kinase (ERK) kinase (MEK) kinase (MEKK)1 (Pulido, *et al.*, 2003).

The activation of the caspase cascade resulting in apoptosis is regulated by a variety of proteins that act as cofactors such as apoptosis activating factor (Apaf)-1 and inhibitors such as Fas-associated death domain (FADD)-like interleukin-1β converting enzyme inhibitory protein (FLIP) and inhibitors of apoptosis protein (IAP) (Pulido, *et al.*, 2003). Inappropriate caspase activity can have a potentially detrimental effect on cell survival, thus the activation of caspases has to be tightly controlled (Debatin, 2004).

*1.3.1.2. Extrinsic or Death Receptor Pathway of Apoptosis*

The extrinsic pathway of apoptosis is activated when external signals or ligands interact with a death receptor on the plasma membrane resulting in the initiation of a cascade of events that leads to apoptosis (Figure 1-3) (Pulido, *et al.*, 2003). The death receptor family includes TNF receptors (TNFR) such as cell determinant (CD)95 (apoptosis-mediating surface antigen Fas (APO)-1/Fas), Fas, TNF-related apoptosis inducing ligand (TRAIL) receptor death receptors and decoy receptors (Debatin, 2004, Huang, *et al.*, 2004) and consists of an extracellular cysteine-rich ligand binding domain and an intracellular death domain (Pulido, *et al.*, 2003). Once a ligand binds to the death receptor, this receptor interacts with death adaptor proteins such as FADD, receptor-integrating protein (RIP), dishevelled anadaxin domain (DAX) and TNFR-I-associated death domain (TRADD) which in turn activates caspases and signalling pathways such as MAPK and NF-κB (Pulido, *et al.*, 2003). Thereafter, the death domain adaptor proteins remain attached to the activated death receptors and with other signalling molecules form the DISC, which recruits and activates initiator caspases such as caspase-8 and caspase-10 via their death effector domain, which then activate other downstream initiator caspases such as caspase-4 and caspase-9 and effector caspases such as caspase-3, caspase-6, caspase-7, which degrade a variety if cellular components resulting in apoptosis (Debatin, 2004, Pulido, *et al.*, 2003, Scoltock, *et al.*, 2004).

Caspase-8 may also result in the cleavage of Bcl-2-interacting domain death agonist (Bid), a Bcl-2 Homologue (BH)3 domain containing protein of the Bcl-2 family (Figure 1-3). This truncated form of Bid translocates to the mitochondrial membrane where it complexes with Bax and lipids resulting in the release of cytochrome *c* and downstream activation of caspase-9 and thus apoptosis. Thus, Bid results in the initiation of the mitochondrial amplification

loop (Debatin, 2004, Hsu, *et al.*, 2004, Scoltock, *et al.*, 2004). The activation of caspase-6 may feed back into the extrinsic pathway by cleaving caspase-8 (Debatin, 2004).

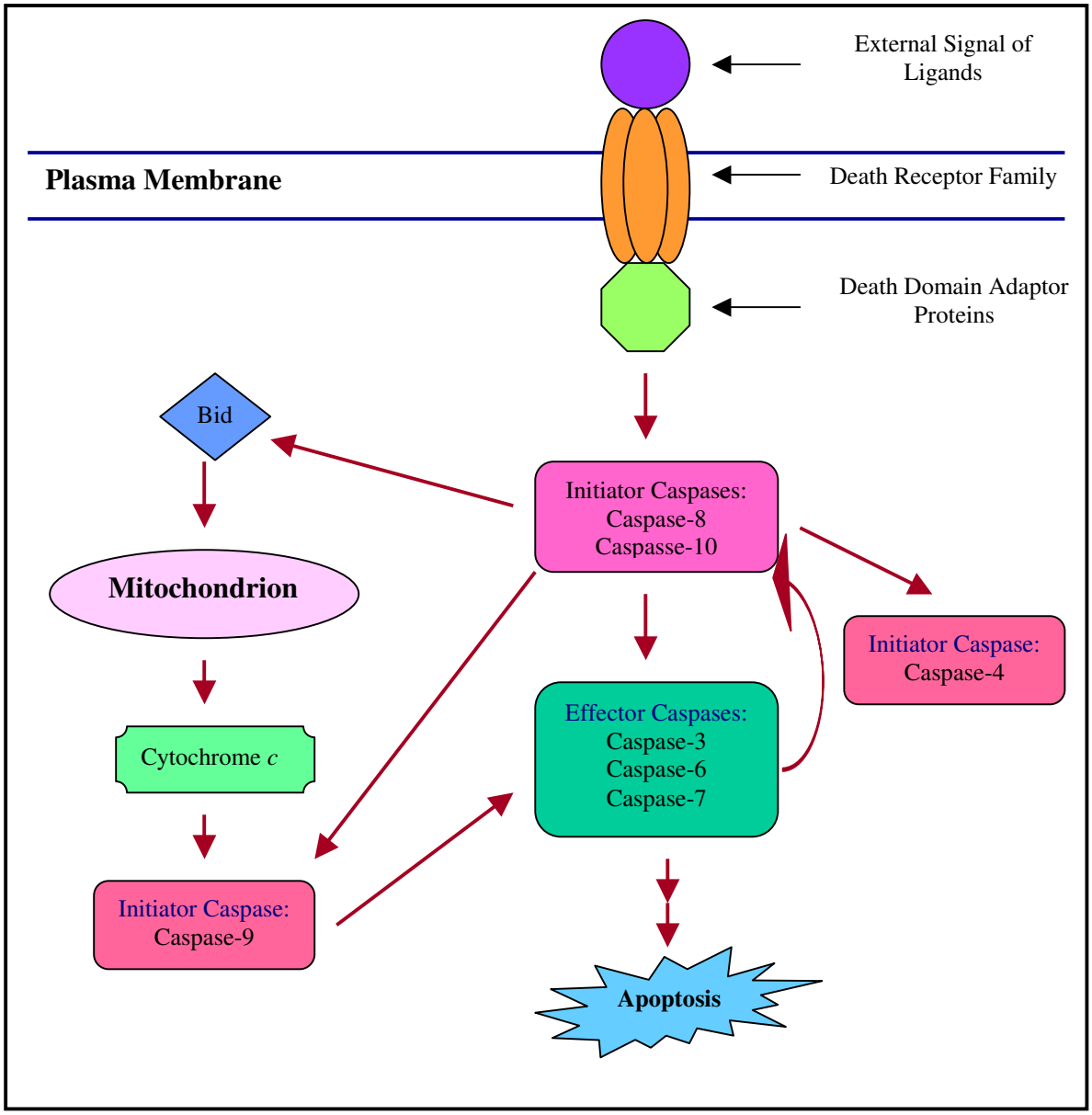



**Figure 1-3: Extrinsic or Death Receptor Pathway of Apoptosis**

#### *1.3.1.2.1. The Influence of Mitogen-Activated Protein Kinase Pathways in Extrinsic Apoptosis Pathway*

The mitogen-activated protein kinase (MAPK) superfamily is made up of three serine/threonine kinase cascades including: (i) the extracellular-signal-related kinases (ERKs) pathway, which respond to growth factors or other external mitogenic signals and functions in the induction of cell proliferation, cell differentiation, cell survival and the inhibition of death signals (Torii, *et al.*, 2004), (ii) the p38 MAPK pathway and (iii) the JNK pathway, both of which are stress-activated kinases that function in the induction of inflammation or in some cases apoptosis (Olson, *et al.*, 2004). Hence, the activation of the p38 MAPK pathway has pro-apoptotic effects while the activation of the ERK pathway has anti-apoptotic effects and cell survival, thus functioning as opposing faces of each other (Pulido, *et al.*, 2003, Sutter, *et al.*, 2004).

Activated death receptors also activate other signalling pathways that play a significant role in apoptosis. For example, the activation of TNFR results in the initiation of the JNK/MAP kinase pathway leading to the phosphorylation of pro-apoptotic and anti-apoptotic proteins and the regulation of gene expression and the activation of caspase-3 results in the activation of the JNK pathway through the cleavage of MEKK (Pulido, *et al.*, 2003). The JNK pathway is also thought to play a role in the inhibition of Bcl-2 and in the phosphorylation of an essential transcription factor *c-jun* (Pulido, *et al.*, 2003).

1.3.1.2.1.1. The Extracellular-Signal-Related Kinase Pathway

In quiescent cells, ERK is located in the cytoplasm in association with MAPK kinases (MAPKKs), MEK1 and MEK2, dual specificity kinases that phosphorylates ERK (Figure 1-4). Extracellular stimuli such as growth factors that bind to a receptor on the plasma membrane stimulates the activation of the Ras family of oncoproteins and protein kinase (PK)C, which stimulates the activation of riboflavin-aldehyde forming enzyme (Raf)1, which in turn stimulates the phosphorylation MEK1/2 and the downstream phosphorylation of ERK, which results in the dissociation of ERK from MEK1/2 (Fang, *et al.*, 2005, Sutter, *et al.*, 2004, Torii, *et al.*, 2004). PKC stimulates the binding of guanosine triphosphate (GTP) to members of the Ras family leading to Raf1 activation while members of the Ras family guanosine triphosphatases (GTPases) switch from the inactive guanosine diphosphate (GDP)-bound form to the active GTP-bound form, which interacts with and activates Raf1 (Fang, *et al.*, 2005). Several subtypes of the ERK family of protein exist including ERK-1, ERK-2, ERK-3, ERK-5 and ERK-6 (Fang, *et al.*, 2005). The released ERK activates cytoplasmic targets such as membrane proteins or is translocated to the nucleus via three mechanisms: (i) passive diffusion of a monomer, (ii) active transport of a dimer that is mediated by GTPase Ras-related protein (Ran) and the importin-β family and (iii) Ran/importin-β family independent transport that is mediated by direct interaction of ERK with the nuclear complex (Fang, *et al.*, 2005). When in the nucleus ERK phosphorylates and activates a variety of nuclear targets including transcription factors such as c-Fos and Elk-1 that function in the induction of cell proliferation, differentiation, cell survival and in the inhibition of apoptosis as well as protecting cell against apoptosis (Fang, *et al.*, 2005, Torii, *et al.*, 2004).

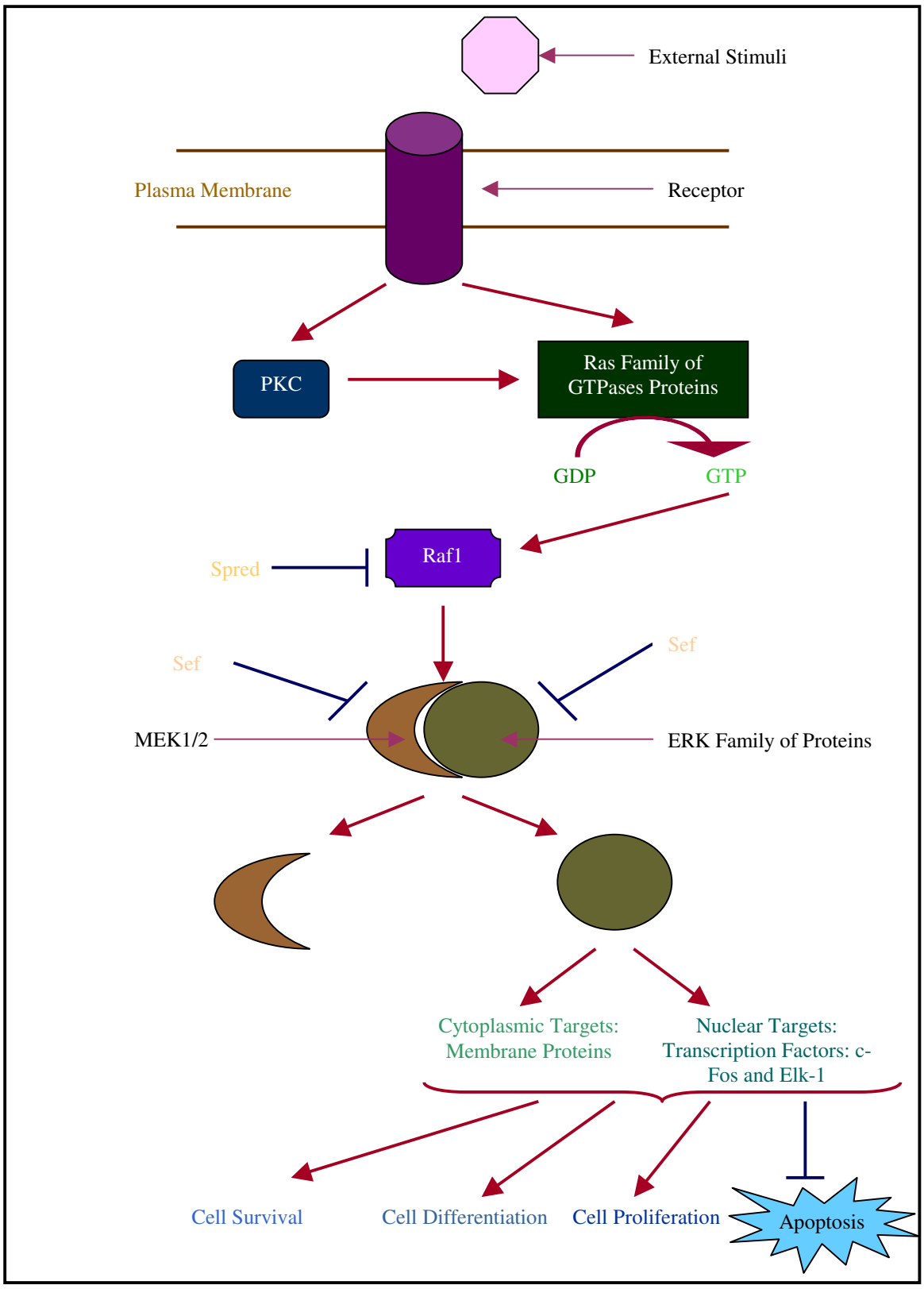



**Figure 1-4: The Extracellular Signal-Related Pathway**

The ERK signalling pathway is inhibited by Sprouty through various proteins and Sprouty-related protein with Enabled (Ena)/ vasodilator-stimulated phosphoprotein (VASP) homology (EVH)-1 domain (Spred) at the level of Raf by binding to Ras and Raf (Figure 1-4) (Torii, *et al.*, 2004). Sef is another protein that is a negative feed back inhibitor of the ERK signalling pathway. It is thought to act downstream or at MEK and inhibits phosphorylation of ERK or specifically blocks ERK nuclear translocation without inhibiting its activity in the cytoplasm (Figure 1-4) (Torii, *et al.*, 2004).

1.3.1.2.1.2. The p38 Mitogen-Activated Protein Kinase Pathway

The p38 MAPK pathway, which was first described in 1994, regulates a variety of cellular responses in response to stress, inflammation and other signals (Olson, *et al.*, 2004). There are four different isoforms of p38 MAPK, namely p38 MAPK-α, p38 MAPK-β, p38 MAPK-γ and p38 MAPK-δ. The p38 MAPK-α and p38 MAPK-β are expressed in most tissues while the p38 MAPK-γ and the p38 MAPK-δ have a limited tissue expression (Olson, *et al.*, 2004).

Stimuli including environmental stresses such as heat shock, inflammatory cytokines, TNF-α and interleukin-1 are delivered to p38 MAPK pathway via small GTPases of the rennin angiotensin system homology (Rho) family that includes Rac, Rho and Cdc42 (Figure 1-5). The Rho family induces the phosphorylation of MAPKK-3 and MAPKK-6. Apoptotic stimuli activate apoptosis signal-regulating kinase (ASK)-1, which directly activates MAPKK-3 and MAPKK-6. MAPKK-3 and MAPKK-6 then phosphorylates and activates the unphosphorylated and inactive p38 MAPK. This active p38 MAPK then phosphorylates and activates activating transcription factor (ATF)-2, CCAAT/Enhancer binding protein (C/EBP) homologous protein (CHOP)-1, myocyte enhancer factor (MEF)-2 and other transcription factors, cell cycle regulators p53 and p73 and immediate targets such as MNK-1, mitogen and

stress-activated kinase (MSK)-1/2, Elk-1, MAPK-activated protein (MAPKAP)-2, MAPKAP kinase (MAPKAPK)-3 and heterogeneous nuclear ribonuclear protein (hnRNP). These phosphorylated proteins than result in the activation of various cellular processes, including cell-cycle arrest, apoptosis, cytokine production, regulation of RNA splicing and cell differentiation. In addition, it indirectly induces the cyclic adenosine monophosphate responsive element binding protein (CREB) cycle via the activation of MSK-1 (Olson, *et al.*, 2004).

The active p38 MAPK is inactivated by phosphatases such as protein phosphatase 1, protein phosphatase 2A or MAPK phosphatase. These phosphatases are activated by the phospho-p38 MAPK, which suggest that there is a tight regulation of active p38 MAPK (Olson, *et al.*, 2004).

#### *1.3.1.3. Intrinsic or Mitochondrial Pathway of Apoptosis*

##### *1.3.1.3.1. <u>The Mitochondrial Permeability Transition Pore</u>*

The mitochondrial permeability transition pore (MPTP), which is also known as the mega channel or multiple conductance channel, is a large multiprotein complex formed at the contact site between the inner and the outer mitochondrial membranes (Casellas, *et al.*, 2002, Hans, *et al.*, 2005, Jordà, *et al.*, 2005). Although the exact structure of the MPTP is not known, it is thought to be composed of six proteins including: (i) the hexokinase located in the cytosol that converts glucose to glucose-6-phosphate, which is the initial phosphorylated intermediate in the glycolytic pathway and is an important precursor of many cellular building blocks, (ii) the voltage-dependent anion channel (VDAC), which is also known as the mitochondrial porin located in the outer membrane functions as the main pathway in metabolite diffusion across the outer mitochondrial membrane, (iii) creatine kinase located in

the intermembrane space facilitates the production and export of phosphocreatine into the cytosol after which it enters into the creatine/phosphocreatine circuit and thus provides an efficient buffering and transport system connecting energy production sites (mitochondria and glycolysis) with energy consumption sites (adenosine triphosphatases (ATPases)), (iv) the adenine nucleotide carrier (ANC), which is also known as the adenine nucleotide transporter (Veenman, *et al.*, 2004) located in the inner membrane functions as an antiporter for the exchange of adenosine triphosphate (ATP) and adenosine diphosphate (ADP) as part of oxidative phosphorylation, (v) cyclophilin D located in the mitochondrial matrix where it interacts with the ANC and (vi) the peripheral benzodiazepine receptor (PBR) (Figure 1-6) (Decaudin, *et al.*, 2002, Casellas, *et al.*, 2002).

MPTP also functions as the critical area for the metabolic coordination between the cytosol, the mitochondrial intermembrane space and the mitochondrial matrix as it helps regulate matrix calcium ion concentration, hydrogen ion concentration (pH), transmembrane electrochemical gradient that drives ATP synthesis, and mitochondrial volume by acting as a calcium-gated channel, voltage-gated channel, pH-gated channel and a redox-gated channel with several levels of conductance and little ion selectivity (Casellas, *et al.*, 2002).

Furthermore, the MPTP functions in the process of cell damage and death, that is, in the initiation and regulation of apoptosis in various cells including hepatocytes, fibroblasts, and thymocytes and is also thought to function in several oncogenic processes (Decaudin, *et al.*, 2002, Jordà, *et al.*, 2005). Therefore, it is considered the central executioner of cell fate (Casellas, *et al.*, 2002) and is believed to be the key regulator of stress-associated signals (Maaser, *et al.*, 2005). Exposure to factors such as growth factor removal, exposure to cytokines like TNF-α and high calcium concentrations coupled with low adenine nucleotide

concentrations, high phosphate concentrations, oxidative stress and the Bcl-2 family of proteins results in the opening of the MPTP, which leads to either necrosis if ATP production is severely impaired or to apoptosis when ATP production remains normal (Hans, *et al.*, 2005). Pharmacological inhibition of this pore prevents cell death (Decaudin, *et al.*, 2002).

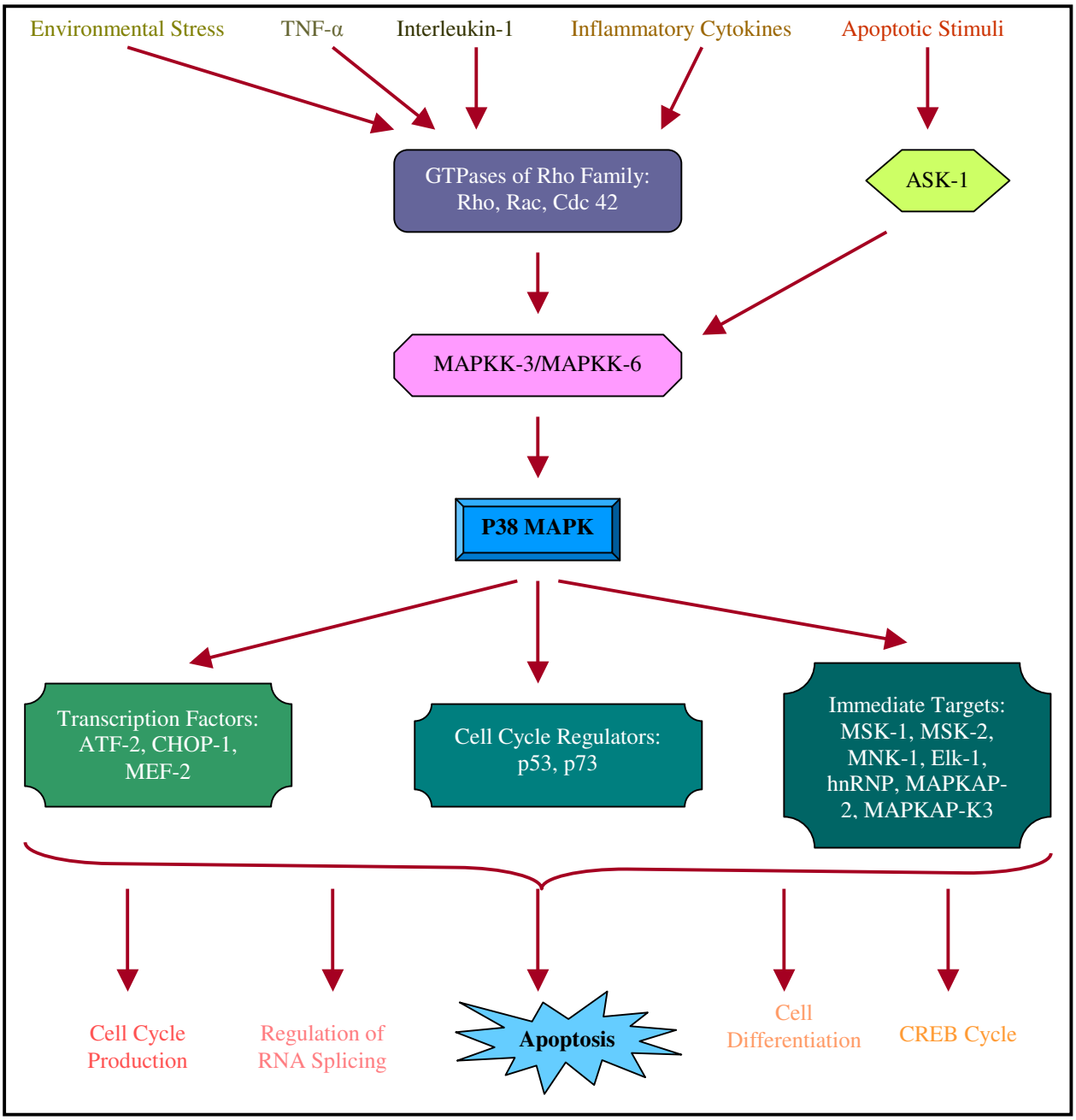



**Figure 1-5: The p38 Mitogen-Activated Protein Kinase Pathway**

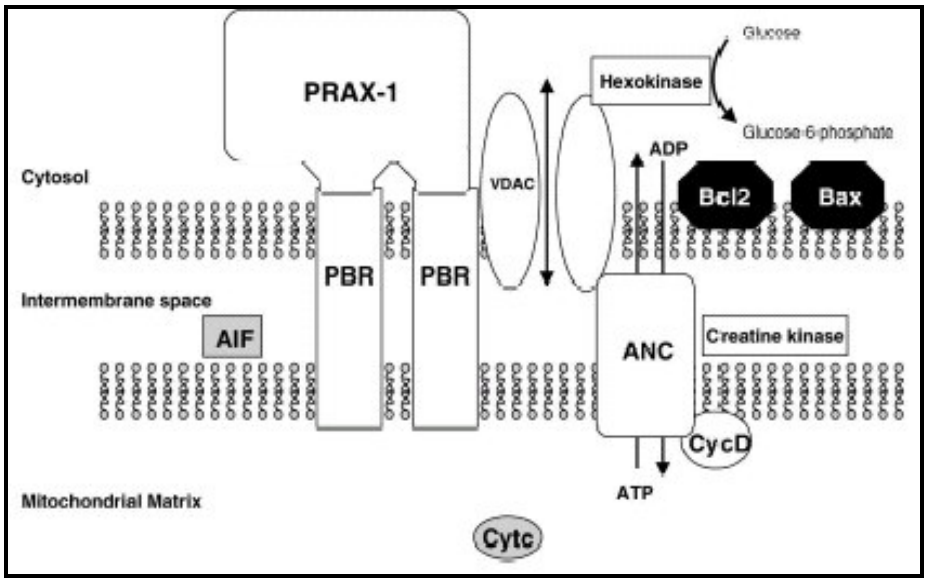



**Figure 1-6: Schematic Structure of the Mitochondrial Permeability Transition Pore**

(Reference: Casellas, *et al.*, 2002)

### *1.3.1.3.2. The Mitochondrial Permeability Transition Pore and the Intrinsic Pathway of Apoptosis*

The intrinsic pathway of apoptosis occurs through three general mechanisms including: (i) the caspase-dependent pathway, which involves the activation of caspases that coordinate downstream events often associated with apoptosis, (ii) the caspase-independent pathway and (iii) loss of mitochondrial functions that are essential for cell survival (Green, *et al.*, 2004). These events all occur as a result of mitochondrial membrane permeabilisation (Green, *et al.*, 2004).

#### 1.3.1.3.2.1. Caspase-Dependent Pathway of Apoptosis

The intrinsic pathway is initiated within the cell, most often through the disruption of cellular homeostasis resulting in the opening of the MPTP that is extensive and prolonged after which the mitochondrial membrane permeability suddenly increases and results in the loss of mitochondrial transmembrane potential ($\Delta\psi_m$) before, during or after mitochondrial

membrane permeabilisation, which in turn results in the uncoupling of the mitochondria and causes swelling, thus putatively serving as the initial event leading to apoptosis (Casellas, *et al.*, 2002, Green, *et al.*, 2004, Pulido, *et al.*, 2003, Hans, *et al.*, 2005, Maaser, *et al.*, 2005, Strohmeier, *et al.*, 2002). This instability of the mitochondrial membrane results in the release of intermembrane apoptogenic proteins, that is proteins located between the inner and the outer mitochondrial membrane such as apoptosis inducing factor (AIF), cytochrome *c*, procaspase-2 or procaspase-9, second mitochondrial activator of caspases (Smac)/direct IAP binding protein with low isoelectric point (pI) (Diablo), Omi/high temperature requirement protein (Htr) A2 and endonuclease G into the cytosol (Figure 1-7A) (Debatin, 2004, Green, *et al.*, 2004). Smac/Diablo and Omi/HtrA2 induce caspase activation by neutralising the inhibitory effects of IAPs and cytochrome *c* forms a complex with Apaf-1 and procapase-9 via its caspase recruitment domain (CARD) domain, which is known as the apoptosome resulting in the activation of a proteolytic cascade that cleaves procaspase-9 to active caspase-9, which in turn leads to the activation of caspase-3 from procaspase-3 (Debatin, 2004, Hans, *et al.*, 2005, Huang, *et al.*, 2004, Pulido, *et al.*, 2003).

Caspase-3, which is the executioner of the caspase cascade, then activates a variety of enzymes that are critical for inducing the structural changes of the nucleus, cytoskeleton and plasma membrane that is characteristic of apoptosis and the repair proteins (Huang, *et al.*, 2004, Hsu, *et al.*, 2004, Casellas, *et al.*, 2002). These include proteins such as Poly (ADP-Ribose) Polymerase (PARP), apoptotic chromatin condensation inducer in the nucleus (Acinus), fodrin, gelsolin, actin, plectrin, cytokeratin, inhibitor of caspase-activated deoxyribonuclease (ICAD), X-linked IAP (XIAP), signal transducer and activator of transcription (STAT)-1, topoisomerase-1, vimentin, lamin, Rb (Debatin, 2004, Hsu, *et al.*, 2004). ICAD is the inhibitor of endonuclease caspase-activated deoxyribonuclease (DNase)

(CAD) that functions in the cleavage of DNA into characteristic oligomeric fragments while Acinus functions in DNA condensation (Debatin, 2004). Proteolysis of cytoskeletal proteins such as gelsoloin, actin, plectrin, and cytokeratin results in loss of overall cell shape and lamin results in nuclear shrinking and budding (Debatin, 2004). It should be noted that PARP and lamin might also be activated by caspase-7 and caspase-6 (Hsu, *et al.*, 2004).

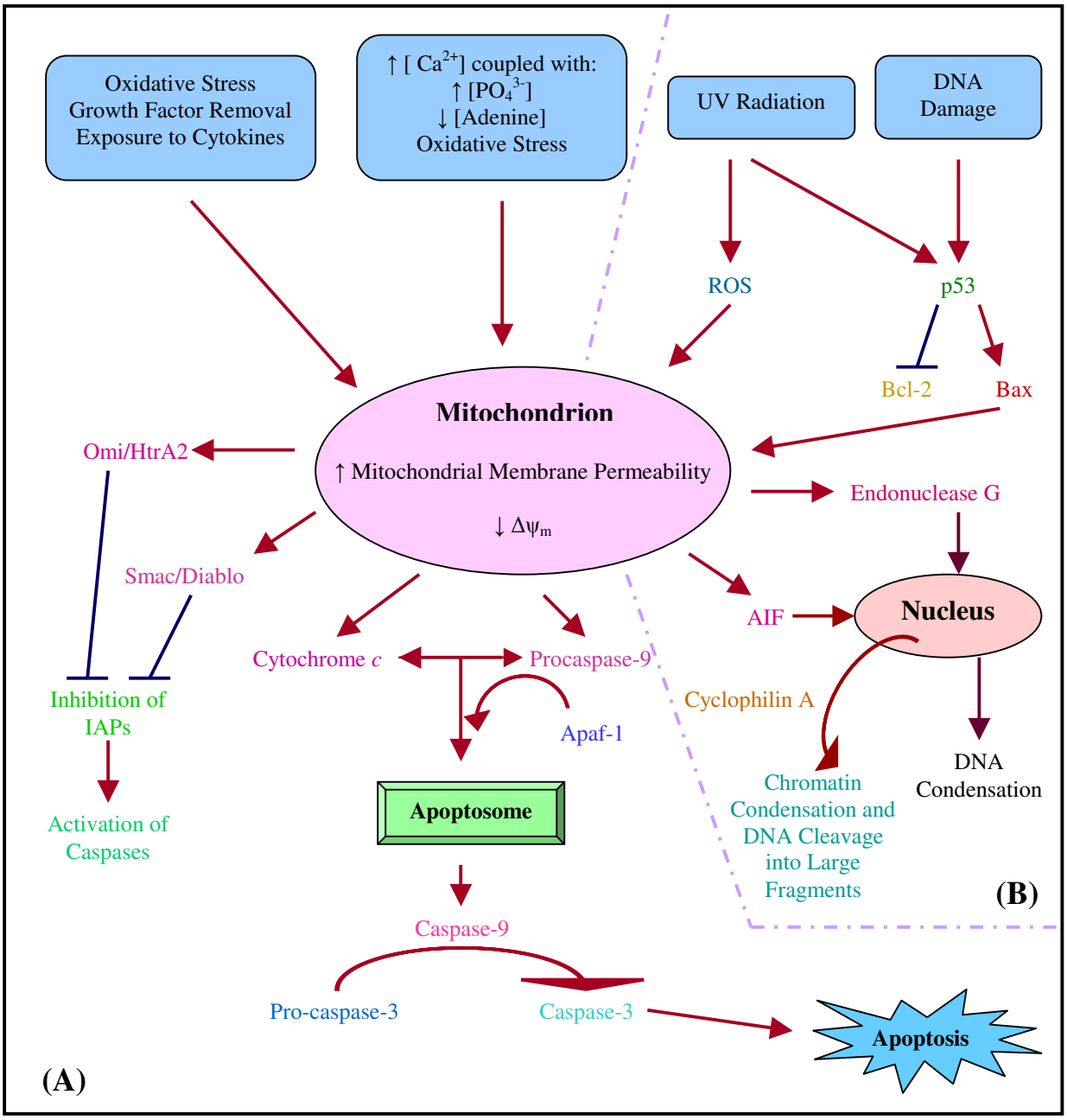



**Figure 1-7: Intrinsic or Mitochondrial Pathway of Apoptosis**

1.3.1.3.2.2. Caspase-Independent Pathway of Apoptosis

Mitochondrial-induced apoptosis may also involve a caspase-independent pathway (Huang, *et al.*, 2004). In this case, an apoptotic stimulus results in an increase in mitochondrial membrane permeability and thus decrease in $\Delta\psi_m$, which allows for the release of AIF in the presence of cyclophilin A and endonuclease G, which activates a DNase that causes DNA cleavage and thus ultimately leads to apoptosis (Figure 1-6B) (Green, *et al.*, 2002, Pulido, *et al.*, 2003).

The excessive generation of reactive oxygen species (ROS) in apoptosis as a result of stimuli such as UV radiation is an important factor in apoptosis because the mitochondria are the source and target of excessive ROS production (Pulido, *et al.*, 2003, Scoltock, *et al.*, 2004). Excessive ROS production results in an increase in mitochondrial membrane permeability and damage of the respiratory chain that results in further increased ROS production. Disruption in the mitochondrial membrane results in the release of cytochrome *c* from the mitochondria, which initiates events leading to apoptosis (Pulido, *et al.*, 2003). Further, it is thought that ROS production plays a role in TNFR and Fas receptor-mediated apoptosis although the mechanism by which this occurs is not known (Pulido, *et al.*, 2003).

Tumour suppressor genes are able to induce apoptosis. For example, p53, which functions in the regulation of gene expression, is activated in response to DNA damage and UV radiation (Pulido, *et al.*, 2003, Scoltock, *et al.*, 2004). p53 may induce apoptosis by suppression of Bcl-2 and the transactivation of several genes that contribute to apoptosis such as Bax and Fas. Also, p53 may function in a caspase-independent manner by activating Bax, which in turn results in the release of cytochrome *c*, which then activates caspase-9. Furthermore, p53 up

regulates the expression of genes involved in ROS production and metabolism (Pulido, *et al.*, 2003).

*1.3.1.3.3.* *Regulatory Mechanisms Involved in Intrinsic Pathway of Apoptosis*

The exact mechanisms regulating the opening of the MPTP and the release of apoptogenic factors are not completely understood but it may vary in different cell lineages and types of stress (Maaser, *et al.*, 2005).

1.3.1.3.3.1. The Bcl-2 Family of Proteins

A family of proto-oncogenes known as the Bcl-2 family regulates mitochondrial membrane permeability as it localises to the mitochondrial membrane and thus induces or suppresses apoptosis (Casellas, *et al.*, 2002, Debatin, 2004, Pulido, *et al.*, 2003, Maaser, *et al.*, 2005). The Bcl-2 family of proto-oncogenes can be divided into three types: the anti-apoptotic members such as Bcl-2, Bcl-$X_L$ and Mcl-I, the pro-apoptotic members such as Bax, Bak and Bcl-2-antagonist of cell death protein (Bad) and the BH3 domain-only molecules that link the extrinsic pathway to the intrinsic pathway such as Bid, Bcl-2-interacting mediator of cell death (Bim), a microtubule-associated protein, Puma and nicotinamide adenine dinucleotide hydrogenase (NADH) oxidase (Noxa), which are p53-induced proteins (Debatin, 2004, Huang, *et al.*, 2004, Pulido, *et al.*, 2003). Thus, a balance between the anti-apoptotic members and the pro-apoptotic members determines cell fate (Pulido, *et al.*, 2003).

When activated by BH3 domain-only proteins, Bax and its family members with multidomains, which resides in the cytosol translocates and is inserted into the outer mitochondrial membrane where it interacts with ANC and oligomerises to form a pore-like structure that results in the release of cytochrome *c*. Bax and its family members also induce an increase in mitochondrial membrane permeability and $\Delta\psi_m$ that promotes the release of

cytochrome *c*, which in turn results in apoptosis (Figure 1-8) (Casellas, *et al.*, 2002, Debatin, 2004, Pulido, *et al.*, 2003).

Bcl-2 and its related proteins when activated however, inhibits the ability of Bax to increase $\Delta\psi_m$ and thus prevents the release of cytochrome *c* and thus inhibits apoptosis induction (Decaudin, *et al.*, 2002, Casellas, *et al.*, 2002, Pulido, *et al.*, 2003). Bcl-2 and Bcl-$X_L$ exert this anti-apoptotic function in part by sequestering of BH3 domain-only proteins in stable mitochondrial complexes, which prevents the activation and translocation of Bax or Bak to the mitochondria (Debatin, 2004). Bcl-2 and Bcl-$X_L$ inhibit apoptosis by preventing cytochrome *c* release through a direct effect on the MPTP by inhibiting its opening or through VDAC (Casellas, *et al.*, 2002, Debatin, 2004). The Bcl-2 proteins are located in the outer mitochondrial membrane in close proximity to the MPTP, and acts to stabilise the integrity of the mitochondrial membrane (Figure 1-8) (Casellas, *et al.*, 2002).

## 1.4. The Peripheral Benzodiazepine Receptor

### *1.4.1. Introduction*

The peripheral benzodiazepine receptor (PBR) was initially described as a binding site for benzodiazepines such as diazepam outside the nervous system but was later found to be expressed in most mammalian tissues including the central nervous system (CNS) (Hans, *et al.*, 2005, Strohmeier, *et al.*, 2002, Sutter, *et al.*, 2004, Veenman, *et al.*, 2004). It was so named because Braestrup and Squires first described it in 1977 as a high affinity-binding site for diazepam in the rat kidney as well as other peripheral tissues (Bribes, *et al.*, 2004, Casellas, *et al.*, 2002, Lacapère, *et al.*, 2003). Alternative names proposed for the PBR include mitochondrial benzodiazepine receptor, mitochondrial DBI receptor, omega $(\omega)_3$ receptor and p-sites (Casellas, *et al.*, 2002, Miettinen, *et al.*, 1995). The PBR has been implicated in

numerous biological processes; however, to the date the precise function of the PBR remains an enigma (Bribes, *et al.*, 2004. Casellas, *et al.*, 2002).

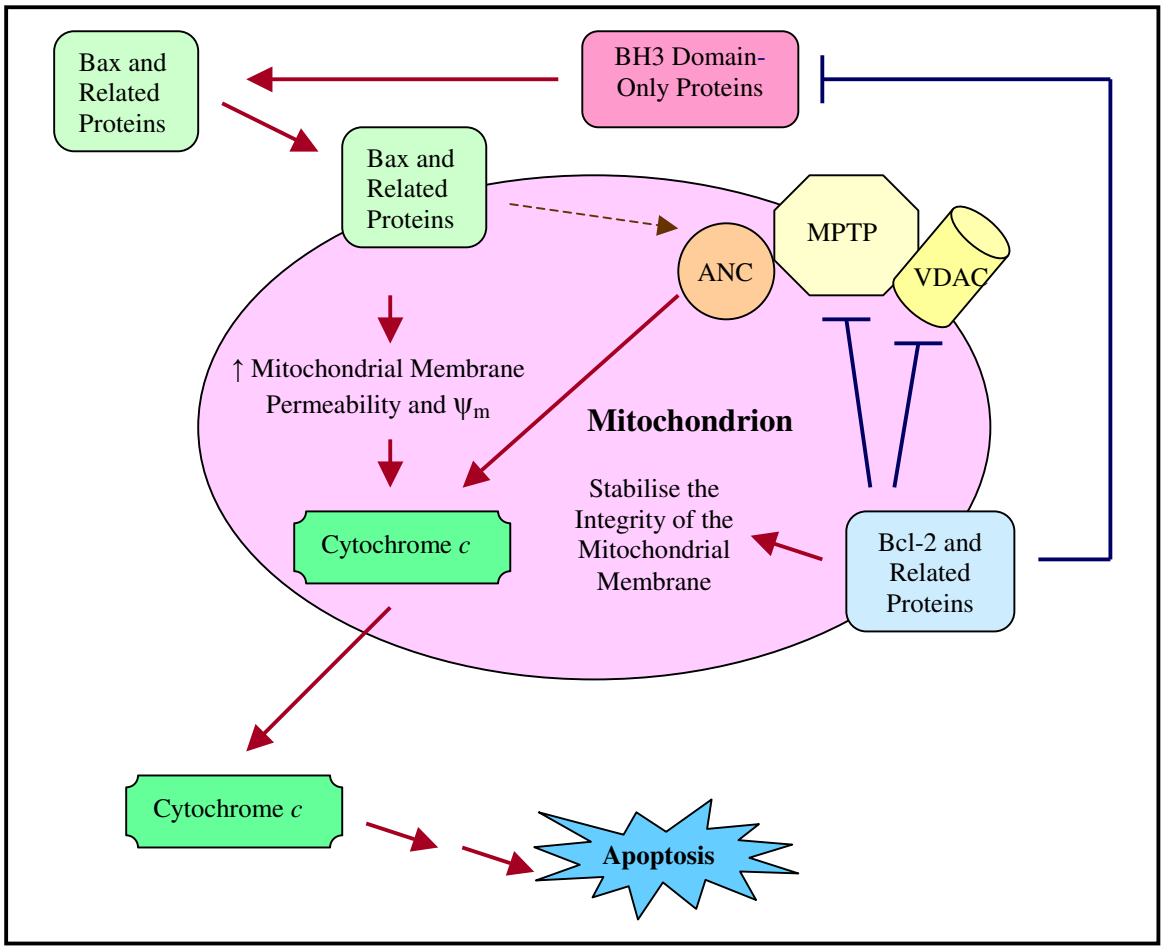



**Figure 1-8: Regulatory Mechanisms of the Bcl-2 Family of Proteins in the Control of Apoptosis**

PBR has been extensively characterised pharmacologically, biochemically, structurally and its cell and tissue expression patterns have also been determined (Bribes, *et al.*, 2004, Casellas, *et al.*, 2002). It is distinct from the central benzodiazepine receptor (CBR) as it lacks coupling to the γ-aminobutyric acid ($GABA_A$) supramolecular complex (Leducq, *et al.*, 2003, Vin, *et al.*, 2004). The CBR is expressed exclusively in the central nervous system (CNS) on the neuronal plasma membrane and interacts with binding sites on the $GABA_A$ supramolecular

complex (Casellas, *et al.*, 2002, Kletsas, *et al.*, 2004, Miettinen, *et al.*, 1995), in their anatomical distribution, pharmacological and biological functions, its structure and its relative affinities for specific ligands (Kassiou, *et al.*, 2004, Sutter, *et al.*, 2004). Diazepam binds with high affinity to both classes of receptors (Casellas, *et al.*, 2002). PBR and CBR can be distinguished from one another by their affinities for different signals where Ro5-4864 and PK11195, which exhibits no anxiolytic activity, binds with nanomolar affinity to PBR but with micromolar affinity to CBR while clonazepam, fumazenil and iomazenil binds with high affinity to the CBR but with extremely low affinity that is less than micromolar affinity to PBR (Casellas, *et al.*, 2002, Kassiou, *et al.*, 2004, Sutter, *et al.*, 2003).

### *1.4.2. Molecular Identity of the Peripheral Benzodiazepine Receptor*

The human *PBR* gene is located on the long arm of chromosome 22 in the region q13.3 and consists of 10 kb to 13 kb (Riond, *et al.*, 1991, Woods, *et al.*, 1996). The *PBR* gene consists of four exons disrupted by three introns, with the first exon and half of the fourth exon being untranslated to form the PBR protein (Figure 1-9). This gene consists of one transcription initiation site (Gavish, *et al.*, 1999, Woods, *et al.*, 1996). A study has reported that an alternatively spliced variant of the PBR mRNA is found in human tissue where a 211 bp internal deletion is observed, that is the exon 2 sequences has been spliced out resulting in an altered reading frame that is unable to translate to form a second type of PBR protein (Gavish, *et al.*, 1999, Woods, *et al.*, 1996). However, it should be noted that this alternative form is expressed at ten times the level to the PBR mRNA but the function of this alternative form is not known (Woods, *et al.*, 1996).

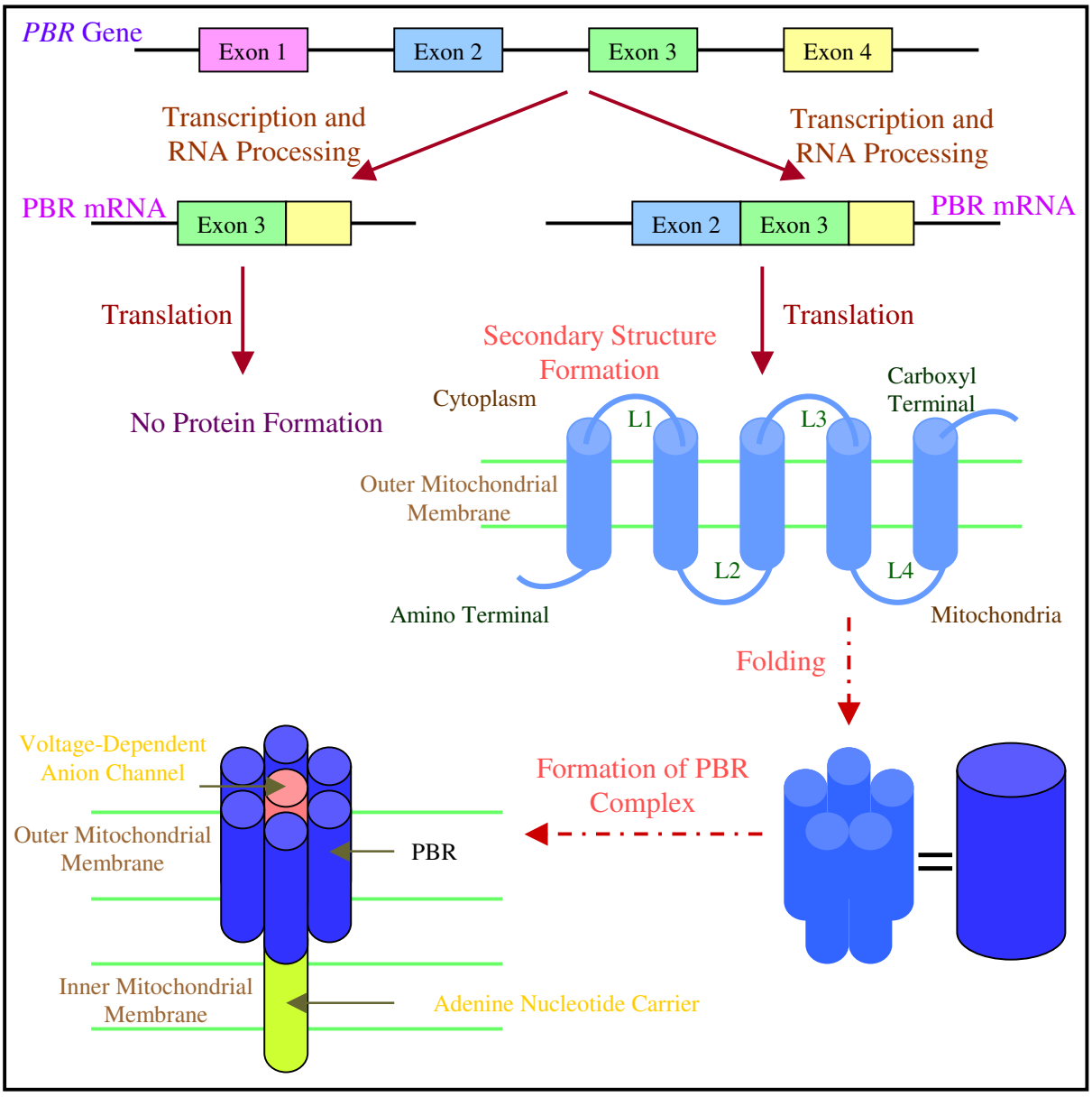



**Figure 1-9: Molecular Identity of the Peripheral Benzodiazepine Receptor**

The PBR is an 18 kDa intracellular ubiquitous isoquinoline and carboxamide binding protein consisting of 169 amino acids (Carmel, *et al.*, 1999, Casellas, *et al.*, 2002, Ferzaz, *et al.*, 2002, Jordà, *et al.*, 2005, Riond, *et al.*, 1991, Veenman, *et al.*, 2004). It is highly hydrophobic, rich in tryptophan and has a positive charge with a pI of 9.6 (Bribes, *et al.*, 2004, Casellas, *et al.*, 2002, Kletsas, *et al.*, 2004). Three-dimensional modelling and hydrophobicity analysis of PBR has revealed that PBR consists of a short intramitochondrial amino-terminal region, five putative amphipatic α-helices consisting of 21 amino acids and linked by hydrophilic loops

that are associated with the outer mitochondrial membrane or span the membrane lipid bilayer and an extramitochondrial carboxyl-terminal tail (Figure 1-9) (Casellas, *et al.*, 2002, Joseph-Liauzun, *et al.*, 1998, Lacapère, *et al.*, 2003, Riond, *et al.*, 1991, Vin, *et al.*, 2004). In its native form PBR exists at various higher molecular mass complexes ranging from 30 kDa to 200 kDa, which occurs as a result of the 18 kDa protein forming polymers both *in vitro* and *in vivo* in response to reactive oxygen species (Corsi, *et al.*, 2005, Corsi, *et al.*, 2004). In addition, these polymeric complexes exhibit a higher binding affinity for PBR ligands (Corsi, *et al.*, 2004).

### *1.4.3. Proteins Associated with the Peripheral Benzodiazepine Receptor*

PBR forms a trimeric protein complex with the 32 kDa voltage-dependent anion channel (VDAC) and 30 kDa adenine nucleotide carrier (ANC) in the outer mitochondrial membrane (Casellas, *et al.*, 2002, Kassiou, *et al.*, 2004, Weisinger, *et al.*, 2004), which together associates with creatine kinase and the Bcl-2 family of proteins (Veenman, *et al.*, 2004) and with other proteins results in the formation of the MPTP (Bribes, *et al.*, 2004, Maaser, *et al.*, 2005, Sutter, *et al.*, 2003). Thus, the PBR has been implicated in the regulation of the MPTP (Vin, *et al.*, 2005). Although, the exact way in which these proteins are arranged is not known, a study in mouse Leydig tumour cells (MA-10) mitochondria focused on the topographical analysis of the receptor distribution on the mitochondrial membrane has indicated that the trimeric receptor complex is formed by clusters of four to six PBR subunits associated with one VDAC molecule that forms the core of the complex that is located on the outer mitochondrial membrane and inner membrane contact site resulting in the formation of "single pores" (Figure 1-9) (Kassiou, *et al.*, 2004, Lacapère, *et al.*, 2003, Veenman, *et al.*, 2004). The role of ANC is not clear while VDAC functions in increasing the ability of PBR to bind to benzodiazepines (Lacapère, *et al.*, 2003). Furthermore, studies have shown that the

ratio of PBR to VDAC and ANC is tissue-specific and condition-specific (Veenman, *et al.*, 2004). The trimeric protein complex is also thought to associate with other proteins resulting in the formation of a 200 kDa complex (Kassiou, *et al.*, 2004). Thus, the molecular structure of the trimeric protein complex is dependent on the interaction of the different binding domains with other proteins (Kassiou, *et al.*, 2004).

Cytosolic proteins have been reported to be associated with the PBR. These are the 10 kDa protein that was co-immunoprecipitated with PBR localised in the mitochondrial fractions that has not been further identified and the PBR-associated protein-1 (PRAX-1), a 240 kDa protein that is located in the cytoplasm and on association with the carboxyl-terminus of the PBR exhibits several motifs implicated in protein-protein interactions such as the linking and dimerisation of the 10 kDa protein to PBR (Casellas, *et al.*, 2002, Kassiou, *et al.*, 2004). PRAX-1 interacts with PBR in a 1:2 PRAX-1:PBR stoichiometry (Casellas, *et al.*, 2002) and is expressed in the brain and thymus but is absent from steroidogenic tissues and liver (Lacapère, *et al.*, 2003). The role of PRAX-1 is undefined, although it is thought to be involved in the recruitment of additional targets to the vicinity of the PBR so as to modulate the function of PBR (Casellas, *et al.*, 2002). Another cytosolic protein that associates with PBR is the PBR-associated protein (PAPs). In particular PAP7 shows high affinity for PBR and has a tissue distribution close to that of PBR (Lacapère, *et al.*, 2003). Both PRAX-1 and PAP7 are proteins that contain glutamic acid stretches (Lacapère, *et al.*, 2003).

Other mitochondrial membrane proteins that have been identified to associate with the PBR proteins include a 170 kDa to 210 kDa protein that was eluted with PBR photolabeled with PK14105, a nitrophenyl derivative of an isoquinoline carboxamide which is an analogue of PK11195 (Bribes, *et al.*, 2004) when detergent solubilised, a 30 kDa to 35 kDa protein identified in liver and manganese-dependent dismutase (MnSOD) (Lacapère, *et al.*, 2003).

### *1.4.4. Evolutionary Conservation of the Peripheral Benzodiazepine Receptor*

The cDNA that encodes the PBR protein has been cloned from various species of mammals including rodents, cows and humans and shows a 71% identity and 80% sequence homology between species (Casellas, *et al.*, 2002, Lacapère, *et al.*, 2003, Woods, *et al.*, 1996). Furthermore, highly similar proteins have been identified in plants, yeast and bacteria, which suggests that it is a highly conserved protein and plays a fundamental role in the cell (Gavish, *et al.*, 1999, Lacapère, *et al.*, 2003). Riond, *et al.* reported that the first methionine in the open reading frame in the cDNA encoding the rat PBR is highly similar to the amino-terminal sequence of the Chinese hamster ovary (Riond, *et al.*, 1991). Studies have shown that the PBR promoter in both rat and humans does not contain a TATAA box but does contain multiple stimulatory protein (Sp) 1 boxes, which suggests further that PBR has a "housekeeping gene" function (Gavish, *et al.*, 1999).

PBR has also been identified in vegetable such as potato (*Solanum tuberosum*). It was found that an increase of PBR occurred in the nuclei of the cells during germination. In particular meristematic cells, which have a great proliferation ratio showed a high density of PBR in the perinuclear/nuclear region when compared to the parenchymal tissue where PBR expression was barely detectable (Corsi, *et al.*, 2005, Corsi, *et al.*, 2004).

The tryptophan-rich sensory protein (TspO), a 17 kDa protein that is very similar to the PBR, is located as a homodimer on the outer membrane in *Rhodobacter sphaeroides* 2.4.1. and is thought to consist of five membrane-spanning domains (Woods, *et al.*, 1996, Yeliseev, *et al.*, 2000). TspO functions in the negative regulation of transcriptional expression of highly specific photosynthesis genes belonging to the PspR-repressor regulon in response to oxygen or light and in the transport or efflux of tetrapyrrole intermediates of the heme/bacteriochlorophyll biosynthetic pathway (Yeliseev, *et al.*, 2000). In one study where the rat PBR was expressed in *Rhodobacter sphaeroides* TSPO1 cells; the rat PBR was functionally substituted for its bacterial homologue and negatively affected the transcription of specifically targeted photosynthesis genes in the presence of oxygen (Casellas, *et al.*, 2002, Yeliseev, *et al.*, 2000). Also, it was found that the rat PBR was located on the outer membrane of *Rhodobacter sphaeroides* as TspO and that it still binds benzodiazepines with the same affinity as when expressed on the outer mitochondrial membrane (Yeliseev, *et al.*, 2000).

PBR exhibits a 32% sequence homology with the CrtK protein of *Rhodobacter capsulatus*, a photosynthetic bacterium, which suggests that these proteins are homologues that descended from a common ancestor (Casellas, *et al.*, 2002). It is interesting to note that *Rhodobacter capsulatus* is a member of the subdivision of purple bacteria that are the likely sources of the endosymbiont that gave rise to the mitochondrion (Casellas, *et al.*, 2002). TspO, which is an analogue of CrtK in *Rhodobacter sphaeroides,* suggests that CrtK and its cognate signal transduction pathway may be a progenitor of mammalian PBR (Casellas, *et al.*, 2002).

Thus, the above-mentioned results and others suggest a close evolutionary and functional relationship between the bacterial and mammalian receptors. This suggests that this receptor plays a similar biological role in their respective cell types (Yeliseev, *et al.*, 2000).

### *1.4.5. Expression and Subcellular Localisation of the Peripheral Benzodiazepine Receptor*

Subcellularly, PBR is expressed mainly in the outer mitochondrial membrane in close association with the mitochondrial enzymes cytochrome oxidase, succinate dehydrogenase and monoamine oxidase and is concentrated near the inner mitochondrial membrane and outer mitochondrial membrane contact sites (Hans, *et al.*, 2005, Kletsas, *et al.*, 2004, Lacapère, *et al.*, 2003). However, it may be located on the inner mitochondrial membrane as is seen in rat lung mitochondria (Gavish, *et al.*, 1999). It is also expressed on the plasma membranes of some cells such as erythrocytes, which are devoid of mitochondria, non-mitochondrial fractions in hepatocytes, in the nucleus and perinuclear area, in the Golgi apparatus, lysosomes, peroxisomes and is associated with the cell membrane of the liver, specifically the non-parenchymal/biliary epithelial cells (Woods, *et al.*, 1996), heart, adrenal glands and testes (Bribes, *et al.*, 2004, Casellas, *et al.*, 2002, Gavish, *et al.*, 1999, Kassiou, *et al.*, 2004, Maaser, *et al.*, 2002, Sutter, *et al.*, 2004).

PBR is expressed with varying degrees of density in the majority of tissues tested especially steroid-producing tissues (Corsi, *et al.*, 2005, Kletsas, *et al.*, 2004, Weisinger, *et al.*, 2004). High expression of PBR have been seen in glandular and secretory tissues such as the pineal gland, adrenal glands, ependyma, pituitary gland and gonads, testis, ovary and uterus intermediate expression of PBR have been seen in renal and myocardial tissue and lung and low expression of PBR have been seen in liver, brain in areas such as the olfactory bulb and the cerebellum, with highest expression seen in the cerebellum, and spinal cord (Bribes, *et al.*,

2004, Casellas, *et al.*, 2002 Galiègue, *et al.*, 2004, Kassiou, *et al.*, 2004, Miettinen, *et al.*, 1995, Venturini, *et al.*, 1998).

Further, it has been found that the tissue distribution of the protein within a given organ was not homogenous. For example, in the adrenal glands, the medulla is virtually devoid of PBR while in the cortical density the expression of PBR is high (Bribes, *et al.*, 2004, Casellas, *et al.*, 2002). Another example is that of the kidney where it was found that there is a selective localisation of PBR in the distal convoluted tubule and the thick ascending limbs of the loop of Henle (Bribes, *et al.*, 2004, Casellas, *et al.*, 2002). This tissue distribution has also been noticed in the thymus (Bribes, *et al.*, 2004).

PBR is expressed in non-neuronal tissue or the ependyma, epithelial cells of choroid plexus olfactory epithelium and predominantly in glial cells and in some neuronal cell types such as neuroblastoma cells, cultured cortical neurons of the CNS and particularly the brain and in peripheral nervous system (PNS) (Ferzaz, *et al.*, 2002, Jordà, *et al.*, 2005, Kassiou, *et al.*, 2004, Miettinen, *et al.*, 1995, Veenman, *et al.*, 2004), all human peripheral blood leukocyte subsets, particularly in monocytes and polymorphonuclear cells such as neutrophils shows high expression, lymphocytes shows intermediate expression and platelets and erythrocytes show low expression (Casellas, *et al.*, 2002, Woods, *et al.*, 1996) and in the skin of healthy donors PBR is up regulated in the superficial differentiated layers of the epidermis (Bribes, *et al.*, 2004). Low expression of PBR is seen in the normal gut mucosa (Maaser, *et al.*, 2002). Also, the expression of PBR is seen at high levels in bronchopulmonary structures such as the submucosal glands, epithelium, ductal smooth muscles and type II alveolar cells (Bribes, *et al.*, 2003).

### *1.4.6. Ligands of the Peripheral Benzodiazepine Receptor*

Two types of ligands bind to PBR with high affinity. These are the endogenous ligands and synthetic ligands.

#### *1.4.6.1. Endogenous Ligands*

Endogenous ligands that bind to the PBR with high affinity include the diazepam binding inhibitor (DBI), its derived fragments, porphyrins such as protoporphyrin IX, a dicarboxylic porphyrin, mesoporphyrin IX, deuteroporphyrin IX and hemin that binds to PBR with nanomolar affinity and cholesterol (Bribes, *et al.*, 2004, Casellas, *et al.*, 2002, Hans, *et al.*, 2005, Venturini, *et al.*, 1998). These endogenous ligands are capable of competitively inhibiting PBR binding (Venturini, *et al.*, 1998).

DBI is an 11 kDa polypeptide consisting of 86 amino acids that binds to PBR with nanomolar affinity and is capable of displacing benzodiazepine binding (Casellas, *et al.*, 2002, Strohmeier, *et al.*, 2002, Venturini, *et al.*, 1998). It is highly expressed in steroidogenic cells, preferentially localised in the periphery of mitochondria and has the ability to bind to long chain acyl-coenzyme A (CoA)-esters (Lacapère, *et al.*, 2003, Miettinen, *et al.*, 1995). DBI is thought to function in the regulation of multiple biological processes such as stimulation of cell growth, stimulation of steroidogenesis where it functions in directly loading cholesterol to the inner mitochondrial membrane side chain cleavage cytochrome P-450 ($P\text{-}450_{scc}$) (Gavish, *et al.*, 1999) and inhibition of glucose-induced insulin secretion from the pancreas with expression been restricted to special cell types in a given organ such as seen in the brain where high concentrations have been detected in circumventricular organs and cerebellum but not in the normal cerebral cortex with particular expression seen in ependymal cells, glial cells and neurons (Miettinen, *et al.*, 1995). This protein is identical to the acyl-CoA binding

protein (ACBP) that has a broad range of distribution throughout tissues and species from animal to the plant kingdom and thus has been suggested to function as a housekeeping gene (Lacapère, *et al.*, 2003).

Porphyrins modulate enzymatic activity of several enzymes such as tryptophan pyrrolase, guanylate cyclase and gluthathione-*S*-transferase and several mitochondrial proteins (Gavish, *et al.*, 1999). Cholesterol, which binds to PBR to the carboxyl-terminal part of PBR (Lacapère, *et al.*, 2003, Yeliseev, *et al.*, 2000) with high affinity (Corsi, *et al.*, 2005) encompasses the lipid bilayer and maintains membrane fluidity (Akech, *et al.*, 2005).

*1.4.6.2. Synthetic Ligands*

Synthetic drug ligands that bind to PBR are diverse in chemical nature (Kletsas, *et al.*, 2004) that can be divided into three main families: (i) the benzodiazepines such as the 4' chloro derivative of diazepam Ro5-4864 [7-choloro-1,3-dihydro-1-methyl-5(4'-cholorphenyl)2H-1,4-benzodiazepine] (Figure 1-10A), (ii) isoquinoline carboxamides such as PK11195 [1-(2-chlorphenyl)-*N*-methyl-*N*-(1-methylpropyl)-3-isoquinoline carboxamide] (Figure 1-10B) and (iii) indoacetamide derivatives such as FGIN-1-27 [*N*, *N*-di-*n*-hexyl-2-(4-fluotophenyl)indole-3-acetamide] (Figure 1-10 C) (Hans, *et al.*, 2005, Veenman, *et al.*, 2004). Studies determining the role of the PBR have been inferred from the biological effects of these ligands (Hans, *et al.*, 2005).

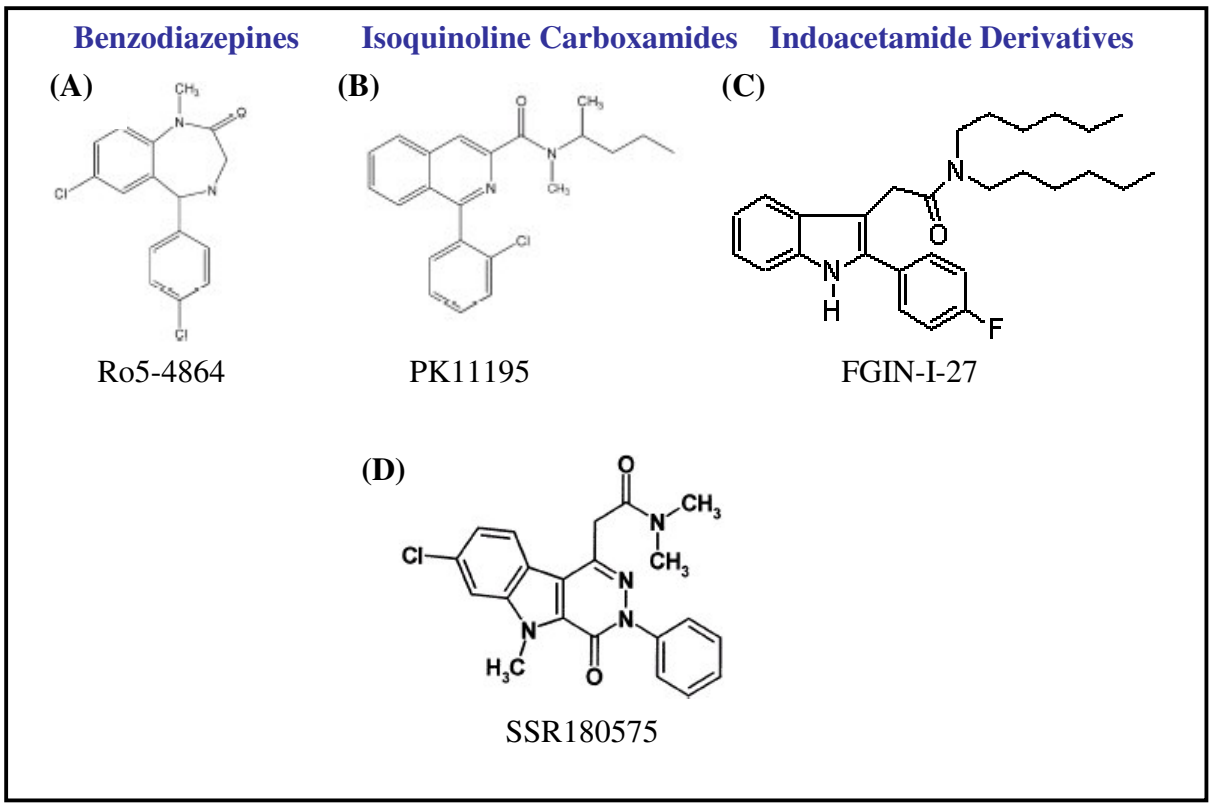



**Figure 1-10: Chemical Structures of Synthetic Ligands that bind to the Peripheral Benzodiazepine Receptor**

(Reference: Casellas, *et al.*, 2002, http://www.chemexper.com/chemicals/supplier/cas/142720-24-9.html, Ferzaz, *et al.*, 2002)

Ro5-4864 binds to PBR with nanomolar affinity in rodents but with a two-fold lower affinity in human and the interaction of Ro5-4864 with PBR is highly species dependent (Bribes, *et al.*, 2004, Carmel, *et al.*, 1999, Casellas, *et al.*, 2002). This variation in binding affinity may be due to amino acid differences that occur in the region near the carboxyl-terminal end of the PBR (Lacapère, *et al.*, 2003). PK11195 is the most widely used PBR ligand that binds to PBR with high (nanomolar) affinity from all species (Bribes, *et al.*, 2004, Casellas, *et al.*, 2002). PK11195 was classified as an antagonist while Ro5-4864 was classified as an agonist based on the entropy and enthalpy driven nature of ligand-receptor interactions (Casellas, *et al.*, 2002). This distinctive property displayed by both classes of ligands suggest that their binding domains either overlap or are allosterically coupled (Casellas, *et al.*, 2002). PK11195 interacts

directly with the PBR protein while Ro5-4864 and other benzodiazepines binds to a site that is made up of the PBR protein and VDAC (Gavish, *et al.*, 1999, Kassiou, *et al.*, 2004). However, it should be noted that under some physiological conditions both ligands induce similar effects (Casellas, *et al.*, 2002). Further, mutation studies have shown that conserved amino acid such as glutamic acid (Glu)$^{29}$, arginine (Arg)$^{32}$ and lysine (Lys)$^{39}$ as well as non-conserved amino acids Leu$^{31}$ and Arg$^{24}$ located in the first putative cytoplasmic loop are involved in the binding of benzodiazepines but not that of binding isoquinoline carboxamides (Yeliseev, *et al.*, 2000). However, the first cytoplasmic loop is involved in binding PK11195 (Lacapère, *et al.*, 2003).

FGIN-1-27 displays high affinity to PBR (Maaser, *et al.*, 2005). SSR180575 is a novel pyridazinoindole derivative that binds to PBR irreversibly with nanomolar affinity (Figure 1-10D) (Bribes, *et al.*, 2004, Vin, *et al.*, 2004).

The order of potency with which different ligands bind to PBR is as follows from the most potent to the least potent: PK11195 > Ro5-4864 > SSR180575 > diazepam > clonazepam (Vin, *et al.*, 2004).

### *1.4.7. Functions of the Peripheral Benzodiazepine Receptor*

The exact function of PBR remains controversial although it is thought to function in several physiological and pathological processes including the regulation of steroidogenesis and cholesterol transport, regulation of cellular proliferation (growth) and differentiation, immunomodulation (immune and phagocytic host defence response) by inducing moncoyte chemotaxis, inflammation, oxygen consumption, porphyrin transport and heme biosynthesis, anion transport, responses to stress and regulation of apoptosis (Casellas, *et al.*, 2002, Hans, *et*

*al.*, 2005, Kassiou, *et al.*, 2004, Maaser, *et al.*, 2005, Riond, *et al.*, 1991, Veenman, *et al.*, 2004). These different functions have been suggested to be tissue-specific (Weisinger, *et al.*, 2004). Furthermore, the PBR is involved in regulatory processes and metabolic functions pertaining to the tissue in which they are present such as calcium homeostasis and modulation of the VDAC and thus functions in the regulation of the opening of the MPTP (Kassiou, *et al.*, 2004, Leducq, *et al.*, 2003, Miettinen, *et al.*, 1995, Veenman, *et al.*, 2004).

PBR is also thought to function in the respiratory system. It is thought to be involved in bronchomotor tonus modulation and epithelial functions such as ionic transport modulation, ciliary and/or anti-inflammatory function via Clara cells (Bribes, *et al.*, 2003). Further, PBR is thought to play a role in the cardiac system, in the pathogenesis of hypertension and in renal and salt-water balance (Katz, *et al.*, 1989).

However, the best characterised function of PBR is in steroidogenesis where PBR is a functional component of the steroidogenic machinery functioning in the transport of cholesterol from the outer mitochondrial membrane to the inner mitochondrial membrane that forms the rate-limiting step (Casellas, *et al.*, 2002, Ferzaz, *et al.*, 2002, Joseph-Liauzun, *et al.*, 1998, Venturini, *et al.*, 1998) and functions in the conversion of cholesterol to pregnenolone, a precursor of all steroids, P-$450_{scc}$ enzyme that is located on the inner mitochondrial membrane (Ferzaz, *et al.*, 2002, Kassiou, *et al.*, 2004). The induction of steroidogenesis has been observed in adrenal glands, the placenta and the nervous tissues such as brain and endocrine tissues (Brown, *et al.*, 2000, Ferzaz, *et al.*, 2002).

PBR is thought to have a function in the regulation of oxidative process (mitochondrial respiration, oxidative phosphorylation) via two aspects (Bribes, *et al.*, 2004, Veenman, *et al.*, 2004). Firstly, it may function as an oxygen sensor by transducing an oxygen-triggered signal that leads to an adaptive cellular response, which is done through the regulation of mitochondrial swelling and the activity of the succinate-cytochrome *c* oxidoreductase (site II), which is a complex multi-subunit enzyme that functions as both a component of the electron transport chain and an essential enzyme of the tricarboxylic acid cycle (TCA) cycle (Ackrell, 2002, Casellas, *et al.*, 2002, Ferzaz, *et al.*, 2002). Secondly, it may mediate protective effects on the mitochondria against ROS (radical) damage where production of ROS leads to the inhibition of oxidative phosphorylation and increases the permeability of the mitochondrial membrane through the opening of the MPTP that ultimately leads to the uncoupling of the oxidative phosphorylation, psi (δ) collapse, mitochondrial swelling and the release of cytochrome *c*, which leads to the activation of caspases and thus cell death via necrosis and/or apoptosis (Casellas, *et al.*, 2002, Leducq, *et al.*, 2003). PBR is also thought to function mitochondrial electrophysiology (Joseph-Liauzun, *et al.*, 1998).

### 1.5. The Peripheral Benzodiazepine Receptor and Cell Proliferation

The role that PBR plays in cell proliferation was mainly investigated using PBR-specific high affinity drug ligands such as PK11195 and Ro5-4864. Results from these investigations have suggested that it may induce or suppress cell proliferation, which probably reflects the tissue-specificity of PBR function (Kletsas, *et al.*, 2004). However, studies have also shown that PBR-specific ligands may also affect cell proliferation independent of their ability to bind to PBR (Kletsas, *et al.*, 2004).

### *1.5.1. The Effect of the Peripheral Benzodiazepine Receptor in the Induction of Cell Proliferation*

PBR is thought to function in the induction of cell proliferation (Veenman, *et al.*, 2004). For example, it was found that PBR knockout Leydig cells grew much slower than their wild-type counterparts and in breast cancer cell lines, it was found that the level of PBR expression correlated inversely with the doubling time and positively with the ability of the tumours to grow *in vivo* in severe combined immunodeficiency (SCID) mice (Galiègue, *et al.*, 2004, Maaser, *et al.*, 2005). It is also thought to increase tumour proliferation in glial tumours (Veenman, *et al.*, 2004) and gene-silencing approaches have shown that PBR is required for epithelial breast cell proliferation (Kletsas, *et al.*, 2004).

PBR ligands in the presence of nerve growth factor caused an induction of c-fos, which regulates the synthesis and replenishment of phospholipids required for signal transduction pathways and thus subsequently regulates enzymes that are involved in the genesis of new membranes necessary for cell growth. Furthermore, high expression of PBR and ligand binding induces cell proliferation when induced by c-fos and phosphotidylcholine synthesis in different breast cancer epithelial cell lines (Akech, *et al.*, 2005).

Concentrations of PK11195 in the receptor binding range, that is nanomolar range, can stimulate DNA synthesis (mitosis) concomitant with increased cholesterol transport in the nuclear membrane (Akech, *et al.*, 2005, Venturini, *et al.*, 1998). High concentration of PBR ligands such as Ro5-4864 could inhibit cell proliferation by inhibiting DNA synthesis in different mammalian cell lines (Akech, *et al.*, 2005, Sänger, *et al.*, 2000). Thus, a biphasic effect on cell proliferation occurs depending on the concentration of the PBR ligands (Sänger, *et al.*, 2000). Nanomolar concentrations of PBR ligands stimulate proliferation in aggressive

breast cancer cells while it inhibits cell proliferation in mildly aggressive breast cancer cells, which is inversely correlated with nuclear cholesterol uptake (Brown, *et al.*, 2000).

PBR has been suggested to stimulate cell proliferation in glioma and breast cancer cell proliferation where the receptor has been linked to the growing aggressive potential of the tumour cells *in vitro* and *in vivo* (Corsi, *et al.*, 2005).

### *1.5.2. The Effect of the Peripheral Benzodiazepine Receptor in the Suppression of Cell Proliferation*

PBR ligands such as FGIN-1-27 and PK11195 have been shown to inhibit cell proliferation and thus reverse the growth-promoting properties of PBR in various tumours such as that of the skin, colon, oesophagus, breast and brain (Maaser, *et al.*, 2005, Maaser, *et al.*, 2004, Sutter, *et al.*, 2004, Veenman, *et al.*, 2004). The mechanisms by which this occurs is still been investigated but it has been shown that the anti-proliferative effects of PBR ligands are due to both induction of apoptosis and cell cycle arrest (Maaser, *et al.*, 2005, Sutter, *et al.*, 2004, Sutter, *et al.*, 2003, Veenman, *et al.*, 2004).

In gastrointestinal cancers and oesophageal cancer cells as well as haematopoietic and epithelial cells PBR ligands induce cell cycle arrest at the $G_1$/S checkpoint only, in breast cancer cells PBR ligands induce cell cycle arrest at both the $G_1$/S and $G_2$/M checkpoint while in lung and melanoma cells PBR ligands induce cell cycle arrest at the $G_2$/M checkpoint only (Maaser, *et al.*, 2005, Sutter, *et al.*, 2004, Sutter, *et al.*, 2003, Veenman, *et al.*, 2004).

The mechanisms by which PBR induces cell cycle arrest is not known, however, recently the signalling molecules that are involved in PBR ligand-induced $G_1$ arrest have been identified (Maaser, *et al.*, 2005, Maaser, *et al.*, 2004). These signalling molecules are mitochondrial alterations, cyclin D1 and $p21^{CIP1}$/$p27^{Kip1}$ and the activation of the p38 MAPK pathway, which results in the overexpression of the *growth arrest and DNA damage-inducible* (*gadd*) genes, specifically *gadd153* and *gadd45* (Maaser, *et al.*, 2004, Sutter, *et al.*, 2004, Sutter, *et al.*, 2003).

Sutter *et al.* also found that PBR ligands induced a MEK-dependent activation of ERK1/2 in oesophageal cancer cells and when PBR ligands were combined with MEK1/2 kinase inhibitors, they induced apoptosis and cell cycle arrest. This suggests that the induction of ERK1/2 compromises the anti-neoplastic effects of PBR ligands and thus serves a protective role (Sutter, *et al.*, 2004). Treatment with both PBR ligands and 3-hydroxy-3-methylglutaryl coenzyme A reductase (HMG-CoAR) inhibitors also showed the synergistic inhibition of cell proliferation in hepatocellular carcinoma cells by inducing apoptosis and cell cycle arrest (Sutter, *et al.*, 2005).

### 1.6. The Peripheral Benzodiazepine Receptor and Apoptosis

It is thought that the PBR has a role in the induction and suppression of apoptosis (Strohmeier, *et al.*, 2002).

### *1.6.1. The Effect of the Peripheral Benzodiazepine Receptor in the Induction of Apoptosis*

The direct apoptotic effects of PBR ligands were observed in colorectal, oesophageal and hepatocellular cancer cells (Maaser, *et al.*, 2005). The molecular mechanism(s) of PBR ligands-induced cell death is not well understood, however, most studies haves suggested that it functions in apoptosis induction (Hans, *et al.*, 2005). PBR ligands have been shown to induce apoptosis by the: (i) activation of caspase-3 and caspase-9, (ii) the cytosolic release of cytochrome *c*, (iii) and increase in ROS production, (iv) activation of the p38 MAPK pathway and (v) the opening of the MPTP (Hans, *et al.*, 2005, Maaser, *et al.*, 2004). Also, to date very little is known about other transcriptional responses than the ones mentioned in this section when cancer cells are treated with PBR-specific ligands (Sutter, *et al.*, 2003).

The role of PBR in the opening of the MPTP is thought to be the most important since the PBR is thought to be a component of the MPTP (Hans, *et al.*, 2005). It is thought that PBR ligands can activate the opening of the MPTP without further addition of calcium and thus functions in the regulation of the MPTP in producing apoptosis because of PBR's close association with the proteins of the MPTP (Casellas, *et al.*, 2002, Maaser, *et al.*, 2005). Furthermore, it is thought that Ro5-4864 and PK11195, that have been classified as a pharmacological agonist and antagonist respectively, maintain their identity in regulating the MPTP (Casellas, *et al.*, 2002). It has been shown that induction of apoptosis by FGIN-1-27 is dependent on the opening of the MPTP and the decrease of $\Delta\psi_m$ while PK11195 induced apoptosis without any alteration in $\Delta\psi_m$ in colorectal and oesophageal cancer cells (Maaser, *et al.*, 2005, Sutter, *et al.*, 2003). Thus, PK11195 is thought to function in the facilitation of the dissipation of the $\Delta\psi_m$, which results in the release of apoptogenic factors (Decaudin, *et al.*, 2002). To date, very little evidence is available that suggests that PBR ligands directly triggers the opening of the MPTP and it is thought that the loss of $\Delta\psi_m$ seen is due to a

downstream event occurring in many apoptotic processes where mitochondria acts as executioners (Hans, *et al.*, 2005).

Bcl-2 is an anti-apoptotic protein that is overexpressed in many cancers (Sutter, *et al.*, 2005). PBR ligands have been shown to overcome Bcl-2 mediated chemoresistance in lung cancer (Sutter, *et al.*, 2004). PK11195 eradicates the inhibition of Bcl-2 via a direct effect on mitochondria (Decaudin, *et al.*, 2002). Thus, it has been successfully applied for combination therapy with several cytotoxic drugs *in vitro* and *in vivo* (Sutter, *et al.*, 2004). Furthermore, PBR ligands induced apoptosis in conjunction with the down regulation of Bcl-2 expression and dephosphorylation of PKB and Bad in hepatic stellate cells (Sutter, *et al.*, 2003).

PBR ligands such as PK11195 when it interacts with the MPTP has been shown to have an indirect pro-apoptotic effect as seen when the susceptibility of cells to the induction of apoptosis was enhanced by a variety of different stimuli such as DNA damage, ligation of the glucocorticoid receptor and ceramide, a proapoptotic second messenger, and the reverse suppression of apoptosis by Bcl-2 (Decaudin, *et al.*, 2002, Casellas, *et al.*, 2002, Jordà, *et al.*, 2005, Strohmeier, *et al.*, 2002). Thus, it has been suggested that the collapse of the $\Delta\psi_m$ could modulate apoptotic process as any alterations in the mitochondrial structure plays a crucial role in the release of apoptotic factors from the mitochondria (Jordà, *et al.*, 2005).

Studies have been reported showing the indirect anti-neoplastic effect of PBR-specific ligands where the PBR ligands increased apoptosis induced by other cytostatic drugs (Maaser, *et al.*, 2005). In hepatocellular carcinoma PK11195 and FGIN-1-27 enhanced the chemosensitivity of tumour cells to paclitaxel, docetaxel, doxorubicin and the Bcl-2 inhibitor HA14-1 (Maaser, *et al.*, 2005). In thymocytes, PBR ligands such as PK11195 enhanced apoptosis as a result of

cells becoming more sensitive to actinomycin D, cycloheximide and the protein kinase inhibitor H7, which suggest a requirement for protein synthesis and phosphorylation (Strohmeier, *et al.*, 2002, Sutter, *et al.*, 2003). Furthermore, similar sensitising effects were observed by the use of tamoxifen, lonidamine, anti-CD95, etoposide, gemtuzumab ozogamicin, dexamethasone, daunomycin and γ-irradiation in different tumours cell lines (Decaudin, *et al.*, 2002, Maaser, *et al.*, 2005).

The induction of apoptosis by PK11195 is only observed at concentrations of a thousand fold higher than what is required for its binding to PBR (Decaudin, *et al.*, 2002). Micromolar concentrations of a series of pyrrolo-1, 5-benzoxazepines as well as PK11195 and Ro5-4864 resulted in the induction of apoptosis in leukaemic cells (HL60) (Strohmeier, *et al.*, 2002). Nanomolar concentrations of PK11195 enhanced the apoptotic effect of TNF-α while it inhibited the anti-apoptotic effect of Ro5-4864 (Strohmeier, *et al.*, 2002).

### *1.6.2. The Effect of the Peripheral Benzodiazepine Receptor in the Suppression of Apoptosis*

However, other studies have reported contrasting effects where the action of PBR ligands on cellular survival has reported pro-survival effects (Hans, *et al.*, 2005). For example, transfection and subsequent overexpression of PBR protected cells against UV-induced apoptosis and hydrogen peroxide-induced apoptosis exhibited a delayed $\Delta\psi_m$ drop (Ferzaz, *et al.*, 2002, Maaser, *et al.*, 2005, Strohmeier, *et al.*, 2002).

Ro5-4864 and PK11195 failed to induce apoptosis in cell lines of haematopoietic and epithelial origin (Strohmeier, *et al.*, 2002). Furthermore, nanomolar concentrations (concentration in the binding range) of Ro5-4864 resulted in anti-apoptotic activities in human pleural effusion histiocytic lymphoblastoid (U937) cells as well as in PBR-transfected leukaemic Jurkat cells where it protected the cells from undergoing TNF-α apoptosis (Casellas, *et al.*, 2002, Leducq, *et al.*, 2003, Strohmeier, *et al.*, 2002). This suggests the pharmacological modulation of the PBR may influence cell survival (Ferzaz, *et al.*, 2002).

### 1.7. The Peripheral Benzodiazepine Receptor and Cancer

An increase expression of PBR has been seen in a wide variety of malignant cells and tissues (Casellas, *et al.*, 2002, Hans, *et al.*, 2005, Veenman, *et al.*, 2004). Increase in PBR densities has been observed in ovarian carcinoma, breast cancers, hepatic carcinoma and colonic carcinomas (colorectal cancers), colon adenocarcinoma, oesophageal cancers, endometrial carcinomas, astrocytomas and gliomas when compared to their untransformed counterpart (Casellas, *et al.*, 2002, Sutter, *et al.*, 2004, Sutter, *et al.*, 2003). It is thought to function as the hallmark of cancerogenesis in some tissues such as gliomas (Hans, *et al.*, 2005).

Many studies have been devoted to the effects of PBR ligands on cell survival and especially on their toxicity towards tumour cell lines (Hans, *et al.*, 2005). From these studies it may be deduced that PBR may be involved in growth control because it is overexpressed in a variety of tumour models and specific PBR ligands inhibit cell proliferation (Maaser, *et al.*, 2004, Sutter, *et al.*, 2005). It may also be involved in cell proliferation of carcinogenic tissue that is controlled by the cell's apoptotic and mitogenic properties (Veenman, *et al.*, 2004). For example, in human breast cancer cell lines the expression of PBR and the mitochondrial density correlates with the high mitotic activity of the cells (Corsi, *et al.*, 2005) while in C6

glioma cells PBR ligands such as benzodiazepines affect proliferation rate in a dose-dependent manner, which suggests the role of PBRs in the mitotic process (Corsi, *et al.*, 2004).

Further, it has been found that PBR expression correlates with tumour malignancy grade and patient survival. The nature by which this up regulation occurs is not known (Hardwick, *et al.*, 2002). A study conducted showed that normal breast tissue and mildly aggressive breast cancer cells express very low levels of PBR mRNA levels, ligand binding sites and protein that are located in the mitochondria while highly aggressive human breast cancer cells, rapidly proliferating breast cancer cells and metastatic human breast tumours have high PBR mRNA levels, PBR ligand binding sites and protein located mainly in the nucleus (Akech, *et al.*, 2005, Bribes, *et al.*, 2004, Brown, *et al.*, 2000, Casellas, *et al.*, 2002, Hardwick, *et al.*, 2002, Sänger, *et al.*, 2000). Also, in brain tumours such as human astrocytomas, the expression of PBR correlates positively with tumour malignancy and proliferation rate and inversely with patient survival (Corsi, *et al.*, 2005, Galiègue, *et al.*, 2004, Guo, *et al.*, 2001).

An increased binding of ligands has been seen in different brain tumours. For example, studies in rat C6 glioma PBR densities increased by up to 30-fold when compared to its surrounding neocortex while in human post-mortem tissue, high levels of PBR ligand binding was observed in intact glioma cells and not in necrotic areas of the tumour and the surrounding normal tissue (Veenman, *et al.*, 2004). Further studies have suggested that the binding of PK11195 to human gliomas may be used to differentiate between high-grade and low-grade gliomas (Veenman, *et al.*, 2004). In rat C6 glioma cells and human T98G glioma cells, PK11195 and Ro5-4864 induced morphological changes of the tumour cells and

treatment with nanomolar concentrations of PK11195 resulted in an increase in growth rate and thymidine incorporation by up to 20 to 30% (Veenman, *et al.*, 2004).

Nuclear and perinuclear localisation of PBR has been found in glioblastoma biopsies, highly aggressive breast cancer cell lines and metastatic human breast tumour biopsies (Casellas, *et al.*, 2002, Galiègue, *et al.*, 2004, Hardwick, *et al.*, 2002). This nuclear localisation seen in breast cancers and gliomas suggests a role of PBR in the development and progression of the disease, as it would regulate cell proliferation by facilitating cholesterol transport into the nucleus (Galiègue, *et al.*, 2004). Thus, it has been hypothesised that the presence of PBR may be a determinant factor for the aggressive phenotype of the tumour and the expression of PBR may be monitored in tumour samples for diagnostic and/or prognostic purposes in the clinic (Galiègue, *et al.*, 2004).

A study demonstrated the prognostic relevance of PBR in colorectal cancer. In this study conducted by Maaser, *et al.*, it was shown that the over-expression of PBR protein resulted in the reduction of the mean patient survival rate by 35% with stage III colorectal cancer tissue (Galiègue, *et al.*, 2004, Maaser, *et al.*, 2002, Veenman, *et al.*, 2004).

## 1.8. Rationale

One of the major problems of chemotherapy is the resultant of drug resistance, which results in treatment failure that leads to progressive disease (Sutter, *et al.*, 2005, Sutter, *et al.*, 2004). Drug resistance may be induced by potential mechanisms that include the activation of the Ras/Raf/MEK/ERK signal transduction cascade, overexpression of the anti-apoptotic protein Bcl-2, overexpression of epidermal growth factor receptor (EGFR) and the increase in cholesterol in cancer cells (Sutter, *et al.*, 2005, Sutter, *et al.*, 2004). Furthermore, failure of cell death induction leads to the induction of cancer cells to antitumour therapies, thus overcoming this apoptotic resistance and the consequent induction of cytotoxic effects is a challenge in the improvement of chemotherapy (Decaudin, *et al.*, 2002).

Data thus far obtained on the expression level and tissue distribution of PBR have been done in other species and very few studies have been performed in humans (Bribes, *et al.*, 2004). The increase of PBR expression in various cancers suggests the role of PBR in the growth control of various cancers (Maaser, *et al.*, 2005). PBR is also thought to be involved in the regulation of MPTP activity in response to signals triggering apoptosis, however the precise mode of action is not known (Casellas, *et al.*, 2002). Thus, it appears to be a pharmacological target for apoptosis modulation (Decaudin, *et al.*, 2002). The level of PBR expression has been suggested to serve as a clinically relevant prognosis factor, which has led many researchers to believe that it may serve as a promising drug target in the field of cancer by the use of specific exogenous PBR ligands (Hans, *et al.*, 2005, Maaser, *et al.*, 2005, Sutter, *et al.*, 2004) or as receptor-mediated drug carriers to selectively target anticancer drugs (Guo, *et al.*, 2001). Furthermore, the increase expression of PBR in cancers has suggested that PBR ligands alone or in combination with other agents may be good candidates as

chemotherapeutic or at the very least as chemosensitising agents (Hans, *et al.*, 2005, Sutter, *et al.*, 2005).

## 1.9. Objectives

The general objective of this study was to determine the expression pattern and tissue distribution of the PBR mRNA in different human cancer tissues. Specific objectives were: (i) to localise the expression of the PBR mRNA in various normal and in various human cancer tissues via *in situ* hybridisation, (ii) to determine whether the expression levels of PBR mRNA varies between the different types of normal tissues, between the different types of cancerous tissues and between the normal and the diseased state via *in situ* hybridisation and quantitative reverse transcriptase (RT) real-time-polymerase chain reaction (PCR) and (iii) to isolate the PBR protein. Thus, the question here was to determine whether PBR mRNA is expressed in all cancer tissues, whether the expression levels differ in the different cancer tissues and whether the expression levels are increased or decreased between the normal and diseased state of a specific tissue.

# 2. MATERIALS AND METHODS

## 2.1. Materials

Ethics clearance (Protocol Number: M050223) and higher degrees approval was obtained from the University of the Witwatersrand Research Committee and the Faculty of Science Postgraduate Committee respectively.

### *2.1.1. Cell Lines*

The following cell lines were used: Graham 293 cell line, which is a normal human embryonic kidney cell line, MRC5 cell line, which is a normal human embryonic fibroblast-like lung cell line, A549 cell line, which is a human epithelial cell lung carcinoma cell line, HeLa cell line, which is a human epithelial cell cervical carcinoma cell line and HepG2 cell line, which is a human liver hepatocellular carcinoma cell line. All these cell lines were purchased from Highveld Biological (Pty) Ltd (Johannesburg, South Africa).

### *2.1.2. Human Tissue Array*

Tissue arrays of multiple organs containing normal and diseased tumour tissues that was formalin-fixed were purchased from Cybrdi Inc. (Frederick, Maryland, USA), catalogue number: CC00-11-002. Each of the tissue arrays contained 48 dots in the array panel, which represented a disease or normal tissue spot from a specimen that was selected and pathologically confirmed. The array dot diameter was 1.5 mm and the section thickness was 5 µm. The total number of cases on this tissue array was obtained from 46 individual patients (normal and diseased combined) (Appendix 1 Tables 1-3).

**2.2. Methodology** *(For composition of solutions refer to Appendix 2)*

### *2.2.1. Preparation of Competent Cells*

Normally *Escherichia coli* cells do not possess the ability to take up DNA from the environment. However, if their cell walls are altered, these bacterial cells become more likely to incorporate foreign DNA and thus these cells are said to be "competent". These cells can be made competent by chemical or physical treatment. Chemical treatment includes the calcium chloride method while physical treatment includes electroporation whereby the bacterial cell is shocked with 2500 V. In addition, bacterial cells that are undergoing rapid growth, that is bacterial cells in the log phase can become competent more easily than bacterial cells that are in the other stages of growth.

The chemical treatment method was used in order to make MC1061 *Escherichia coli* cells (Fermentas Life Sciences, Hanover, MD, USA) and BL-2 *Escherichia coli* (donated from the University of the Western Cape, Department of Biotechnology) competent. The MC1061 strain was used for cloning while the BL-2 strain was used in the expression of the PBR protein.

1. The night before making competent cells the desired bacterial strain was plated on 10 mM Magnesium Chloride ($MgCl_2$) Luria-Bertani (LB) agar (LA) plates.
2. A single colony of the desired strain was added to 20 ml Tryptone Yeast Extract $MgCl_2$ (TYM) Broth in a 500 ml conical flask and grown at 37 ˚C overnight, shaking constantly at 300 rpm.
3. 1 ml of cells in the TYM Broth were added to 100 ml fresh TYM Broth in a 2 l conical flask. The cells were grown for a further 2-3 hours or until optical density at 550 nm equals 0.2 at 37 ˚C, shaking constantly at 300 rpm.

4. Thereafter, 400 ml of fresh TYM broth was added to the 2 l conical flask and cells allowed to grow for a further 2-3 hours or until optical density at 550 nm lies between 0.4 and 0.6 at 37 ˚C, shaking constantly at 300 rpm.
5. Bacterial cells were rapidly cooled in ice water, shaking constantly after which they were centrifuged in two 125 ml propylene tubes at 3000 rpm for 10 minutes at 4 ˚C using the JA-10 rotor and J2-21 Beckman centrifuge (Beckman Coulter, Inc., Fullerton, CA, USA).
6. The supernatant was discarded and the pellet resuspended in 125 ml Tfb1. This solution was allowed to incubate for 30 minutes on ice after which the bacterial cells were centrifuged at 3000 rpm for 10 minutes at 4 ˚C using the JA-10 rotor and J2-21 Beckman centrifuge.
7. The bacterial cells were gently resuspended in 80 ml Tfb2 after which 300 µl were aliquoted into 0.5 ml eppendorf tubes and frozen in liquid nitrogen or dry ice. These aliquoted cells were then stored at -70 ˚C for further use.

### *2.2.2. Expression of the Peripheral Benzodiazepine Receptor mRNA in Various Human Cancer Tissues*

*2.2.2.1. Molecular Cloning*

*2.2.2.1.1. <u>RNA Extraction</u>*

RNA extraction is the technique by which total ribonucleic acid (RNA) can be extracted from tissues or cell line samples. Total RNA can be extracted using the TRIzol™ LS Reagent method, which can be divided into four stages namely, the disruption stage, the homogenisation stage, the phase separation stage and the RNA precipitation stage. During the disruption stage a complete disruption of the cell wall and plasma membrane of the cell and organelles found in the cell occurs allowing for the release of all the RNA contained in the sample. At homogenisation the viscosity of the cell lysates produced during disruption is

reduced and the shearing of high molecular weight genomic DNA and other high molecular weight cellular components occurs using the TRIzol™ LS Reagent. RNA is separated from the rest of the lysate using chloroform while RNA is isolated by RNA precipitation using isopropyl propanol.

Total RNA was extracted and purified from the Graham 293 cell line, which was cultured in a 25 $cm^3$ tissue culture plate with 10 % Foetal Bovine Serum (FBS)-Dulbecco's Modified Eagle Media (DMEM) (Invitrogen Corporation, Life Technologie, Carlsbad, CA, USA) until cells became confluent. These cells were grown in monolayer and washed with phosphate buffered saline (PBS) prior to RNA extraction.

1. The confluent cells were homogenised by the addition of 2 ml of TRIzol™ LS reagent (Invitrogen Corporation, Life Technologie, Carlsbad, CA, USA) per 25 $cm^3$ of culture plate and vigorously shaken for 2 hours.
2. Cells were passed through a pipette several times to ensure that the cells were completely homogenised after which the homogenate was transferred to a 2 ml eppendorf tube.
3. 1 ml of chloroform (Merck Chemicals (Pty) Ltd, Saarchem, Wadeville, Gauteng, South Africa) was added to the homogenate and vigorously vortexed for 15 seconds.
4. The mixture was then incubated at room temperature for 10 minutes after which it was centrifuged at 15000 rpm at 4 ˚C for 1 hour in order to allow for phase separation.
5. The top aqueous layer was transferred to a fresh 2 ml eppendorf tube, to which 1 ml isopropyl alcohol (Merck Chemicals (Pty) Ltd, Saarchem, Wadeville, Gauteng, South Africa) was added, mixed thoroughly by inverting the tube and left to incubate at room temperature for 1 hour after which it was incubated overnight at 4˚C.

6. The following day the sample was centrifuged at 3000 rpm for 30 minutes at 4 ˚C after which the supernatant was discarded.
7. The RNA pellet was then washed with 70 % (v/v) ethanol by centrifuging the mixture at 3000 rpm for 5 minutes at 4 ˚C.
8. The pellet was resuspended in 100 µl of 0.1 % (v/v) diethyl pyrocarbonate (DEPC)-treated water ($H_2O$), which was then stored at –70 ˚C for further use.
9. The quality of the RNA extracted was determined by formaldehyde agarose gel electrophoresis (Section 2.2.5.1.).

*2.2.2.1.2. Reverse Transcription/Complementary DNA Synthesis*

Reverse transcription is the technique that involves the synthesis of complementary deoxyribonucleic acid (cDNA) through a two-step process. This involves isolation of messenger RNA (mRNA) from total RNA using oligo-deoxythymidines (dT) primers, which are specific for mRNA, after which it is reverse transcribed into single-stranded cDNA using the enzyme reverse transcriptase. All mRNA have poly-adenosines (poly-A) tail at its 3' end, thus enabling oligo-dT primers to bind to them.

Reverse transcription was performed using a First Strand cDNA Synthesis Kit for RT-PCR (AMV) purchased from Roche Diagnostics GmbH (Manneheim, Germany). 1-2 ng of total RNA sample was used as the template for reverse transcription via AMV reverse transcriptase. mRNA was isolated from total RNA using the oligo-p$(dT)_{15}$ primers. The reverse transcription reaction was carried out in a total volume of 20 µl that was composed of the reagents seen in Appendix 3 Table 1. A negative control was used, which was to perform reverse transcription in the absence of total RNA. The reaction was carried out under the

following conditions seen in Appendix 3 Table 2 after which samples were cooled by placing it on ice for 10 minutes. Thereafter, the cDNA was stored at 4 ˚C for further use.

*2.2.2.1.3.* *Polymerase Chain Reaction*

Polymerase chain reaction (PCR) is the technique that results in the selective amplification of the region of interest in the deoxyribonucleic acid (DNA) molecule through three cyclic steps. These three steps are denaturation, annealing and extension. The gene of interest is amplified using primers that are complementary to the sequence of interest. Denaturation is the step at which double-stranded DNA is denatured. Annealing is the step at which the forward and reverse primers anneal to the template DNA. Extension is the step at which DNA polymerase usually *Taq* polymerase in the presence of $MgCl_2$, dNTPs and PCR buffer synthesises new DNA. This repetitive cycle is carried out for a number of cycles to amplify the region of interest resulting in the exponential multiplication of the region of interest.

The PBR gene transcript was amplified from cDNA by using primers specific for the *PBR* gene. These primers were 5'-*TTCACAGAGAAGGCTGTGGTTC*-3' and 5'-*GCCATACGCAGTAGTTGAGTGT*-3', which represent the forward and reverse primers respectively. This results in the amplification of a region of the *PBR* gene constituting 247 bp located between the mRNA positions 283 and 532 (Appendix 4 Figure 1).

PCR was carried out in a total volume of 25 µl using the reagents as indicated in Appendix 3 Table 3. A negative control was used, which was to perform PCR in the absence of template DNA. The PCR reaction was performed in a GeneAmp® PCR System 9700 thermocycler (Applied Biosystems, Foster City, CA, USA) under the conditions indicated in Appendix 3

Table 4. Results were analysed by agarose gel electrophoresis (Section 2.2.5.2.) and the product stored at 4 ºC for further use.

*2.2.2.1.4. Cloning*

Cloning is the technique by which the DNA segment of interest is inserted into an autonomously replicating DNA molecule (cloning vector) so that the DNA segment of interest is replicated with the vector. Cloning involves two steps: ligation and transformation.

2.2.2.1.4.1. Ligation

Ligation is the technique by which recombinant DNA molecules are constructed by joining together the vector molecule and the DNA segment of interest using DNA ligase usually T4 DNA ligase.

The PCR product was ligated into pGEM-T Easy vector (Appendix 5 Figure 1). pGEM-T Easy vectors are convenient vectors by which PCR products can be cloned. The vectors are prepared by cutting pGEM-T Easy vectors with *Eco*RV restriction enzyme and adding 3' terminal thymidines (T) to both ends. These 3' T overhangs at the insertion site improves the efficiency of ligation of a PCR product into plasmids by preventing recircularisation of the vector and providing a compatible overhang for certain thermostable polymerases that often add a single adenosine (A), in a template-independent fashion, to the 3' ends of the amplified fragments. Thus, the vector has T tails that can be ligated to the A overhangs of *Taq* polymerase PCR reaction products.

The ligation reactions were carried out using the LigaFast™ Rapid Ligation System (Promega Corporation, Madison WI, USA). Ligation reactions were carried out in a total volume of 10 µl consisting of the reagents indicated in Appendix 3 Table 5. Two controls were used, a negative control performed in the absence of pGEM-T Easy vector and PCR product and the other performed in the absence of PCR product, that is only containing the pGEM-T Easy vector. These reactions were then incubated at room temperature for 1 hour after which transformation was performed.

2.2.2.1.4.2. Transformation

Transformation is the technique that ultimately allows for the selection and propagation of plasmid DNA via competent bacterial cells taking up the plasmid DNA. Positive selection for bacterial cells containing the plasmid DNA is accomplished by growth on medium containing an appropriate antibiotic since the plasmid DNA is engineered to contain the corresponding antibiotic resistant gene.

Two controls used in this protocol include the ligation mixtures from the above protocol, that is, a negative control performed in the absence of pGEM-T Easy vector and PCR product and the other performed in the absence of PCR product, that is only containing only the pGEM-T Easy vector.

1. Transformation was performed by the addition of 100 µl of MC1061 *Escherichia coli* competent cells (refer to Section 2.2.2.) to each 10 µl ligation mixture.
2. All three reactions were incubated on ice for 30 minutes followed by incubation at 37 ˚C for 5 minutes after which the reactions were immediately placed on ice for 2 minutes.
3. Thereafter, 900 µl LB broth was added and incubated at 37 ˚C for 1 hour.

4. 100 µl of each reaction was plated on warmed 269 mM ampicillin-containing agar plates as well as on agar plates containing no ampicillin and incubated at 37˚C overnight.
5. An image of the plates was captured using a scanner.

*2.2.2.1.5. Colony Polymerase Chain Reaction*

Colony PCR is a technique by which the success of cloning can be measured by screening for positive colonies, that is, colonies that are positive in the sense that they have acquired the right recombinant DNA molecule. PCR amplifies the insert found in the recombinant DNA molecule.

Gene specific primers for the *PBR* gene were used to amplify the insert in the recombinant DNA molecule. The template DNA was the colony dissolved in 10 µl of sterile distilled water ($sdH_2O$). The negative control used, was to perform the PCR reaction in the absence of template DNA. The PCR reactions were performed using the protocols stated in Section 2.2.2.1.3. and the results were analysed using agarose gel electrophoresis (Section 2.2.5.2).

*2.2.2.1.6. Miniprep Analysis/Plasmid DNA Extraction*

Miniprep analysis, which is also known as the alkaline lysis or the plasmid DNA extraction method is the technique by which plasmid DNA is extracted from bacterial cells such as *Escherichia coli*. The yield of plasmid will vary depending on a number of factors including copy number, cell density of bacterial culture, type of culture medium and the bacterial strain used.

Production of alkaline lysates involves four basic steps: resuspension, lysis, neutralization and clearing of lysates. Resuspension involves the resuspending of harvested bacterial cells in Tris (hydroxymethyl) aminomethane (Tris) - hydrochloric acid (HCl) - ethylenediamine tetra acetic acid (EDTA) buffer containing ribonuclease (RNase) A. RNase A ensures that liberated cellular RNA is digested during lysis. Lysis results in the disruption of the integrity of the bacterial cell wall and membrane and in the denaturation of cellular proteins, which in turn results in the isolation of plasmid DNA. This is achieved with the ionic detergent sodium dodecyl sulphate (SDS). Sodium hydroxide (NaOH) denatures the chromosomal DNA, plasmid DNA and proteins. Neutralization of the lysate is achieved by the addition of sodium potassium acetate. This high salt concentration causes potassium dodecyl sulphate (KDS) to precipitate the denatured proteins and chromosomal DNA. Cellular debris is co-precipitated in the unstable salt-detergent complexes. Plasmid DNA being circular and closed renatures quickly and remains in solution while chromosomal DNA also begins to renature but because it is much larger, the renaturation step is interrupted. Clearing of lysates involves the removal of precipitated debris by either centrifugation or filtration.

The Promega WizardPlus® SV Miniprep Purification System (Promega Corporation, Madison, WI, USA) was used to purify plasmid DNA.

1. The rest of the colony mix prepared for colony PCR was mixed with 5 ml LB broth containing 5 µl 269 mM ampicillin.
2. The mixture was left to grow overnight (12-16 hours) at 37 ˚C with vigorous shaking.
3. The overnight bacterial culture was centrifuged at 10000 rpm for 5 minutes at room temperature after which the supernatant was discarded.
4. The pellet was resuspended in 250 µl Cell Resuspension Solution after which 250 µl Cell Lysis Solution was added and incubated at room temperature for 5 minutes.

5. 10 µl Alkaline Protease Solution was added and incubated at room temperature for 5 minutes.
6. 350 µl of Neutralization Solution was added and centrifuged at top speed for 10 minutes at room temperature.
7. The cleared lysate was decanted into a spin column that had been inserted into a collection tube, which was then centrifuged at top speed for 1 minute at room temperature.
8. The flow through was discarded followed by the addition of 250 µl Wash Solution, which was then centrifuged at top speed for 1 minute at room temperature.
9. The column was transferred to a 1.5 ml eppendorf tube, to which 100 µl of nuclease free $H_2O$ was added followed by centrifugation at top speed for 1 minute resulting in the elution of the plasmid DNA, which was stored at –20 ˚C for further use.
10. To determine if plasmid DNA was isolated the results were analysed by agarose gel electrophoresis (Section 2.2.5.2.).

*2.2.2.1.7.* *Restriction Digestion*

Restriction digestion is a technique used to determine the presence of the insert by ascertaining the size of the insert. The recombinant DNA molecule is usually digested with restriction endonucleases. Restriction endonucleases are bacterial enzymes that bind and cleave DNA at specific target sequences. Type II restriction endonucleases are nucleases that cleave DNA at very specific recognition sequences consisting of a short palindromic sequence, cleaving within this site to generate specific termini. These termini are either cohesive which can have either 5’ or 3’ overhangs of generally between 2 to 4 bases or blunt which have no overhangs and their termini are flush.

*Eco*RI, which recognises the recognition sequence G↓AATTC[1] at the T7 promoter region and the SP6 promoter region of the pGEM-T Easy vector (Appendix 5 Figure 1), cuts on either side of the insert resulting in its release. *Pst*I, which recognises the recognition sequence CTGCA↓G at the SP6 promoter region of the pGEM-T Easy vector (Appendix 5 Figure 1), results in the linearisation of the recombinant DNA molecule.

Restriction digestions were performed using restriction enzymes purchased from Roche Diagnostics GmbH (Manneheim, Germany). The restriction digestion reactions were carried out in a total volume of 30 µl composed of the reagents indicated in Appendix 3 Table 6. As indicated in Appendix 3 Table 6 either 1 µl of *Eco*RI was added to the reaction or 1 µl of *Pst*I was added to the reaction.

1. The reactions were incubated at 37 ˚C for 1 hour in a waterbath.
2. Thereafter, the reactions were incubated at 65 ˚C for 5 minutes, which terminated the reactions.
3. Results were analysed using agarose gel electrophoresis (Section 2.2.5.2.). Controls used on the gel were the undigested clone and the colony PCR product, that is, the PBR fragment to determine if the insert was released.

*2.2.2.1.8. <u>Sequencing</u>*

The purified clone was sent to Inqaba Biotechnical Industries (Pty) Ltd (Pretoria, Gauteng, South Africa), to determine the sequence of the PBR fragment. Results were analysed using CHROMAS, version 1.62 (Technelysium (Pty) Ltd, Helensville, Queensland, Australia) and BLAST from the National Centre for Biomedical Information (NCBI) at URL:

[1] ↓ indicates where restriction endonucleases cuts the DNA

http://www.ncbi.nlm.nih.gov to compare the sequence obtained to a reference sequence (Accession Number: BT006949).

*2.2.2.1.9. Linearisation of Recombinant DNA Molecules*

Restriction digestion was done to linearise the recombinant DNA molecule in preparation for *in vitro* transcription. *Pst*I and *ApaI* were used to linearise the recombinant DNA molecule. *Apa*I recognises the recognition sequence GGGCC↓C[2] and cleaves the pGEM-T Easy vector at the T7 promoter region (Appendix 5 Figure 1). Thus, the linearised fragment digested by *Pst*I is used for the generation of the anti-sense strand while the linearised fragment digested by *Apa*I is used for the generation of the sense strand.

The protocol was followed as mentioned in Section 2.2.2.1.7. However, it should be noted that the *Apa*I restriction digestion reaction was incubated at 30 ˚C and the reaction was performed in Restriction Buffer A. This enzyme was purchased from Roche Diagnostics (Manneheim, Germany). In the case of *Pst*I, 3 µl of the enzyme and 16 µl of sd$H_2O$ were required and an incubation period of 3 hours was required in order to perform the reaction. This discrepancy occurs as in this case *PstI* was purchased from Fermentas Life Sciences, (Hanover, MD, USA) and thus the restriction buffer used was Restriction Buffer $O^+$. Results were analysed agarose gel electrophoresis (Section 2.2.5.2). The control used on the gel was undigested plasmid DNA.

[2] ↓ indicates where restriction endonuclease cuts the DNA

*2.2.2.1.10. Purification of Linearised Recombinant DNA Molecules*

DNA fragments can be extracted and purified from any agarose gel in Tris-Acetate/EDTA (TAE) or Tris-Borate/EDTA (TBE) buffers without phenol extraction and ethanol precipitation. This procedure is based on the ability of DNA to bind to silica membranes in the presence of chaotropic salts. DNA of 100 bp to 10 kb can be isolated using microcentrifugation to force the dissolved gel slice through the membrane while simultaneously binding the DNA on the surface of the silica. After, electrophoresis, which separates the DNA fragments, the band(s) of interest is excised and dissolved in the presence of guanidine thiocyanate. The washing steps follow this, which removes small contaminating molecules.

The linearised DNA fragments were purified using the Promega Wizard® SV Gel and PCR Clean-Up System (Promega Corporation, Madison, WI, USA).

1. The DNA band of interest was visualized on the agarose gel using an UV light transilluminator (UMP, California, USA) and cut out from the gel using a sterile blade.
2. The gel was dissolved in 10 µl Membrane Binding Solution per 10 mg of the gel slice by incubating this solution at 65 ˚C.
3. The dissolved gel mixture was then transferred to a Minicolumn assembly and incubated at room temperature for 1 minute followed by centrifugation at 10000 rpm for 1 minute at room temperature.
4. The flow through was discarded and 700 µl Membrane Wash Solution added followed by centrifugation at 10000 rpm for 1 minute at room temperature.
5. The flow through was discarded and 500 µl Membrane Wash Solution added followed by centrifugation at 10000 rpm for 5 minutes at room temperature.

6. The Minicolumn was then transferred to a 1.5 ml eppendorf tube to which 30 µl of DEPC-treated $H_2O$ was added followed by centrifugation at 10000 rpm for 1 minute at room temperature resulting in the elution of the purified linearised DNA, which was stored at – 20 ˚C for further use.
7. The results were analysed by quantification using a Milton Roy Spectronic Genesys 5 spectrophotometer (Biomed Device Engineering, San Francisco, CA, USA) where absorbance was measured at 260 nm and 280 nm. In order to quantify the DNA solution, 5 µl of the linearised DNA solution was dissolved in 0.995 µl DEPC-treated $H_2O$ and the control used was DEPC-treated $H_2O$ alone.
8. Results were further analysed by agarose gel electrophoresis (Section 2.2.5.2).

*2.2.2.2. Sense and Anti-Sense Probe Synthesis*

*2.2.2.2.1. <u>In Vitro Transcription of Digoxigenin Labelled Sense and Anti-Sense Transcripts</u>*

*In vitro* transcription is the technique by which small amounts of RNA can be synthesized from a DNA template under the suitable control of a promoter for RNA polymerase such as SP6, T3 and T7 RNA polymerase. Thereafter, each RNA copy is labelled with digoxigenin (DIG)-deoxyuridine triphosphate (dUTP) at every 20-25th nucleotide position. DIG is a steroid that is isolated from the digitalis plant, thus allowing for the detection of the sequence of interest during *in situ* hybridisation when bound to anti-DIG conjugates.

DIG-labelled anti-sense and sense complementary RNA (cRNA) transcripts were generated using 2 ng/ml linearised purified pGEM-T Easy vectors containing the *PBR* gene that was digested with *Pst*I and *Apa*I respectively and the DIG RNA Labelling Kit (SP6/T7) purchased from Roche Diagnostics GmbH (Manneheim, Germany). The anti-sense probe was generated in the presence of T7 RNA polymerase while the sense probe was generated in the presence

of SP6 RNA polymerase. To determine the specificity of labelling a control cRNA was also generated from control DNA PSPT 18-Neo/PvuII in the presence of SP6 RNA polymerase. All three reactions were carried out under the same conditions in a total volume of 20 µl containing the following reagents as seen in Appendix 3 Table 7.

1. These reactions were incubated at 37 ˚C for 2 hours in a GeneAmp® System 2700 thermocycler (Applied Biosystems, Foster City, CA, USA).
2. The reactions were terminated by the addition of 2 µl of 0.2 M EDTA, pH 8.0 after which it was briefly vortexed and centrifuged.
3. 2.2 µl of 4 M lithium chloride (LiCl) was added to each reaction.
4. The reactions were precipitated by the addition of 75 µl of cold absolute ethanol (Merck Chemicals (Pty) Ltd, Saarchem, Wadeville, Gauteng, South Africa) followed by brief vortexing and centrifugation after which the reactions were incubated at –20 ˚C for 2 hours.
5. The precipitate was pelleted at 13000 rpm for 15 minutes at 4 ˚C after which the supernatant was discarded.
6. The pellet was washed with the addition of 100 µl of cold 70 % (v/v) ethanol after which the pellet was precipitated by centrifugation at 13000 rpm for 15 minutes at 4 ˚C.
7. The supernatant was discarded and the pellet dried for 2 hours in an air lamina flow.
8. The pellet was dissolved in 25 µl of DEPC-treated $H_2O$ and left to stand at 4 ˚C for 1 hour after which the DIG labelled transcripts were stored at –70 ˚C in aliquots of 10 µl in tight capped 0.5 ml eppendorf tubes.

*2.2.2.2.2. Estimation of Minimal Concentration of Probes*

The minimal concentration of the probe that can be detected was estimated using the guideline described in the DIG's user guide (Roche Diagnostics GmbH, Manneheim, Germany). This was done by 10-fold serial dilutions of the DIG-labelled cRNA transcripts synthesised in Section 2.2.2.2.1. and DIG-labelled control RNA having a concentration of 10 µg/100 µl provided in the DIG RNA Labelling Kit in $sdH_2O$ as tabulated in Appendix 3 Table 8.

The optimal concentrations of the sense and anti-sense probes were determined by the comparing the spot intensities of each of the probes to the DIG-labelled control cRNA.

1. 1 µl of each dilution was spotted on a nylon membrane (Hybond, Amersham Biosciences, California, USA), where spots were lightly marked with a pencil after which the membrane was allowed to air-dry in a lamina flow for 10 minutes.
2. The probe was fixed onto the membrane by placing it under UV light for 5 minutes.
3. 50 ml 1X Washing Buffer was used to wash the membrane, shaking constantly for 5 minutes after which the membrane was blocked using 50 ml 1X Blocking Solution, shaking constantly for 30 minutes.
4. The membrane was incubated with 50 ml of sheep anti-DIG Alkaline Phosphatase (AP) Immunoglobulin (Ig) G (Roche Diagnostics GmbH, Manneheim, Germany) that was diluted 1:10000 with 1X Blocking Solution, shaking constantly for 30 minutes.
5. Thereafter, the membrane was washed twice with 50 ml 1X Washing Buffer, shaking constantly for 15 minutes after which 50 ml 1X Detection Buffer was used to immerse the membrane, shaking constantly for 2 minutes.

6. This membrane was then incubated overnight in the dark in 50 ml nitroblue tetrazolium (NBT)/5-bromo-4-chloro-3-indolyl phosphate (BCIP) (Roche Diagnostics GmbH, Manneheim, Germany) that was diluted 1:50 with 1X Detection Buffer with constant shaking. This allowed for the colour reaction to occur.
7. The reaction was terminated by placing the membrane in 1X Tris-HCl/EDTA (TE) buffer for 5 minutes after which the membrane was air-dried and the minimal concentration of the sense and anti-sense probes determined by comparing it with DIG-labelled control cRNA.

*2.2.2.3. <u>In Situ</u> Hybridisation*

*In situ* hybridisation is the process by which specific mRNA sequences are localized and detected in morphologically preserved tissue sections or cell preparations by hybridising a complementary strand of a nucleotide probe to the sequence of interest. This technique can be divided into three major steps: pre-hybridisation, hybridisation and post-hybridisation. Pre-hybridisation is the step at which tissue sections are dewaxed and treated with various chemicals such as acetic anhydride and HCl to reduce background staining. Hybridisation is the step at which the DIG-labelled RNA probes bind to the mRNA sequence of interest in the tissue sections. Post-hybridisation is the step at which excess probe is removed and the labelled mRNA sequence of interest can be colorimetrically and fluorescently detected.

Two controls were used to perform this technique. The first was a negative control, which was prepared by the localisation of the sense probe on a tissue preparation, thus allowing for one to determine if localisation occurred when tissue preparations were hybridised with the anti-sense probe. The other control used was to compare the diseased tissue to the normal tissue, both of which were hybridised with the anti-sense probe.

*2.2.2.3.1. Pre-Hybridisation*

1. The tissue sections were dewaxed in fresh xylene (Merck Chemicals (Pty) Ltd, Saarchem, Wadeville, Gauteng, South Africa) for 30 minutes, which consisted of 3 changes of 10 minutes each.
2. Thereafter, the tissue sections were rehydrated in fresh 100% ethanol for 6 minutes, which consisted of 2 changes of 3 minutes each. This was followed by serial hydration of the tissue sections for 3 minutes each in 90%-, 70%-, 50%-ethanol and DEPC-$H_2O$.
3. The tissue sections were fixed in 4% paraformaldehyde (PFA) for 20 minutes after which it was washed in fresh Tris Buffer Saline (TBS) for 3 minutes, which consisted of 3 changes of 1 minute each.
4. The proteins in the tissue sections were denatured in 0.1 M HCl for 10 minutes at room temperature followed by washing in fresh TBS for 3 minutes, which consisted of 3 changes of 1 minute each.
5. This was followed by the limitation of non-specific labelling with freshly prepared 0.5% acetic anhydride for 10 minutes after which it was washed in fresh TBS for 3 minutes, which consisted of 3 changes of 1 minute each.
6. Subsequently, the cell membrane was permeabilised with 10µg/µl Proteinase K (Promega Corporation, Madison, WI, USA) dissolved in TBS for 20 minutes at 37 ˚C followed by washing with fresh TBS for 3 minutes, which consisted of 3 changes of 1 minute each.
7. Proteinase K activity was terminated by placing tissue sections in TBS for 5 minutes at 4 ˚C.
8. This was followed by the serial dehydration of the tissue slides for 1 minute each in 50%-, 70%- and 90%-ethanol. The tissue sections were further dehydrated in 100% ethanol for 2 minutes, which consisted of 2 changes of 1 minute each.

9. Thereafter, the tissue sections were dried in chloroform (Merck (Pty) Ltd, Saarchem, Wadeville, Gauteng, South Africa) for 10 minutes in the fume hood.
10. The tissue sections were then stored in a dust-free environment for days at room temperature for further use.

*2.2.2.3.2. Hybridisation*

1. Probes were prepared for hybridisation. The probes were thawed on iced. 2 µl 10 µg/ml Herring Sperm DNA (Promega Corporation, Madison, WI, USA) was dissolved in 198 µl of hybridisation buffer and vortexed vigorously after which 1 µl in the case of the sense probe and 0.8 µl in the case of the anti-sense probe was added. 0.8 µl was used in the case of anti-sense probe because the concentration of the probe was very high, which results in increase trapping during hybridisation and thus a lower value was used to prevent this. These probe preparations were than boiled for 5 minutes followed by placing it immediately on ice for 2 minutes.
2. 100 µl of the probe was placed on each slide that was enclosed with a GENE Frame (Southern Cross Biotechnology, Cape Town, South Africa).
3. Hybridisation was allowed to take place by placing slides in a Hybaid Omnislide Flat Block Humidity Chamber (Thermo Electron Company, Massachusetts, USA) containing a solution composed of 50% (v/v) formamide and 5% (v/v) 20X NaCl sodium citrate solution (SSC), which prevents the evaporation of the hybridisation solution, overnight (± 16 hours) at 55 ˚C.

*2.2.2.3.3. Post-Hybridisation*

The Roche Diagnostics Washing and Blocking Kit (Roche Diagnostics GmbH, Manneheim, Germany) were used to conduct this protocol.

1. The slides were removed from the humid chamber and the excess probe was removed by dropping it off after which GENE Frames were removed.
2. Slides were then washed in 2X SSC for 30 minutes at 37 ˚C in a wash module after which they were washed in 1X SSC, 0.5X SSC and 0.1X SSC for 20 minutes each at 55 ˚C.
3. The slides were then washed in fresh TBS for 3 minutes, which consisted of 3 changes of 1 minute each.
4. Thereafter, 100 µl of 1X Blocking Solution was added to each slide and incubated at room temperature for 15 minutes in a humidity chamber. This allows for the blocking of non-specific binding sites on tissue sections.

The protocol hereafter varies depending on the detection method used.

2.2.2.3.3.1. Colorimetric Detection

DIG-labelled probes that have hybridised to the target sequence can be detected colorimetrically with AP conjugated to anti-DIG. This occurs when the tissue sections are incubated with a suitable substrate such as NBT/BCIP allowing for AP activity to occur, which results in the formation of a purple/blue precipitate, which can be viewed under a light microscope.

1. Tissue sections were incubated with 100 µl sheep anti-DIG-AP IgG diluted 1:500 in 1X blocking solution per slide and incubated in a humid chamber for 1 hour at room temperature.
2. The tissue slides were washed in fresh TBS for 3 minutes, which consisted of 3 changes of 1 minute each.

3. Thereafter, tissue sections were incubated with 100 µl of chromogen NBT/BCIP diluted 1:50 in 1X Detection Buffer per slide and left to develop in a dark humid chamber overnight at room temperature.
4. The reaction was terminated by incubating the slides with 100 µl of 1X TE for 5 minutes after which the slides were washed in running tap water for 5 minutes.
5. Tissue sections were counterstained with 5 drops of Mayer's Haematoxylin (Sigma Diagnostics, St. Louis, MO, USA) per slide for 1 minute followed by washing in running tap water for 10 minutes.
6. Thereafter, tissue sections were mounted with aqueous glycerol jelly and allowed to dry at 37 ˚C for ± 1 hour.
7. Tissue sections were viewed and images captured using the AxioCam (MRm/MRc) camera and AxioVision software package (Carl Zeiss AG, Oberkochen, Germany).

2.2.2.3.3.2. Fluorescent Detection

DIG-labelled RNA probes that have hybridised to the target sequence can be detected fluorescently with fluorescein isothiocyanate (FITC) conjugated to anti-DIG. FITC does not require the presence of a suitable substrate in order to emit a colour substrate. When FITC is excited at 490 nm, it results in the emission of an apple green colour, which can be viewed under a fluorescent microscope.

1. The slides were washed in TBS-Tween for 5 minutes after which they were incubated in a Tri-Sodium-Blocking (TNB) solution at 37 ˚C for 30 minutes.
2. Tissue sections were then incubated at 37 ˚C with 75 µl anti-DIG fluorescein for 30 minutes after which the slides were washed in TBS-Tween for 15 minutes, which consisted of 3 changes of 5 minutes each.

3. The tissue sections were mounted with Molecular Probes SlowFade® Light Antifade Kit (Molecular Probes, Eugene, Oregon, USA) using the manufacturer's instructions.
    3.1. Slides were mounted by placing a drop of component C that is Equilibration Buffer on tissue samples. These slides were then incubated at room temperature for 10 minutes or until dry.
    3.2. Thereafter, a drop of component A that is the Mounting Media was added to which a coverslip was placed.
4. Tissue sections were then viewed under the fluorescence microscope and images captured using the AxioCam (MRm/MRc) camera and AxioVision software package.

### *2.2.3. Expression Levels of the Peripheral Benzodiazepine Receptor mRNA in Various Human Cancer Tissues*

#### *2.2.3.1. RNA Isolation*

RNA was isolated from MRC5, A549, HeLa and HepG cultured cells using the High Pure RNA Isolation kit purchased from Roche Diagnostic GmbH (Manneheim, Germany).

1. Cells were resuspended in 200 µl PBS after which 400 µl of Lysis/Binding Buffer was added and vortexed for 15 seconds.
2. The sample was then transferred to a High Pure filter tube inserted into a collection tube after which the sample was centrifuged for 15 seconds at 10000 rpm at room temperature and the flow through discarded.
3. 90 µl DNase Incubation Buffer and 10 µl DNase I was added into a sterile reaction tube, mixed, after which the solution was transferred into the High Pure filter tube. This was left to incubate for 15 minutes at 15 ˚C.

4. 500 µl Wash Buffer I was added to the filter tube assembly and centrifuged at 10000 rpm for 15 seconds at room temperature.
5. The flow through was discarded and 500 µl Wash Buffer II added to the filter tube assembly. This was centrifuged at 10000 rpm for 15 seconds at room temperature.
6. The flow through was again discarded and 200 µl Wash Buffer II added to the filter tube assembly. This was centrifuged at 10000 rpm for 2 minutes at room temperature, which ensured the removal residual Wash Buffer.
7. The collection tube containing the flow through was discarded and the High Pure filter tube was inserted into a 1.5 ml eppendorf tube. 100 µl Elution Buffer was added to the filter tube assembly and centrifuged at 10000 rpm for 1 minute at room temperature. This was then stored at –80 ˚C for further use.

*2.2.3.2. Relative Quantitative Reverse Transcriptase- Real-Time Polymerase Chain Reaction*

Quantitative reverse transcriptase-real-time PCR is the process by which mRNA can be quantified both in relative terms and absolute terms. It is a two-step process involving reverse transcription and real-time PCR. The quantification of the PCR product relies on the detection of a fluorescent signal proportional to the amount of product. PCR products can be measured in real-time by the used of double-stranded DNA-binding dye, namely SYBR Green I, which binds to double-stranded DNA, that is the PCR product. The amount of PCR product can be directly measured in real time using a fluorimeter. Quantification is based on a threshold cycle, that is the first PCR cycle with detectable fluorescence. By monitoring during the period when PCR amplification is exponential provides precise data for accurate quantification.

*2.2.3.2.1. Reverse Transcription/Complementary DNA Synthesis*

Reverse transcription was performed using an ImProm-II™ Reverse Transcription System purchased from Promega Corporation (Madison, WI, USA). 1-2 ng of total RNA samples was used as a template for reverse transcriptase. mRNA was isolated from total RNA using the oligo-$(dT)_{15}$ primers. The reverse transcription reaction was carried out in a total volume of 20 µl that was composed of the reagents indicated in Appendix 3 Table 9. A negative control was used, which was to perform reverse transcription in the absence of total RNA. The reaction was carried out under the following conditions as seen in Appendix 3 Table 10 after which samples were cooled by placing on ice for 10 minutes. The concentration of the cDNA was spectrophotometrically determined using an Ultraspec2000 (Amersham Pharmacia Biotech, Picataway, NJ, USA) after which the cDNA was stored at 4 ˚C for further use.

*2.2.3.2.2. Real-Time Polymerase Chain Reaction*

Real-Time PCR was carried out in a total volume of 25 µl using the reagents as indicated in Appendix 3 Table 11. The negative control used was to perform real-time PCR in the absence of both the forward and reverse primers and template DNA. The relative quantitative PCR was performed in a Bio-Rad MJ Mini Personal Thermal Cycler (Bio-Rad Laboratories, Hercules, CA, USA) under the conditions indicated in Appendix 3 Table 12. Results were analysed by quantitation and melting curves using the Opticon 3.1 software (Bio-Rad Laboratories, Hercules, CA, USA) and agarose gel electrophoresis (Section 2.2.5.2.).

### *2.2.4. Peripheral Benzodiazepine Receptor Protein Expression*

#### *2.2.4.1. Restriction Digestion of the Peripheral Benzodiazepine Receptor Insert and pGEX-6P-2 Expression Vector*

The insert that is the DNA fragment of interest (PBR) was digested from the pGEM-T Easy vector using *Bam*HI and *Xho*I. These two recognition sequences had been built in with the PCR primers, thus allowing for the insert to contain the two recognition sequences found on the multiple cloning site of the protein expression vector, pGEX-6P-2 (Appendix 5 Figure 2), that is pGEX-6P-2 recognises the recognition sequence for *Bam*HI G↓GATTC[3] and *Xho*I C↓TCGAG[3].

The protocol was followed as mentioned in Section 2.2.3.1.7. However it should be noted that *Bam*HI and *Xho*I digestion were purchased from Fermentas Life Sciences (Hanover, MD, USA), thus the Restriction Buffer for *Bam*HI was Buffer *Bam*HI and the Restriction Buffer for *Xho*I was Buffer R. The Restriction Buffer used for double digestion was Buffer Tango. Three controls were used. These included the undigested clone, digesting the clone with *Bam*HI only and digesting the clone with *Xho*I only. The protocol in Section 2.2.3.1.7. varied as follows: the two controls that is the clone digested with *Bam*HI only and the clone digested with *Xho*I only required 3 µl of restriction enzyme and 16 µl $sdH_2O$, the clone digested with both *Bam*HI and *Xho*I required 3 µl of each restriction enzyme, 2 µl Restriction Buffer and 12 µl $sdH_2O$ and each of the reaction were incubated for 3 hours. The restriction digestion reactions were carried out for the clone containing the *PBR* gene and the pGEX-6P-2 expression vector and the controls used for each were as mentioned above. Results were analysed using agarose gel electrophoresis (Section 2.5.2).

[3] ↓ indicates where restriction nucleases cuts the DNA

*2.2.4.2. Purification of the Peripheral Benzodiazepine Receptor Insert and pGEX-6P-2 Expression Vector*

The released insert and the pGEX-6P-2 vector digested with *Bam*HI and *Xho*I were purified by the protocol seen in Section 2.2.3.1.10. after which results were analysed by agarose gel electrophoresis.

*2.2.4.3. Cloning*

The purified insert was ligated into the protein expression vector, pGEX-6P-2 after which the recombinant molecules were transformed into competent MC1061 *Escherichia coli* cells (Section 2.2.1.) as described in Section 2.2.2.1.4. Two controls were used, a negative control performed in the absence of pGEX-6P-2 vector and the purified insert and the other performed in the absence of the PCR product, that is, only containing the pGEX-6P-2 vector. An image was captured using a scanner.

*2.2.4.4. Colony Polymerase Chain Reaction*

Colony PCR was done to determine the success of cloning by amplifying the insert found in the recombinant DNA molecule via PCR using the protocol as described in Section 2.2.2.1.5. The negative control used, was to perform the PCR reaction in the absence of template DNA. Results were analysed by agarose gel electrophoresis (Section 2.2.5.2.).

*2.2.4.5. Miniprep Analysis/Plasmid DNA Extraction*

The recombinant DNA molecules, that is the insert ligated to the pGEX-6P-2 expression vector was extracted from the bacterial cells via miniprep analysis or plasmid DNA extraction as described in Section 2.2.1.6. Results were analysed by agarose gel electrophoresis (Section 2.2.5.2.).

*2.2.4.6. Restriction Digestion*

Restriction digestion was done to determine the presence of the insert using the protocol in Section 2.2.2.1.7. with the variations as described in 2.2.4.2. Four controls used include the undigested clone, digesting the clone with *Bam*HI only, digesting the clone with *Xho*I only and the colony PCR product. Results were analysed by agarose gel electrophoresis (Section 2.2.5.2.).

*2.2.4.7. Sequencing*

The purified clone was sent to Inqaba Biotechnical Industries (Pty) Ltd to determine the sequence of the PBR fragments. Results were analysed using CHROMAS, version 1.62 and BLAST from NCBI to compare the sequence obtained to a reference sequence (Accession Number: BT006949) and to determine the orientation of the PBR fragment. The sequence was then converted into an amino acid sequence using DNAMAN, trial version 6.0 (Lynonn Corporation, Vaudreuil, Quebec, Canada) in order to determine the size of the protein that will be synthesised when expressed.

*2.2.4.8. Optimisation of the Gluthathione-S-Transferase Fusion Protein using Isopropyl-β-D-Thiogalactopyranoside*

Gluthathione-*S*-Transferase (GST) fusion protein that is GST fused with PBR was synthesised by inducing the cloned pGEX-6P-2 vector with isopropyl-β-D-thiogalactopyranoside (IPTG), which binds to the *lac* repressor, encoded by the *lac* $^{Iq}$ gene thus allowing for the transcription of all genes downstream of the *tac* promoter in the pGEX-6P-2 expression vector.

1. 2 µl PBR ligated into pGEX-6P-2 expression vectors were transformed into competent BL-2 *Escherichia coli* cells (refer to Section 2.2.1) as described in Section 2.2.2.1.3.
2. A single colony was inoculated in 5 ml LB containing 5 µl of 269 mM ampicillin and grown overnight at 37 ˚C, shaking constantly at 110 rpm.
3. 1 ml of this overnight culture was then added to 60 ml fresh LB containing 60 µl of 269 mM ampicillin after which it was incubated at 37 ˚C, shaking constantly at 110 rpm for ± 2 hours until the optical density at 550 nm was ± 0.4.
4. Thereafter, 10 ml of culture were transferred to six different sterile tubes where they were induced with different concentrations of 0.5 M IPTG, namely 0.1 mM, 0.3 mM, 0.5 mM, 0.7 mM and 0.9 mM. The control used was bacterial culture uninduced with IPTG. These cultures were then allowed to shake at 110 rpm at 25 ˚C overnight.
5. The overnight induced cultures were transferred to six 50 ml isopropylene tubes and centrifuged at 10000 rpm for 5 minutes at 4 ˚C using the JA-20 rotor and J2-21 Beckman centrifuge.
6. The supernatant was discarded and the pellet resuspended in 2 ml PBS.
7. The resuspended culture was freeze-thawed by placing it at 37 ˚C for 15 minutes and –80 ˚C for 15 minutes. This step was repeated twice.
8. Thereafter, the resuspended culture was centrifuged at 10000 rpm for 30 minutes at 4 ˚C using the JA-20 rotor and J2-21 Beckman centrifuge.
9. The supernatant was transferred to a 1.5 ml eppendorf tube and stored at –80 ˚C for further use. Results were analysed using SDS-PAGE (Section 2.2.5.3.).

### *2.2.5. Electrophoresis*

*2.2.5.1. Formaldehyde Agarose Gel Electrophoresis*

Formaldehyde agarose gel electrophoresis is the technique by which RNA can be separated according to size. This can occur because formaldehyde prevents the RNA from forming a secondary structure, thus it acts as a denaturing agent. The nucleic acid material is loaded onto the formaldehyde agarose gel, to which an electric current is applied. Due to the negative charge of the RNA, which results from the phosphate molecules on the RNA backbone, the RNA migrates towards the positive electrode. The agarose gel, which contains randomly, distributed pores acts a "molecular sieve", separating the molecules according to size. The RNA fragments are visualised by staining the gel with ethidium bromide. Ethidium bromide intercalates between the bases of the RNA, which can then be visualised under UV light as the ethidium bromide fluoresces under these conditions.

1. The formaldehyde agarose gel was prepared by dissolving 1 g of agarose-D-1-LE (Hispanagar, Whitehead Scientific (Pty) Ltd, Brackenfell, South Africa) in 10 ml of 10X 3-[N-morpholino] propane sulfonic acid (MOPS) and 85 ml DEPC-treated $H_2O$.
2. The solution was allowed to reach 50 ˚C after which 5.4 ml 37% formaldehyde (v/v) was added followed by addition of 10 mg/ml ethidium bromide (Merck KGoA, Darmstadt, Germany) and the gel allowed to set on a casting tray.
3. Thereafter, 10 µl of freshly prepared formaldehyde gel loading buffer was added subsequent to which the mixture was heated at 65 ˚C for 5 minutes, which allowed for the denaturation of RNA.
4. This mixture was then cooled on ice for 10 minutes before it was loaded onto the gel.
5. The gel was electrophoresed with 1X MOPS at 50 V and allowed to run until the loading dye reached three-quarters of the gel after which it was viewed and image captured under

a Bio-Rad Universal Hood II UV transilluminator (Bio-Rad Laboratories-Segrate, Milan, Italy) and using the QuantityOne-D-Analysis Software (Bio-Rad Laboratories, Hercules, CA, USA) or a UVP BioDoc-It™ System SG (The Scientific Group).

*2.2.5.2. Agarose Gel Electrophoresis*

Agarose gel electrophoresis is the technique by which DNA can be separated according to its size. The nucleic acid material is loaded onto the agarose gel, to which an electric current is applied. Due to the negative charge of the DNA, which results from the phosphate molecules on the DNA backbone, the DNA migrates towards the positive electrode. The agarose gel, which contain randomly distributed pores acts as a "molecular sieve", separating the molecules by size. The DNA fragments are visualised by staining the gel with ethidium bromide. Ethidium bromide intercalates between the bases of the DNA, which can then be visualised under UV light as the ethidium bromide fluoresces under these conditions.

1. A 1% agarose gel was prepared by dissolving 1 g of agarose in 100 ml TBE buffer. 0.3 µg/ml ethidium bromide was added to the solution once it reached about 50 ˚C and the gel allowed to set on a casting tray.
2. DNA samples were mixed with a fifth of the sample volume bromophenol loading dye.
3. DNA samples were run with a DNA molecular weight marker of 100 to 1050 bp known as DNA Molecular Weight Marker XIV (Roche Diagnostics, Manneheim, Germany) (Appendix 6 Figure 1A) or 80 to 1031 bp known as GeneRuler™ 100 bp DNA Ladder (Fermentas Life Sciences, Hanover, MD, USA) (Appendix 6 Figure 1B) or 50 to 1031 bp known as GeneRuler™ 50 bp DNA Ladder (Fermentas Life Sciences, Hanover, MD, USA) (Appendix 6 Figure 1C).

4. The DNA samples and the DNA molecular weight marker were loaded onto the gel and run at 70 V in 1X TBE buffer. The gel was allowed to run until the bromophenol blue dye reached three-quarters of the gel after which the gel was viewed and image captured using a UV transilluminator.

*2.2.5.3. Sodium Dodecyl Sulphate-Polyacrylamide Gel Electrophoresis*

Sodium dodecyl sulphate (SDS)- polyacrylamide gel electrophoresis (PAGE) is the technique by which proteins can be separated according to their size. SDS is an anionic detergent which means it is a detergent which denatures proteins to their primary structures by "wrapping around" the polypeptide backbone thus binding to proteins in a mass ration of 1.4:1 and conferring a negative charge to the denatured protein. Thus, all proteins in the gel will migrate to the positive electrode when placed in an electric field. β-mercaptoethanol or dithiothreitol (DTT) reduces disulphide bridges in proteins, which allows for the random configuration necessary for separation by size. N, N, N', N'-tetramethylenediamine (TEMED) is a free radical stabilizer that catalyses the decomposition of the persulphate ion in ammonium persulphate to give a free radical, which in turn results in the initiation of polymerisation of acrylamide. The polyacrylamide gel is a polymer of acrylamide monomers that are polymerised in a head-to-tail fashion into a long chain and bis-acrylamide, which is a cross-linking agent that is occasionally built into the growing acrylamide chain thus inducing a second site for chain extension resulting in the formation of a cross-linked matrix that functions as a "molecular sieve" to separate proteins according to their size when placed under an electric field. Proteins can be visualised by staining the gel with Coomassie Brilliant Blue, a sulphated trimethlyamine in a methanol: $H_2O$: glacial acetic acid mixture. This glacial acetic acid-methanol mixture acts as a denaturing agent by precipitating or fixing the protein in the gel preventing it from being washed away during staining and functions in complexing

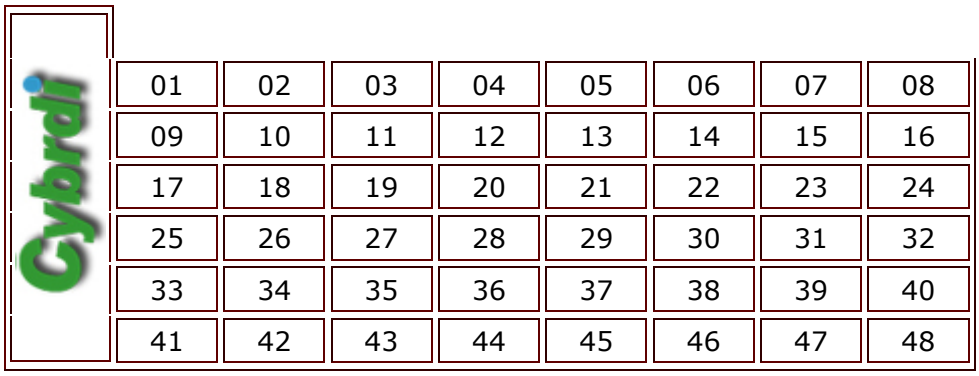
the Coomassie Brilliant Blue to the protein. Thereafter, the gel is destained with Destaining Solution to remove excess staining solution.

1. Two glass plates, one notched and one having spacers were assembled by clamping the two plates together. The clamped plates were placed on a sponge in order to clamp the bottom and held in an upright position.
2. A 12% (v/v) separating gel was prepared as indicated in Appendix 3 Table 13 and poured between the plates until three-quarters filled. This gel was then allowed to stand until it solidified.
3. A 7% (v/v) stacking gel was prepared as indicated in Appendix 3 Table 13 and poured between the plates until completely filled after which a comb was inserted between the two plates and allowed to solidify.
4. After solidification, the comb was removed and the plate placed in a bucket containing Electrophoresis Buffer in a manner that each well was submerged with the buffer.
5. 30 µl of protein samples were mixed with 10 µl of 2X sample dye, boiled for 4 minutes at 95 ˚C after which it was loaded onto the gel with PageRuler$^{TM}$ Prestained Protein Ladder (Fermentas Life Sciences, Hanover, MD, USA) (Appendix 6 Figure 2).
6. The gel was allowed to run at 150 V until the loading dye reached ±0.5 cm from the bottom of the gel.
7. The gel was then removed from the glass plates by lifting the plate using a spatula and stained overnight with Coomassie Brilliant Blue, shaking constantly. The Coomassie Brilliant Blue was removed and the gel rinsed with $dH_2O$ to remove excess stain.
8. Thereafter, the gel was destained overnight with Destain Solution shaking constantly. The gel was washed with $dH_2O$ after which the image was captured using a Bio-Rad Universal

Hood II Transilluminator (Bio-Rad Laboratories-Segrate, Milan, Italy) and using the QuantityOne-D-Analysis Software (Bio-Rad Laboratories, Hercules, CA, USA).

# APPENDIX 1: Information of Tissue Array Panel

**Table 1: Tissue Array Panel Display**




| Number | Age | Sex | Organ | Pathology Diagnosis | Grade |
|---|---|---|---|---|---|
| 1 | 46 | Male | Liver | Hepatocellular Carcinoma | II |
| 2 | 78 | Female | Colon | Adenocarcinoma | III |
| 3 | 57 | Female | Epiploon | Squamous Cell Carcinoma | III |
| 4 | 66 | Male | Prostate | Adenocarcinoma | III |
| 5 | 60 | Female | Breast | Infiltrating Duct Carcinoma | No Grade |
| 6 | 57 | Male | Lung | Adenocarcinoma | III |
| 7 | 60 | Female | Kidney | Chromophobe Carcinoma | No Grade |
| 8 | 67 | Male | Brain | Astrocytic Carcinoma | II |
| 9 | 41 | Male | Liver | Hepatocellular Carcinoma | III |
| 10 | 66 | Male | Colon | Adenocarcinoma | II |
| 11 | 52 | Male | Epiploon | Squamous Cell Carcinoma | III |
| 12 | 64 | Male | Prostate | Adenocarcinoma | II |
| 13 | 49 | Female | Breast | Infiltrating Duct Carcinoma | No Grade |
| 14 | 46 | Male | Lung | Squamous Cell Carcinoma | III |
| 15 | 53 | Female | Kidney | Clear Cell Carcinoma | No Grade |

| | | | | | |
|---|---|---|---|---|---|
| 16 | 49 | Female | Brain | Lymphoma | - |
| 17 | 77 | Male | Liver | Hepatocellular Carcinoma | II |
| 18 | 57 | Male | Colon | Adenocarcinoma | I |
| 19 | 60 | Male | Epiploon | Squamous Cell Carcinoma | III |
| 20 | 72 | Male | Prostate | Adenocarcinoma | III |
| 21 | 48 | Female | Breast | Infiltrating Duct Carcinoma | No Grade |
| 22 | 36 | Female | Lung | Small Cell Carcinoma | No Grade |
| 23 | 45 | Male | Kidney | Clear Cell Carcinoma | No Grade |
| 24 | 57 | Male | Brain | Ependymoblastoma | - |
| 25 | 48 | Male | Liver | Normal Tissue | - |
| 26 | 66 | Male | Colon | Normal Tissue | - |
| 27 | 65 | Male | Stomach | Normal Tissue | - |
| 28 | 67 | Male | Prostate | Proliferative Tissue | - |
| 29 | 43 | Female | Breast | Normal Tissue | - |
| 30 | 46 | Male | Lung | Normal Tissue | - |
| 31 | 45 | Male | Kidney | Normal Tissue | - |
| 32 | 67 | Male | Brain | Normal Tissue | - |
| 33 | 37 | Male | Liver | Normal Tissue | - |
| 34 | 52 | Female | Colon | Normal Tissue | - |
| 35 | 74 | Female | Stomach | Normal Tissue | - |
| 36 | 78 | Male | Prostate | Proliferative Tissue | - |
| 37 | 42 | Female | Breast | Normal Tissue | - |
| 38 | 36 | Female | Lung | Normal Tissue | - |
| 39 | 51 | Female | Kidney | Normal Tissue | - |
| 40 | 67 | Male | Brain | Normal Tissue | - |

| | | | | | |
|---|---|---|---|---|---|
| 41 | 48 | Male | Liver | Normal Tissue | - |
| 42 | 57 | Male | Colon | Normal Tissue | - |
| 43 | 64 | Female | Epiploon | Greater Omentum | - |
| 44 | 68 | Male | Prostate | Proliferative Tissue | - |
| 45 | 51 | Female | Breast | Harden Adenosis Tissue | - |
| 46 | 57 | Male | Lung | Normal Tissue | - |
| 47 | 49 | Female | Kidney | Normal Tissue | - |
| 48 | 59 | Male | Brain | Normal Tissue | - |

1. Case numbers 1-24 represent diseased tissues, case numbers 25-27, 29-35, 37-43 and 45-48 represent normal tissues and case numbers 28, 36 and 44 represents hyperplastic tissues.
2. Grade indicates the level of malignancy of a tumour. Tumours are graded based on their mitotic index (growth rate), vascularity, presence of necrotic centres, invasive potential (border distinctness) and similarity to normal cells. Malignant tumours contain several grades of cells, however the most malignant cell found in the tumour determines the grade for the entire tumour even if most of the tumour is a lower grade. According to the World Health Organization grading system, grade I tumours are the least malignant and these tumours grow slowly and microscopically appear almost normal. Grade II tumours grow slightly faster than grade I tumours, have slightly abnormal microscopic appearance and these tumours may invade surrounding normal tissue. Grade III tumours are malignant containing actively reproducing normal cells that invade surrounding normal tissue. Grade IV tumours are the most malignant invading wide areas of surrounding tissue that reproduce rapidly. These tumours have an unusual microscopic appearance and are necrotic in the centre. In addition, Grade IV tumours have new blood vessels forming that maintain the rapid growth of the tumour.

(Reference: URL: http://www.cybrdi.com/viewproduct.php?id=245 and URL: http://www.abta.org/pdf/ABTA%20Primer-Chapter%202.pdf)

**Table 2: Summary of the Number of Patients with Cancer on the Tissue Array Panel**

| Organ | Type of Cancer | Grade | Number of Patients |
|---|---|---|---|
| Liver | Hepatocellular Carcinoma | II | 2 |
| | | III | 1 |
| Colon | Adenocarcinoma | I | 1 |
| | | II | 1 |
| | | III | 1 |
| Stomach/Epiploon | Squamous Cell Carcinoma | III | 3 |
| Prostate | Adenocarcinoma | II | 1 |
| | | III | 2 |
| Breast | Infiltrating Ductal Carcinoma | - | 3 |
| Lung | Adenocarcinoma | III | 1 |
| | Squamous Cell Carcinoma | III | 1 |
| | Small Cell Carcinoma | - | 1 |
| Kidney | Chromophobe Carcinoma | - | 1 |
| | Clear Cell Carcinoma | - | 2 |
| Brain | Astrocytic Carcinoma | II | 1 |
| | Lymphoma | - | 1 |
| | Ependymoblastoma | - | 1 |

**Table 3: Summary of the Number of Normal Patients on the Tissue Array Panel**

| Organ | Number of Patients |
|---|---|
| Liver | 2 |
| Colon | 3 |
| Stomach | 2 |
| Epiploon | 1 |
| Prostate (Proliferative Tissue) | 3 |
| Breast (Normal Tissue) | 2 |
| Breast (Adenosis Tissue) | 1 |
| Lung | 3 |
| Kidney | 3 |
| Brain | 2 |

# APPENDIX 2: Composition of Reagents and Solutions

| Solution | Composition |
|---|---|
| 0.5% Acetic Anhydride (v/v) | 0.25 ml 100% Acetic Anhydride (v/v) (Merck Chemicals (Pty) Ltd, Saarchem, Wadeville, Gauteng, South Africa) in 5 ml 1M Tris, pH 7.5 and 45 ml DEPC-treated $H_2O$ |
| 10% Ammonium Persulphate (w/v) | Dissolve 0.1 g ammonium persulphate (Promega Corporation, Madison, WI, USA) in 1 ml $dH_2O$. Prepare fresh for every use |
| 269 mM Ampicillin | 0.1g Ampicillin (Roche Diagnostics GmbH, Manneheim, Germany) in 1 ml $sdH_2O$ |
| Anti-DIG-AP IgG Diluted in 1:500 in 1X Blocking Solution | Add 1 µl Anti-DIG-AP IgG to 500 µl 1X Blocking Solution |
| Anti-DIG-AP Diluted 1:10000 in 1X Blocking Solution | Add 5 µl Anti-DIG-AP IgG to 50 ml 1X Blocking Solution |
| 10X Blocking Stock Solution | Dissolve Blocking Reagent (Roche Diagnostics GmbH, Manneheim, Germany) in 10% 10X Maleic Acid Buffer (v/v) constantly stirring at 65 ˚C. Store at 2-8 ˚C. |
| 1X Blocking Solution | Dilute 1:10 10X Blocking Solution<br>Dilute 1:10 10X Maleic Acid Buffer<br>Make solution up to final volume with $sdH_2O$ |
| Bromophenol Blue Loading Dye | 30% Glycerol (v/v) (Merck Chemicals (Pty) Ltd, Saarchem, Wadeville, Gauteng, South Africa)<br>15 mM EDTA (Merck Laboratory Supplies (Pty) Ltd, |

| | |
|---|---|
| | Saarchem, Midrand, Gauteng, South Africa), pH 8.0<br>0.05% Bromophenol Blue (w/v) (Riedel-de-Haën, Sigma Aldrich Laborchemikalien GmbH, Seelze) |
| Buffer *Bam*HI | 10 mM Tris-HCl, pH 8.0<br>5 mM $MgCl_2$<br>100 mM Potassium Chloride (KCl)<br>1 mM 2-Mercaptoethanol<br>0.02% Triton X-100<br>0.1 mg/ml BSA |
| Buffer R | 10 mM Tris-HCl, pH 8.5<br>10 mM $MgCl_2$<br>100 mM KCl<br>0.1mg/ml BSA |
| Buffer Tango, pH 7.9 | 33 mM Tris-Acetate<br>100 mM Magnesium Acetate<br>66 mM Potassium Acetate<br>0.1 mg/ml BSA |
| Cell Resuspension Solution | 100 µg/ml RNase A<br>25 mM Tris-HCl, pH 7.5<br>10 mM EDTA |
| Cell Lysis Solution | 1 % SDS (w/v)<br>0.2 % NaOH (w/v) |
| Coomassie Brilliant Blue | 0.025% (w/v) Coomassie Brilliant Blue R250<br>(Searle Diagnostics, High Wycombe Bucks, England)<br>40% (v/v) Methanol |

| | |
|---|---|
| | (Merck Chemicals (Pty) Ltd, Saarchem, Wadeville, Gauteng, South Africa)<br>7% (v/v) Glacial Acetic Acid<br>(Merck Chemicals (Pty) Ltd, Saarchem, Wadeville, Gauteng, South Africa) |
| 0.1 % DEPC-Treated $H_2O$ (v/v) | 1 ml DEPC (Sigma-Aldrich Chemie GmbH, Steinheim, Switzerland) in 1 l $dH_2O$.<br>Shake at 37 ˚C overnight and autoclave. |
| Destain Solution | Ratio 13: 2: 5 – $dH_2O$: Glacial Acetic Acid: Ethanol |
| 10X Detection Buffer (Roche Diagnostics GmbH, Manneheim, Germany) | 0.1 M Tris-HCl, pH 9.5<br>0.1 M Sodium Chloride (NaCl) |
| 1X Detection Buffer | Dilute 1:10 10X Detection Buffer<br>Make solution up to final volume with $sdH_2O$ |
| 40% Dextran (v/v) | Dissolved 40 g Dextran Sulphate Sodium Salt (Sigma-Aldrich Chemie GmbH, Steinheim, Germany) in 70 ml DEPC-treated $H_2O$ by heating at 68 ˚C for 3-4 hours and making up to a final volume of 100 ml with DEPC-treated $H_2O$. Store at 4 ˚C. |
| DNA Molecular Weight Marker XIV | 10 mM Tris-HCl, pH8.0<br>1 mM EDTA |
| DNase Incubation Buffer | 1 M NaCl<br>20 mM Tris-HCl, pH 7.0<br>10 mM (Manganese Chloride) $MnCl_2$ |
| dNTP Mix (First Strand | 10 mM Deoxyadenine Triphosphate (dATP) |

| | |
|---|---|
| cDNA Synthesis Kit) | 10 mM Deoxycytosine Triphosphate (dCTP)<br>10 mM dT Triphosphate (dTTP)<br>10 mM Deoxyguanine Triphosphate (dGTP) |
| dNTP Mix (ImProm-II™ Reverse Transcription System) | 10 mM dATP<br>10 mM dTTP<br>10 mM dCTP<br>10 mM GTP |
| 0.5 M EDTA, pH 8.0 | Dissolved 18.62 g EDTA in 50 ml sd$H_2O$. Added 1.0 M drops of NaOH until pH reaches 8.0 and made up to 100 ml with DEPC-treated $H_2O$ |
| Electrophoresis Buffer | 3 g Tris (Merck Chemicals (Pty) Ltd, Saarchem, Wadeville, Gauteng, South Africa)<br>14.4 g Glycine (Riedel-de-Haën, Sigma-Aldrich Laborchemikalien GmbH, Seelze)<br>1.0 g SDS (Roche Diagnostics GmbH, Manneheim, Germany)<br>Dissolve in 1 l d$H_2O$ |
| Elution Buffer | Nuclease-Free, Sterile, Double d$H_2O$ |
| 90% Ethanol (v/v) | 45 ml 100% Ethanol in 5ml DEPC-treated $H_2O$ |
| 70 % Ethanol (v/v) | 35 ml 100 % Ethanol in 15 ml DEPC-treated $H_2O$ |
| 50% Ethanol (v/v) | 25 ml 100% Ethanol in 25 ml DEPC-treated $H_2O$ |
| 37% Formaldehyde (v/v) | Add 3.7 ml to 6.3 ml DEPC-treated $H_2O$ |
| Formaldehyde Gel Loading Buffer | 720 µl Formamide (Fluka Chemie GmbH, Sigma-Aldrich Chemie Gmbh, Steinheim, Switzerland)<br>160 µl 10X MOPS Buffer |

| | |
|---|---|
| | 260 µl 37% Formaldehyde (v/v)<br>(Riedel-de-Haën, Sigma-Aldrich Laborchemikalien GmbH, Seelze)<br>100 µl sd$H_2O$<br>10 mg/ml Ethidium Bromide<br>80 µl Bromophenol Blue in DEPC-treated $H_2O$ |
| 50% Formamide (v/v) | 12.5 ml 100% Formamide in 12.5 ml DEPC-treated $H_2O$ |
| GeneRuler$^{TM}$ 100 bp DNA Ladder/ GeneRuler$^{TM}$ 50 bp DNA Ladder (ready to use ladders) | 10 mM Tris-HCl, pH7.6<br>1 mM EDTA<br>0.005% Bromophenol Blue<br>0.005% Xylene Cyanol FF<br>10% Glycerol (v/v) |
| 0.1 M HCl | Dilute 10 ml 9 M HCl (v/v) (Merck Chemicals (Pty) Ltd, Saarchem, Wadeville, Gauteng, South Africa) with 990 ml DEPC-treated $H_2O$ |
| Hybridisation Buffer | 1 ml 20X SSC<br>2.5 ml 40% Dextran (v/v)<br>20 µl 10% SDS<br>5 ml 100% Formamide<br>1.4 ml DEPC-treated $H_2O$<br>Store at –20 ˚C in 1 ml aliquots. |
| 0.5 M IPTG | Dissolved 0.12 g IPTG (Fermentas Life Sciences, Hanover, MD, USA) in 1 ml d$H_2O$ |
| IQ$^{TM}$ SYBR® Green Supermix | 100 mM KCl<br>40 mM Tris-HCl, pH 8.4 |

| | |
|---|---|
| | 0.4 mM dATP<br>0.4 mM dCTP<br>0.4 mM dGTP<br>0.4 mM dTTP<br>*Taq* DNA Polymerase (50 units/ml)<br>6 mM $MgCl_2$<br>SYBR Green I<br>20 nM Fluorescein |
| LB Broth | 1% Bacto-Tryptone (w/v) (Merck Chemicals (Pty) Ltd, BioLab Diagnostics (Pty) Ltd, Wadeville, Gauteng, South Africa)<br>0.5% Bacto-Yeast Extract (w/v) (Merck Chemicals (Pty) Ltd, BioLab Diagnostics (Pty) Ltd, Wadeville, Gauteng, South Africa)<br>1% NaCl (w/v)<br>Bring to 1 litre with $dH_2O$ and autoclave. |
| LB Agar (LA) containing 269 mM Ampicillin | 1.4% Nutrient Agar (w/v) (Fluka Chemie Gmbh, Sigma-Aldrich Chemie GmbH, Steinheim, Switzerland)<br>Boil to dissolve and autoclave. Dissolve 50 µl 269 mM Ampicillin to slightly cooled LA and swirl to mix. Pour agar in petri dishes and store at 4 ˚C |
| LB Plates containing $MgCl_2$ | 1.4% Nutrient Agar (w/v)<br>10 mM $MgCl_2$ (Merck Chemicals (Pty) Ltd, Saarchem, Wadeville, Gauteng, South Africa)<br>Boil to dissolve and autoclave. |

| | |
|---|---|
| 4 M LiCl | Dissolved 8.478 g LiCl (Sigma-Aldrich GmbH & Co KG, Steinheim, Germany) in 50 ml sd$H_2O$ |
| Lysis/-Binding Buffer, pH 6.6 | 4.5M Guanidine-HCl<br>50 mM Tris-HCl<br>30% Triton X-100 (w/v) |
| 10X Maleic Acid Buffer<br>(Roche Diagnostics GmbH, Manneheim, Germany) | 0.1 M Tris-HCl<br>0.15 M NaCl<br>Adjust to pH 7.5 with NaOH (solid) |
| Membrane Binding Solution | 4.5 M Guanidine Isothiocyanate<br>0.5 M Potassium-Acetate, pH 5.0 |
| Membrane Wash Solution | 10 mM Potassium Acetate, pH 5.0<br>80 % Ethanol<br>16.7 µM EDTA, pH 8.0 |
| 10X MOPS Buffer | 400 mM MOPS (Fluka Chemie Gmbh, Sigma-Aldrich Chemie GmbH, Steinheim, Switzerland)<br>48 mM EDTA<br>400 mM Sodium Citrate |
| 1X MOPS Buffer | Add 100 ml 10X MOPS to 900 ml DEPC-treated $H_2O$ |
| 5 M NaCl | 73.05g NaCl (Merck Chemicals (Pty) Ltd, Saarchem, Wadeville, Gauteng, South Africa) dissolved in 250 ml $dH_2O$. Autoclave. |
| 1.0 M NaOH | Dissolved 36.9 g NaOH (Merck Chemicals (Pty) Ltd, Saarchem, Wadeville, Gauteng, South Africa) in 100 ml $dH_2O$. |
| NBT/BCIP Diluted 1:50 in 1X | Add 40 µl NBT/BCIP to 2 ml 1X Detection Buffer |

| | |
|---|---|
| Detection Buffer | |
| Neutralization Solution, pH 4.2 | 0.75 M Potassium Acetate (Kac)<br>2.12 M Glacial Acetic Acid<br>4.09 M Guanidine Hydrochloride |
| 10X NTP Labelling Mix | 10 mM ATP<br>10 mM Cytosine Triphosphate (CTP)<br>10 mM Guanidine Triphosphate (GTP)<br>6.5 mM Uridine Triphosphate (UTP)<br>3.5 mM DIG-11-UTP |
| PageRuler$^{TM}$ Prestained Protein Ladder | 0.1-0.2 mg/ml of each protein in 62.5 mM Tris-$H_3PO_4$, pH 7.5<br>1 mM EDTA<br>2% SDS (w/v)<br>10 mM DTT<br>1 mM $NaN_3$<br>33% Glycerol (w/v) |
| 0.01 M PBS, pH 7.4 | Dissolved 5 PBS (Sigma-Aldrich Chemie GmbH, Steinheim, Germany) tablets in 1 l $dH_2O$ and autoclaved. |
| 2X PCR Master Mix | 50 units/ml *Taq* DNA Polymerase<br>400 µM dATP<br>400 µM dCTP<br>400 µM dGTP<br>400 µM dTTP<br>3mM $MgCl_2$ |
| 4% PFA | 2.5 g PFA (Merck Chemicals (Pty) Ltd, Saarchem, |

| | |
|---|---|
| | Wadeville, Gauteng, South Africa) dissolved in 25 ml 200 mM Phosphate Buffer by slow heating to 60 ˚C until solution becomes clear. |
| 200 mM Phosphate Buffer, pH7.4 | 4.3 g Disodium Hydrogen-Orthophosphate ($Na_2HPO_4$) Anhydrous (Merck Chemicals (Pty) Ltd, Saarchem, Wadeville, Gauteng, South Africa)<br>3.1 g Sodium Dihydrogen Phosphate ($NaH_2PO_4$) (Riedel-de-Haën, Sigma-Aldrich Laborchemikalien GmbH, Seelze)<br>Add 250 ml DEPC-treated $H_2O$ and autoclave. |
| 2X Rapid Ligation Buffer | 60 mM Tris-HCl, pH 7.8<br>20 mM $MgCl_2$<br>20 mM DTT<br>2 mM ATP<br>10% Polyethylene Glycol (PEG) |
| 10X Reaction Buffer, pH 8.3 (First Strand cDNA Synthesis Kit) | 100 mM Tris<br>500 mM KCl |
| 5X Reaction Buffer (ImProm-II™ Reverse Transcription System) | 250 mM Tris-HCl, pH 8.3<br>375 mM KCl<br>50 mM DTT |
| 10X Restriction Buffer A, pH 7.9 | 330 mM Tris-Acetate<br>660 mM Potassium Acetate<br>100 mM Magnesium Acetate<br>5 mM DTT |
| 10X Restriction Buffer H | 500 mM Tris-HCl, pH 7.5 |

| | |
|---|---|
| | 1 M NaCl<br>100 mM $MgCl_2$<br>10 mM DTT |
| Restriction Buffer $O^+$ | 50 mM Tris-HCl, pH 7.5<br>10 mM $MgCl_2$<br>100 mM NaCl<br>0.1 mg/ml Bovine Serum Albumin (BSA) |
| 2X Sample Dye | 0.09 M Tris-HCl, pH 6.8<br>20% (v/v) Glycerol<br>2% (w/v) SDS<br>0.02% (w/v) Bromophenol Blue<br>0.1 M DTT (Roche Diagnostics GmbH, Manneheim, Germany) |
| 10% SDS (w/v) | Dissolve 10 g SDS in 100 ml DEPC-treated $H_2O$ |
| 10% SDS (w/v)<br>(Electrophoresis) | Dissolve 10 g SDS in 100 ml $dH_2O$ |
| 20X SSC | Dissolve 175.3 g NaCl, 88.2 g Tri-Sodium Citrate (Merck Chemicals (Pty) Ltd, Saarchem, Wadeville, Gauteng, South Africa) in 800 ml DEPC-treated $H_2O$. Adjust to pH 7.0 with 1 M HCl and make up to a final volume 1 l DEPC-treated $H_2O$ |
| 5X SSC | 1.625 ml 20X SSC in 18.75 ml DEPC-treated $H_2O$ |
| 2X SSC | 40 ml 20X SSC in 360 ml $dH_2O$ |
| 1X SSC | 20 ml 20X SSC in 380 ml $dH_2O$ |
| 0.5X SSC | 10 ml 20X SSC in 390 ml $dH_2O$ |

| | |
|---|---|
| 0.1X SSC | 2 ml 20X SSC in 398 ml $dH_2O$ |
| 10X TBS | 50 ml 1 M Tris, pH 7.5<br>30 ml 5 M NaCl<br>Make up to 1 l with DEPC-treated $H_2O$ |
| 20X TBS-Tween 20 | 5 ml of Tween 20 (Merch-Schuhardt) per 1 l TBS |
| 10X TBE Buffer, pH 8.2 | 0.89 M Tris<br>0.89 M Boric Acid (Riedel-de-Haën, Sigma-Aldrich Laborchemikalien GmbH, Seelze)<br>25 mM EDTA<br>Adjust to pH 8.2 with 1 M HCl |
| 1X TBE Buffer, pH 8.2 | Add 100 ml of 10X TBE Buffer to 900 ml $dH_2O$ |
| 1X TE Buffer, pH 8.0 | 10 mM Tris<br>1 mM EDTA<br>Adjust to pH 8.0 using 9M HCl |
| Tfb1 | 30 mM KAc (Fluka Chemie Gmbh, Sigma-Aldrich Chemie GmbH, Steinheim, Switzerland)<br>50 mM $MnCl_2$ (Riedel-de-Haën, Sigma-Aldrich Laborchemikalien GmbH, Seelze)<br>100 mM KCl (Riedel-de-Haën, Sigma-Aldrich Laborchemikalien GmbH, Seelze)<br>10 mM Calcium Chloride ($CaCl_2$) (Riedel-de-Haën, Sigma-Aldrich Laborchemikalien GmbH, Seelze)<br>15% (v/v) Glycerol<br>Solution was sterilised by filtration |
| Tfb2 | 10 mM MOPS, pH7.0 |

| | |
|---|---|
| | 75 mM $CaCl_2$<br>10 mM KCl<br>15% (v/v) Glycerol<br>Solution was sterilised by filtration |
| TNB | 2 ml Maleic Acid<br>2.5 ml Blocking Buffer<br>45 ml TBS |
| 0.5 M Tris-HCl, pH 6.8 | Dissolve 6.05 g Tris in 95 ml $dH_2O$. Adjust to pH 6.8 with 9M HCl. Make the solution up to 100 ml with $dH_2O$. |
| 1 M Tris, pH 7.5 | 6.1 g Tris dissolved in 50 ml $dH_2O$<br>Adjust pH to 7.5 with 1 M HCl and autoclave. |
| 1.5 M Tris-HCl, pH 8.8 | Dissolve 18.15 g Tris in 95 ml $dH_2O$. Adjust to pH 8.8 with 9 M HCl. Make the solution up to 100 ml with $dH_2O$. |
| TYM Broth | 2.0 % Bacto-Tryptone (w/v)<br>0.5 % Bacto-Yeast Extract (w/v)<br>0.1 M Sodium Chloride (NaCl)<br>10 mM $MgCl_2$<br>pH to 7.0 with 1.0 M NaOH. Autoclave. |
| 1X Washing Buffer (Roche Diagnostics GmbH, Manneheim, Germany) | 0.1 M Maleic Acid Buffer<br>0.15 M NaCl<br>0.3% Polyethylene Sorbitan Monolaurat (Tween 20) (v/v) |
| Wash Buffer I | 5 M Guanidine Hydrochloride<br>20 mM Tris-HCl, pH 6.6<br>20 ml 100% Ethanol |
| Wash Buffer II | 20 mM NaCl |

| | |
|---|---|
| | 1 mM Tris-HCl, pH 7.5<br>40 ml 100% Ethanol |
| Wash Solution | 60.0 mM KAc, pH 7.5<br>8.3 mM Tris-HCl, pH 7.5<br>40 μM EDTA, pH 8.0<br>60 % Ethanol (v/v) |

# APPENDIX 3: Composition of Reactions and Procedures

**Table 1: Composition of Reverse Transcription Reaction**

| Reagents | Volume (µl) |
|---|---|
| 10X Reaction Buffer | 2 |
| 25 mM $MgCl_2$ | 4 |
| 10 mM Deoxyribonucleotide Triphosphate (dNTP) Mix | 2 |
| Oligo-p$(dT)_{15}$ Primer (0.8 µg/µl) | 2 |
| RNase Inhibitor | 1 |
| Total RNA Sample | 1 |
| AMV Reverse Transcriptase | 1 |
| Nuclease-Free $H_2O$ | 7 |
| Total Volume | 20 |

**Table 2: Reverse Transcription Conditions used to Synthesise Complementary DNA**

| Step | Temperature (˚C) | Time (min) |
|---|---|---|
| Annealing of oligo-p(dT) Primer | 25 | 10 |
| Reverse Transcription | 42 | 60 |
| Denaturation | 99 | 5 |

**Table 3: Composition of Polymerase Chain Reaction (PCR) Reaction**

| Reagents | Volume (µl) |
|---|---|
| 2X PCR Master Mix (Promega Corporation, Madison, WI, USA) | 12.5 |
| Forward Primer | 1.0 |
| Reverse Primer | 1.0 |
| 25 mM $MgCl_2$ Stock Solution (Promega Corporation, Madison, WI, USA) | 2.0 |
| Nuclease Free $H_2O$ | 7.5 |
| Template DNA (cDNA) | 1.0 |
| Total Volume | 25.0 |

**Table 4: PCR Conditions used to amplify the Region of Interest**

| Step | Temperature (˚C) | Time (s) | Cycle |
|---|---|---|---|
| Denaturation | 95 | 120 | 1 |
| Denaturation | 95 | 30 | |
| Annealing | 58 | 30 | 30 |
| Extension | 72 | 60 | |
| Extension | 72 | 60 | 1 |

**Table 5: Composition of Ligation Reaction**

| Reagents | Volume (µl) |
|---|---|
| 2X Rapid Ligation Buffer | 5 |
| 10 ng/µl pGEM-T Easy Vector | 1 |
| PCR Product | 1 |
| T4 DNA Ligase | 1 |
| Nuclease Free $H_2O$ | 3 |
| Total Volume | 10 |

**Table 6: Composition Restriction Digestion Reaction**

| Reagents | Volume (µl) |
|---|---|
| Purified Clone | 10 |
| 10X Restriction Buffer H | 1 |
| Restriction Enzyme: *Eco*RI or *Pst*I | 1 |
| $SdH_2O$ | 18 |
| Total Volume | 30 |

**Table 7: Composition of *In Vitro* Transcription Reactions**

| Reagent | Control cRNA (µl) | Sense Probe (µl) | Anti-Sense Probe (µl) |
|---|---|---|---|
| Control DNA PSPT 18-Neo/PvuII | 4 | - | - |
| ApaI Digested Linearised Clone | - | 6 | - |
| PstI Digested Linearised Clone | - | - | 6 |
| 10X NTP Labelling Mix | 2 | 2 | 2 |
| 10X Transcription Buffer | 2 | 2 | 2 |
| SP6 RNA Polymerase | 2 | 2 | - |
| T7 RNA Polymerase | - | - | 2 |
| DEPC-Treated $H_2O$ | 10 | 8 | 8 |
| Total Volume | 20 | 20 | 20 |

**Table 8: Serial Dilutions of Probes to Estimate Minimal Concentrations of Probes**

| Dilution | DIG-Labelled Control cRNA | DIG-Labelled cRNA of Control PSPT 18-Neo/PvuII | PBR Probes (Sense and Anti-Sense) |
|---|---|---|---|
| Initial Concentration | 10 µg/100 µl | 250 ng/50 µl | 5 µg/25 µl |
| Dilution 1 [20 ng/µl] | (1:5) 1 µl + 4 µl $sdH_2O$ | - | (1:10) 1 µl + 9 µl $sdH_2O$ |
| Dilution 2 [1 ng/µl] | (1:20) 2 µl + 38 µl $sdH_2O$ | (1:5) 2 µl + 8 µl $sdH_2O$ | (1:20) 2 µl + 38 µl $sdH_2O$ |
| Dilution 3 [100 pg/µl] | (1:10) 5 µl + 45 µl $sdH_2O$ | (1:10) 5 µl + 45 µl $sdH_2O$ | (1:10) 5 µl + 45 µl $sdH_2O$ |
| Dilution 4 [10 pg/µl] | (1:10) 5 µl + 45 µl $sdH_2O$ | (1:10) 5 µl + 45 µl $sdH_2O$ | (1:10) 5 µl + 45 µl $sdH_2O$ |
| Dilution 5 [1 pg/µl] | (1:10) 5 µl + 45 µl $sdH_2O$ | (1:10) 5 µl + 45 µl $sdH_2O$ | (1:10) 5 µl + 45 µl $sdH_2O$ |
| Dilution 6 [0.1 pg/µl] | (1:10) 5 µl + 45 µl $sdH_2O$ | (1:10) 5 µl + 45 µl $sdH_2O$ | (1:10) 5 µl + 45 µl $sdH_2O$ |
| Dilution 7 [0.01 pg/µl] | (1:10) 5 µl + 45 µl $sdH_2O$ | (1:10) 5 µl + 45 µl $sdH_2O$ | (1:10) 5 µl + 45 µl $sdH_2O$ |

**Table 9: Composition of Reverse Transcription Reaction**

| Reagents | Volume (µl) |
|---|---|
| 5X Reaction Buffer | 4 |
| 25 mM $MgCl_2$ | 4 |
| 10 mM dNTP Mix | 2 |
| Primer Oligo-$(dT)_{15}$ (0.5 mg/ml) | 2 |
| RNase Inhibitor (20-40 units/µl) | 1 |
| Nuclease Free $H_2O$ | 5.2 |
| ImProm-II™ Reverse Transcriptase | 0.8 |
| RNA (Template) | 1 |
| Total Volume | 20 |

**Table 10: Reverse Transcription Conditions used to Synthesise Complementary DNA**

| Step | Temperature (˚C) | Time (min) |
|---|---|---|
| Annealing of Oligo-dT Primer | 25 | 10 |
| Reverse Transcription | 42 | 60 |
| Denaturation | 99 | 5 |

**Table 11: Composition of Relative Quantitative Polymerase Chain Reaction (PCR)**

| Reagents | Volume (µl) |
|---|---|
| iQ™ SYBR® Green Mix (Bio-Rad Laboratories, Hercules, CA, USA) | 12.5 |
| Forward Primer (10 pmol/µl) | 1.0 |
| Reverse Primer (10 pmol/µl) | 1.0 |
| 25 mM $MgCl_2$ Stock Solution (Promega Corporation, Madison, WI, USA) | 2.0 |
| $sdH_2O$ | *x* |
| Template DNA (cDNA) (1 µg/µl) | *y* |
| Total Volume | 25 |

1. *x* and *y* are variable depending on the concentration of the template (cDNA).

**Table 12: Relative Quantitative PCR Conditions used to Amplify Region of Interest**

| Step | Temperature (˚C) | Time (s) | Plate Read | Cycle |
|---|---|---|---|---|
| Denaturation | 95 | 120 | - | 1 |
| Denaturation<br>Annealing<br>Extension | 95<br>58<br>72 | 30<br>30<br>60 | -<br>-<br>Yes (Single) | 40 |
| Extension | 72 | 600 | - | 1 |
| Melting Curve | 55-95<br>(rises in 1 ˚C increments) | 10 (at each temperature) | Yes<br>(Continuous) | 1 |
| Cooling | 20 | Forever | - | 1 |

**Table 13: Reagents used in Preparation of SDS-PAGE**

| Reagent | Separating Gel (ml) | Stacking Gel (ml) |
|---|---|---|
| $dH_2O$ | 3.35 | 6.1 |
| 1.5 M Tris-HCl, pH8.8 | 2.5 | - |
| 0.5 M Tris-HCl, pH 6.8 | - | 2.5 |
| 40% Acrylamide-Bis Stock Solution (Promega Corporation, Madison, WI, USA) | 4.0 | 1.3 |
| 10% SDS (w/v) | 0.1 | 0.1 |
| 10% Ammonium Persulphate (w/v) | 0.05 | 0.05 |
| TEMED (Promega Corporation, Madison, WI, USA) | 0.01 | 0.01 |

# APPENDIX 4: Sequence

```
1   atggccccgc cctgggtgcc cgccatgggc ttcacgctgg cgcccagcct ggggtgcttc
61  gtgggctccc gctttgtcca cggcgagggt ctccgctggt acgccggcct gcagaagccc
121 tcgtggcacc cgccccactg ggtgctgggc cctgtctggg gcacgctcta ctcagccatg
181 gggtacggct cctacctggt ctggaaagag ctgggaggct tcacagagaa ggctgtggtt
241 ccctgggcc tctacactgg gcagctggcc ctgaactggg catggccccc catcttcttt
301 ggtgcccgac aaatgggctg ggccttggtg gatctcctgc tggtcagtgg ggcggcggca
361 gccactaccg tggcctggta ccaggtgagc ccgctggccg cccgcctgct ctacccctac
421 ctggcctggc tggccttcgc gaccacactc aactactgcg tatggcggga caaccatggc
481 tggcatgggg gacggcggct gccagagtag
```

**Figure 1: Sequence of the *Peripheral Benzodiazepine Receptor* (*PBR*) Gene**

The sequence of the *PBR* gene was obtained from GenBank at NCBI and has an Accession Number of BT006949. The bold nucleotides in the sequence represent the region at which the forward primer and reverse primer bind respectively to the PBR product. The blue coloured portion of sequence represents the fragment of the *PBR* gene that is amplified and is located between mRNA position 283 and 532. The PBR fragment amplified is 247 bp in size.

(Reference: URL: http://www.ncbi.nlm.nih.gove/entrez/viewer.fcgi?db=nucleotide&val=30582736)

# APPENDIX 5: Vectors

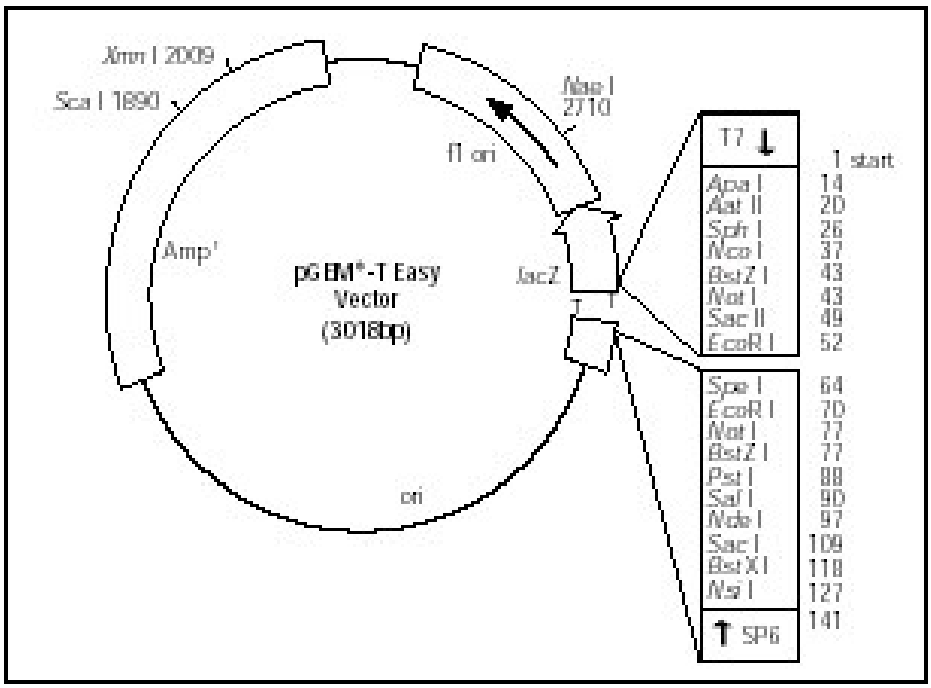



**Figure 1: Schematic Diagram of the pGEM-T Easy Vector**

The pGEM-T Easy vector is made up of 3018 bp. The T7 RNA polymerase transcription initiation site occurs at position 1, SP6 RNA polymerase initiation sites occurs at position 141, the T7 RNA polymerase promoter region occurs between 3002 and 3006, the SP6 RNA polymerase promoter region occurs between position 136 and 158, the multiple cloning site occurs between positions 10 and 128. In addition, the position at which restriction enzymes cleave the vector is indicated. (Reference: URL: http://www.tcd.ie/Genetics/staff/Noel.Murphy/recombinat%20dna%20ge4021/pgem.pdf)

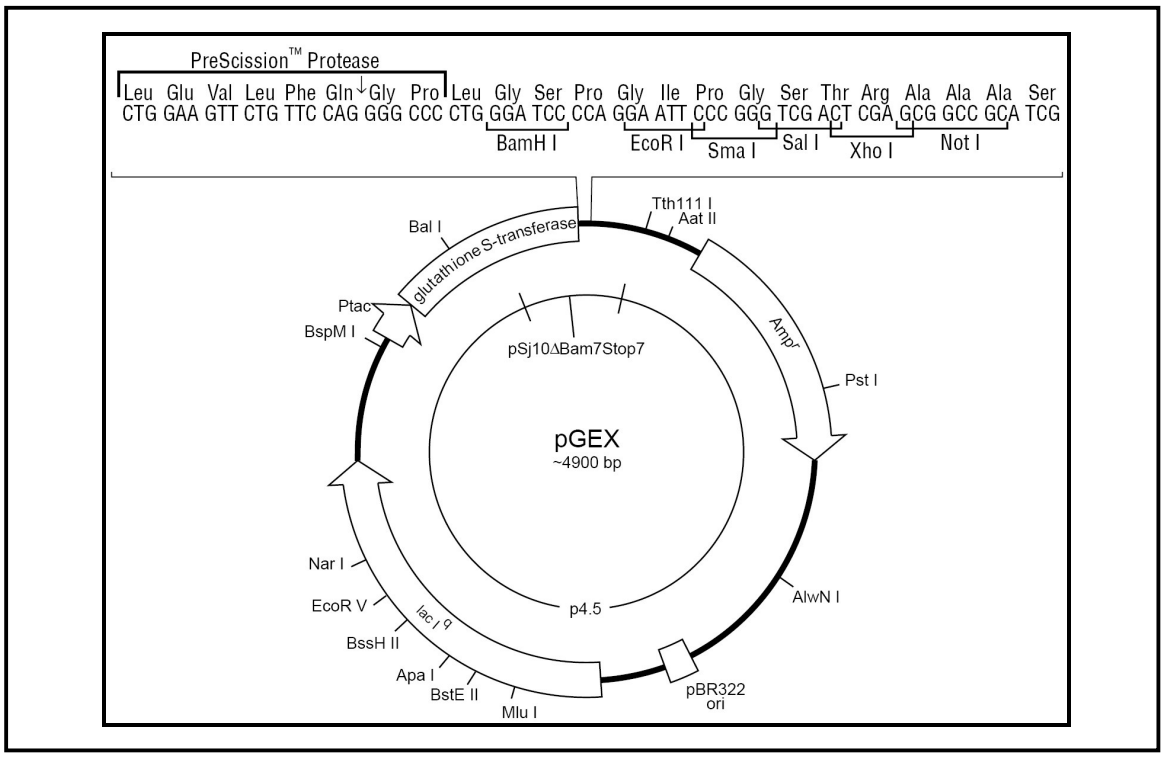



**Figure 2: Schematic Diagram of pGEX-6P-2 Expression Vector**

The pGEX-6P-2 expression vector is approximately 4900 bp in size and consists of a *tac* promoter that makes the expression vector chemically inducible, allows for a high level of expression and controls the expression of gluthathione-*S*-transferase, an internal *lac* $I^q$ gene that encodes for the *lac* repressor which allows for the expression of genes downstream of the *tac* promoter when induced with isopropyl-β-D-thiogalactopyranoside (IPTG), PreScission™ Protease recognition sites for cleaving the desired protein from the fusion product and an ampicillin resistant gene. (Reference: URL: http://www4.amershambiosciences.com/pdfs/970004M2-01.pdf)

# APPENDIX 6: DNA and Protein Ladders

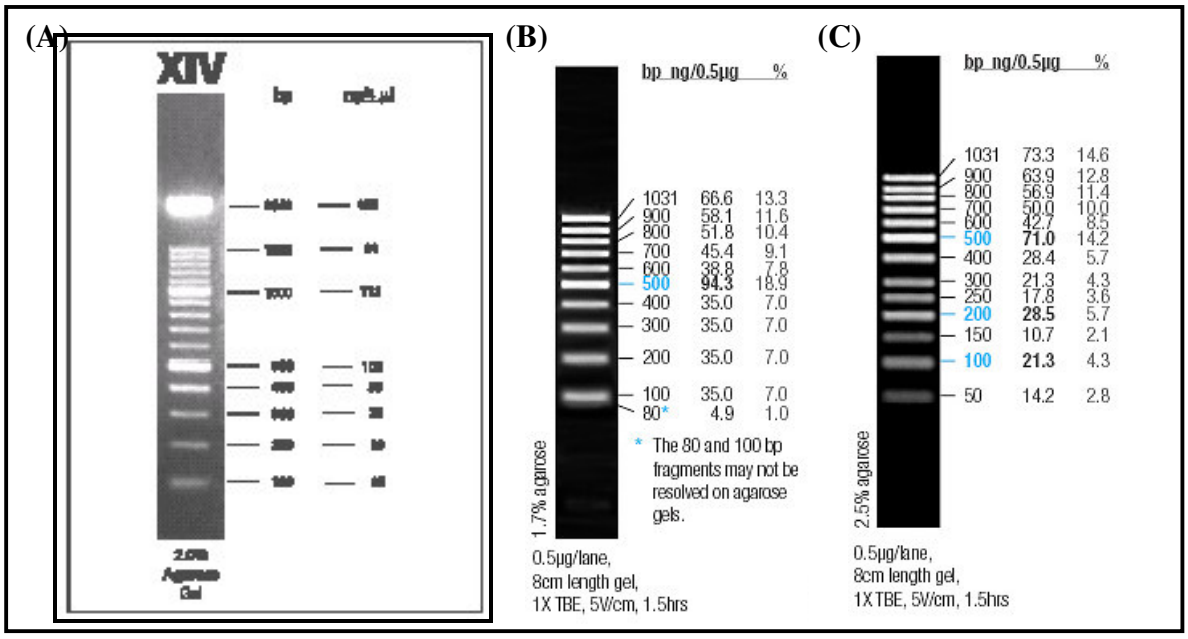



**Figure 1: DNA Molecular Weight Ladders**

DNA molecular weight ladders allows for the accurate sizing of DNA fragments generated by PCR or restriction digest in agarose gels. (A) The DNA molecular weight marker XIV allows for the accurate sizing of DNA fragments of between 100 and 1050 bp. The DNA ladder mixture consists of 15 bands plus an additional band of 2462 bp when placed under agarose gel electrophoresis. (Reference: URL: http://www.roche-applied-science.com/pack-insert/1721933a.pdf). (B) GeneRuler™ 100bp DNA Ladder allows for the accurate sizing of DNA fragments of between 80 and 1031 bp. The DNA ladder mixture results in a ladder consisting of 11 discrete bands when placed under agarose gel electrophoresis. (C) GeneRuler™ 50 bp DNA Ladder allows for the accurate sizing of DNA fragments of between 50 and 1031 bp. The DNA ladder mixture results in a ladder consisting of 13 discrete bands when placed under agarose gel electrophoresis. (Reference: URL: http://www.fermentas.com/catalog/electrophoresis/generuler.htmGenePlus)

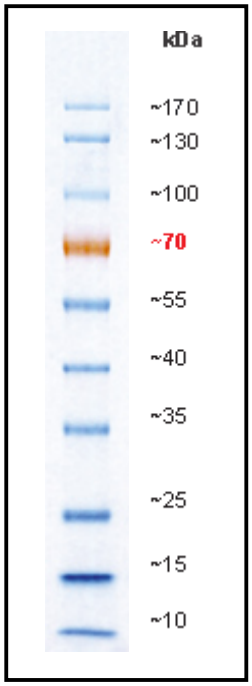



**Figure 2: Protein Molecular Weight Ladder**

Protein molecular weight ladders allow for the accurate sizing of denatured proteins generated by induction with IPTG in SDS-PAGE gels. The PageRulerT$^{M}$ Prestained Protein Ladder (Fermentas Life Sciences, Hanover, MD, USA) allows for the accurate sizing of protein between approximately 10 kDa to 170 kDa (Reference: http://www.fermentas.com/catalog/electrophoresis/markmo0671.htm).

# 3. RESULTS

## 3.1. Confirmation of the Histology and Histopathology of Normal Tissues and Histopathology of Cancer Tissues

### *3.1.1. Introduction*

Tissue specimen that have been processed, sectioned and mounted on a slide can be viewed microscopically only after it has been stained making the cells visible (Brown, 2002). In histology, the most common used stain for tissue samples fixed in formalin or alcohol is the haematoxylin and eosin stain that is the H&E stain. This stain involves two separate dyes: (i) haematoxylin, which is a dark purplish dye that stains the chromatin within the nucleus resulting in a deep purplish-blue colour and (ii) eosin, which is an orange-pink to red dye that stains cytoplasmic material such as collagen in connective tissue leaving an orange-pink counterstain (Brown, 2002). H&E staining was used to confirm the histology of the different normal tissues studied as well as to determine the histopathologies of the different cancer tissues studied before *in situ* hybridisation results could be analysed.

### *3.1.2. Histology of Normal Tissue and Histopathology of Tumour Disease in Liver*

#### *3.1.2.1. Normal Tissue*

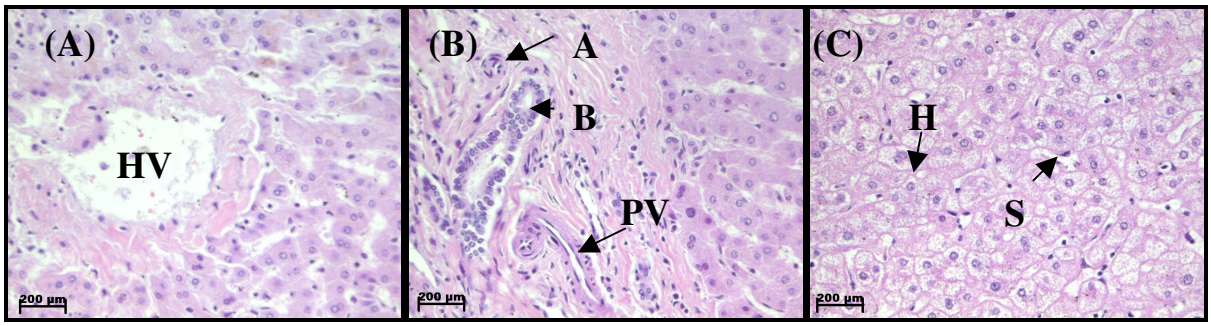



**Figure 3-1: H&E of Normal Liver Tissue**

(A) represents the hepatic venule (HV) that is lined by endothelial cells and is characterised by a clearly defined intimal layer devoid of elastic fibres and a tunica media consisting of one or two layers of smooth muscle fibres surrounded by anastomosing plates of hepatocytes and sinusoids. (B) represents the portal tract consisting of the hepatic portal vein (PV) consisting of a thin wall lined by flattened endothelial cells, a hepatic artery (A) that is thick-walled and consisting of one layer of smooth muscle cells and flattened endothelial cells and a bile duct (B) that is lined by a simple cuboidal or columnar epithelium. (C) represents anastomosing plates of hepatocytes between which the sinusoids are located. Hepatocytes (H) are large polyhedral cells with round nuclei with peripherally dispersed chromatin and prominent nucleoli. Sinusoid lining cells (S) are distinguished by their flattened condensed nuclei and attenuated poorly stained cytoplasm. (Reference: Coltran, *et al.*, 1999, Eroschenko, 2000, Young, *et al.*, 2000) (Magnification 400X)

*3.1.2.2. Hepatocellular Carcinoma*

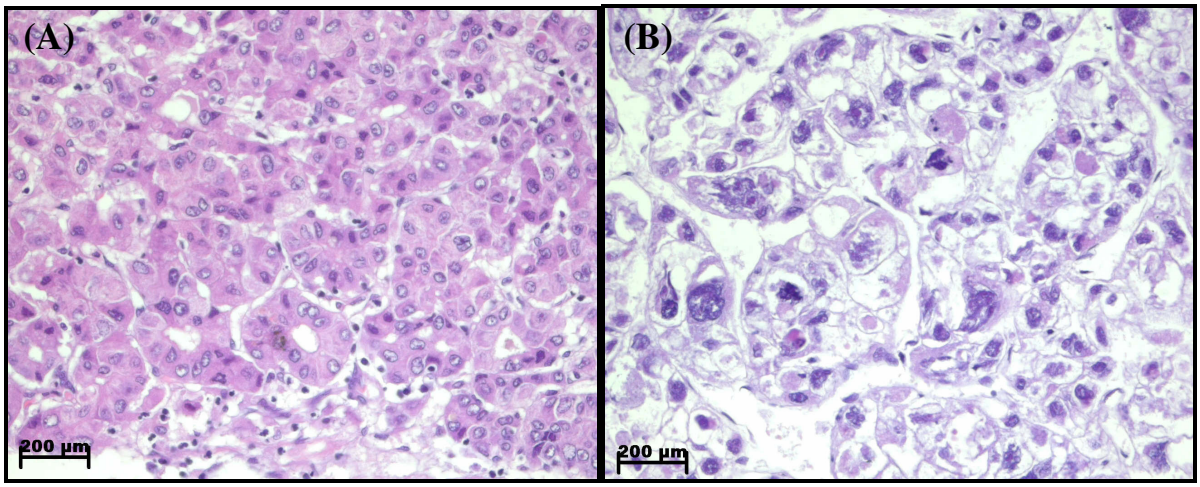



**Figure 3-2: H&E of Hepatocellular Carcinoma**

(A) represents a Grade II hepatocellular carcinoma that is characterised by tumour cells that have a tubular pattern. (B) represents a Grade III hepatocellular carcinoma that is characterised by a pleomorphic appearance with numerous anaplastic giant cells that may become small to resemble spindle cell sarcomas containing prominent nuclei and nucleoli and a scanty cytoplasm that appears basophilic. (Reference: Coltran, *et al.*, 1999, Rosai, 2004) (Magnification 400X)

### *3.1.3. Histology of Normal Tissue and Histopathology of Tumour Disease in Colon*

*3.1.3.1. Normal Tissue*

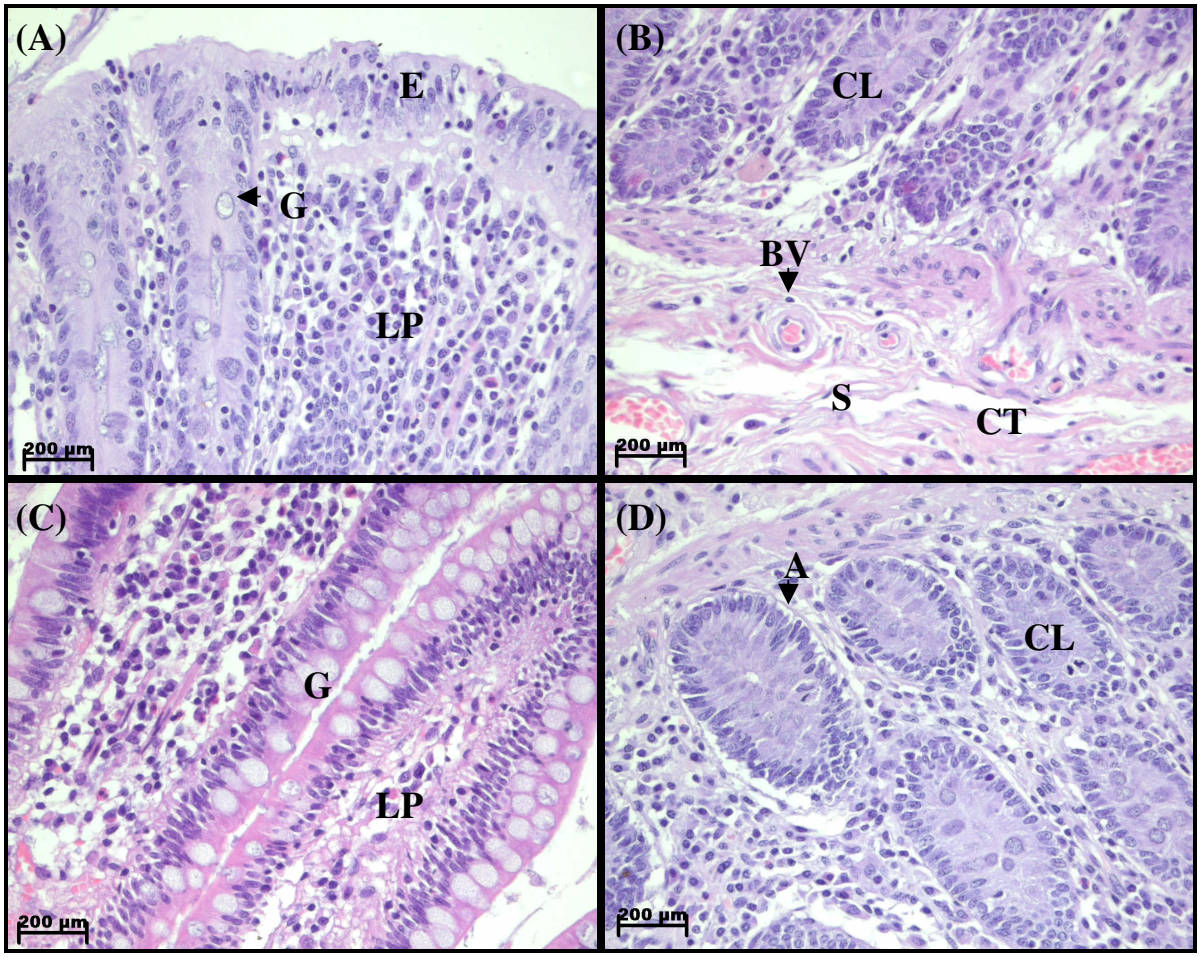



**Figure 3-3: H&E of Normal Colon Tissue**

(A) shows the epithelial layer of the mucosa that consists of columnar epithelial cells (E) with a thin striated border, numerous goblet cells (G) and lamina propria (LP) consisting of abundant lymphatic tissue. (B) shows the submucosa (S) that is found directly below the mucosa containing the crypts of Lieberkhün (CL) consisting of loose collagenous connective tissue (CT) containing large blood vessels (BV). (C) represents a longitudinal section of the crypts of Lieberkhün (CL) showing goblet cells (G) as is indicated by the small and condensed nuclei. Below the goblet cells, the lamina propria (LP) can be seen that consists of abundant lymphatic tissue. (D) represents a traverse section of the crypts of Lieberkhün (CL) showing absorptive cells (A) as is indicated by the tall columnar cells consisting of the oval basal nuclei. (Reference: Coltran, *et al.*, 1999, Eroschenko, 2000, Young, *et al.*, 2000) (Magnification 400X)

*3.1.3.2. Colonic Adenocarcinoma*

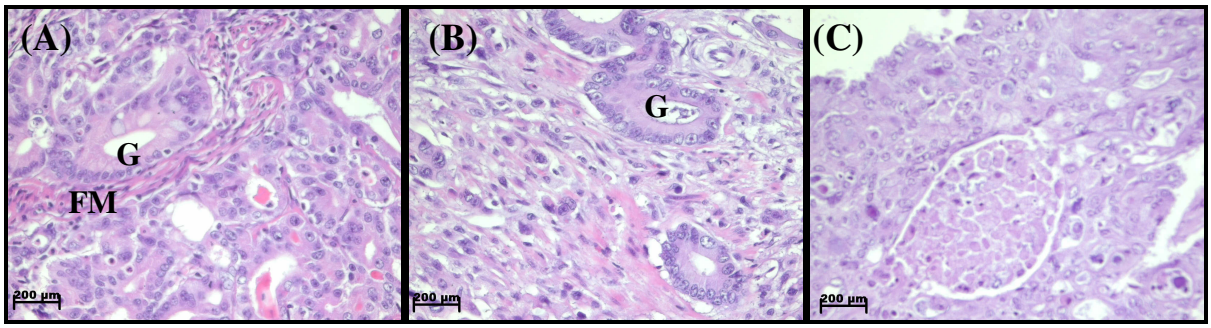



**Figure 3-4: H&E of Colonic Adenocarcinoma**

(A) represents Grade I tubular adenomas characterised adenomatous glands (G) that are well formed, irregular and tubular and surrounded by a fibromuscular (FM) stroma. (B) represents Grade II tubular adenomas characterised by the presence of fewer adenomatous glands (G) and more of the tumour cells arranged as solid sheets. (C) represents Grade III tubular adenomas that is characterised by a predominantly solid pattern with virtually no adenomatous glands. (Reference: Barbatis, 1995, Coltran *et al.*, 1999) (Magnification 400X)

### *3.1.4. Histology of Normal Tissue and Histopathology of Tumour Disease in Epiploon and Stomach*

*3.1.4.1. Normal Tissue*

*3.1.4.1.1. <u>Epiploon Normal Tissue</u>*

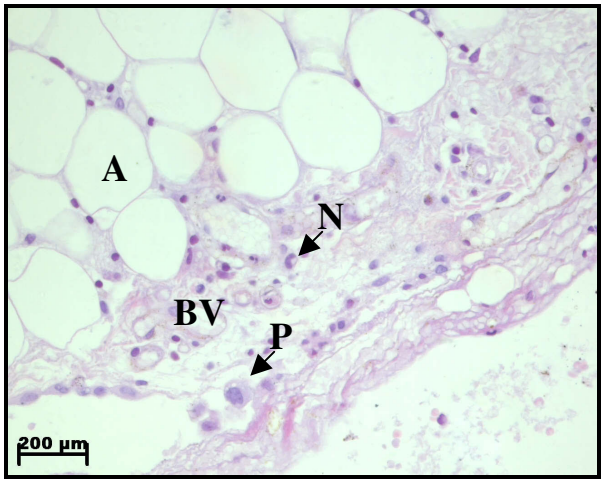



**Figure 3-5: H&E of Normal Epiploon Tissue**

The above figure represents epiploon that comprises loose connective tissue that consists of adipose tissue (A), plasma cells (P), neutrophils (N) and blood vessels (BV). (Reference: Eroschenko, 2000) (Magnification 400X)

*3.1.4.1.2.* *Stomach Normal Tissue*

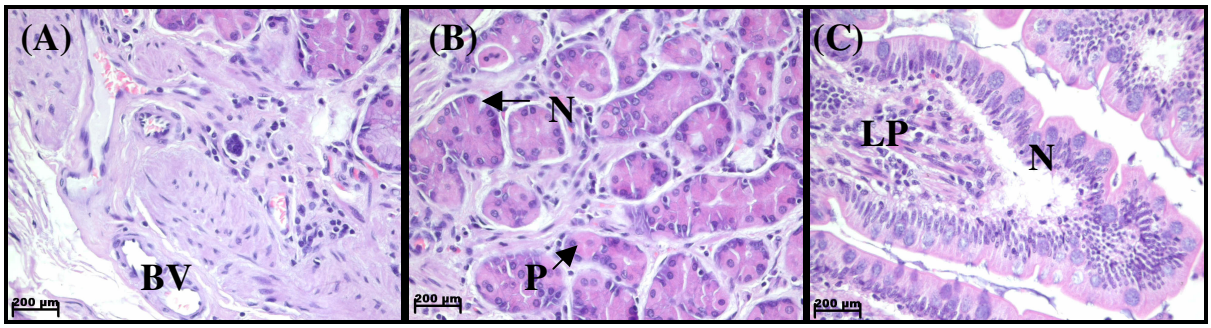



**Figure 3-6: H&E of Normal Stomach Tissue**

(A) represents the submucosa that consists of relatively loose and distensible connective tissue that contains the larger blood vessels (BV) as well as the nerves supplying the mucosa. (B) represents the transverse section of the crypts of Lieberkhün, which show the presence of the parietal cells (P) that are characterised by a rounded shape with an intensely eosinophilic cytoplasm and centrally located nucleus. Neck mucous cells (N) are found lining the glands. (C) represents the longitudinal section of the gastric glands, which shows the surface and neck mucous cells (N) that have a tall columnar shape and the underlying lamina propria (LP) that appears loose, scanty and vascular consisting of collagen and reticular fibres and fibroblasts characterised by oval nuclei. (Reference: Eroschenko, 2000, Young, *et al.*, 2000) (Magnification 400X)

*3.1.4.2. Squamous Cell Carcinoma of the Stomach*

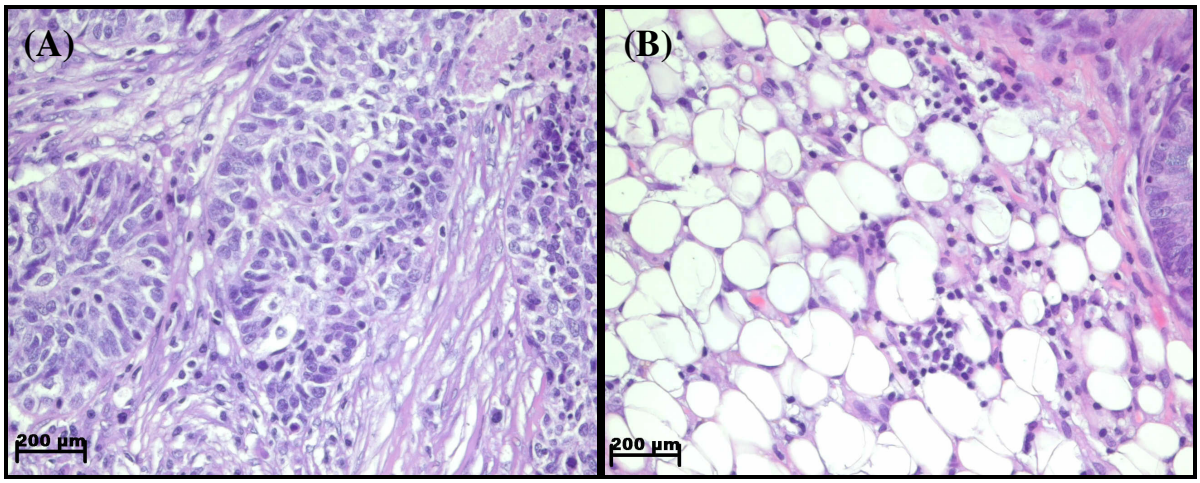



**Figure 3-7: H&E of Stomach Squamous Cell Carcinoma**

The above figure represents Grade III stomach squamous cell carcinoma. (A) represents tumour cells that are characterised by a keratin pearl formation arranged in a mosaic pattern of ectopic squamous cell nests. (B) represents the invasion of tumour cells into the epiploon as is characterised by the presence of tumour cells within the adipose tissue. (Reference: Schmidt, *et al.*, 2001, Yildrim, *et al.*, 2005) (Magnification 400X)

### *3.1.5. Histology of Normal Tissue and Histopathology of Tumour Disease in Prostate*

#### *3.1.5.1. Hyperplastic Tissue*

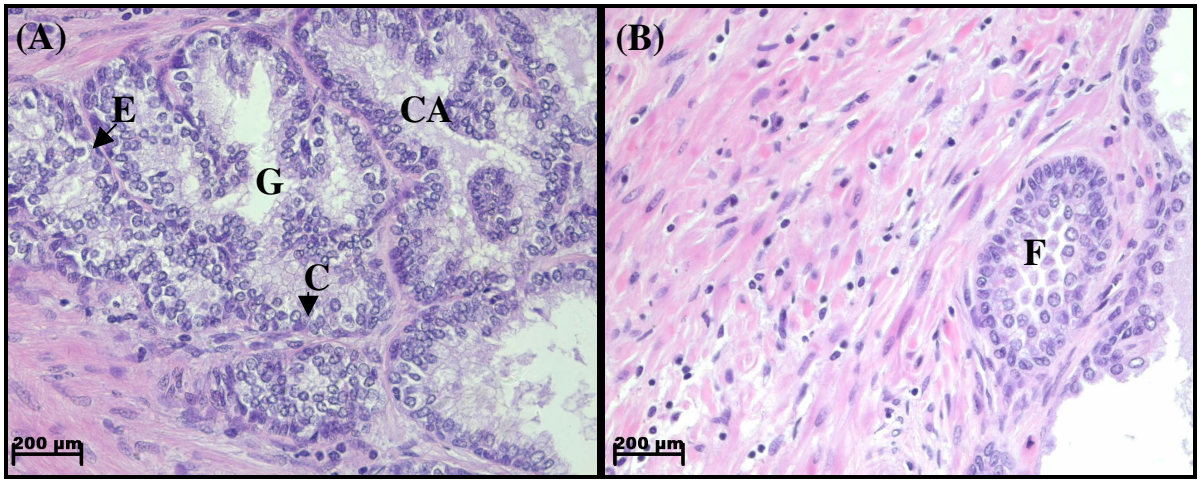



**Figure 3-8: H&E of Hyperplastic Prostate Tissue**

(A) Glandular proliferation takes the form of aggregations of small to large to cystically dilated glands (G) that are lined by an inner columnar (C) and an outer cuboidal to flattened endothelium (E). The epithelium is characteristically thrown up into numerous papillary buds and infoldings. In addition, hyperplastic tissue is characterised by foci of infarction that appear as nests and foci of squamous metaplasia that surrounds the foci of infarction. Corpora amylacea (CA) is a lamellated glycoprotein mass secreted by the prostate glands that becomes progressively calcified to form prostatic concretions with increasing age. (B) indicates hyperplastic tissue characterised by fibrous and muscular proliferation of the fibromuscular stroma. The foci of squamous metaplasia (F) occur in the margins of the foci of infarction as nests of metaplastic but orderly squamous cells (Reference: Coltran, *et al.*, 1999) (Magnification 400X)

*3.1.4.2. Adenocarcinoma of the Peripheral Ducts and Acini*

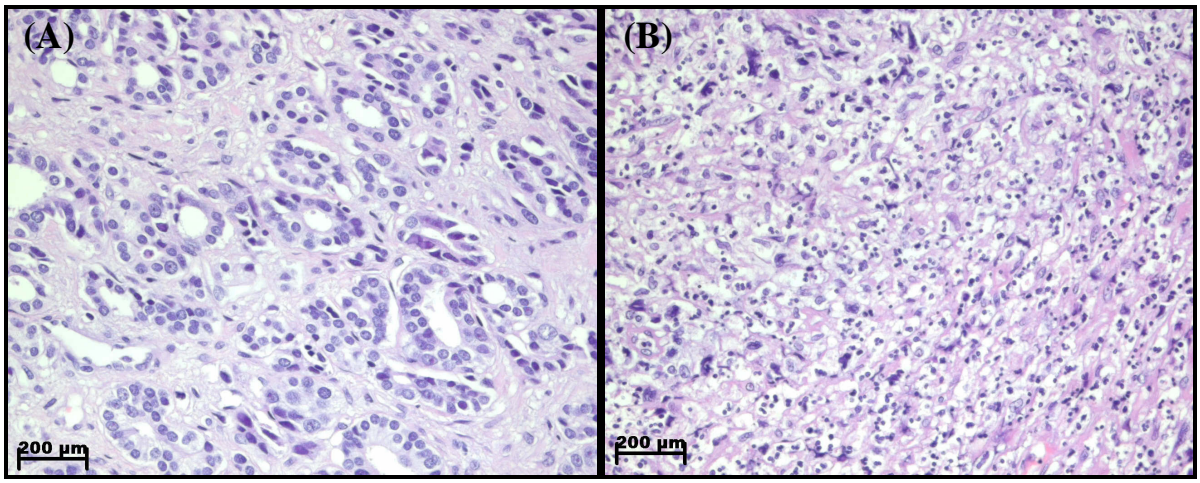



**Figure 3-9: H&E of Adenocarcinoma of the Peripheral Ducts and Acini in the Prostate**

(A) represents a Grade II prostate adenocarcinoma, which is characterised by smaller and more closely packed glands, of irregular outline and smooth inner surface with little intervening stroma between the glands. The gland consists of a single uniform layer of cuboidal to low columnar epithelium. (B) represents Grade III prostate adenocarcinoma, which is characterised by cells that tend to grow in sheets. (Reference: Coltran, *et al.*, 1999) (Magnification 400X)

### *3.1.6. Histology of Normal Tissue and Histopathology of Tumour Disease in Breast*

*3.1.6.1. Normal Tissue*

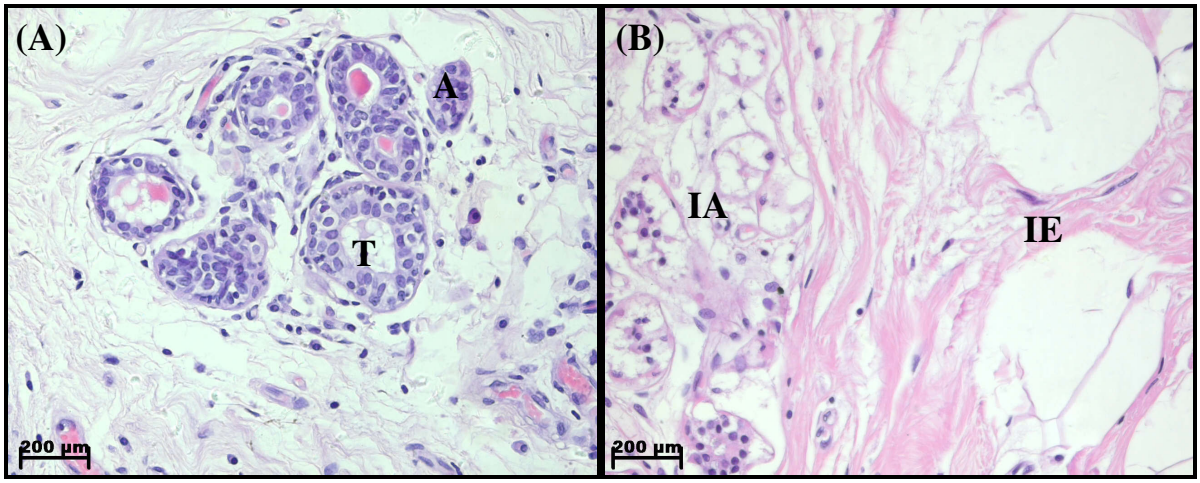



**Figure 3-10: H&E of Inactive Mammary Gland Normal Tissue**

(A) shows terminal ducts (T) and alveoli (A) consisting of two layers of epithelial cells: an outer layer of discontinuous myoepithelial cells and a luminal layer of cuboidal epithelial cells. (B) shows the dense fibroconnective tissue known as the interlobular stroma (IE) that consists of collagen fibres admixed with adipose tissue and the less dense intralobular stroma (IA) that surrounds the ducts within each lobule and consists of collagen and more vascular tissue. (Reference: Coltran, *et al.*, 1999, Eroschenko, 2000, Young, *et al.*, 2000) (Magnification 400X)

*3.1.6.2. Invasive Carcinoma (No Special Type)*

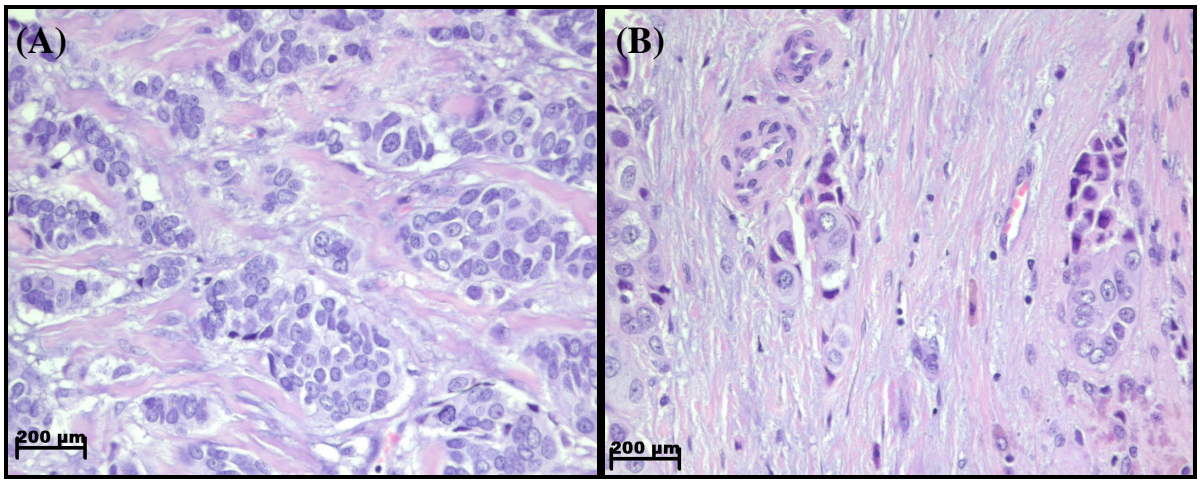



**Figure 3-11: H&E of Invasive Carcinoma (No Specific Type)**

(A) represents tumour cells growing in solid cell nests consisting of fibrotic stroma between the nests and the presence of apocrine metaplasia. (B) shows the presence of a mononuclear inflammatory infiltrate, namely lymphocytes between the tumour and the stroma. (Reference: Coltran, *et al.*, 1999, Rosai, 2004) (Magnification 400X)

### *3.1.7. Histology of Normal Tissue and Histopathology of Tumour Diseases in Lung*

#### *3.1.7.1. Normal Tissue*

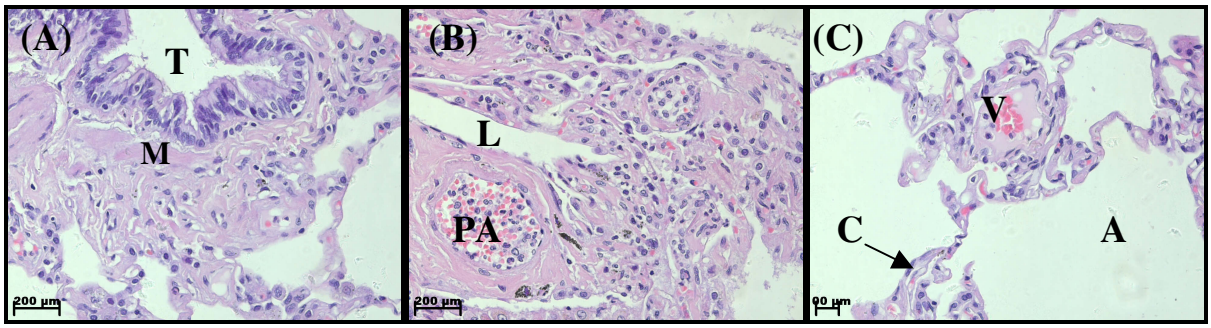



**Figure 3-12: H&E of Lung Normal Tissue**

(A) represents a terminal bronchiole (T) characterised by a prominent mucosal fold that consists of ciliated columnar epithelium and Clara cells characterised by tall, columnar non-ciliated cells. A smooth muscle layer (M) arranged as discrete bundles of various orientations surrounds the mucosal layer. (B) represents the parenchyma consisting of the pulmonary artery (PA), lymph vessel (L) and connective tissue consisting mainly of collagen fibres. (C) represents alveoli (A) lined by flattened epithelial cells that is surrounded by a rich network of pulmonary capillaries (C) that are supplied by pulmonary vessels (V). (Reference: Coltran, *et al.*, 1999, Eroschenko, 2000) (Magnification 400X)

### *3.1.7.2. Bronchogenic Carcinomas*

#### *3.1.7.2.1. Adenocarcinoma*

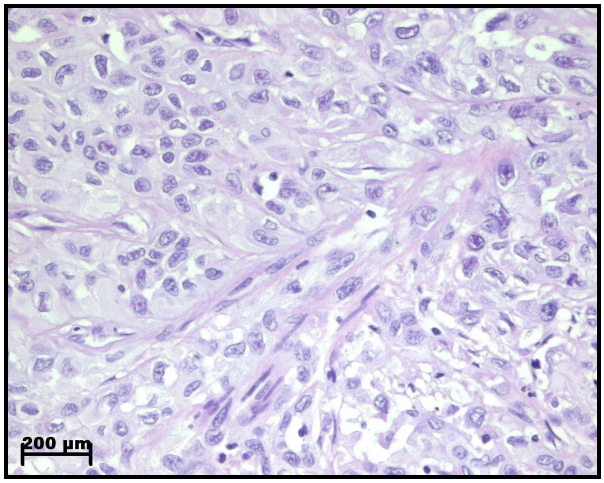



**Figure 3-13: H&E of Lung Adenocarcinoma**

The above figure represents the growth pattern of Grade III lung adenocarcinoma that is characterised by a solid pattern and occasional mucin-producing glands and cells. (Reference: Coltran, *et al.*, 1999) (Magnification 400X)

#### *3.1.7.2.2. Squamous Cell Carcinoma*

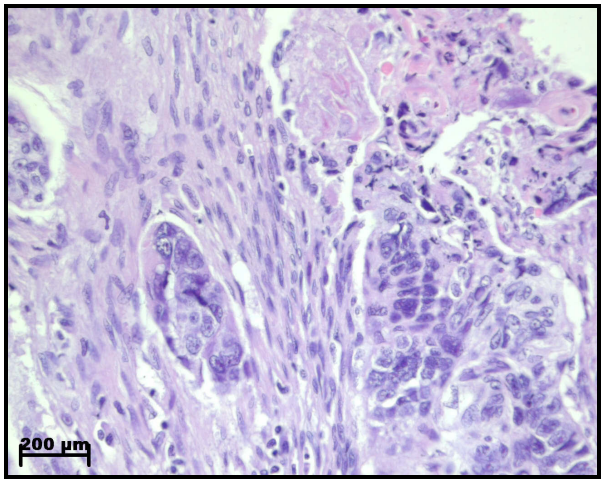



**Figure 3-14: H&E of Lung Squamous Cell Carcinoma**

The above diagram represents Grade III lung squamous cell carcinoma that is characterised by the presence of squamous metaplasia adjacent to the tumour mass. In addition, it shows the merging of the squamous tumour cells with the large cell pattern. (Reference: Coltran, *et al.*, 1999) (Magnification 400X)

*3.1.7.2.3.* *Classic Small Cell Carcinoma*

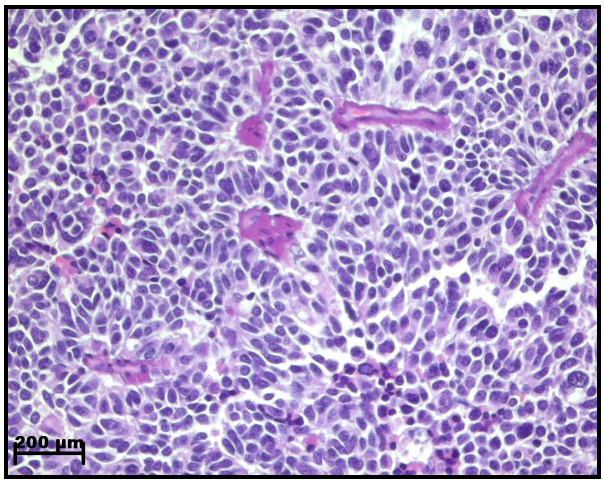



**Figure 3-15: H&E of Lung Classic Small Cell Carcinoma**

The above diagram represents lung classic small cell carcinoma characterised by the growth of tumour cells in clusters. Tumour cells contain small round to oval nuclei that appear to resemble lymphocytes. In addition, the cytoplasm of tumour cells appears scanty. Tumour cells appear spindle-shaped or polygonal. (Reference: Coltran, *et al.*, 1999, Rosai, 2004) (Magnification 400X)

### *3.1.8. Histology of Normal Tissue and Histopathology of Tumour Diseases in Kidney*

*3.1.8.1.Normal Tissue*

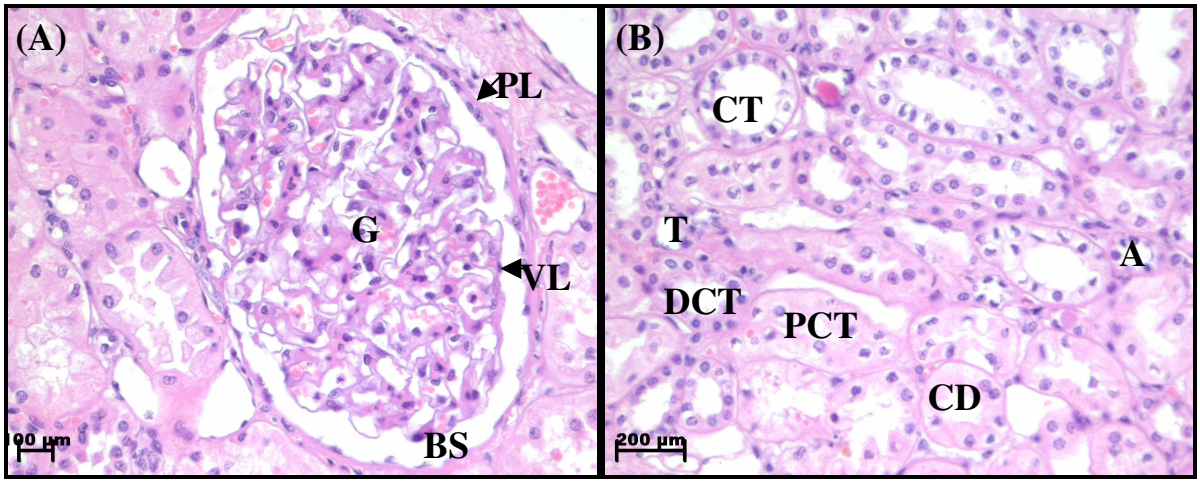



**Figure 3-16: H&E of Normal Kidney Tissue**

(A) represents the renal corpuscle that consists of the glomerulus (G) and Bowman's capsule. Bowman's capsule can be divided into three layers from the outside in: the parietal layer (PL), Bowman's space (BS) and the visceral layer (VS). The parietal layer, which forms the Bowman's capsule proper consists of a single layer of flattened cells resting on the basement membrane derived from the distended blind-end of the renal tubule. Bowman's space is located between the parietal and visceral layers and is continuous with the lumen of the renal tubule. The visceral layer is located closest to the glomerulus and consists of a layer of epithelial cells known as the podocytes that lies on the basement membrane that is also common to the glomerulus and is continuous with the parietal layer around the visceral stalk. Glomerulus can be defined as a glandular network of anastomosing capillaries lined by endothelial cells. (B) represents the different histophysiological zones of the renal tubule. The proximal convoluted tubule (PCT) is lined by a simple cuboidal epithelium with a prominent brush border of tall microvilli. Both the thin ascending and descending limbs (T) have a simple squamous epithelium and a regular round shape. The thick ascending limbs (A) are lined by low cuboidal epithelium and appear round in cross section. Both the ascending and descending limbs have the absence of a brush border. The distal convoluted tubule (DCT) consists of a simple cuboidal epithelium that is characterised by the absence of a brush border and larger more clearly defined lumen than that of the PCT. The collecting tubule (CT) is lined by a simple cuboidal epithelium, however, it appears wider and less regular in shape to the ascending limbs. The collecting duct (CD) is characterised by a large diameter and pale stained simple columnar epithelial lining. (Reference: Coltran, *et al.*, 1999, Eroschenko, 2000, Young, *et al.*, 2000 (Magnification 400X)

### *3.1.8.2. Renal Cell Carcinomas*

#### *3.1.8.2.1. Chromophobe Renal Carcinoma*

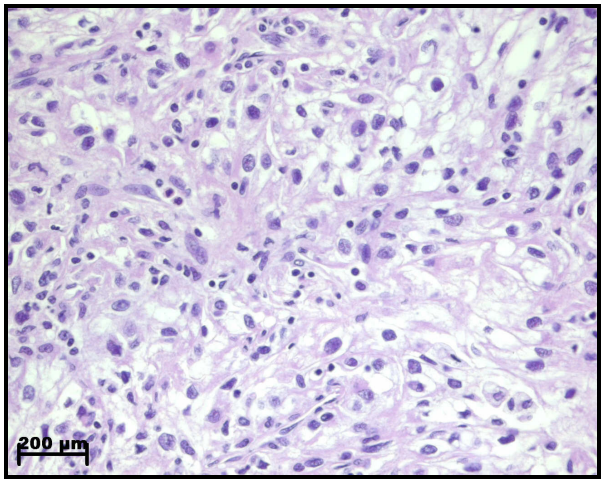



**Figure 3-17: H&E of Chromophobe Renal Carcinoma**

Chromophobe renal carcinomas are characterised by large polygonal tumour cells arranged in solid sheets. Tumour cells consist of pale eosinophilic stained reticular cytoplasm. (Reference: Coltran, *et al.*, 1999, Zambrano, *et al.*, 1999) (Magnification 400X)

*3.1.8.2.2.* *Clear Cell Carcinoma*

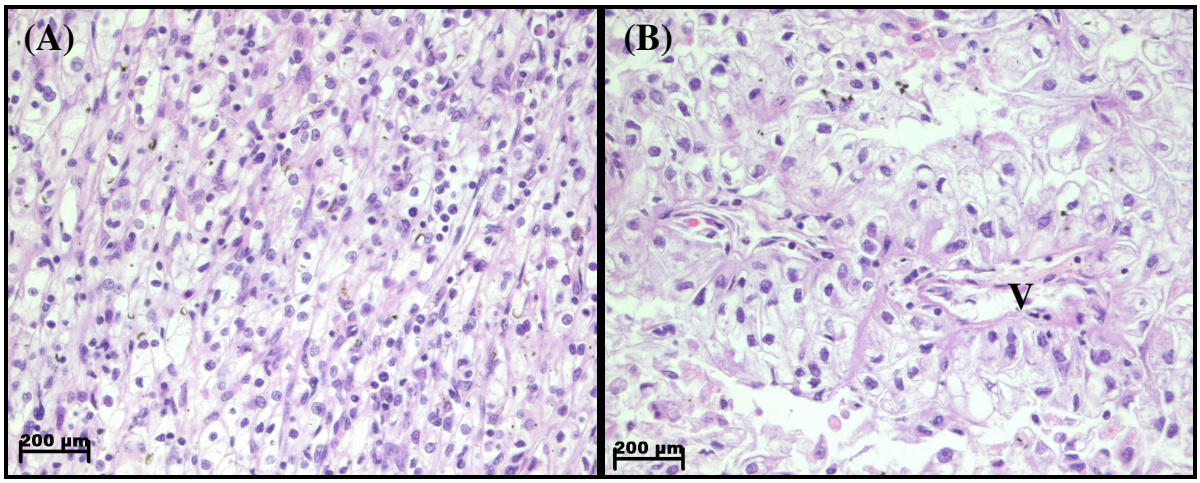



**Figure 3-18: H&E of Clear Cell Carcinoma**

(A) represents diffuse clear cell carcinoma growing in a trabecular of cord-like pattern. Tumour cells are small cells that have a rounded or polygonal shape containing an indistinct cell margin, a pale staining granular or clear, that is a vacuolated cytoplasm and normochromatic nuclei with inconspicuous nucleoli. (B) represents the stroma of the tumour containing a delicate branching vasculature (V) and has a fibromuscular appearance. (Reference: Coltran, *et al.*, 1999, Rosai, 2004) (Magnification 400X)

### *3.1.9. Histopathology of Normal Tissue and Tumour Diseases in Brain*

*3.1.9.1. Normal Tissue*

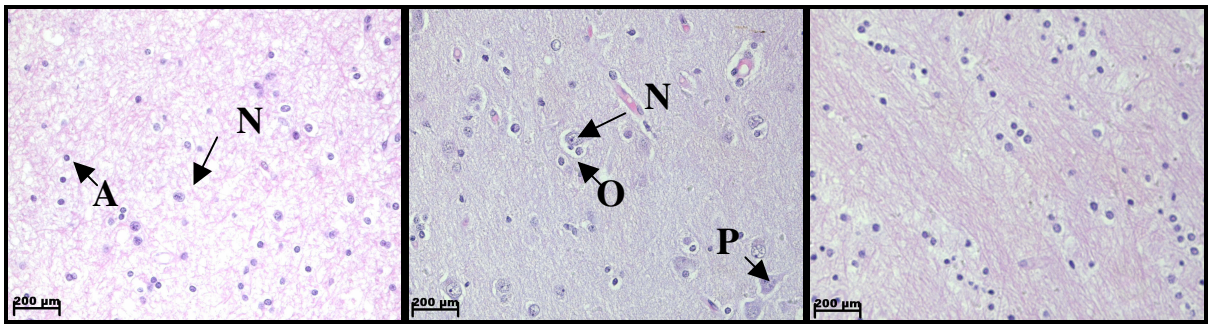



**Figure 3-19: H&E of Normal Brain Tissue**

(A) represents white matter, which shows the presence of neurones characterised by their basophilic granular cytoplasm and glia especially astrocytes (A) that are characterised by round to oval nuclei with evenly dispersed polar chromatin. (B) represents grey matter that is characterised by the presence of neurones (N) such as pseudo-unipolar neurones that are recognised by their basophilic granular cytoplasm and glia especially oligodendrocytes (O) that are characterised by a denser, more homogenous chromatin in rounder, smaller and lymphocyte-like nuclei. Oligodendrocytic cytoplasmic processes wrap around the axons of neurones. Other neurones found include pyramidal cells (P), which are characterised by pyramid-shaped cell bodies, with their apex being directed toward the cortical surface. (C) represents oligodendrocytes arranged in a linear array. All three diagrams show cells lying in a fibrillary network of neural processes. (Reference: Coltran, *et al.*, 1999, Eroschenko, 2000, Young, *et al.*, 2000) (Magnification 400X)

### *3.1.9.2. Brain Cancer*

#### *3.1.9.2.1. Diffuse Fibrillary Astrocytoma*

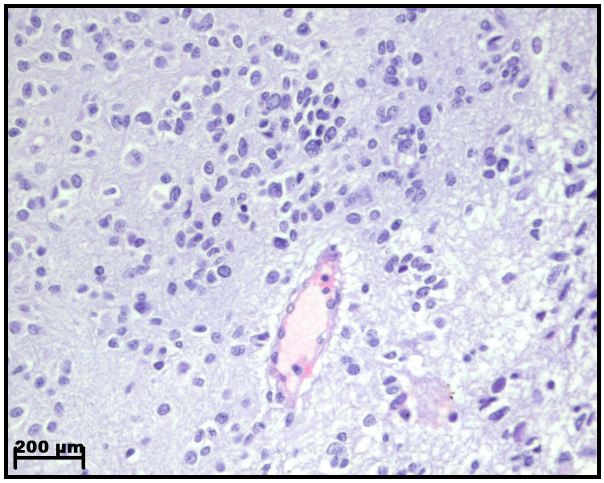



**Figure 3-20: H&E of Diffuse Fibrillary Astrocytoma**

The above diagram represents a Grade II diffuse fibrillary astrocytoma that is characterised by a low to moderate increase in glial cell nuclei that appear oval in shape and an intervening felt work of fine astrocytic cell processes that give the background a fibrillary appearance. (Reference: Coltran, *et al.*, 1999, Rosai, 2004) (Magnification 400X)

*3.1.9.2.2.* *Ependymoma*

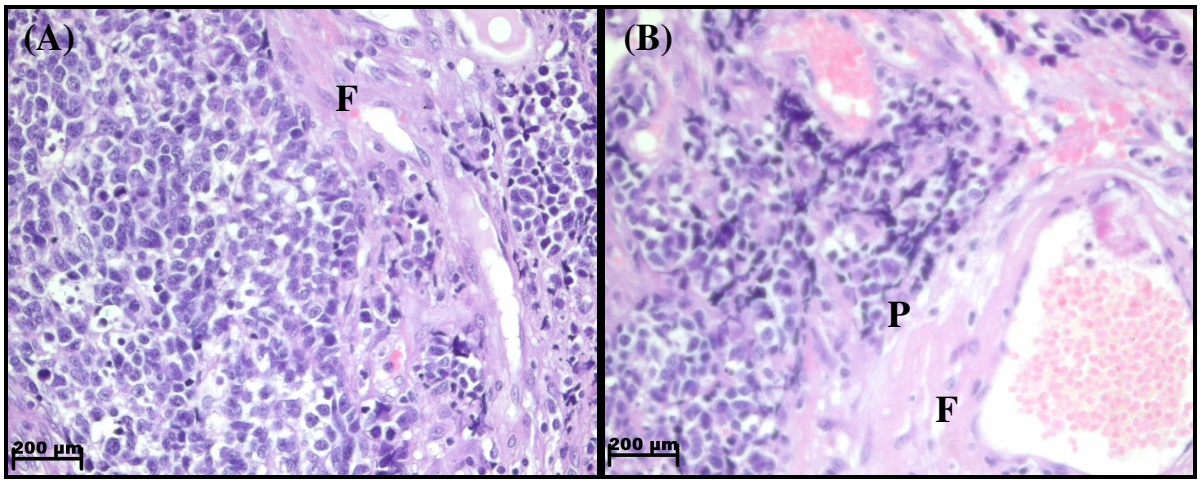



**Figure 3-21: H&E of Ependymoma**

(A) represents ependymoma that is composed of tumour cells with regular, round to oval nuclei with abundant granular cytoplasm. Between the nuclei there is a variably dense fibrillary network (F). (B) represents perivascular pseudorosettes (P) formations where tumour cells and the dense meshwork of fibrillary cytoplasmic processes (F) condense in a collar-like fashion around blood vessels. (Reference: Coltran, *et al.*, 1999, Rosai, 2004) (Magnification 400X)

*3.1.9.2.3. Peripheral Central Nervous System Lymphoma*

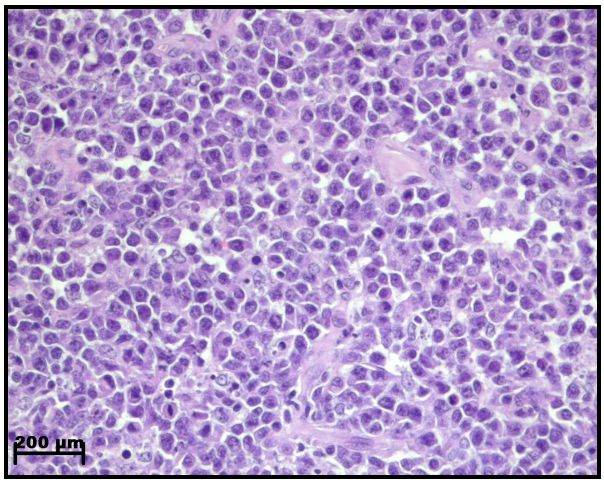



**Figure 3-22: H&E of Primary Central Nervous System Lymphoma**

The above figure represents primary central nervous system lymphoma characterised by the presence of a large cell cytology consisting of mononuclear cells of an undetermined type, which may be a type of lymphocyte that is characterised by round to oval nuclei with prominent nucleoli and a lack of cytoplasmic processes of cellular cohesions. (Reference: Fine, *et al.*, 2003, Rosai, 2004) (Magnification 400X)

### *3.1.10. Summary*

The histology and histopathology section confirmed the histologies of the different normal tissues and histopathologies of the different cancer tissues to be studied via *in situ* hybridisation. This section also further provided an understanding of the main cell types and tissues found in each normal organ, structural changes that occurs between normal and its cancerous counterparts for the various organs as well as structural changes that occur as cancerous tissues become more progressive that is poorly differentiated. This understanding proved valuable when localisation studies were done.

## 3.2. Expression of the Peripheral Benzodiazepine Receptor mRNA in Various Human Cancer Tissues

### *3.2.1. Introduction*

In order to ascertain if PBR mRNA is expressed in normal and cancerous tissues from various organs of the body and whether it is expressed at similar levels between the normal and cancerous states, colorimetric and fluorescent *in situ* hybridisation was performed. *In situ* hybridisation is a qualitative or semi-quantitative technique by which specific mRNA of interest in the cytoplasm or DNA of interest in the nucleus can be localised in morphologically preserved tissue sections or cell preparations through the hybridisation of a complimentary strand of a nucleotide probe to the sequence of interest. The sensitivity of this technique is such that the threshold levels of detection are in the region of 10 to 20 copies of mRNA or DNA per cell. This technique provides considerable information regarding the structure and function of cell within pathological means (Lanlani, *et al.*, 1997). Thus, in order to perform this technique, labelled RNA probes specific for PBR had to be synthesised that binds to the complementary mRNA in tissue sections after which results were seen under light and fluorescent microscopy.

### *3.2.2. Molecular Cloning*

#### *3.2.2.1. RNA Extraction*

Total RNA was extracted using the TRIzol$^{TM}$ RNA extraction method and results analysed by formaldehyde agarose gel electrophoresis (Figure 3-23). This resulted in the formation of a smear, however two distinct bands could be distinguished. These bands were indicative of ribosomal RNA (rRNA), specifically the 18S and 28S rRNA, which have a relative molecular weight of 1.9 kb and 5.0 kb. Smearing seen in the lane indicates that some RNA underwent degradation.

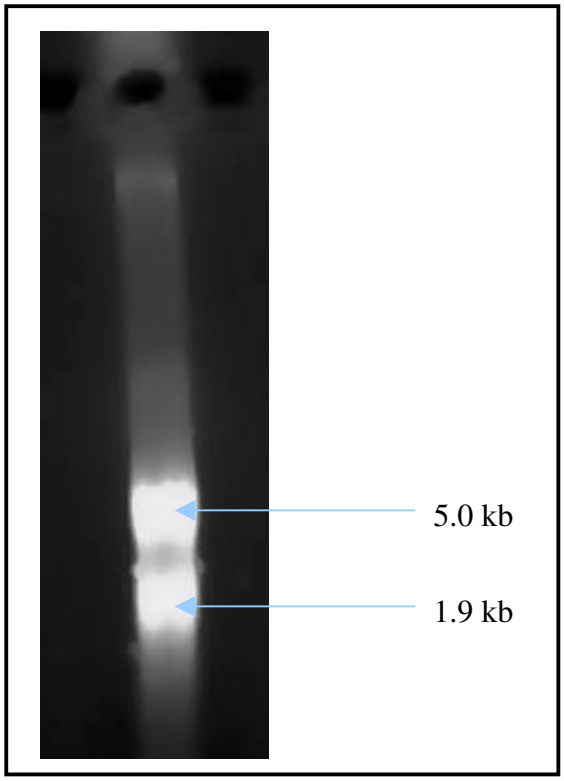



**Figure 3-23: Isolation of Total RNA**

*3.2.2.2. Polymerase Chain Reaction*

The 247 bp region of interest of the *PBR* gene was amplified by PCR using PBR specific primers. The results were analysed by agarose gel electrophoresis where the PCR product was run on a 1% agarose gel (Figure 3-24). It was found that the *PBR* gene was amplified as is indicative of the bold band (Lane 3) as it lied between the 200 bp and 300 bp reference bands (Lane 1). A negative control run with the amplification of the *PBR* gene was to perform PCR in the absence of any template DNA by replacing it with nuclease free $H_2O$, which resulted in no band formation (Lane 2).

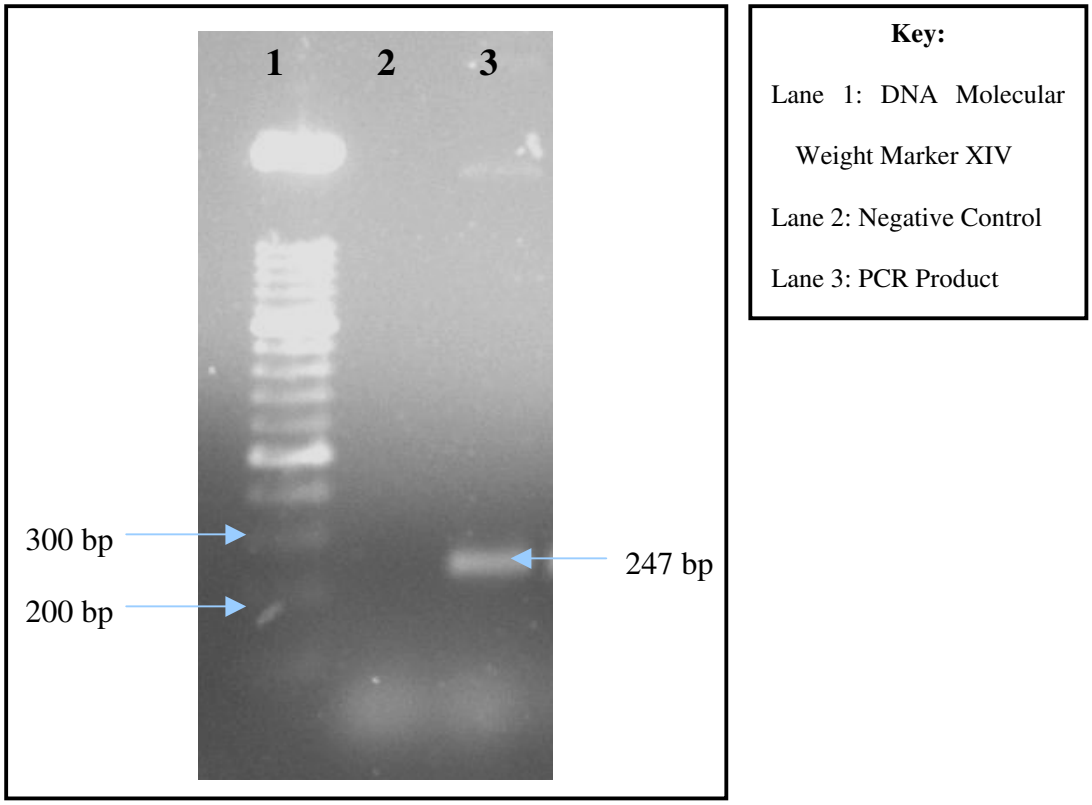



**Figure 3-24: Amplification of the *Peripheral Benzodiazepine Receptor* Gene Region of Interest**

*3.2.2.3. Cloning*

The PCR product was ligated into pGEM-T Easy vector, which contains a multiple cloning site, 3'-T overhangs allowing for the correct ligation of the PCR product and an ampicillin resistant domain, using the LigaFast™ Rapid Ligation System (Promega Corporation, Madison WI, USA) after which it was transformed into competent MC1061 *Escherichia coli* cells and grown on ampicillin-containing nutrient-rich agar plates. Thus, only those bacteria containing the ampicillin resistant gene will grow. To determine if the MC1061 *Escherichia coli* cells were competent, a background control used was to plate the cloning reactions on nutrient-rich agar plates not containing ampicillin. A negative background control used was to allow bacteria to grow in the absence of the vector and the insert. This control served the purpose of determining if the bacterial cells contained the ampicillin resistant gene. A positive

control used was to grow bacteria in the presence of just the pGEM-T Easy vector only. This control serves the purpose to determine if bacterial cells are competent. It was found that growth occurred on ampicillin-negative plates as well as on ampicillin-positive plates where bacterial cells contained the pGEM-T Easy vector plus the insert or the pGEM-T Easy vector only while no growth occurred in bacterial cells that did not contain the pGEM-T Easy vector or insert (Figure 3-25).

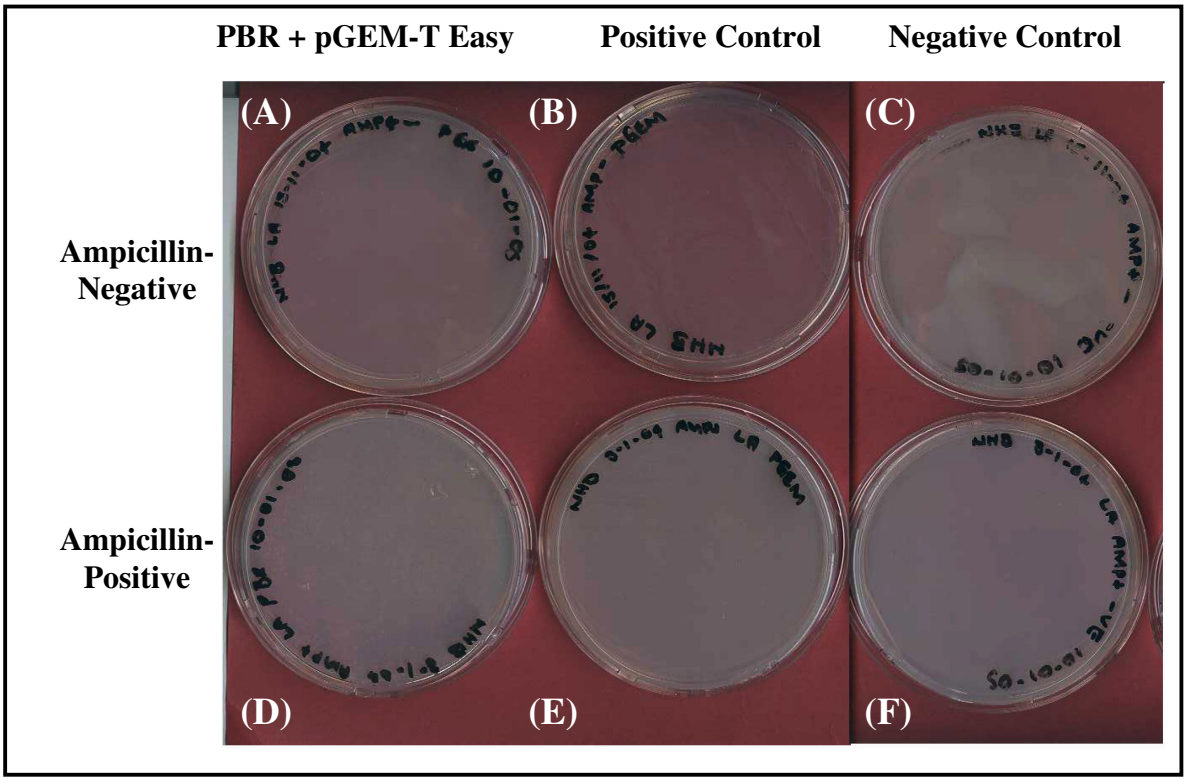



**Figure 3-25: Cloning of the Peripheral Benzodiazepine Receptor Insert into pGEM-T Easy Vector**

*3.2.2.4. Colony Polymerase Chain Reaction*

Colony PCR was done to confirm that the bacterial cells that grew on the ampicillin plates contained the vector plus the insert. Taking colonies at random that grew on the nutrient-rich agar plates and amplifying the region of interest by PCR using PBR specific primers accomplished this. The results were analysed by agarose gel electrophoresis where the PCR

product was run on a 1% agarose gel (Figure 3-26). It was found that the insert was amplified as is indicative of the bold band (Lanes 3-10) as it lied between the 200 bp and 300 bp reference bands (Lane 1). A negative control run with the amplification of the recombinant DNA molecules was to perform PCR in the absence of any recombinant DNA by replacing it with nuclease free $H_2O$, which resulted in no band formation (Lane 2).

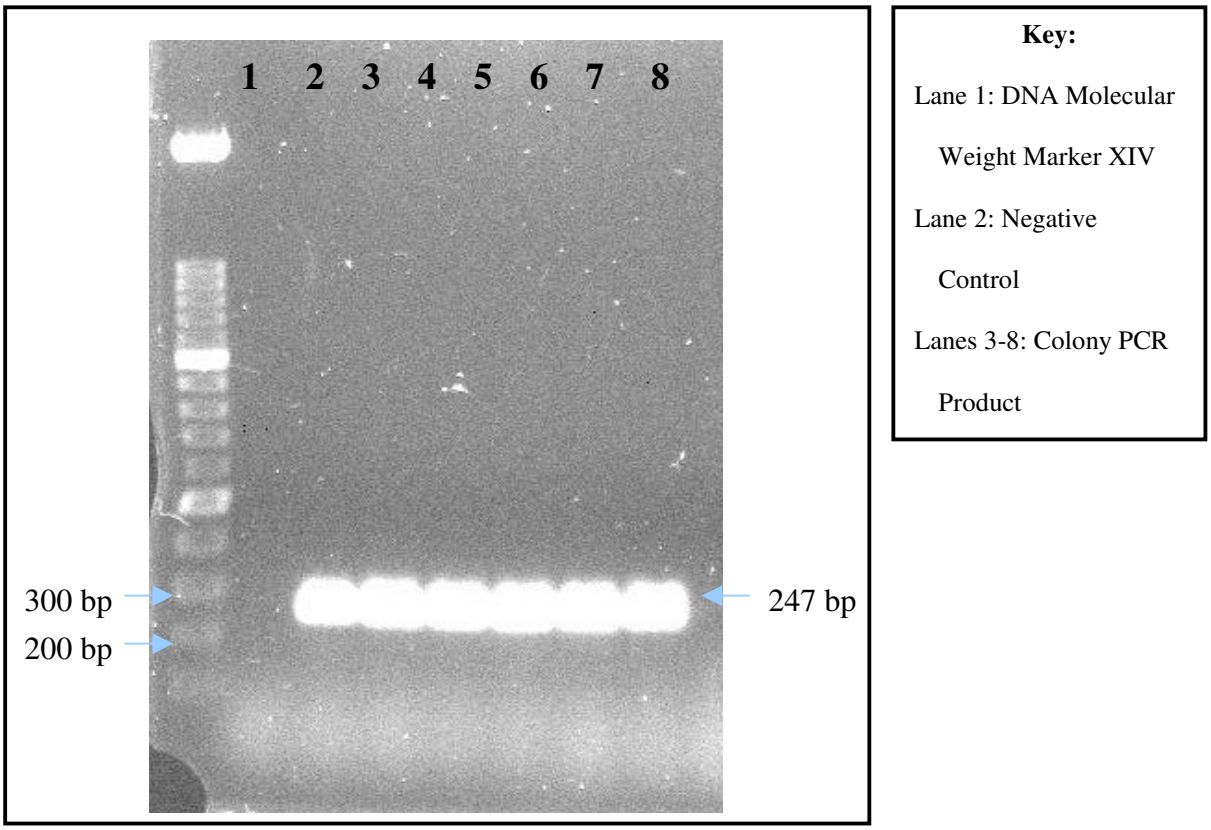



**Figure 3-26: Amplification of the Peripheral Benzodiazepine Receptor Insert via Colony PCR**

*3.2.2.5. Miniprep Analysis/Plasmid DNA Extraction*

The pGEM-T Easy vector containing the insert was isolated from the bacterial cells and purified by plasmid DNA extraction using the WizardPlus® SV Miniprep Purification System (Promega Corporation, Madison, WI, USA). To determine if the clones were isolated, the results were analysed by agarose gel electrophoresis where the clones were run on a 1%

agarose gel (Figure 3-27). The gel showed the formation of three bands greater than 1031 bp reference band (Lane 1), which indicates that pGEM-T Easy vector containing the insert was isolated (Lanes 2, 4-7). The three bands that can be seen are indicative of the different states in which plasmid DNA occurs, namely it may range from supercoiled to completely relaxed. The most tightly supercoiled plasmid DNA will travel furthest in the gel while the most relaxed plasmid DNA will travel the least on the gel. Lane 3 shows no bands, which indicates that the plasmid DNA was lost during the plasmid DNA extraction procedure which could have occurred at a number of steps such as during lysis and washing or another reason could be that the plasmid DNA was too dilute to be seen as a band on the gel.

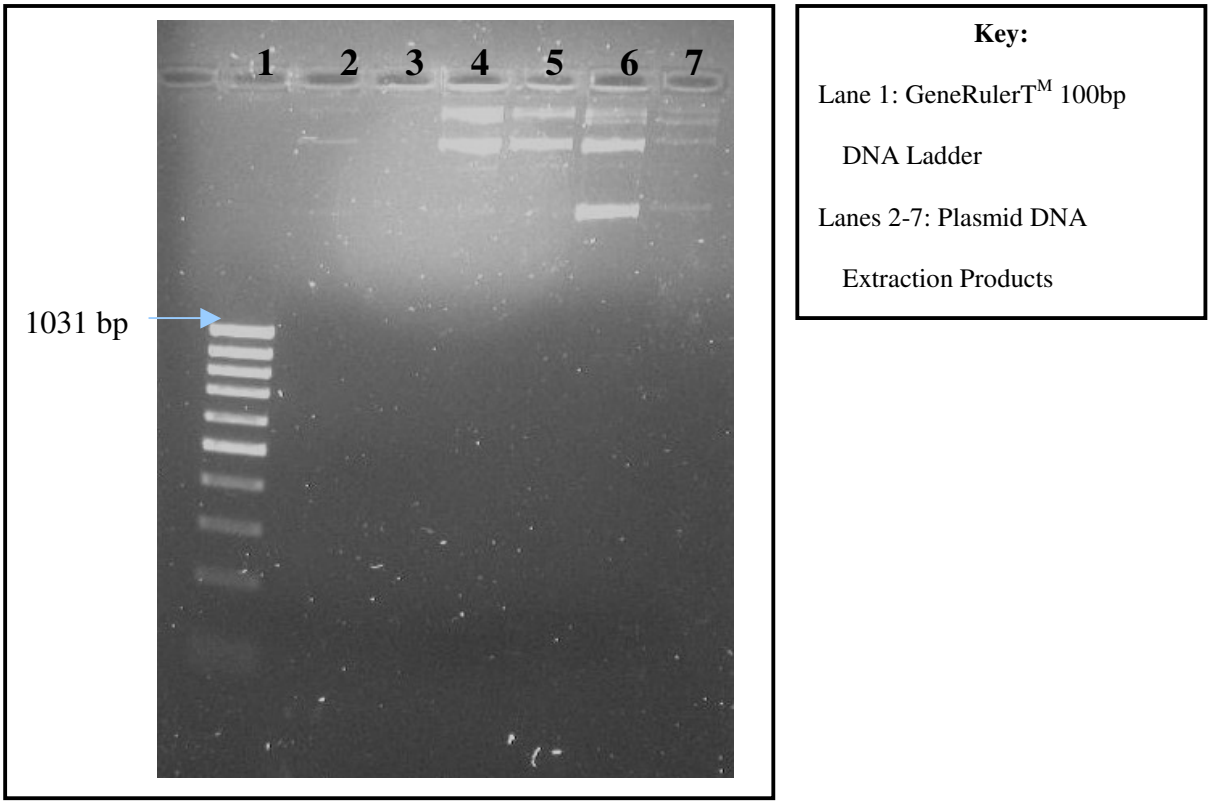



**Figure 3-27: Isolation of Plasmid DNA**

*3.2.2.6. Restriction Digestion*

The purified plasmid DNA was digested with *Eco*RI to determine the presence of the insert in the plasmid DNA and *Pst*I to determine if the plasmid DNA could be linearised to be later used in the synthesis of the anti-sense probe. The results were analysed by agarose gel electrophoresis where the digestions were run on a 1% agarose gel (Figure 3-28). Two controls used in this experiment included the undigested clone (Lane 2), which resulted in the formation of two bands greater than the 1031 bp reference band (Lane 1) that represented the different states of the plasmid DNA, and the colony PCR product (Lane 3) represented by the band located between the 200 bp and 300 bp reference bands (Lane 1). When the recombinant plasmid DNA was digested with *Pst*I, it resulted in the formation of one band (Lane 4) greater than the 1031 bp reference band (Lane 1), which indicates that the recombinant plasmid DNA is linearised by *Pst*I. It was found that when the recombinant plasmid DNA was digested with *Eco*RI, it resulted in the formation of two bands (Lane 5), one band greater than the 1031 bp reference band (Lane 1) and the other lying between the 500 bp and 600 bp reference band (Lane 1). However, the hypothesised result was that the smaller fragment size should have been 247 bp, the size of the PCR product.

Therefore, in order to determine if the recombinant plasmid DNA contains the PBR insert, the recombinant plasmid DNA underwent PCR using PBR-specific primers. Results were analysed using agarose gel electrophoresis where the PCR products were run on a 1% agarose gel (Figure 3-7). This resulted in the formation of a band (Lane 3) that lay between the 200 bp and 300 bp reference bands (Lane 1). A negative control used was to replace the recombinant plasmid DNA with nuclease free $H_2O$, which resulted in no band formation (Lane 2). Thus, PCR confirmed the presence of the insert in the recombinant plasmid DNA, which was then sent for sequencing.

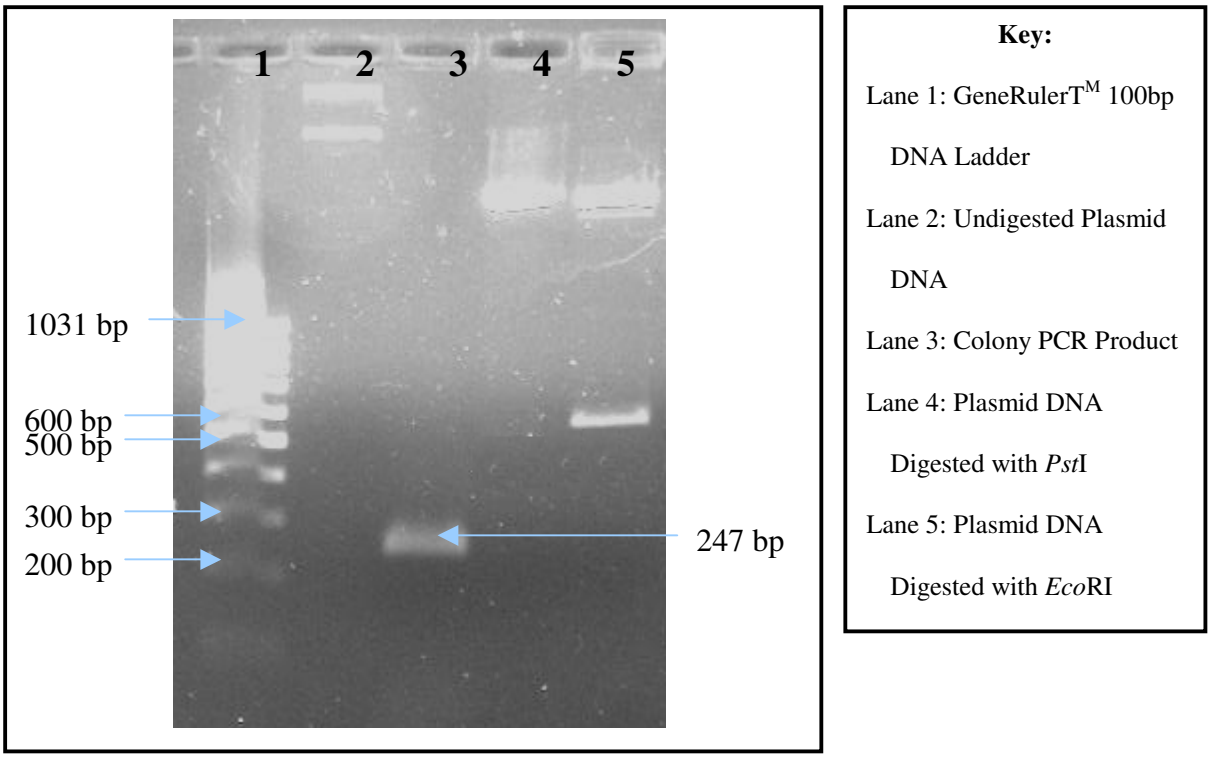



**Figure 3-28: Restriction of Plasmid DNA containing Insert**

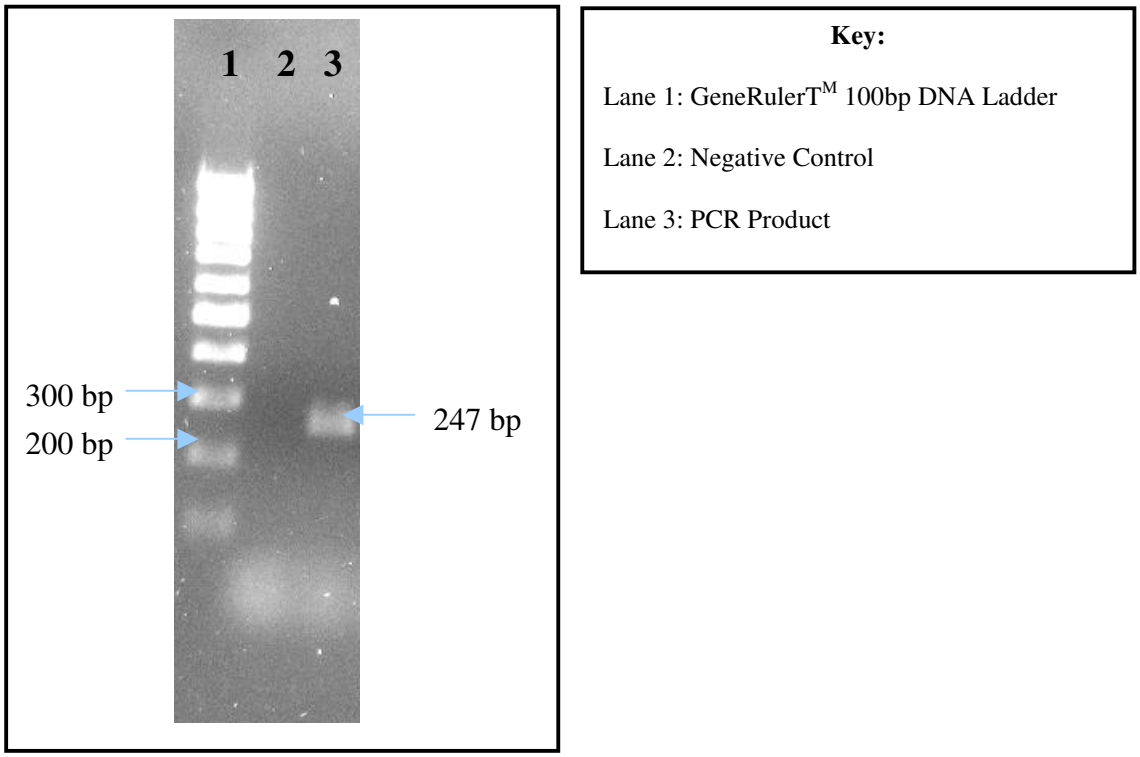



**Figure 3-29: Amplification of Peripheral Benzodiazepine Receptor Insert via Polymerase Chain Reaction**

*3.2.2.7. Sequencing*

The purified recombinant clone containing the region of interest of the *PBR* gene was sent to Inqaba Biotechnical Industries (Pty) Ltd (Pretoria, Gauteng, South Africa) for sequencing to determine if the insert isolated was actually the *PBR* gene. The results were analysed using CHROMAS, version 1.62 (Technelysium (Pty) Ltd, Helensville, Queensland, Australia) and by comparing the clone PBR sequence to that of the *Homo sapiens* benzodiazepine receptor (peripheral) mRNA reference sequence (Accession Number: BT006949) obtained from the Nucleotide database at NCBI. This was done using BLAST at NCBI where two sequences can be compared to each other (Figure 3-30). It was found that the PBR insert was 512 bp in size, which is the size of the entire reference PBR sequence, which means that the entire *PBR* gene was cloned into the pGEM-T Easy vector, which probably occurred as a result of mispriming and spontaneous mutations. The sequence was 98% accurate to the reference sequence and lies in a 5' to 3' orientation.

*3.2.2.8. Linearisation of Clones*

The pGEM-T Easy vectors containing the PBR inserts were digested with *Apa*I and *Pst*I independently in order to synthesise linearised clones, which were later used in the synthesis of sense and anti-sense probes respectively. Results were analysed by agarose gel electrophoresis where purified products were run on a 1% agarose gel (Figure 3-31). It was found that one band (Lanes 3 and 4) greater than the 1031 bp reference band (Lane 1) occurred for both the independent digestion of clones with *Apa*I and *Pst*I. The control used in this experiment was undigested clone that was run concurrently on the gel, which resulted in the formation of two bands that represents the different states in which plasmid DNA occurs.

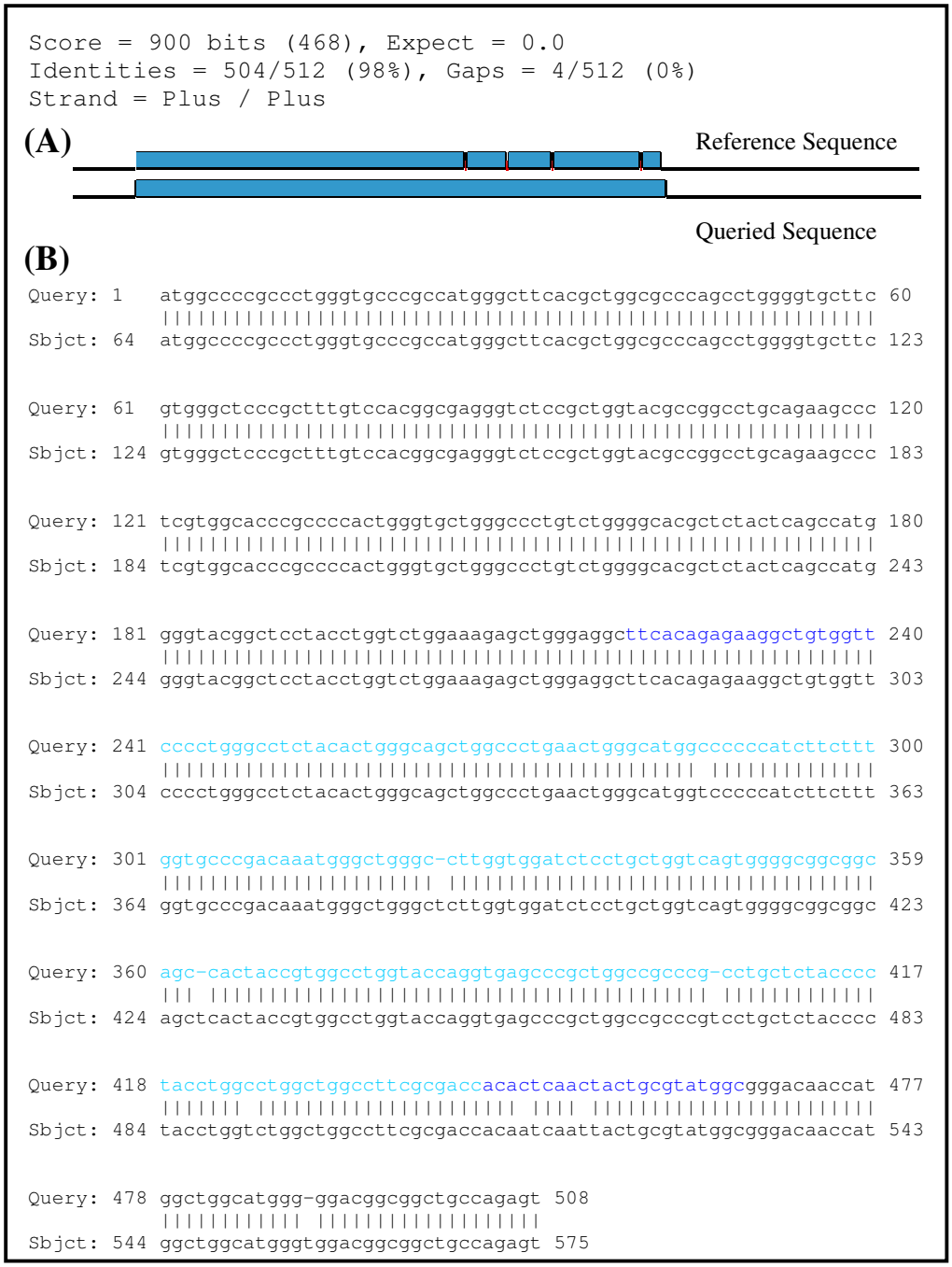
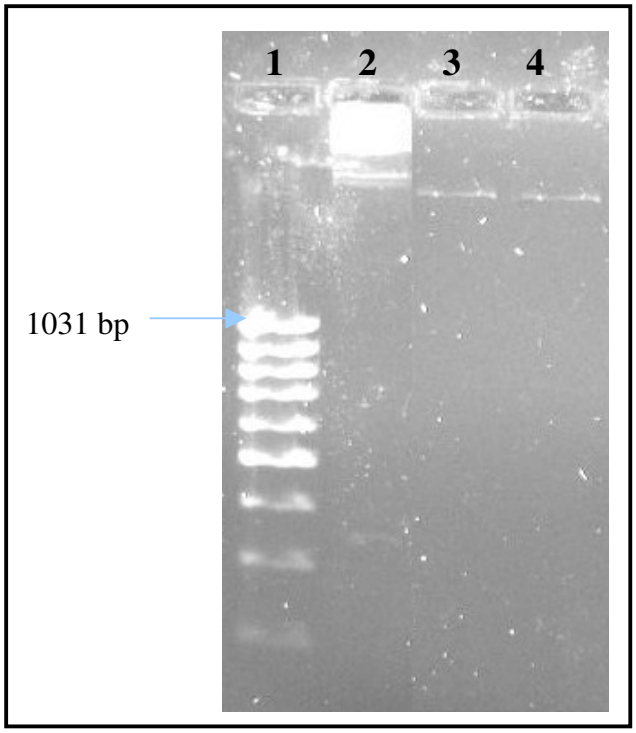



**Figure 3-30: Sequence Alignment of the *Peripheral Benzodiazepine Receptor* Gene**

(A) shows a graphic alignment of the two sequences. (B) shows a detailed alignment of the cloned *PBR* gene to the reference *PBR* gene.




**Key:**

Lane 1: GeneRulerT$^{M}$ 100bp DNA Ladder

Lane 2: Undigested Plasmid DNA

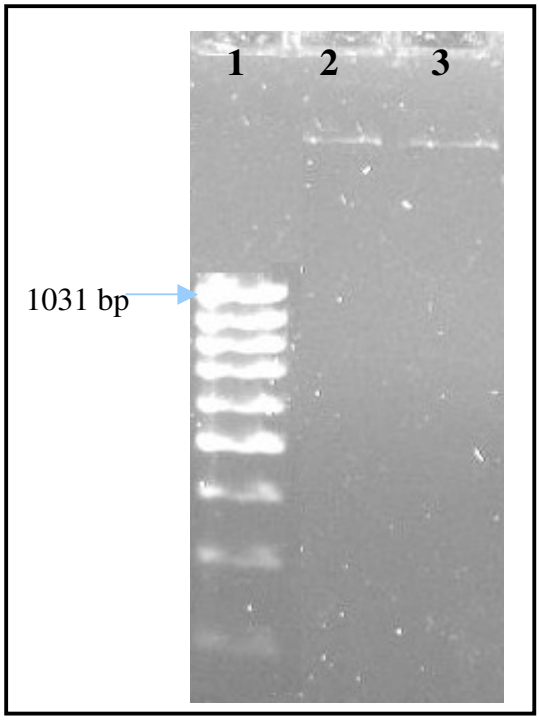
Lane 3: Plasmid DNA Digested with *Apa*I

Lane 4: Plasmid DNA Digested with *Pst*I

**Figure 3-31: Linearisation of Recombinant Plasmid DNA**

*3.2.2.9. Purification of Linearised Clones*

The linearised clones digested with *Pst*I and *Apa*I were purified using the Promega Wizard® SV Gel and PCR Clean-Up System (Promega Corporation, Madison, WI, USA) in order to remove any excess salts and other contaminants. Results were analysed by agarose gel electrophoresis where purified products were run on a 1% agarose gel (Figure 3-32). It was found that both clones digested with *Pst*I and *Apa*I were recovered as is indicative of the formation of a band (Lanes 2 and 3) at a level greater than 1031 bp reference band (Lane 1).




**Key:**

Lane 1: GeneRuler$T^M$ 100bp DNA Ladder

Lane 2: Purified Linearised Clone Digested with *Apa*I

Lane 3: Purified Linearised Clone Digested with *Pst*I

**Figure 3-32: Purification of Linearised Clones**

Thereafter, the linearised clones were quantified to determine the concentration and purity of each clone digested with *Apa*I and *Pst*I. Determining the concentration of each probe was required to determine what volume of each clone would be required to make a final concentration of 2 µg/µl required for the *in vitro* transcription of sense and anti-sense probes. This was done spectrophotometrically by measuring the absorbance at 260 nm and 280 nm for each clone, which was blanked against DEPC-treated $H_2O$ (Table 3-1). 260 nm is the wavelength at which nuclei absorbs light maximally while 280 nm is the wavelength at which protein absorbs light maximally. The purity of the sample can thus be determined by the ratio $A_{260}$:$A_{280}$, which was found to be 1.1 in the case of the *Apa*I digested clone and 1.0 in the case of the *Pst*I digested clone. However, a pure DNA solution should result in a value greater than or equal to 1.8. The reason that the values are lower than 1.8 for the probes may be because the sample solutions used to measure the absorbance may have been too dilute.

**Table 3-1: Absorbance, Purity and Concentration of Sense and Anti-Sense Probes Measured at 260 nm and 280 nm**

| Sample | $A_{260}$ | $A_{280}$ | $A_{260}$:$A_{280}$ | Concentration (µg/ml) [1] |
|---|---|---|---|---|
| *Apa*I Digested Clone | 0.070 | 0.065 | 1.1 | 350 |
| *Pst*I Digested Clone | 0.082 | 0.083 | 1.0 | 410 |

1. Concentration of each probe was determined using the formula: $c = A_{260} \times [A_{260}dsDNA] \times DF$

Concentration of each clone was determined using the formula: $c = A_{260} \times [A_{260}dsDNA] \times DF$, where c is the concentration of the sample, $[A_{260}dsDNA]$ is the concentration of double-stranded (ds) DNA where absorbance at 260 nm is 1.0, which is 50 µg/ml and DF is the dilution factor, which was 100. The concentrations of the clones were found to be 350 µg/ml for the *Apa*I digested clone and 410 µg/ml for the *Pst*I digested clone. The volume required to prepare a solution of concentration 2 µg/µl was determined using ratios and was found to be 5.7 µl for the *Apa*I digested clone and 4.9 µl for the *Pst*I digested clone (For calculation refer to Appendix 7 Calculations of Concentrations Linearised Clones, Volume Required to Synthesise Probes and Purity of Linearised Clones).

### *3.2.3. Sense and Anti-Sense Probe Synthesis*

Clones linearised with *Pst*I and *Apa*I were used to synthesise the anti-sense and sense probes respectively. This was done via *in vitro* transcription where small amounts of RNA is synthesised from a DNA template under the suitable control of a promoter for RNA polymerase after which each RNA copy was labelled with DIG-dUTP at every 20-25th nucleotide position. These labelled RNA probes were later used for *in situ* hybridisation. The sense probe was generated using SP6 RNA polymerase, which generates a 3' to 5' RNA copy, which prevents the sense probe from binding to the mRNA during *in situ* hybridisation

while the T7 RNA polymerase was used to generate the anti-sense probe resulting in the generation of a 5' to 3' RNA copy, which is able to bind to the 3' end of the complementary mRNA strand during *in situ* hybridisation.

*3.2.3.1. Estimation of Minimal Concentration of Probes*

Serial dilutions of sense and anti-sense probes that were labelled with DIG during *in vitro* transcription, was blotted onto a nylon membrane from which the minimal concentration of the sense and anti-sense probes were determined (Figure 3-33). Comparing the intensity of the least dilute blot of both probes that appears on the membrane and comparing it to the same intensity blot of the DIG-labelled control RNA determined the minimal concentration of each probe. For the sense probe, the minimal concentration of the probe was determined to be 0.01 pg/µl and for the anti-sense probe the minimal concentration of the probe was determined to be 0.1 pg/µl.

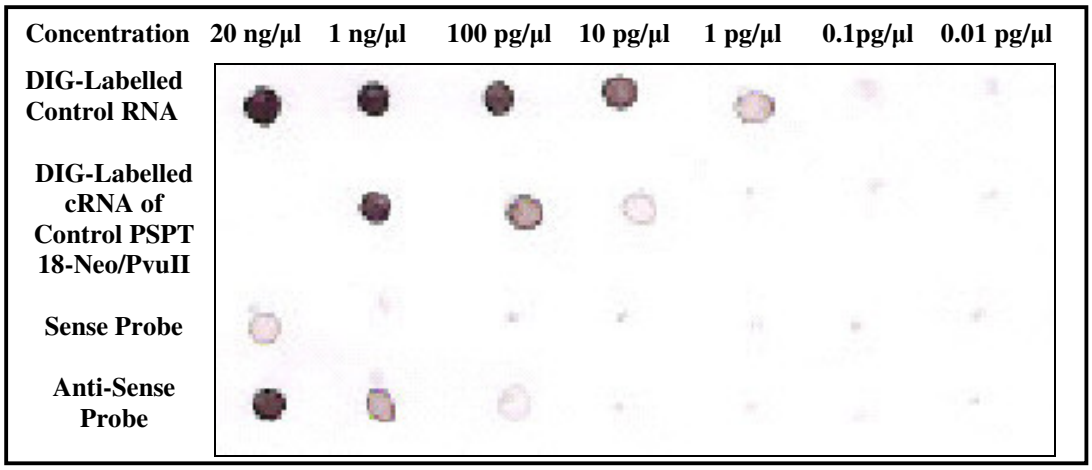



**Figure 3-33: Blot showing Minimal Concentration of DIG-Labelled Sense and Anti-Sense Probes**

### *3.2.4. In Situ Hybridisation*

Colorimetric and fluorescent detection of the DIG-labelled anti-sense RNA probes were used to determine the localisation of the PBR mRNA in tissue preparations. DIG-labelled anti-sense RNA probes hydrogen bonds to the complementary mRNA. DIG-labelled anti-sense RNA probes were colorimetrically detected by the binding of anti-DIG conjugated to AP to the DIG-labelled anti-sense RNA probes, which in the presence of a substrate such as NBT/BCIP allows for enzymatic activity to occur, which results in the formation of a purple/blue precipitate (Figure 3-34A). DIG-labelled anti-sense RNA probes were fluorescently detected by the binding of anti-DIG conjugated to FITC to DIG-labelled anti-sense RNA probes. FITC does not require the presence of a substrate and emits an apple green colour when excited at 490 nm (Figure 3-34B).

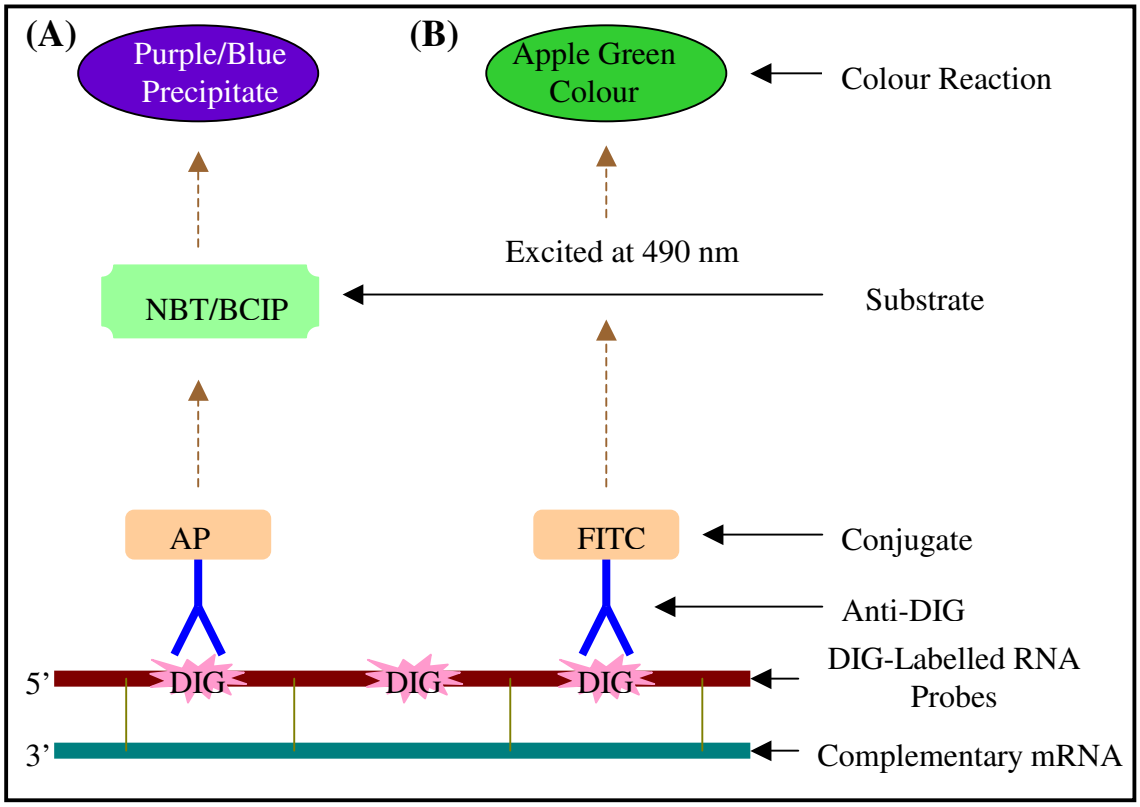



**Figure 3-34: Schematic Diagram of *In Situ* Hybridisation**

In all cases, tissue preparations labelled with DIG-labelled sense probes showed no localization and served as the negative control. In order to determine a pattern of expression, *in situ* hybridisation on the tissue array was done in triplicate (3 tissue array slides were used for the colorimetric detection and 3 tissue array slides were used for the fluorescent detection) as some cancers had only 1 dot on the tissue array.

Increase or decrease in expression of PBR mRNA was determined by looking at the intensity of the staining. It should be noted that for each of the cancers, increase and decrease in expression of PBR mRNA was determined relatively as there was no software available by which the images could be analysed to determine quantitation in absolute terms.

#### *3.2.4.1. Expression of the Peripheral Benzodiazepine Receptor mRNA in Liver Normal and Tumour Tissues*

Expression of PBR mRNA in liver can be determined by comparing the normal and cancerous tissues to the negative control (Figure 3-35). It was found that PBR mRNA is expressed in both normal tissue and hepatocellular carcinoma. All cases showed that PBR mRNA expression varies from the normal to the diseased state, with PBR mRNA expression levels increasing in Grade II and Grade III hepatocellular carcinoma when compared to its normal counterpart. Also, PBR mRNA expression levels varies for the different grades of the tumour showing that PBR mRNA expression levels decreases from Grade II to Grade III hepatocellular carcinoma.

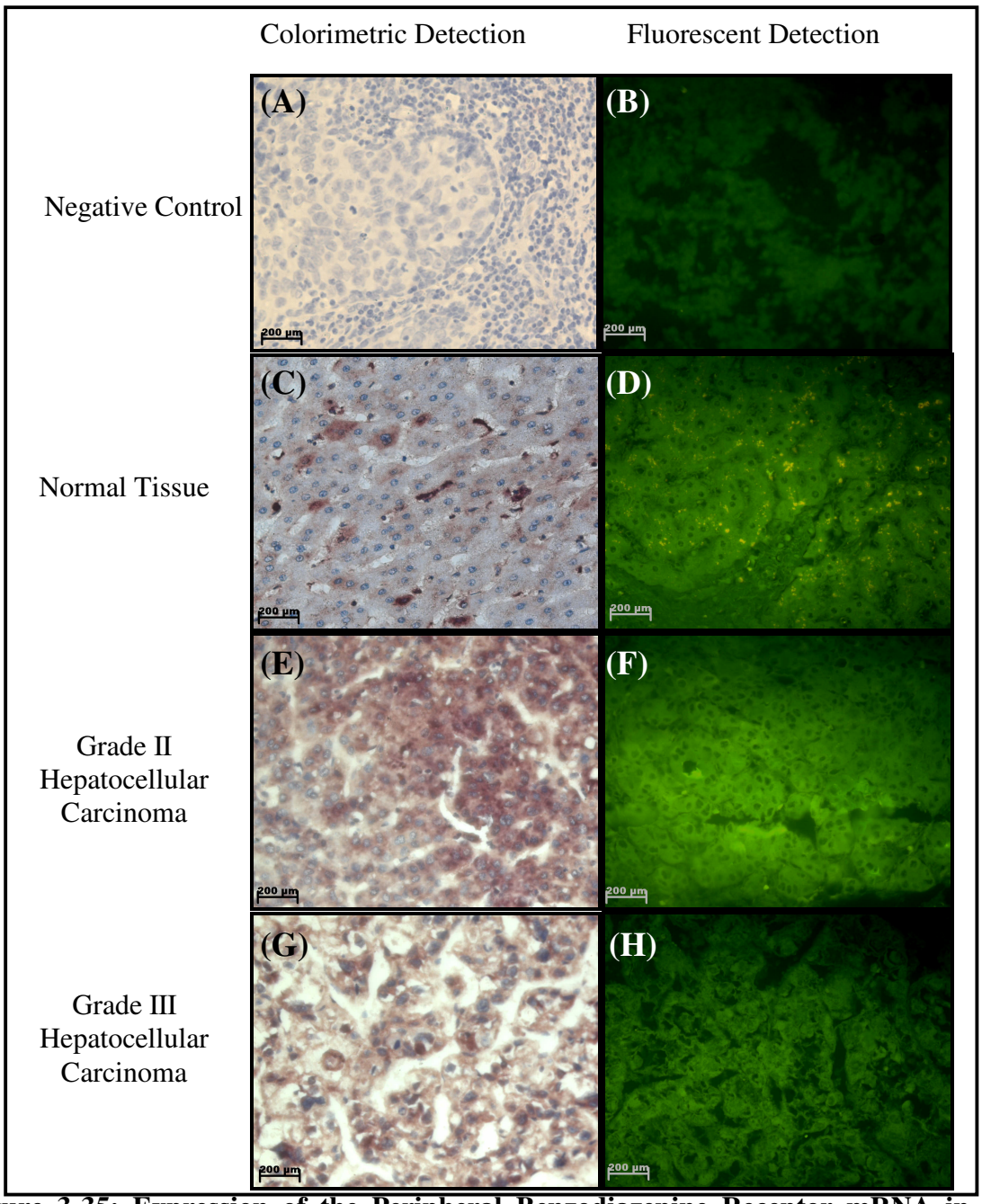



**Figure 3-35: Expression of the Peripheral Benzodiazepine Receptor mRNA in Liver** (Magnification 400X)

The subcellular localisation of the PBR mRNA is determined by comparing a tissue sample to the negative control. In normal liver tissue PBR mRNA is expressed in the cytoplasm of hepatocytes and in the nuclei and cytoplasm of Kupffer cells and endothelial cells of the sinusoids (Figure 3-36).

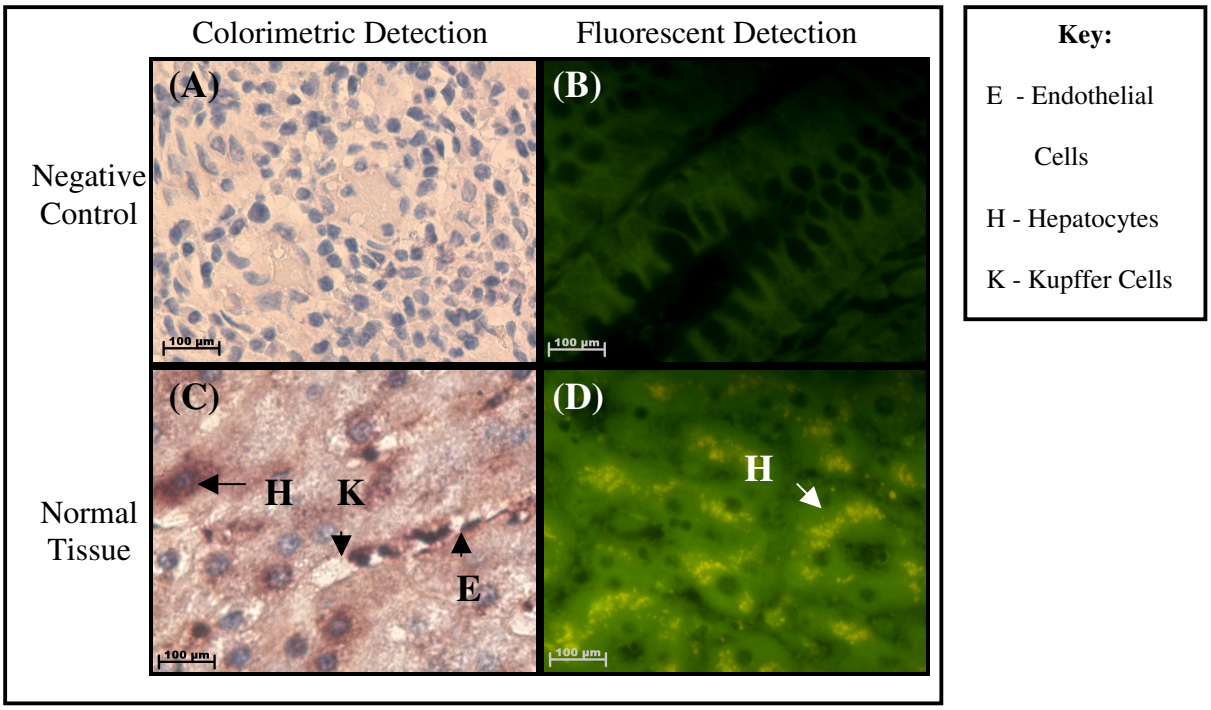



**Figure 3-36: Subcellular Localisation of the Peripheral Benzodiazepine Receptor mRNA in Normal Liver Tissue** (Magnification 1000X)

Grade II hepatocellular carcinoma express PBR mRNA in the cytoplasm of tumour cells having either a trabecular or pseudoglandular pattern while Grade III hepatocellular carcinoma express PBR mRNA in the nuclei and cytoplasm of tumour cells that resemble anaplastic giant cells to spindle-shaped cells (Figure 3-37).

### *3.2.4.2. Expression of the Peripheral Benzodiazepine Receptor mRNA in Colon Normal and Tumour Tissues*

Expression of PBR mRNA in colon can be determined by comparing normal and cancerous tissues to the negative control, which is the localisation of the sense strand to mRNA in tissue resulting in no localisation (Figure 3-38). It was found that PBR mRNA is expressed in both normal tissue and colonic adenocarcinoma. All cases showed that PBR mRNA expression varies from the normal to the diseased state, with PBR mRNA expression levels increasing in Grade I colonic adenocarcinoma when compared to its normal counterpart while decreasing in

Grade II and Grade III colonic adenocarcinoma when compared to its normal counterpart. Also all cases showed that PBR mRNA expression levels varies for the different grades of the tumour showing that PBR mRNA expression levels decreases from Grade I to Grade II and Grade III colonic adenocarcinoma respectively. However, it should be noted that in all cases Grade II colonic adenocarcinoma showed a lower expression level of PBR mRNA than Grade III colonic adenocarcinoma.

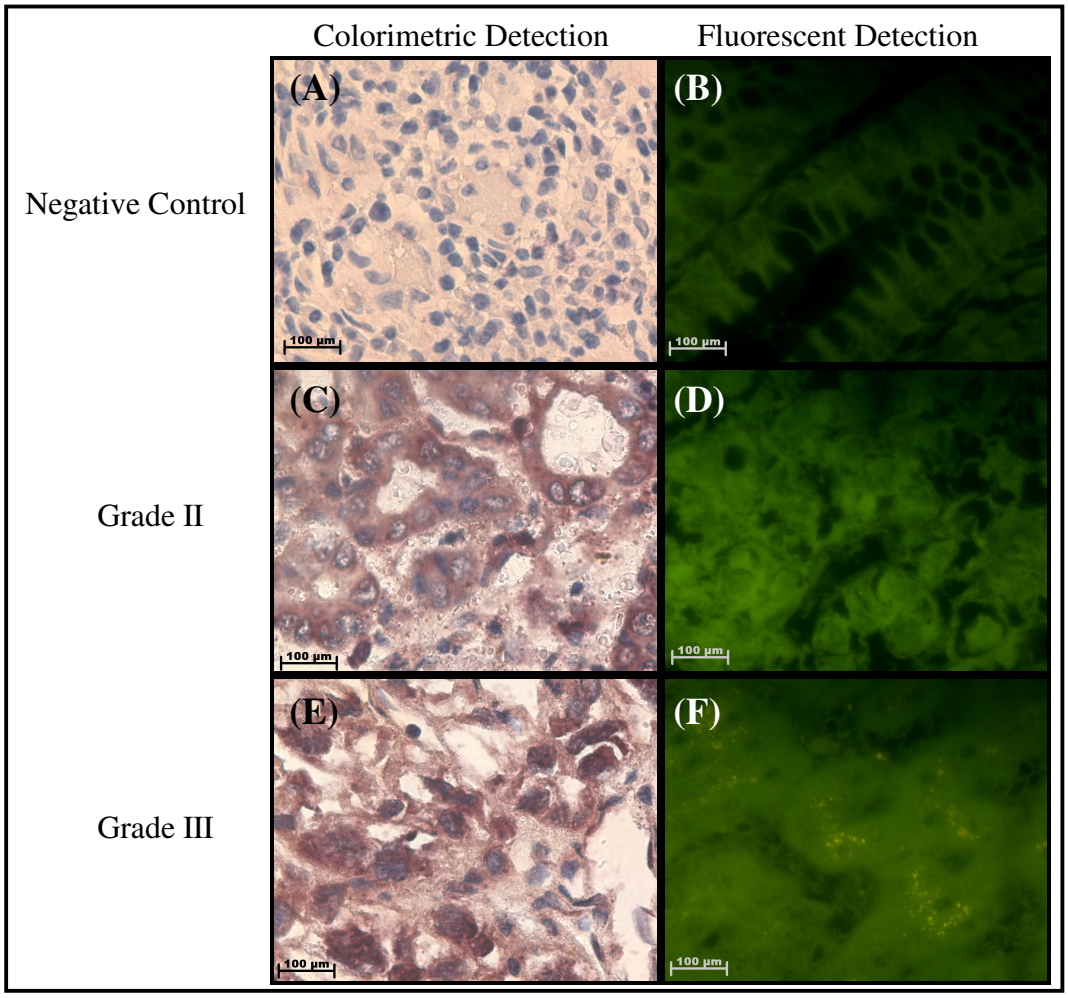



**Figure 3-37: Subcellular Localisation of the Peripheral Benzodiazepine Receptor mRNA in Hepatocellular Carcinoma** (Magnification 1000X)

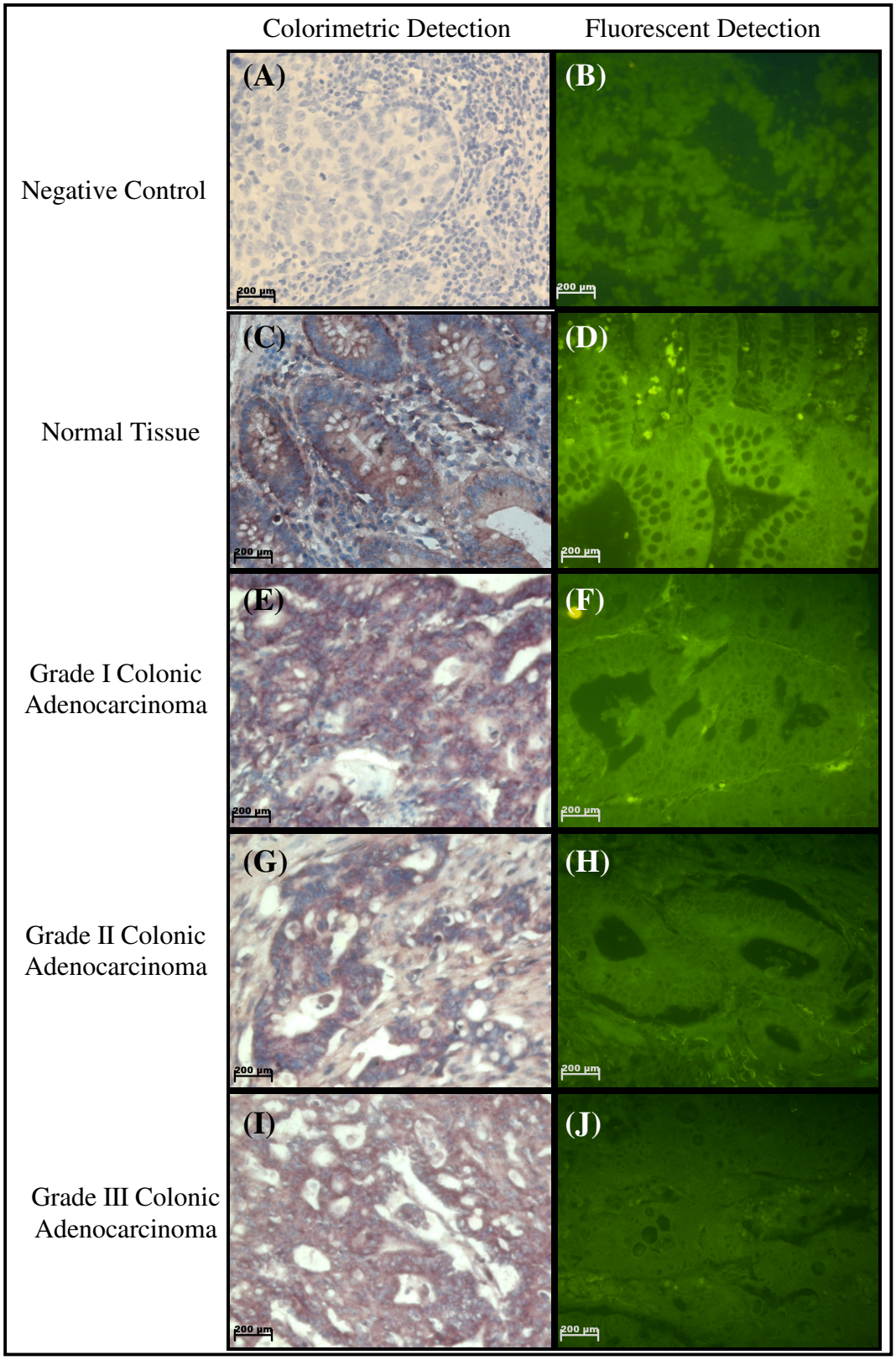



**Figure 3-38: Expression of the Peripheral Benzodiazepine Receptor mRNA in Colon**

(Magnification 400X)

The subcellular localisation of the PBR mRNA is determined by comparing a tissue sample to the negative control. In normal colon tissue PBR mRNA is expressed in the cytoplasm of goblet cells and absorptive cells of the Crypts of Lieberkhün and in the cytoplasm of plasma cells and in the nuclei and cytoplasm of lymphocytes located in the lamina propria (Figure 3-39).

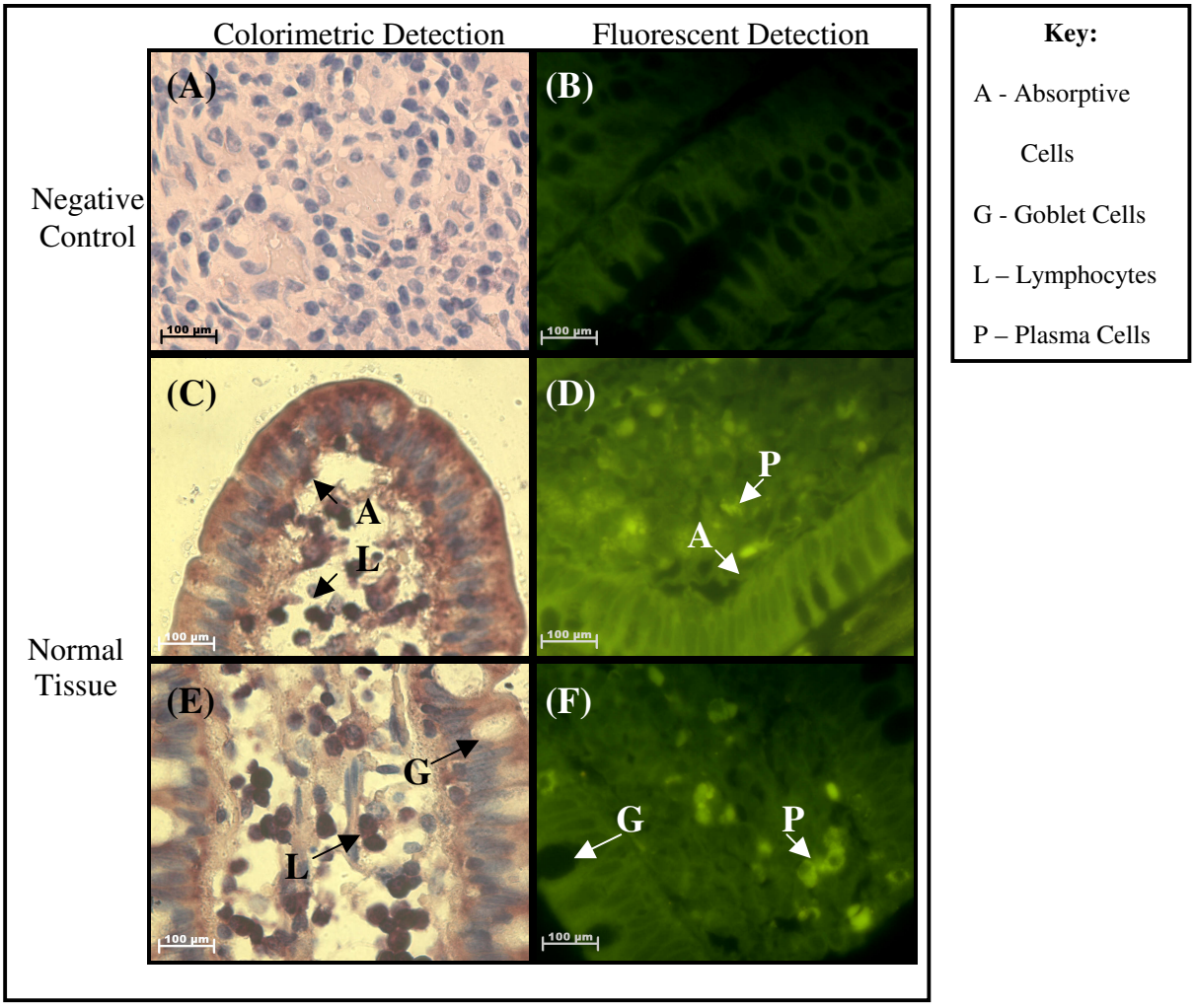



**Figure 3-39: Subcellular Localisation of the Peripheral Benzodiazepine Receptor mRNA in Normal Colon Tissue** (Magnification 1000X)

Grade I colonic adenocarcinoma express PBR mRNA in the cytoplasm of tumour cells that are mucin-secreting and arranged in adenomatous tubular glands and fibromuscular stroma, Grade II colonic adenocarcinomas express PBR mRNA in the cytoplasm of tumour cells arranged as adenomatous glands and tumour cells arranged as solid sheets while Grade III colonic adenocarcinoma express PBR mRNA in the cytoplasm of tumour cells that are predominantly arranged as a solid pattern (Figure 3-40).

### *3.2.4.3.Expression of the Peripheral Benzodiazepine Receptor mRNA in Epiploon Normal and Tumour Tissues*

Expression of PBR mRNA in the epiploon and stomach can be determined by comparing normal and cancerous tissues to the negative control (Figure 3-41). It was found that PBR is expressed in both normal epiploon and stomach and in Grade III stomach squamous cell carcinoma. PBR mRNA expression varies from the normal to the diseased state, with PBR mRNA expression levels increasing in squamous cell carcinoma compared to its normal counterpart. In addition, PBR mRNA may be expressed at a higher level in epiploon than in the stomach of normal tissue as determined by the intensity of the staining because 50% of cases studied showed a high expression level while 50% of the cases studied showed an intermediate expression level.

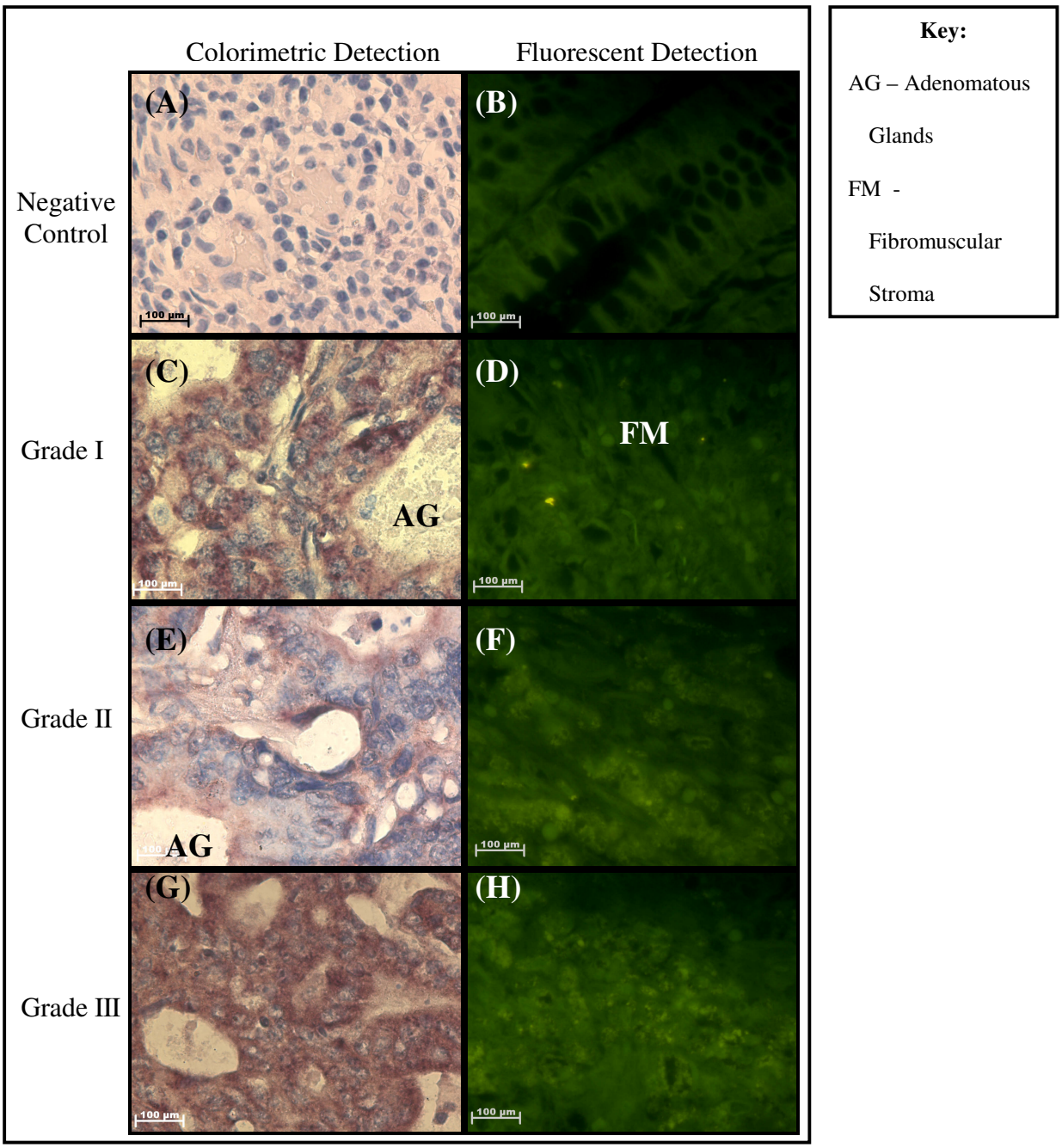



**Figure 3-40: Subcellular Localisation of Peripheral Benzodiazepine Receptor mRNA in Colonic Adenocarcinoma** (Magnification 1000X)

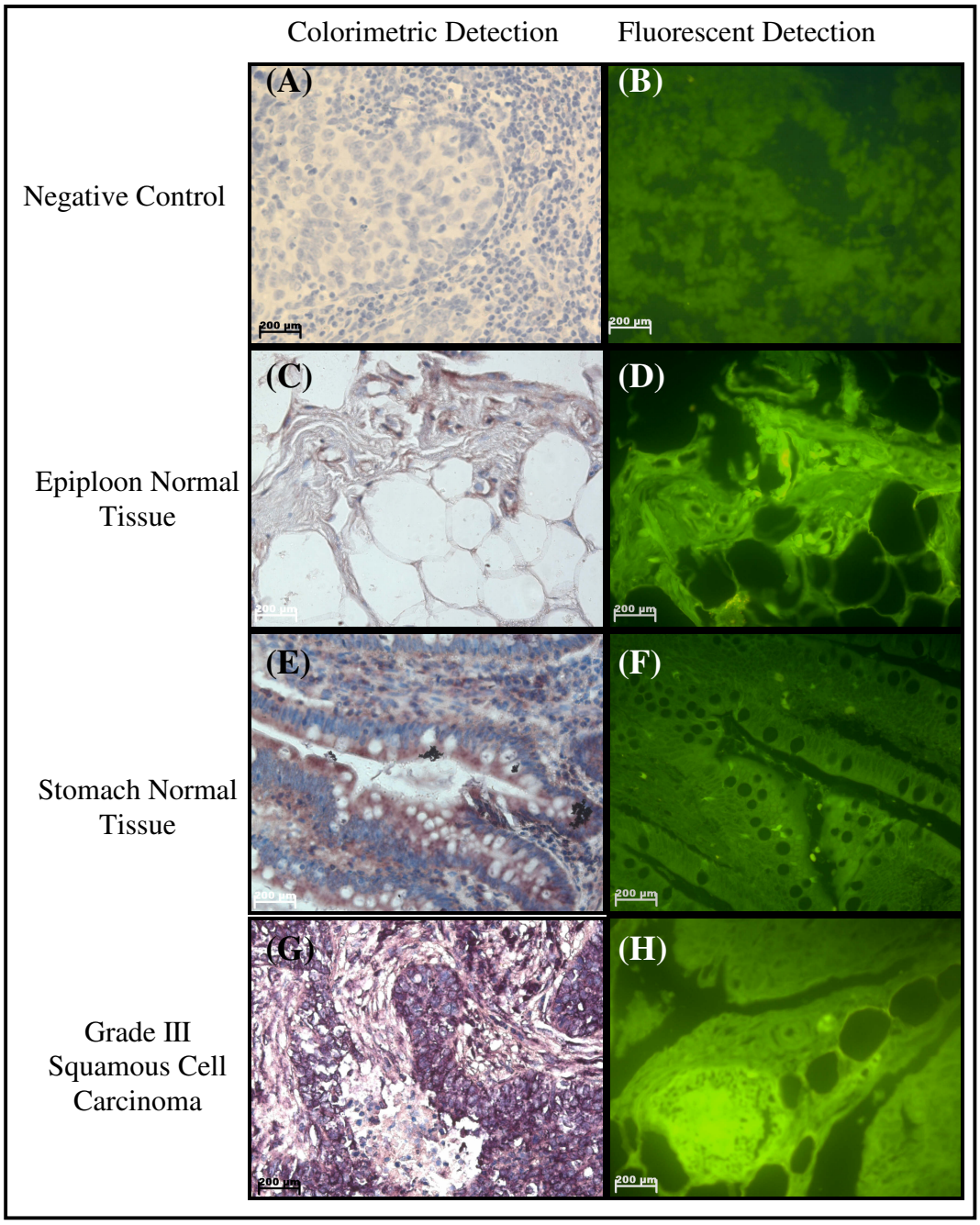



**Figure 3-41: Expression of the Peripheral Benzodiazepine Receptor mRNA in Normal Epiploon and Stomach** (Magnification 400X)

The subcellular localisation of the PBR mRNA is determined by comparing a tissue sample to the negative control. In normal epiploon tissue PBR mRNA is expressed in the cytoplasm of adipose cells, collagen fibres and fibroblasts located between the collagen fibres in the stroma (Figure 3-42).

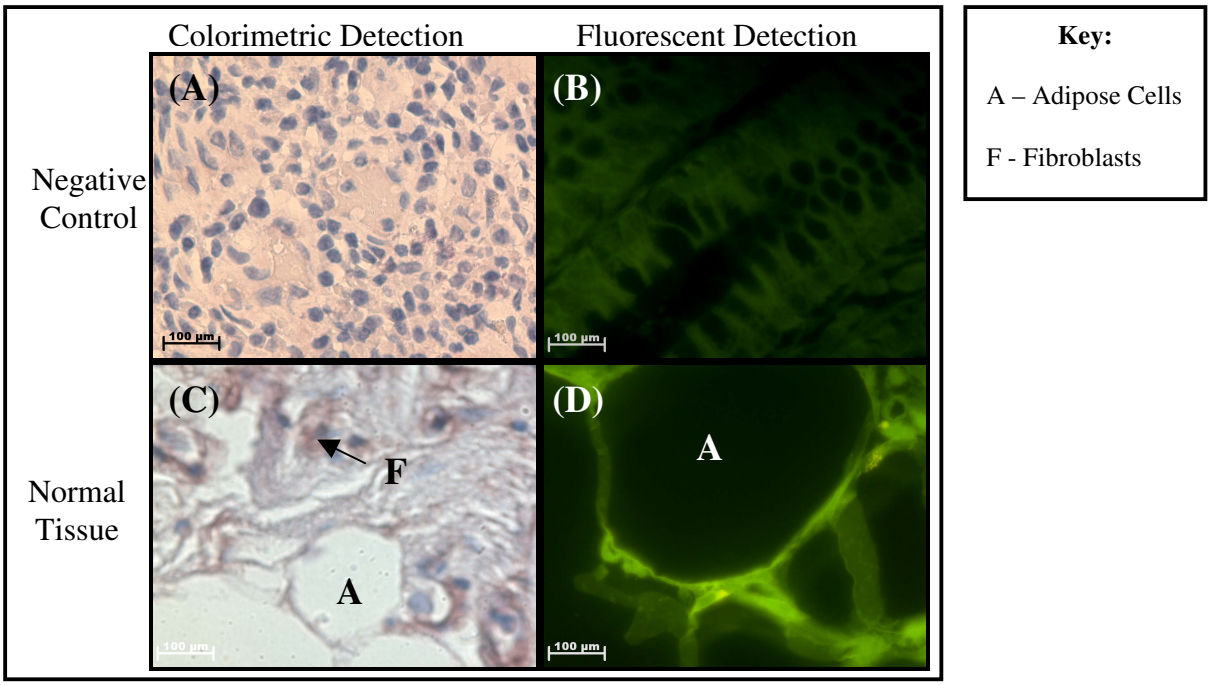



**Figure 3-42: Subcellular Localisation of the Peripheral Benzodiazepine Receptor mRNA in Normal Epiploon Tissue** (Magnification 1000X)

In stomach normal tissue PBR mRNA is expressed in the cytoplasm of parietal cells, chief cells, surface mucous cells and neck mucous cells of the gastric glands and in the cytoplasm of collagen fibres, plasma cells and macrophages and nuclei and cytoplasm of lymphocytes located in the lamina propria (Figure 3-43).

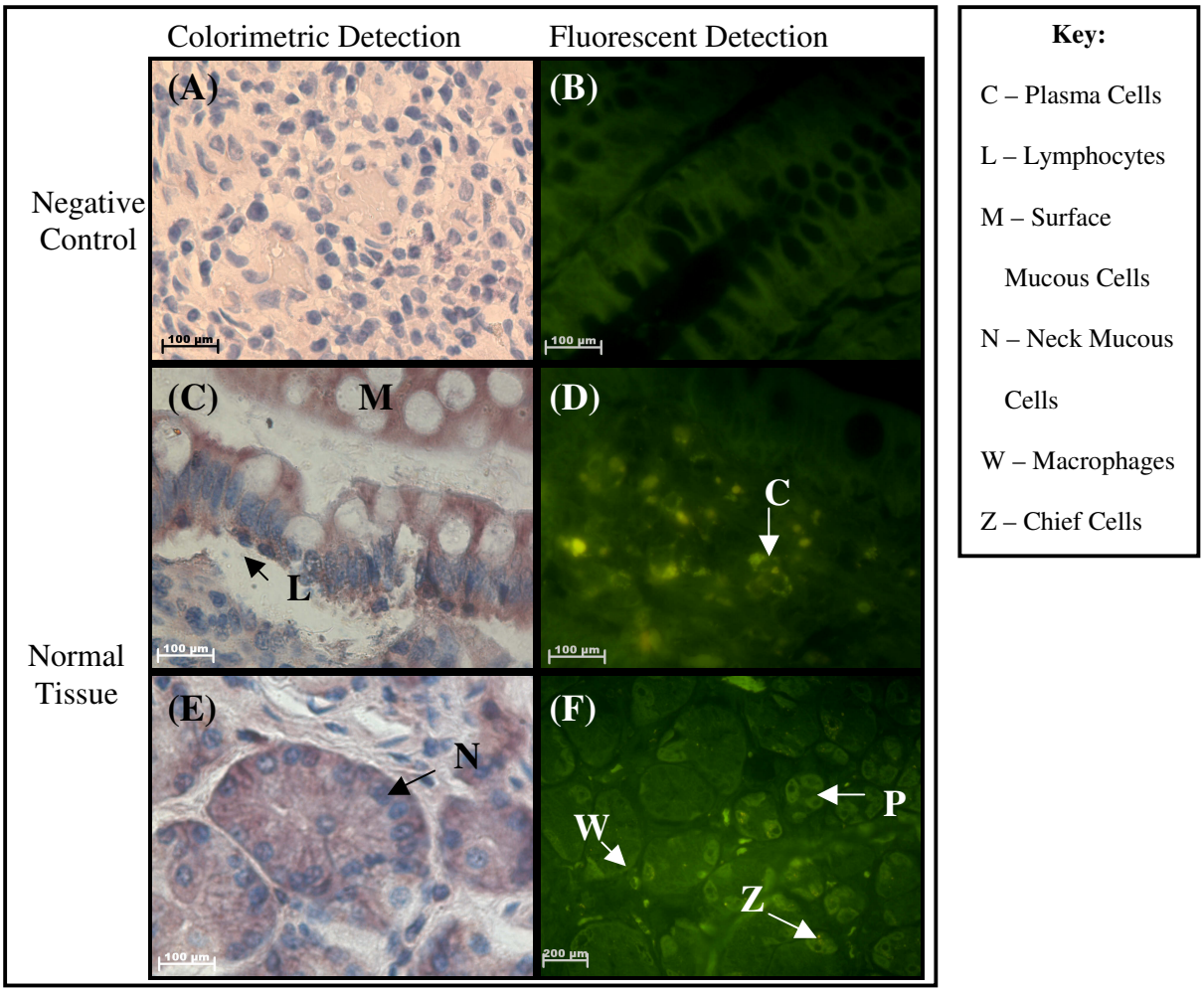



**Figure 3-43: Subcellular Localisation of the Peripheral Benzodiazepine Receptor mRNA in Normal Stomach Tissue** (Magnification 1000X)

In Grade III stomach squamous cell carcinoma PBR mRNA is expressed in the cytoplasm of tumour cells and collagen fibres in the surrounding stroma (Figure 3-44).

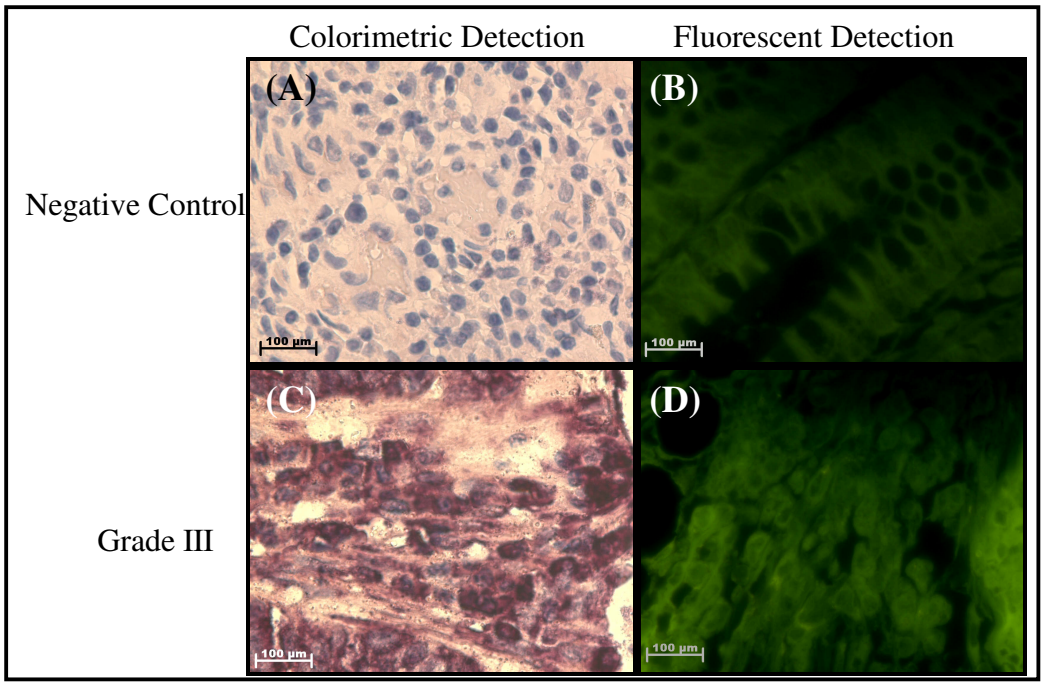



**Figure 3-44: Subcellular Localisation of the Peripheral Benzodiazepine Receptor mRNA in Stomach Squamous Cell Carcinoma** (Magnification 1000X)

*3.2.4.4. Expression of the Peripheral Benzodiazepine Receptor mRNA in Prostate Normal and Tumour Tissues*

Expression of PBR mRNA in prostate can be determined by comparing normal and cancerous tissues to the negative control (Figure 3-45). It was found that PBR mRNA is expressed in both hyperplastic tissue and adenocarcinoma of the peripheral duct and acini. PBR mRNA expression varies from the normal to the diseased state, with all cases showing PBR mRNA expression levels increasing in Grade II and Grade III adenocarcinoma of the peripheral duct and acini when compared to its normal counterpart. Also, PBR mRNA expression levels vary for the different grades of the tumour showing that PBR mRNA expression levels increases from Grade II to Grade III adenocarcinoma of the peripheral duct and acini.

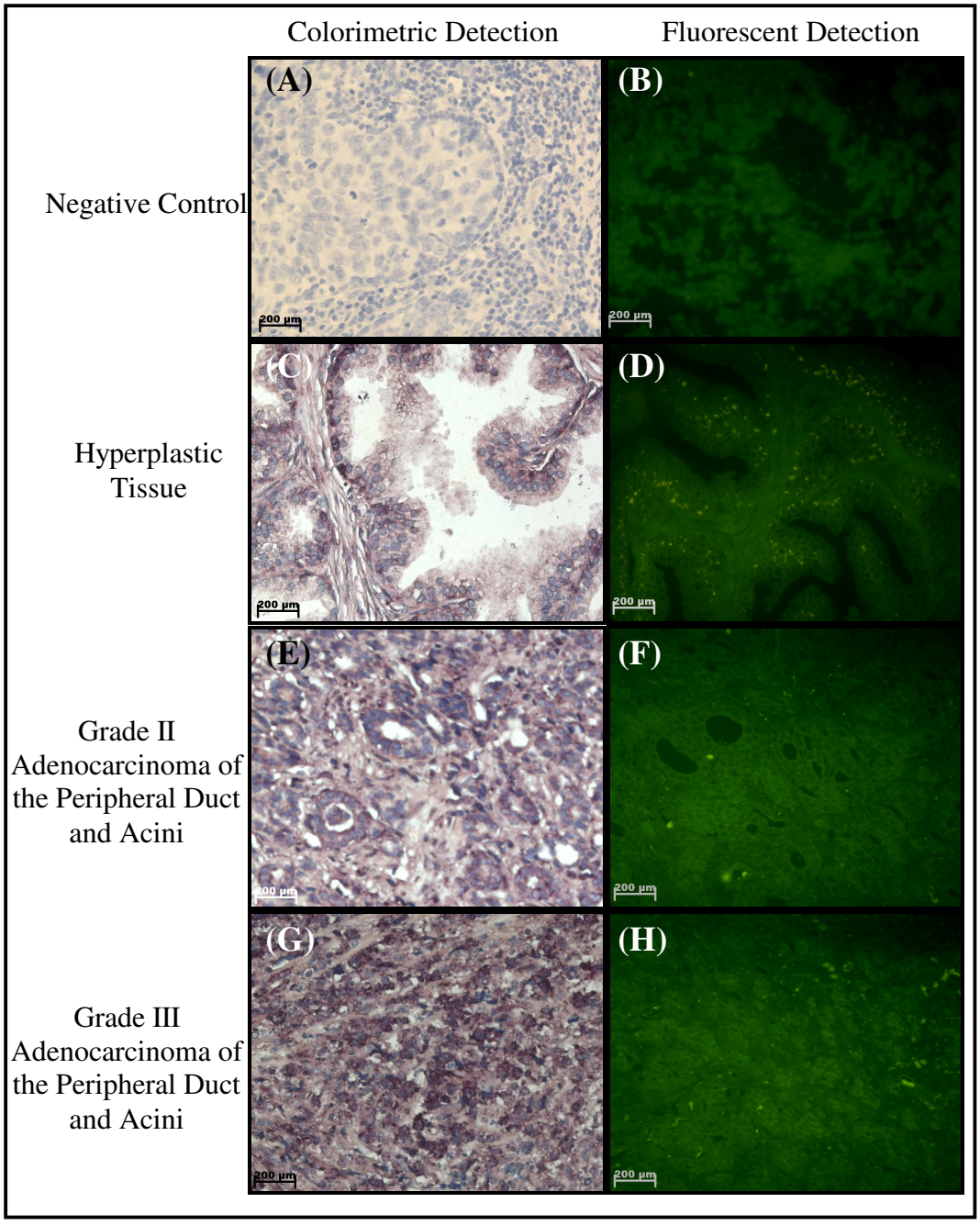



**Figure 3-45: Expression of the Peripheral Benzodiazepine Receptor mRNA in Prostate**

(Magnification 400X)

The subcellular localisation of the PBR mRNA is determined by comparing a tissue sample to the negative control. In hyperplastic prostate tissue PBR mRNA is expressed in the cytoplasm of the inner columnar epithelium and in the cytoplasm and nuclei of the outer cuboidal to flattened endothelial cells that line the glands and in the cytoplasm of the collagen and elastic fibres and in the nuclei of fibroblasts of the fibromuscular stroma (Figure 3-46).

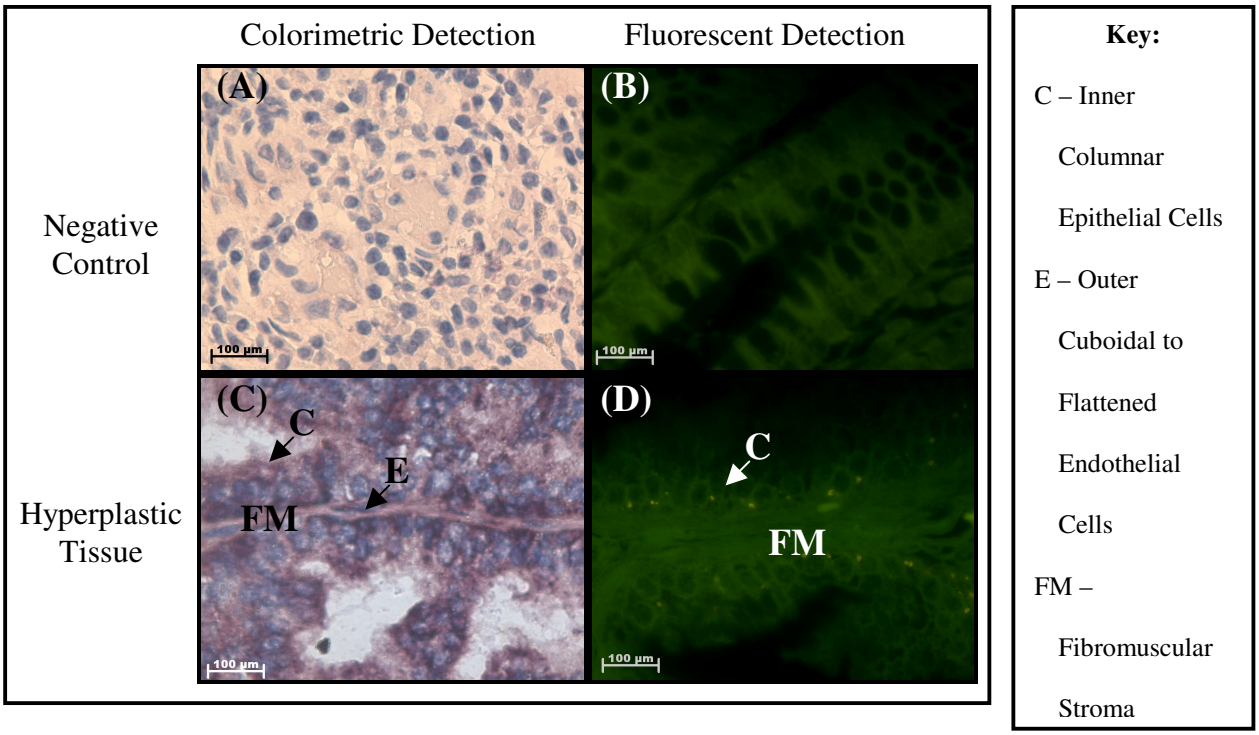



**Figure 3-46: Subcellular Localisation of the Peripheral Benzodiazepine Receptor mRNA in Hyperplastic Prostate Tissue** (Magnification 1000X)

Grade II adenocarcinoma of the peripheral duct and acini expresses PBR mRNA in the cytoplasm of cuboidal to low columnar epithelial cells lining glands and in the collagen fibres located in the stroma and in the nuclei and cytoplasm of lymphocytes and endothelial cells lining blood vessels located in the surrounding stroma while Grade III adenocarcinoma of the

peripheral duct and acini expresses PBR mRNA in the cytoplasm of tumour cells that grow in nests or sheets (Figure 3-47).

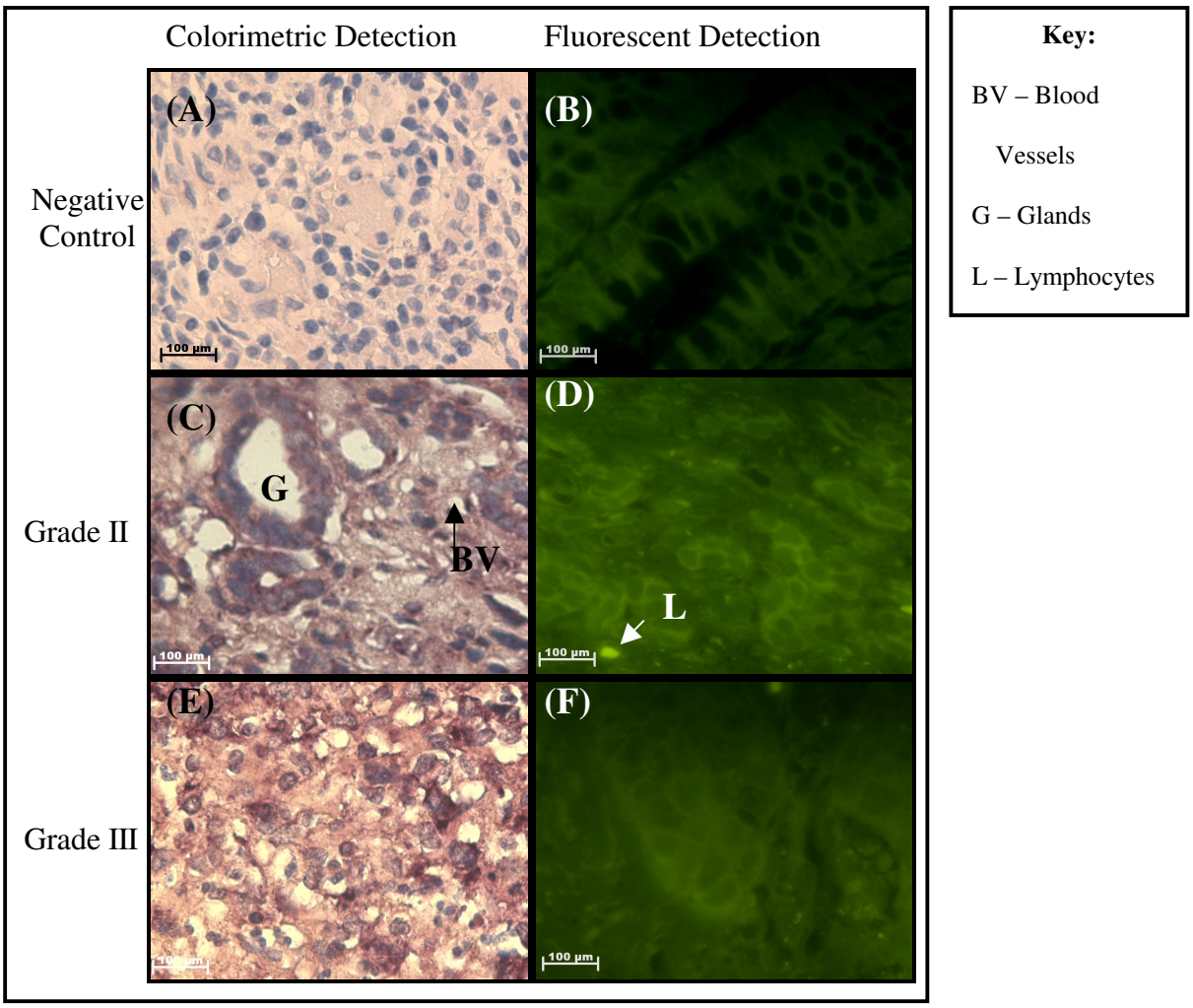



**Figure 3-47: Subcellular Localisation of the Peripheral Benzodiazepine Receptor mRNA in Prostate Adenocarcinoma of the Peripheral Duct and Acini** (Magnification 1000X)

*3.2.4.5. Expression of the Peripheral Benzodiazepine Receptor mRNA in Breast Normal and Tumour Tissues*

Expression of PBR mRNA in breast can be determined by comparing normal and cancerous tissues to the negative control (Figure 3-48). It was found that PBR mRNA is expressed in both normal and Grade III invasive carcinoma (NST). PBR mRNA expression varies from the

normal to the diseased state, with PBR mRNA expression levels increasing in invasive carcinoma (NST) when compared to its normal counterpart.

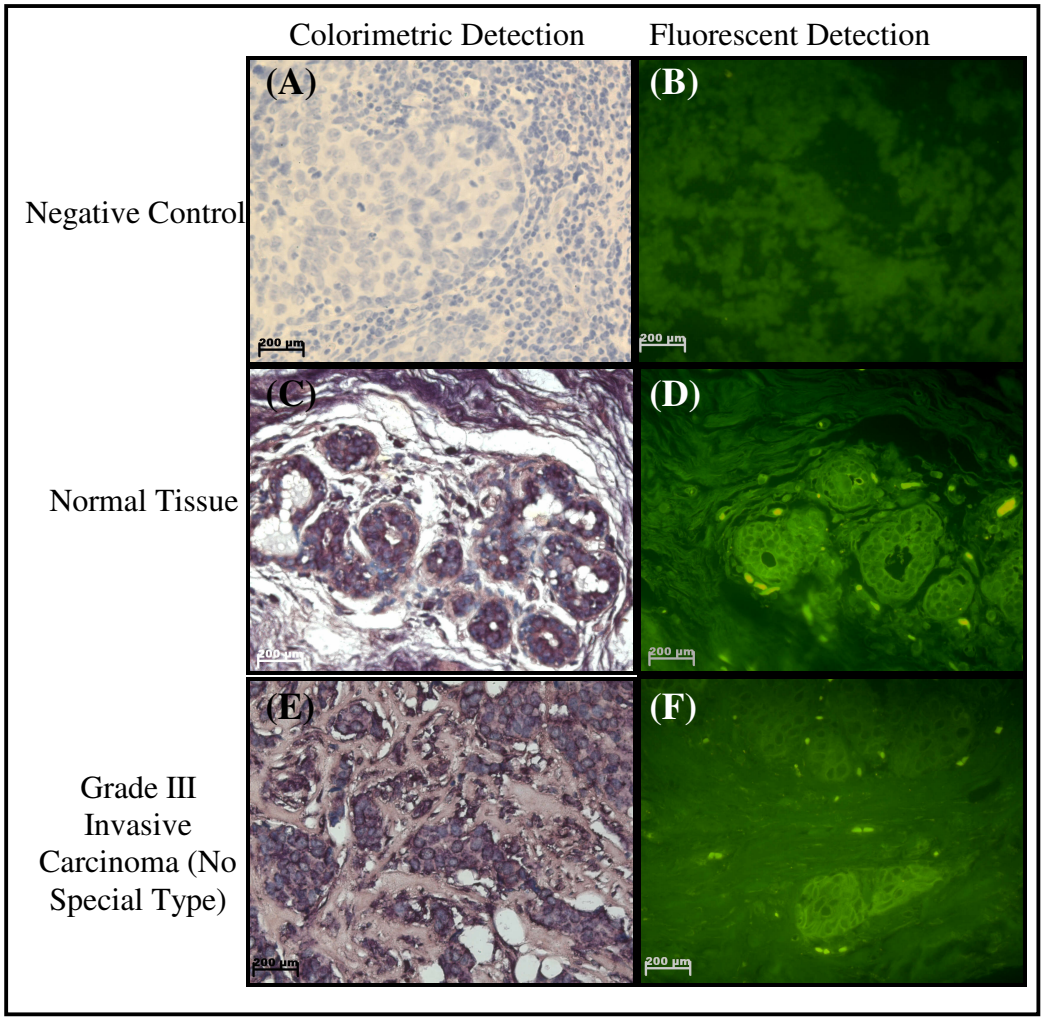



**Figure 3-48: Expression of the Peripheral Benzodiazepine Receptor mRNA in Breast**

(Magnification 400X)

The subcellular localisation of the PBR mRNA is determined by comparing a tissue sample to the negative control. In normal breast tissue PBR mRNA is expressed in the cytoplasm of the luminal layer of cuboidal epithelial cells and the outer layer of discontinuous epithelial cells of the terminal ducts and alveoli, in cytoplasm of collagen fibres of the fibroconnective tissue,

in nuclei and cytoplasm of lymphocytes and in the nuclei of endothelial cells of the vascular tissue located in the intralobular stroma (Figure 4-49).

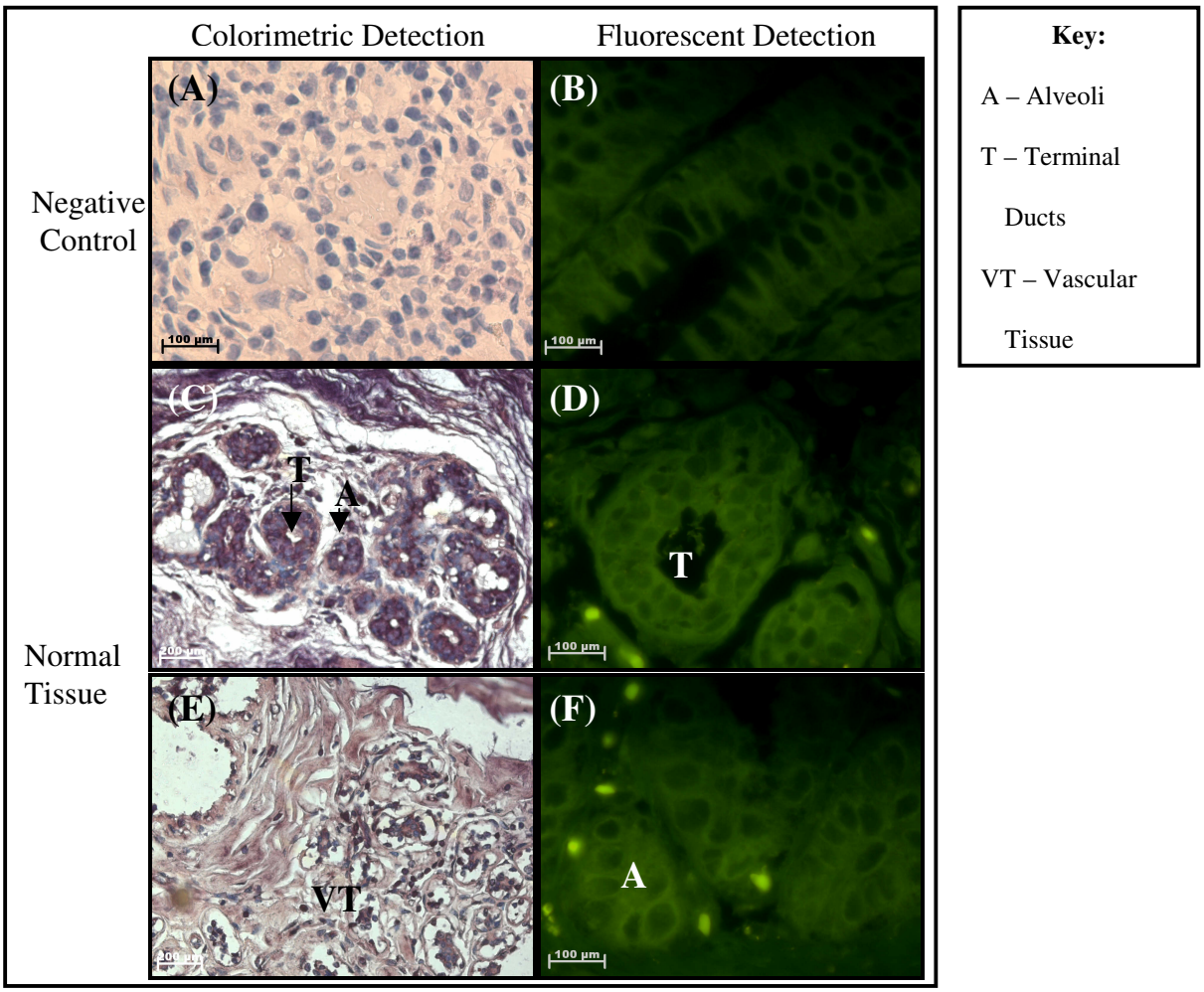



**Figure 3-49: Subcellular Localisation of the Peripheral Benzodiazepine Receptor mRNA in Normal Breast Tissue** (Magnification 1000X)

Grade III invasive carcinoma (NST) expresses PBR mRNA in the cytoplasm of tumour cells arranged as nests and collagen fibres of the fibrotic stroma and in the nuclei and cytoplasm of lymphocytes located between the tumour and stroma, indicating the presence of a mononuclear infiltrate (Figure 3-50).

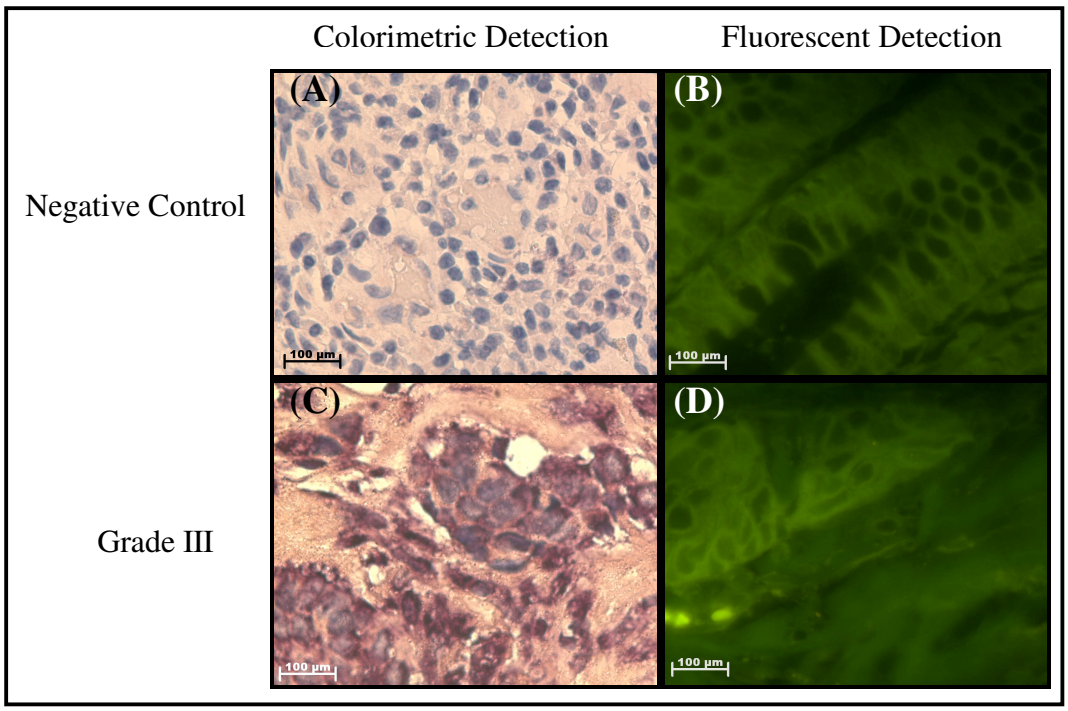



**Figure 3-50: Subcellular Localisation of the Peripheral Benzodiazepine Receptor mRNA in Breast Invasive Carcinoma (No Specific Type)** (Magnification 1000X)

*3.2.4.6. Expression of the Peripheral Benzodiazepine Receptor mRNA in Lung Normal and Tumour Tissues*

Expression of PBR mRNA in lung can be determined by comparing normal and cancerous tissues to the negative control (Figure 3-51). It was found that PBR mRNA is expressed in both normal and cancerous tissues (Grade III adenocarcinoma, Grade III squamous cell carcinoma and small cell carcinoma). PBR mRNA expression varies from the normal to the diseased state, with PBR mRNA expression levels increasing in all cases Grade III squamous cell carcinoma, decreasing in all cases of Grade III adenocarcinoma and 50% cases of small cell carcinoma and showing no expression in 50% cases of small cell carcinoma. Also, the expression of PBR mRNA varies between the different types of cancers, with Grade III squamous cell carcinoma showing the most intense staining while small cell carcinoma showing the least intense staining.

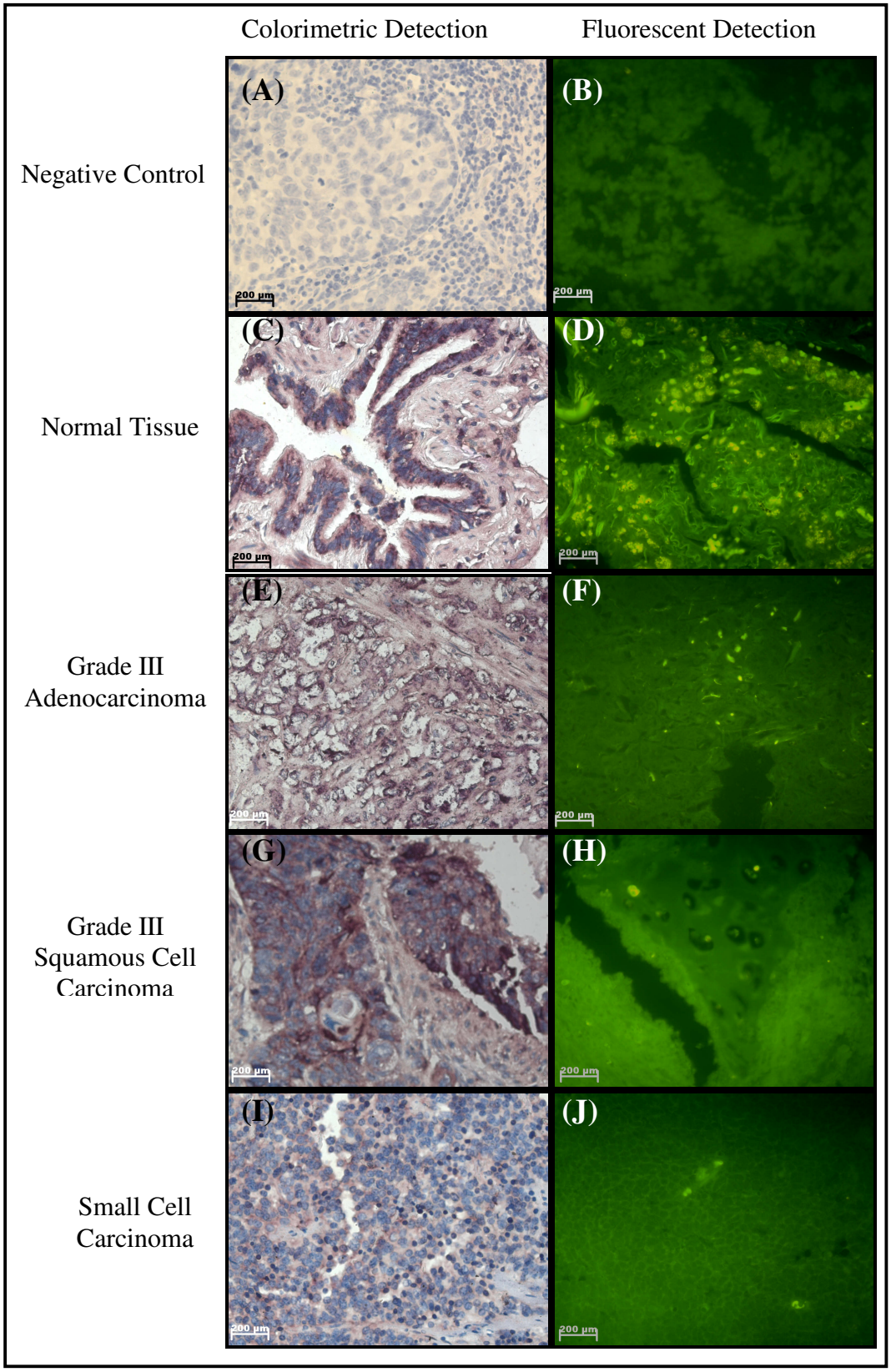



**Figure 3-51: Expression of the Peripheral Benzodiazepine Receptor mRNA in Lung**

(Magnification 400X)

The subcellular localisation of the PBR mRNA is determined by comparing a tissue sample to the negative control. In normal lung tissue PBR mRNA is expressed in the cytoplasm of macrophages, plasma cells and fibroblasts in the surrounding stroma, in the cuboidal cells that line the respiratory bronchiole and in the smooth muscle fibres surrounding the pulmonary artery, and in the nuclei and cytoplasm of the endothelial cells of the pulmonary artery and lymphocytes in the surrounding stroma (Figure 3-53).

Grade III lung adenocarcinoma expresses PBR mRNA in the cytoplasm and nuclei of tumour cells and in the fibres located in the surrounding solid-like stroma (Figure 3-52).

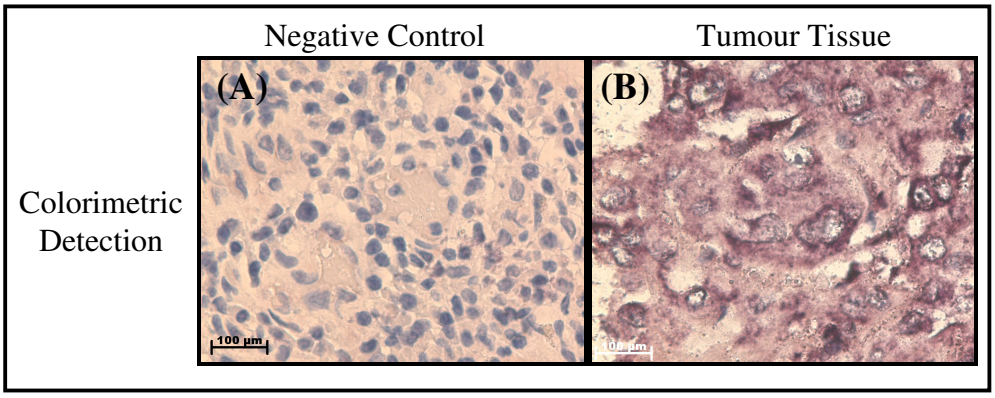



**Figure 3-52: Subcellular Localisation of the Peripheral Benzodiazepine Receptor mRNA in Lung Adenocarcinoma** (Magnification 1000X)

Grade III squamous cell carcinoma expresses PBR mRNA in the cytoplasm and nuclei of tumour cells that is characterised with the merging of tumour cells with the large cell pattern (Figure 3-54).

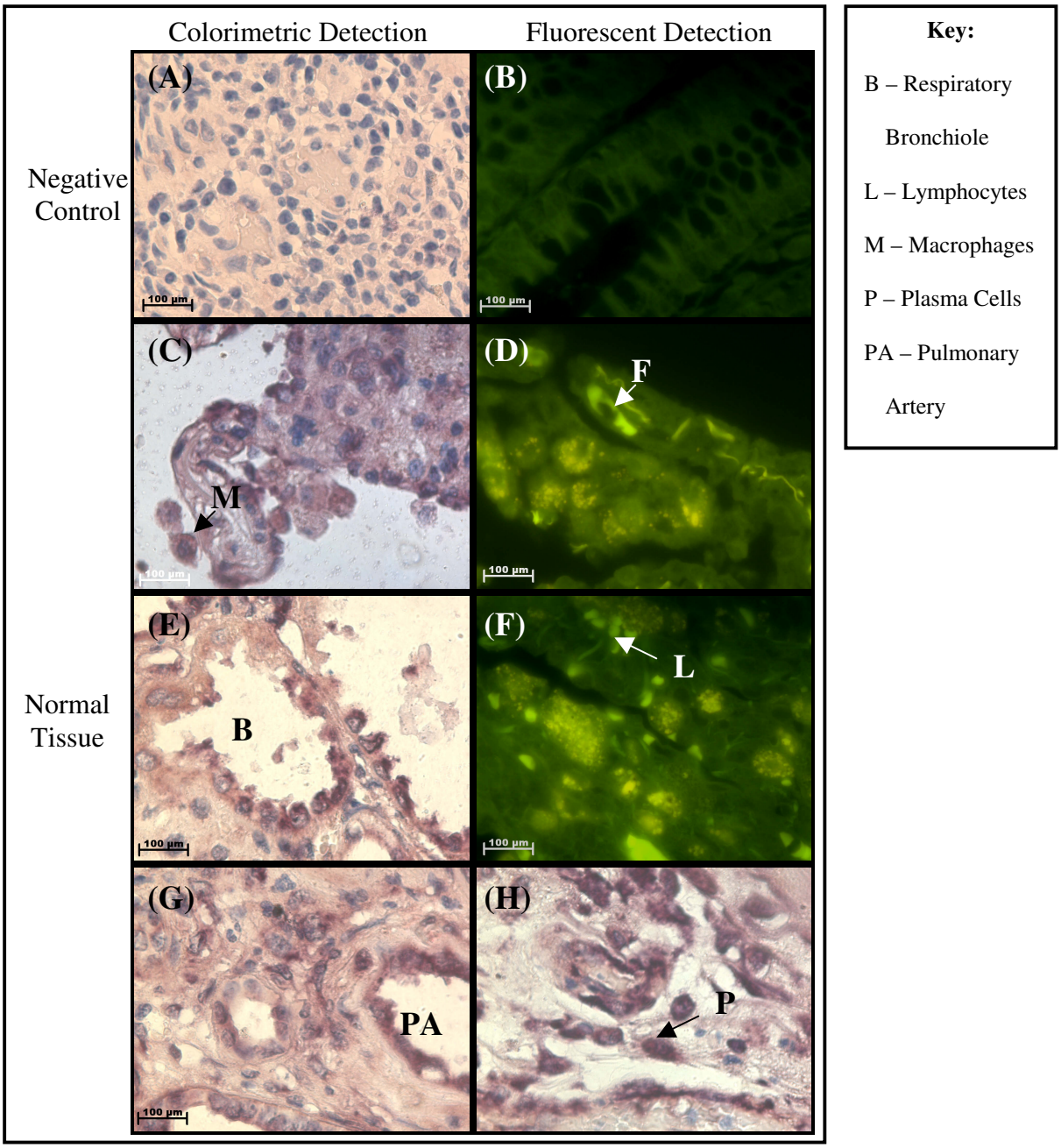



**Figure 3-53: Subcellular Localisation of the Peripheral Benzodiazepine Receptor mRNA in Normal Lung Tissue** (Magnification 1000X)

Lung small cell carcinoma expresses PBR mRNA in the cytoplasm of tumour cells that resemble lymphocytes and have a scanty cytoplasm and in the nuclei of lymphocytes and endothelial cells lining capillaries in the stroma (Figure 3-55).

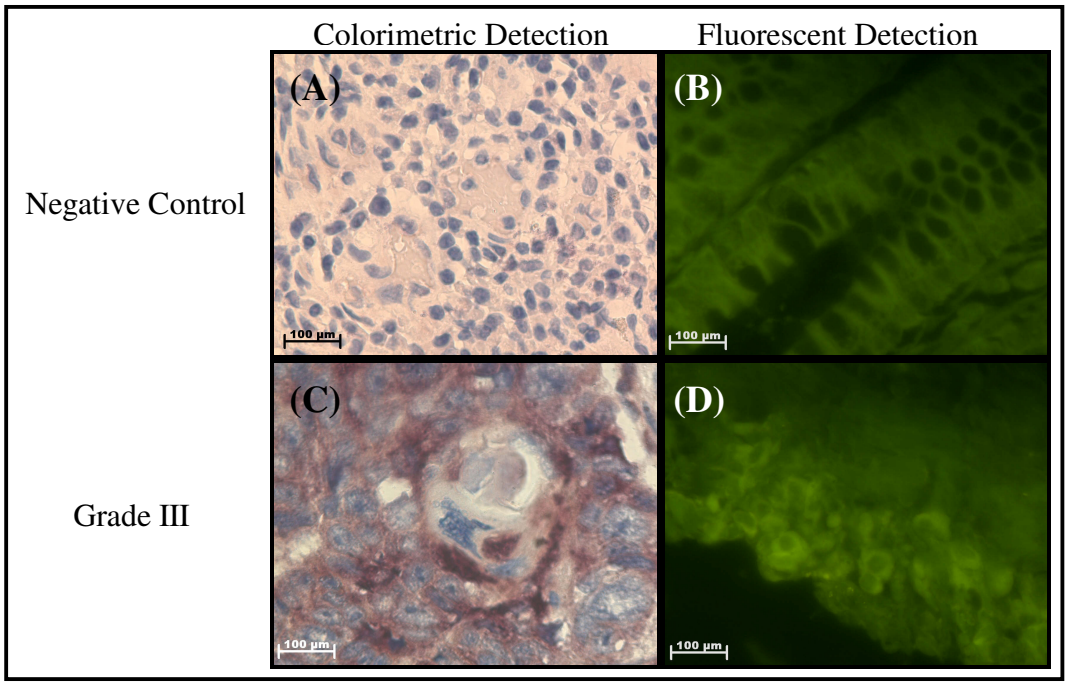



**Figure 3-54: Subcellular Localisation of the Peripheral Benzodiazepine Receptor mRNA in Lung Squamous Cell Carcinoma** (Magnification 1000X)

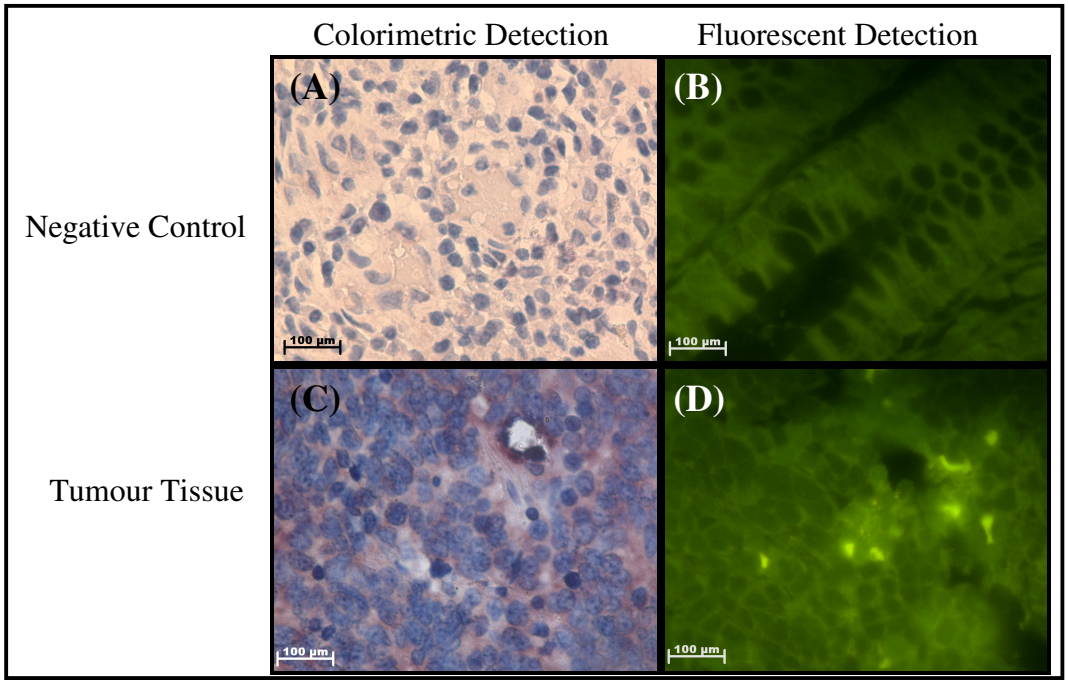



**Figure 3-55: Subcellular Localisation of the Peripheral Benzodiazepine Receptor mRNA in Lung Small Cell Carcinoma** (Magnification 1000X)

### *3.2.4.7. Expression of the Peripheral Benzodiazepine Receptor mRNA in Kidney Normal and Tumour Tissues*

Expression of PBR mRNA in kidney can be determined by comparing normal and cancerous tissues to the negative control (Figure 3-56). It was found that PBR mRNA is expressed in both normal and cancerous tissues (chromophobe renal cell carcinoma and clear cell renal carcinoma). PBR mRNA expression varies from the normal to the diseased state, with PBR mRNA expression levels increasing in all cases of chromophobe renal cell carcinoma and clear cell renal carcinoma. Also, the expression of PBR mRNA varies between the different types of cancers, with chromophobe renal cell carcinoma showing a higher expression of PBR mRNA than clear cell renal carcinoma seen by the intensity of staining.

The subcellular localisation of the PBR mRNA is determined by comparing a tissue sample to the negative control. In normal kidney tissue PBR mRNA is expressed in the cytoplasm of the flattened cells located in the parietal layer of the Bowman's capsule, in the cytoplasm of endothelial cells that lines the anastomosing network of capillaries of in the glomerulus, in the cytoplasm of the simple cuboidal epithelium with a prominent brush border of tall microvilli that lines the proximal convoluted tubule (PCT), in the cytoplasm of the simple squamous epithelium and erythrocytes within the vasa recta characterised by an irregular shape, in the cytoplasm of the simple squamous epithelium that lines the thin ascending and descending limbs characterised by a regular round shape, in the cytoplasm of the low cuboidal epithelium of the thick ascending limb that appear round in cross section, in the cytoplasm of the simple cuboidal epithelium of the distal convoluted tubule (DCT) characterised by the absence of a brush border and a larger more clearly defined lumen than the PCT, in the cytoplasm of the simple cuboidal epithelium of the collecting tubule that appears wider and less regular in

shape to the ascending limb and in the cytoplasm of the simple columnar epithelium that lines the collecting duct (Figure 3-57).

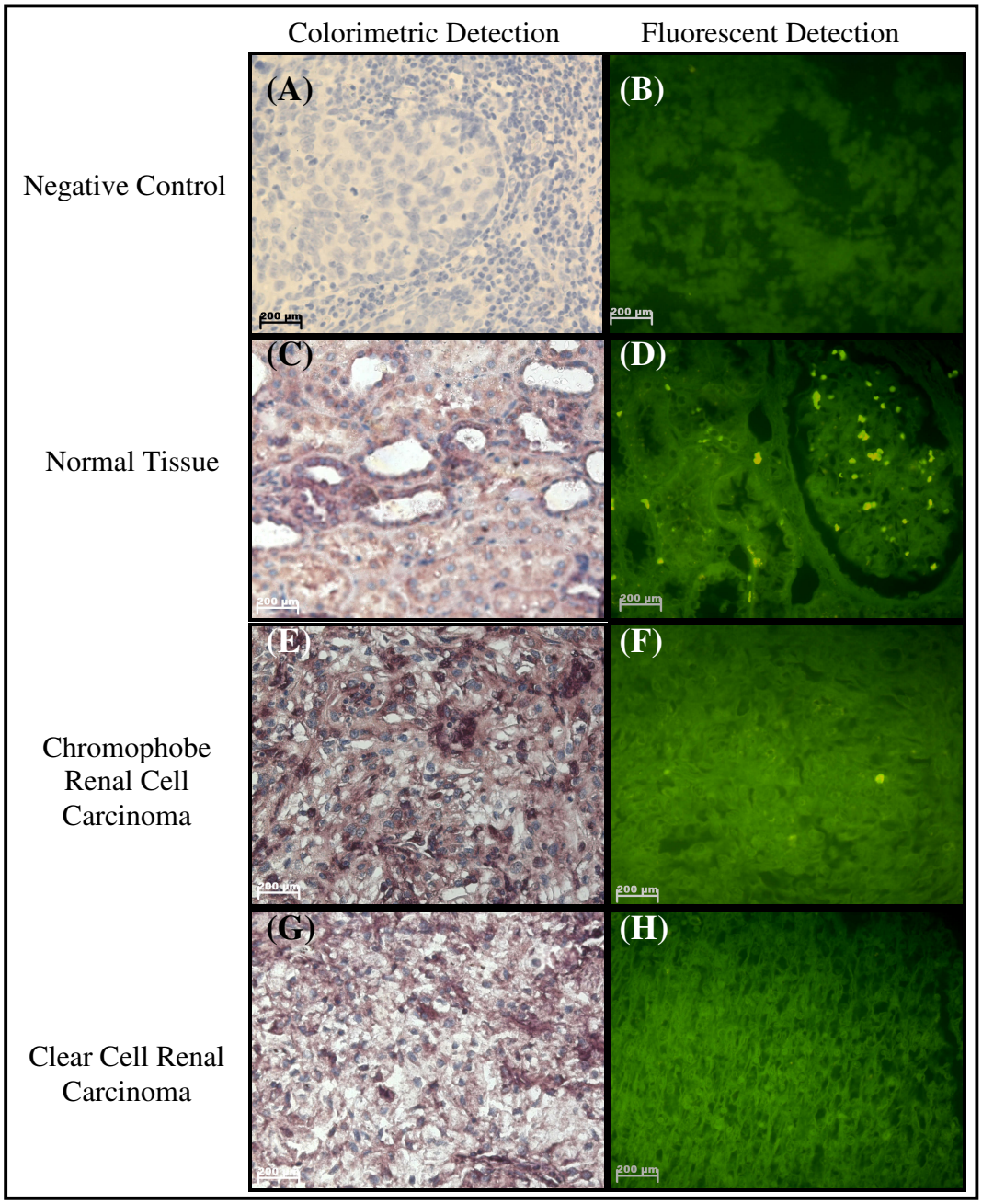



**Figure 3-56: Expression of the Peripheral Benzodiazepine Receptor mRNA in Kidney**

(Magnification 400X)

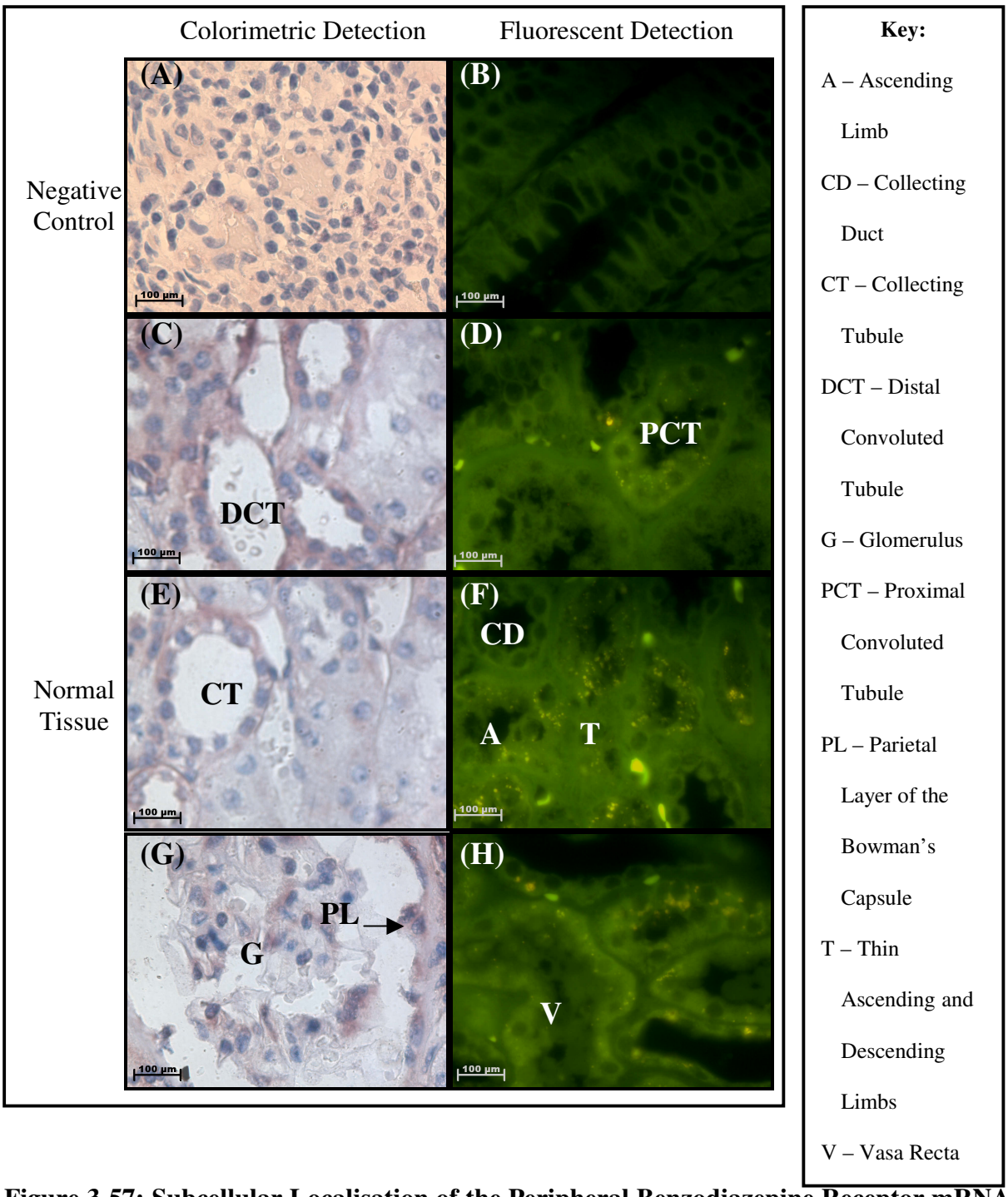



**Figure 3-57: Subcellular Localisation of the Peripheral Benzodiazepine Receptor mRNA in Normal Kidney Tissue** (Magnification 1000X)

Grade III chromophobe renal cell carcinoma shows expression of PBR mRNA in the nuclei and cytoplasm of tumour cells that are usually arranged as a solid pattern with concentrations of the largest cells around the blood vessels (Figure 3-58).

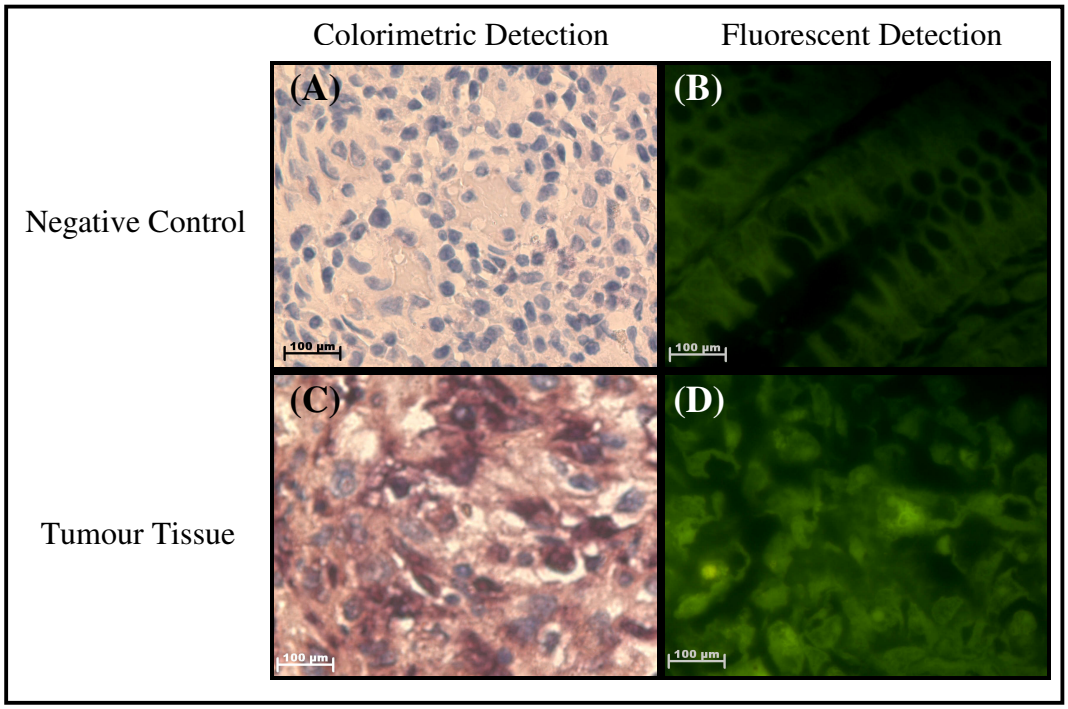



**Figure 3-58: Subcellular Localisation of the Peripheral Benzodiazepine Receptor mRNA in Chromophobe Renal Cell Carcinoma** (Magnification 1000X)

Renal clear cell carcinoma expresses PBR mRNA in the nuclei and cytoplasm of tumour cells and in the cytoplasm of the delicate branching vasculature that appears fibromuscular (Figure 3-59).

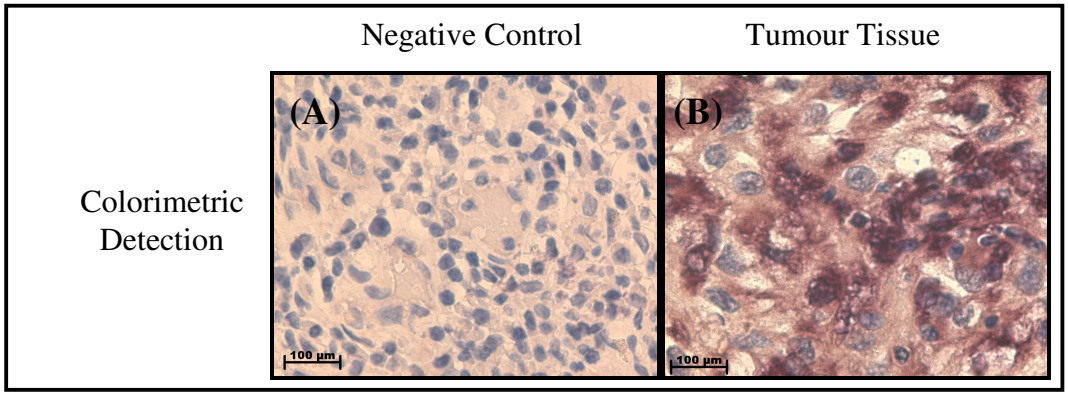



**Figure 3-59: Subcellular Localisation of the Peripheral Benzodiazepine Receptor mRNA in Renal Clear Cell Carcinoma** (Magnification 1000X)

### *3.2.4.8. Expression of the Peripheral Benzodiazepine Receptor mRNA in Brain Normal and Tumour Tissues*

Expression of PBR mRNA in brain can be determined by comparing normal and cancerous tissues to the negative control (Figure 3-60). It was found that PBR mRNA is expressed in both normal and cancerous tissues (Grade II diffuse fibrillary astrocytoma, primary central nervous system lymphoma (PCNSL) and ependymoma). PBR mRNA expression varies from the normal to the diseased state, with PBR mRNA expression levels increasing in all cases of Grade II diffuse fibrillary astrocytoma, PCNSL and ependymoma. Also, the expression of PBR mRNA varies between the different types of cancers; with Grade II diffuse fibrillary astrocytoma showing the highest level of expression and PCNSL showing the lowest level of expression. Furthermore, PBR mRNA expression levels vary between the different types of normal tissue, with grey matter showing a higher PBR mRNA expression than white matter.

The subcellular localisation of the PBR mRNA is determined by comparing a tissue sample to the negative control. In normal brain tissue PBR mRNA is expressed in the cytoplasm of neurones such as pyramidal cells, fusiform cells, in glia such as oligodendrocytes and in the astrocytes and in the cytoplasm of the fibrillary network of white matter and in the cytoplasm of glia such as oligodendrocytes, neurones such as stellate cells and astrocytes and in the cytoplasm of the fibrillary network of grey matter (Figure 3-61).

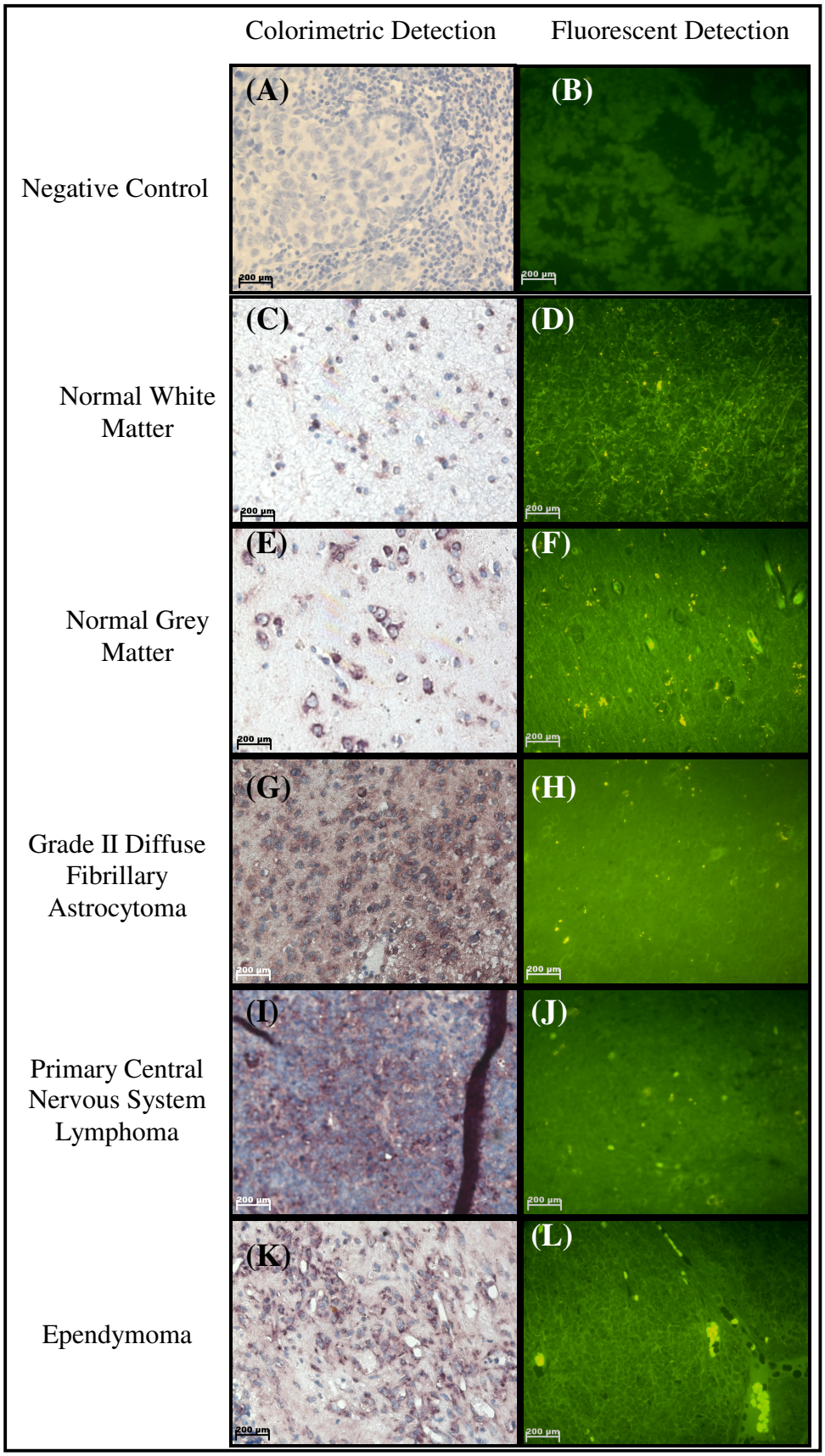



**Figure 3-60: Expression of the Peripheral Benzodiazepine Receptor mRNA in Brain**

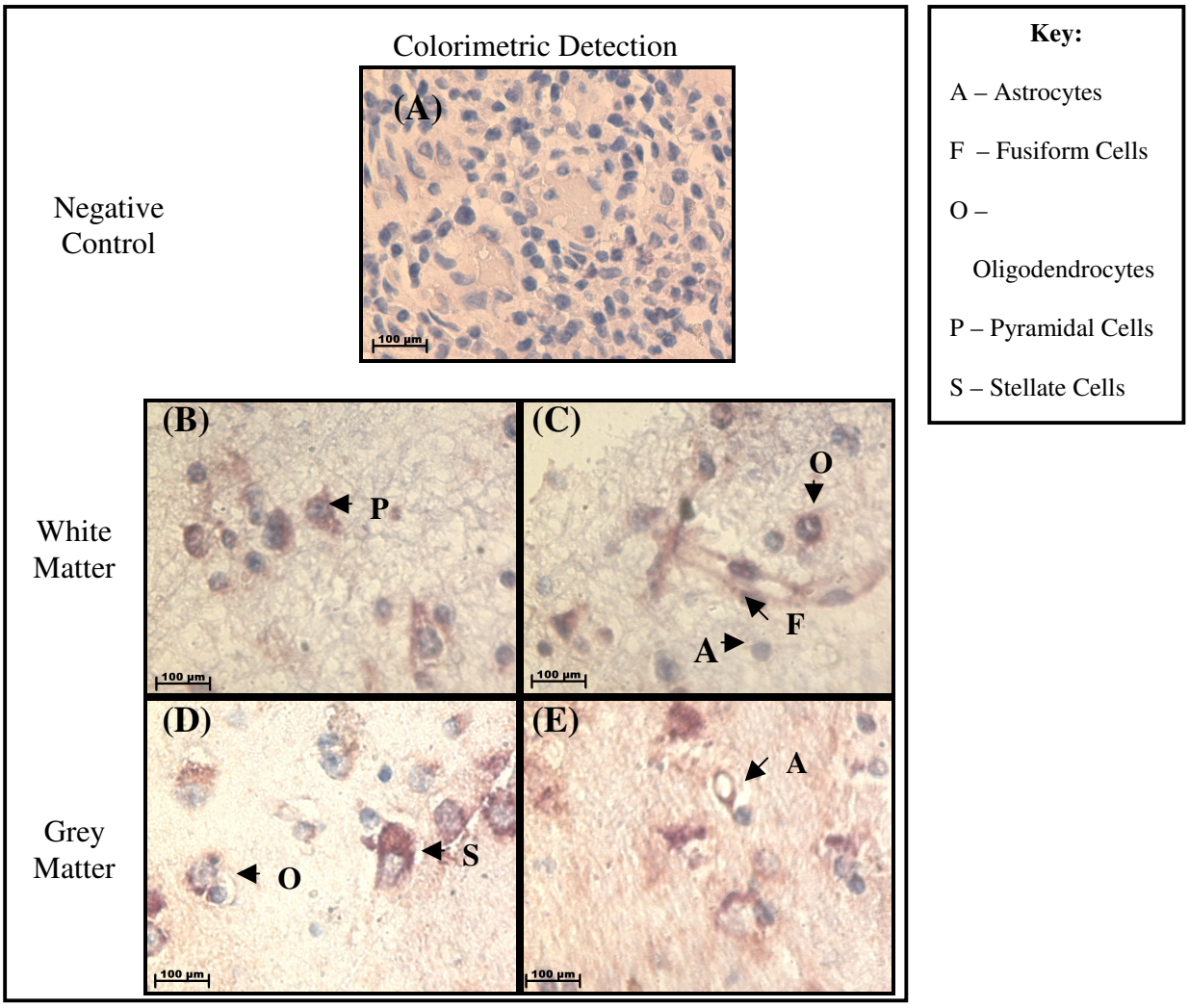



**Figure 3-61: Subcellular Localisation of the Peripheral Benzodiazepine Receptor mRNA in Normal Brain Tissue** (Magnification 1000X)

Grade II diffuse fibrillary astrocytoma expresses PBR mRNA in the cytoplasm of tumour cells that appear as glial cells having an oval shape appearance, neurones such as stellate cells and oligodendrocytes and in the astrocytes, that is, in the astrocytic processes that appears as a fibrillary background, in the nuclei of microglia and in the nuclei and cytoplasm of fusiform cells (Figure 3-62).

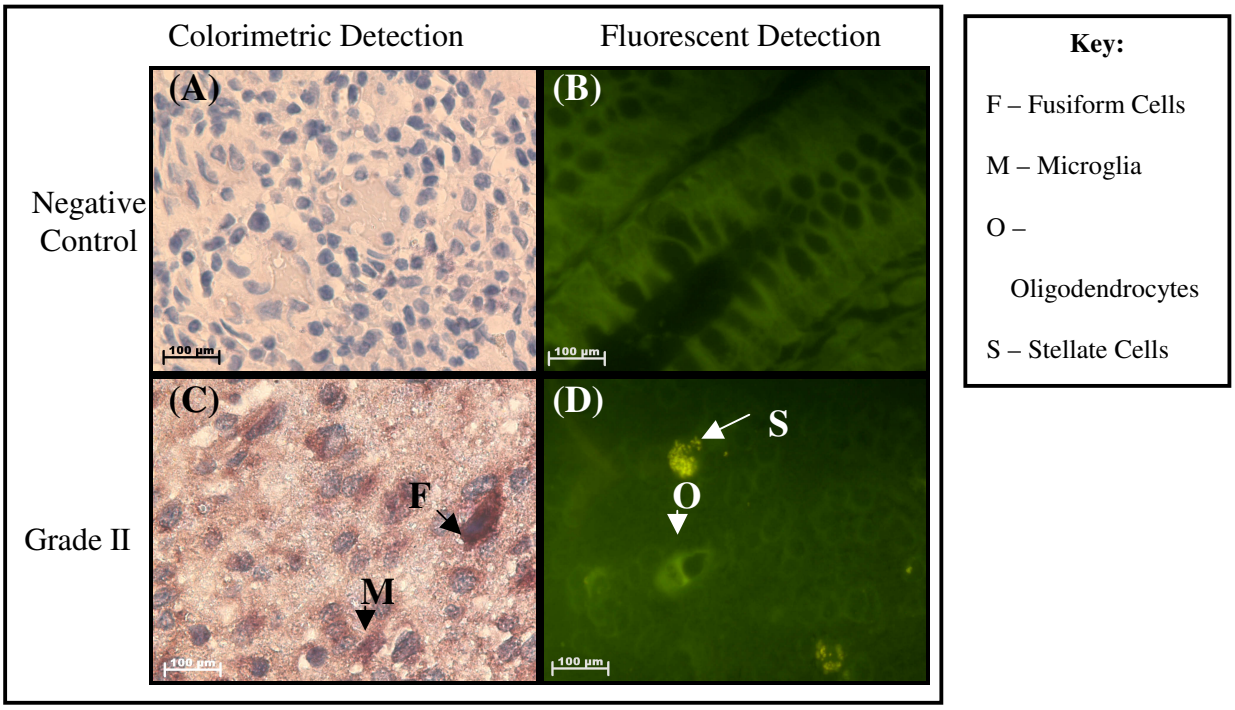



**Figure 3-62: Subcellular Localisation of the Peripheral Benzodiazepine Receptor mRNA in Diffuse Fibrillary Astrocytoma** (Magnification 1000X)

PCNSL expresses PBR mRNA in the cytoplasm of tumour cells that appear lymphocyte-like and neurones such as oligodendrocytes and in the nuclei and cytoplasm of astrocytes, microglia and fusiform cells (Figure 3-63).

Ependymomas expresses PBR mRNA in the nuclei and cytoplasm of tumour cells characterised by round to oval nuclei and an abundant granular cytoplasm and the fibrillary processes and in the nuclei of lymphocytes (Figure 3-64).

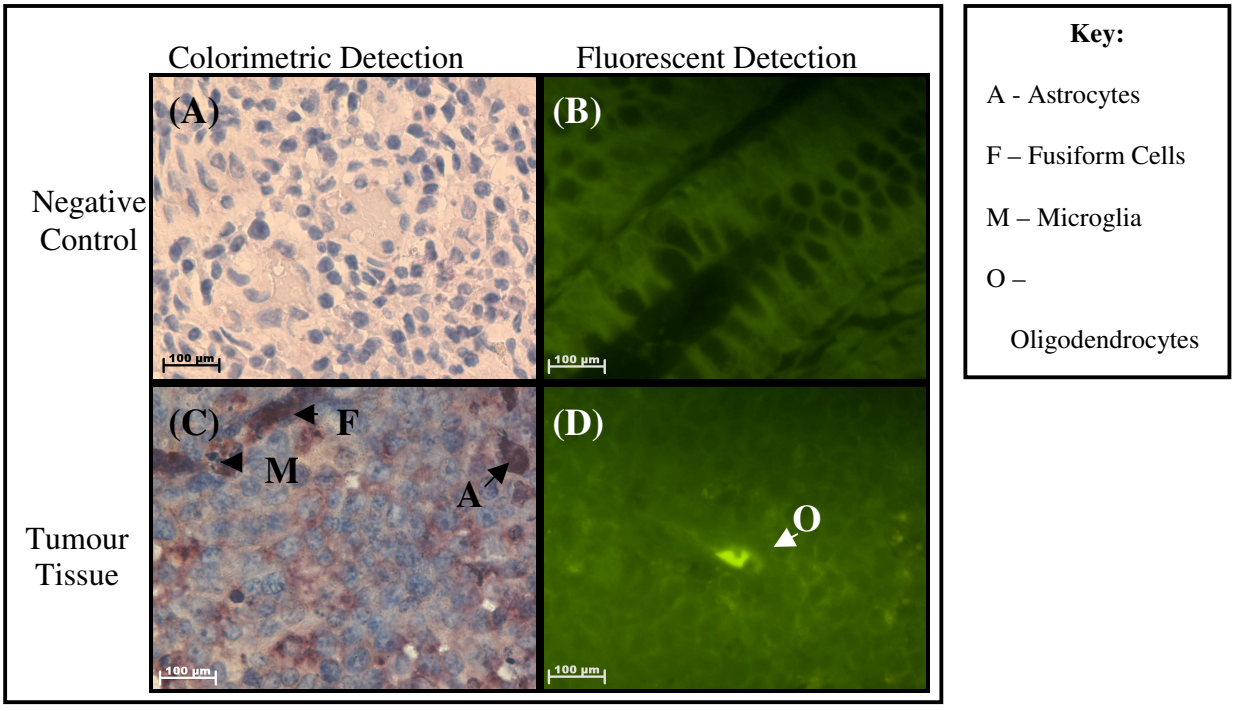



**Figure 3-63: Subcellular Localisation of the Peripheral Benzodiazepine Receptor mRNA in Primary Central Nervous System Lymphoma** (Magnification 1000X)

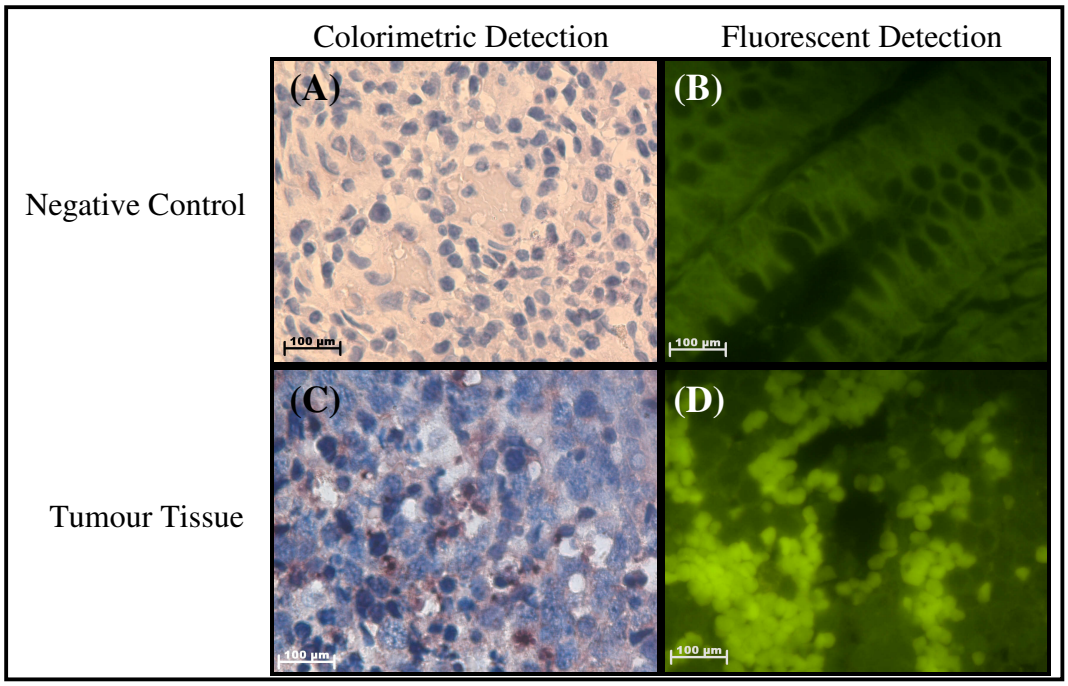



**Figure 3-64: Subcellular Localisation of the Peripheral Benzodiazepine Receptor mRNA in Ependymoma** (Magnification 1000X)

### *3.2.5. Summary*

The PBR mRNA was expressed in all normal and cancerous human tissues studied. The expression of PBR was clearly seen in specific cells within a given organ in both the normal and the diseased state (Appendix 8 Table 1 and Table 2). From the results obtained it is clear that the PBR mRNA is expressed mainly in the cytoplasm, however, nuclear localisation of PBR mRNA were observed.

The level of expression within a given organ varies in the normal and cancerous state (Appendix 8 Table 3 and Table 4). In order to determine if the level of expression of PBR mRNA increased or decreased in the cancerous state, cancerous tissues were compared to its normal counterpart (Appendix 8 Table 5).

Furthermore, the level of PBR mRNA expression varies with tumour malignancy grade (Appendix 8 Table 5). In hepatocellular carcinoma expression of PBR mRNA decreased as tumour invasion increased while in prostate adenocarcinoma of the peripheral duct and acini PBR mRNA level increased as tumour invasion increased. In colon adenocarcinoma expression of PBR mRNA decreased from Grade I to Grade II and Grade III colonic adenocarcinoma. However, Grade III colonic adenocarcinoma had a higher PBR mRNA expression level than Grade II colonic adenocarcinoma.

## 3.3. Expression Levels of Peripheral Benzodiazepine Receptor mRNA in Various Human Cancer Tissues

### *3.3.1. Introduction*

Real-time PCR is a sensitive technique, providing ease and convenience to quantitate differences in mRNA expression, even when the amount of RNA available is low. The real-time PCR machine uses both the logarithmic and linear graphs to examine data. Both graphs may be used because a linear relationship exists between the amount of PCR product and the cycle number when seen on a logarithmic scale as the amount of PCR product increases exponentially. Thus, accurate and precise quantitation of DNA is done when PCR amplification is still in the exponential phase that is in the log phase, which occurs earlier in the PCR reaction. Data is acquired from the threshold cycle ($C_t$), that is the cycle at which the reporter dye fluorescence intensity increases above the background noise. $C_t$ is determined at the most exponential phase of the reaction and is more accurate than the end-point measurements. It should be noted that the $C_t$ value is inversely proportional to the copy number of template DNA, that is the higher the $C_t$ value, the lower the amount of template DNA. Thus, the $C_t$ value is used in quantitation as well as in qualitative analysis as a pass/fail measure. The slope of the log-linear phase is a reflection of the amplification efficiency.

SYBR Green I is a dye that when bound to double-stranded DNA fluoresces very brightly at a ratio that is much higher in the presence of double-stranded DNA than single-stranded DNA. It has an excitation and emission maxima of 494 nm and 594 nm respectively. Since SYBR Green I binds to amplified cDNA, the quantitation curve is the measure of increase in fluorescence as the dye binds to increasing amounts of DNA in the reaction tube. This DNA could be the PCR product but may also be any other DNA in the tube. In order to determine if the PCR product has been amplified and not any other DNA results can be analysed using a

melting curve. Thus, this is a means by which quality control can be maintained, as all products amplified with the same primers should have the same or similar melting temperature. Differences in this melting temperature may occur when there is contamination, mispriming, that is PCR products made due to the annealing of primers to complementary or partially complementary sequences on non-target DNA, or primer dimer formation.

### *3.3.2. Relative Quantitative Real-Time Polymerase Chain Reaction*

Relative quantitative real-time PCR was done to determine level of expression of the PBR mRNA in various cancer tissues, namely lung normal tissue (MRC5), lung adenocarcinoma (A549), cervical carcinoma (HeLa) and liver hepatocellular carcinoma (HepG). This was achieved by extracting RNA from each cell line, reverse transcribing each cell line into cDNA using reverse transcriptase and oligo-$(dT)_{15}$ after which each cell line underwent real-time PCR using PBR specific primers and SYBR Green I. Results were analysed using quantitation and melting curves using the Opticon 3.1 software (Bio-Rad Laboratories, Hercules, CA, USA) and agarose gel electrophoresis where real-time PCR products were run on a 1% agarose gel.

#### *3.3.2.1. Optimisation of the Concentration of Template DNA Required for Real-Time Polymerase Chain Reaction*

In order to determine the optimal concentration of cDNA required to perform this experiment, quantitative real-time PCR was conducted using serial dilutions of MRC5. Results were analysed using quantitation and melting curves.

Quantitation of the PCR product synthesised during the serial dilution of MRC5 is represented by a graph of fluorescence versus the cycle number, that is the amount of SYBR Green I that binds to double-stranded DNA at each cycle (Figure 3-65). The resultant graph for each of the serial dilutions is logarithmic, which eventually plateaus towards the end of the PCR reaction. Quantitation of the PCR product is determined where PCR amplification is still exponential, represented by linear part of the curve. The negative control that was used as a blank containing only $sdH_2O$ was subtracted from the other cell lines in order to remove the background noise. Further, the standard deviation was set at 0.002 in order to further remove background noise. Relatively, serial dilutions of MRC5 showed expression of PBR mRNA and the relationship in decreasing order of PBR mRNA expression is as follows: 1:1000 dilution of MRC5 > 1:100 dilution of MRC5 > 1:10 dilution of MRC5 > 1:10000 dilution of MRC5 > undiluted MRC5.

$C_t$ values and efficiency of PCR was determined in comparison to the negative control containing only $sdH_2O$ (Table 3-2). The efficiency of PCR should lie between 90-100%. However, in this study, only the 1:10000 dilution of MRC5 showed efficiency greater than 100%, which indicates that the result obtained for this cell line is highly efficient. The other serial dilutions of MRC5 showed efficiencies that were lower than 90% ranging from 44% to 81%. Reasons for low efficiency seen could include the length of the PCR product, secondary structure formation, primer quality and concentration of the product. $C_t$ values should not lie higher than 40 because any value higher than this indicates that no amplification of PCR product occurs. In this case, all the $C_t$ values lie below 40 with $C_t$ values increasing as follows: 1:1000 dilution of MRC5 < 1:100 dilution of MRC5 < 1:10 dilution of MRC5 < 1:10000 dilution of MRC5 < undiluted MRC5. This indicates that samples containing

template DNA increases as follows: 1:1000 dilution of MRC5 > 1:100 dilution of MRC5 > 1:10 dilution of MRC5 > 1:10000 dilution of MRC5 > undiluted MRC5.

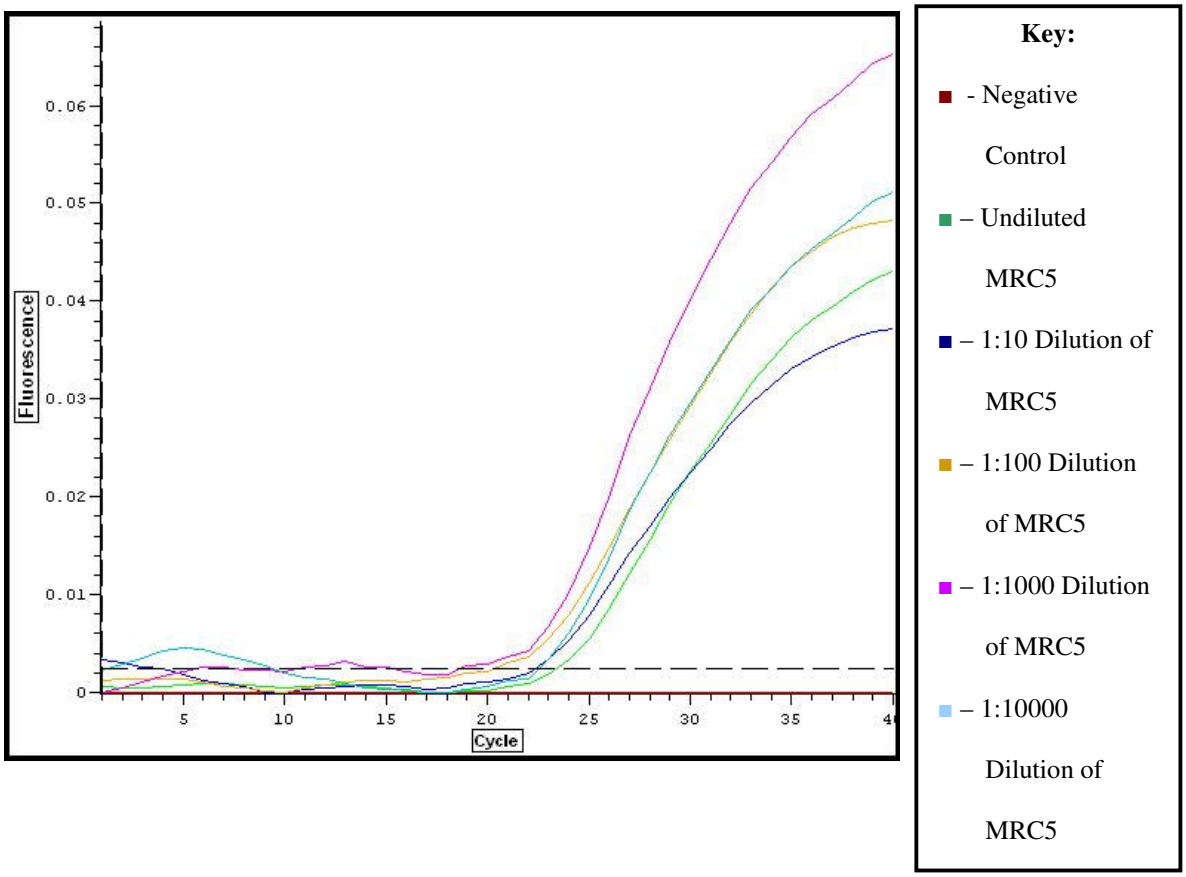



**Figure 3-65: Quantitative Curve of the *Peripheral Benzodiazepine Receptor* Gene in the Serial Dilution of the MRC5 Cell Line**

In order to determine if the *PBR* gene was amplified and not any other product, a melting curve was done. Results are represented as a graph of fluorescence, which is the relative fluorescence units over time ($-dI/dT_{max}$), versus temperature that peaks at the melting temperature ($T_m$) (Figure 3-66) and a table showing the melting temperature for each of the samples (Table 3-3). An additional column is the full width half maximum (FWHM), which represents the width in ˚C of the $–dI/dT_{max}$ peak and thus describes the sharpness of the peak. In order to reduce background noise, the effect of the blank was subtracted from all five samples. It was found that all five samples had a major peak at 84 ˚C. However, even after

subtracting the blank background noise could still be seen which indicates that the PCR product synthesised is probably not very pure and this could have occurred due to contamination.

**Table 3-2: Efficiency and Threshold Cycle Values of PCR Product Synthesised**

| Sample | Efficiency | Threshold Cycle ($C_t$) |
|---|---|---|
| Negative Control | - | - |
| Undiluted MRC5 | 80.85 | 23.42 |
| 1:10 Diluted MRC5 | 64.01 | 22.31 |
| 1:100 Diluted MRC5 | 44.93 | 20.32 |
| 1:1000 Diluted MRC5 | 49.55 | 18.66 |
| 1: 10000 Diluted MRC5 | 134.58 | 22.52 |

It was found that the optimal concentration at which real-time PCR occurred most efficiently and precisely was when the cDNA production was diluted 10000 times that is when the concentration of MRC5 was 0.286 ng/µl (For calculation refer to Appendix 7 Calculations of Concentrations cDNA, Volume Required for Real-Time PCR and Purity of cDNA).

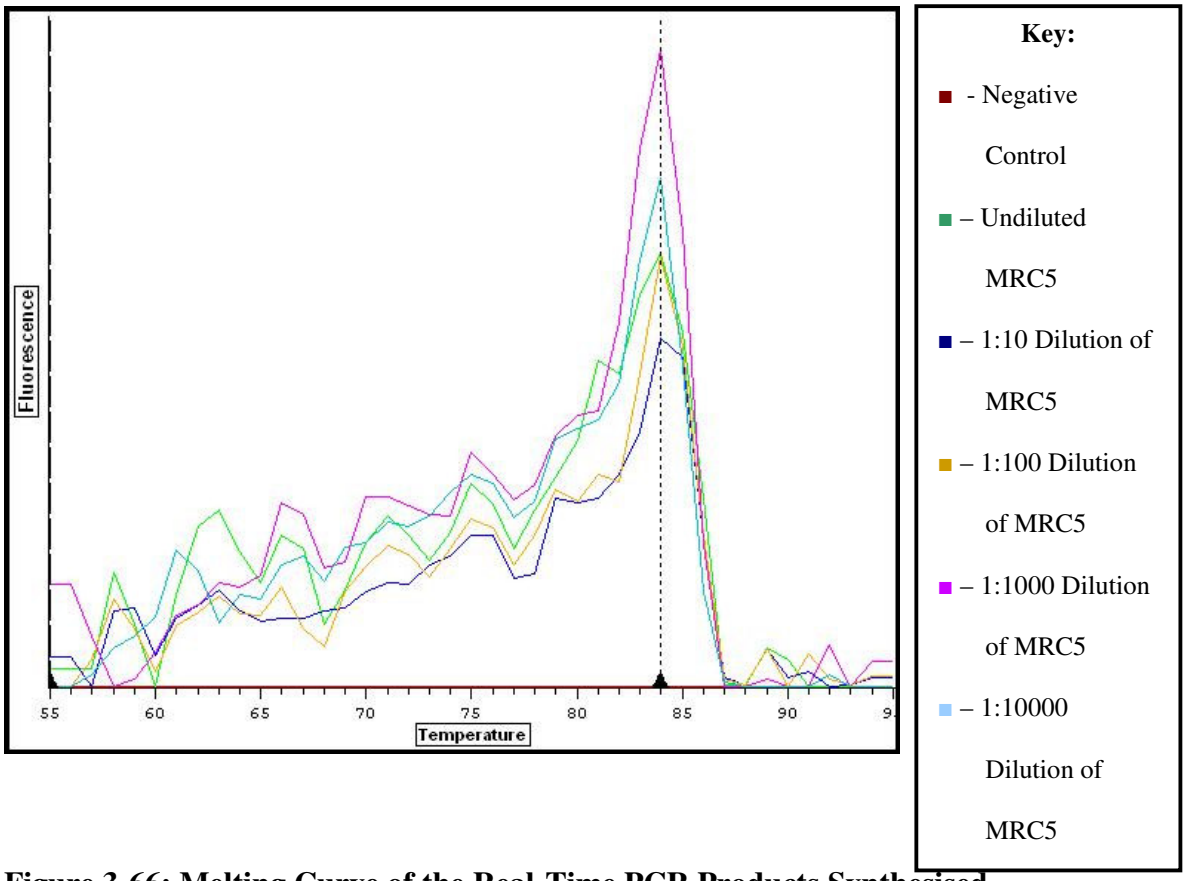



**Figure 3-66: Melting Curve of the Real-Time PCR Products Synthesised**

*3.3.2.2. Determination of Expression of Peripheral Benzodiazepine Receptor mRNA in Various Cell Lines using Optimal Concentration of Template DNA*

The cDNA products for each of the cell lines were quantified to determine the concentration and purity of the cDNA for each. Determining the concentration of each cell line was required to determine what volume of each cell line was required to make a final concentration of 0.216 ng/µl for real-time PCR. This was done spectrophotometrically by measuring the absorbance at 260 nm and 280 nm for each of the cell lines, which was blanked against sd$H_2O$ (Table 3-4). 260 nm is the wavelength at which nuclei absorbs light maximally while 280 nm is the wavelength at which protein absorbs light maximally. A pure DNA solution should result in a value greater than or equal to 1.8. The values obtained were lower than 1.8 for each of the cell lines, which may have occurred because the sample solutions were blanked against

sd$H_2O$, while in actual fact the sample solutions also contained the reagents used in order to construct cDNA.

**Table 3-3: Calculation of Melting Temperatures for the PCR Product Synthesised in Serial Dilution of the MRC5 Cell Line**

| Sample | Full Width Half Maximum (FWHM) | Relative Fluorescent Units over Time ($-dI/dT_{max}$) | Melting Temperature ($T_m$) (˚C) |
|---|---|---|---|
| Negative Control | 0.000 | 0.00000 | 55 |
| Undiluted MRC5 | 6.681 | 0.007354 | 84 |
| 1:10 Diluted MRC5 | 7.045 | 0.007429 | 84 |
| 1:100 Diluted MRC5 | 3.571 | 0.010830 | 84 |
| 1:1000 Diluted MRC5 | 3.945 | 0.017000 | 84 |
| 1: 10000 Diluted MRC5 | 5.67 | 0.01154 | 84 |

Concentration of each clone was determined using the formula: $c = A_{260} \times [A_{260}dsDNA] \times DF$, where c is the concentration of the sample, $[A_{260}dsDNA]$ is the concentration of double-stranded (ds) DNA where absorbance at 260 nm is 1.0, which is 50 µg/ml and DF is the dilution factor, which was 100 and were as tabulated in Table 3-4. The volume required to prepare a cDNA template of concentration 0.216 ng/µl was determined using ratios and was found to be 0.8 µl for MRC5, 1.0 µl for A549, 0.34 µl for HeLa and 1.0 µl for HepG (For calculations see Appendix 7 Calculations of Concentrations cDNA, Volume Required for Real-Time PCR and Purity of cDNA).

**Table 3-4: Absorbance, Purity and Concentration of Sense and Anti-Sense Probes Measured at 260 nm and 280 nm**

| Sample | $A_{260}$ | $A_{280}$ | $A_{260}$:$A_{280}$ | Concentration (µg/ml) [1] | Concentration (ng/µl)[2] |
|---|---|---|---|---|---|
| MRC5 | 0.438 | 0.347 | 1.65 | 2860 | 0.286 |
| A549 | 0.438 | 0.270 | 1.62 | 2190 | 0.219 |
| HeLa | 1.280 | 0.932 | 1.38 | 6430 | 0.643 |
| HepG | 0.432 | 0.266 | 1.62 | 2160 | 0.216 |

1. Concentration of each cell line was determined using the formula: $c = A_{260} \times [A_{260}dsDNA] \times DF$
2. Concentration of each cell line was determined by using a dilution factor of 10000

Quantitation of the PCR product is represented by a graph of fluorescence versus the cycle number (Figure 3-67). The resultant graph for each of the cell lines is logarithmic, which eventually plateaus towards the end of the PCR reaction. Quantitation of the PCR product is determined where PCR amplification is still exponential and is represented by the linear part of the curve. The negative control that was used as a blank containing only $sdH_2O$ was subtracted from the other cell lines in order to remove the background noise. Further, the standard deviation was set at 0.004 in order to further remove background noise. Relatively, the normal MRC5 showed a higher concentration of PBR when compared to it cancerous cell line A549. When comparing the cancerous cell lines HepG showed the highest concentration of PBR while A549 showed the least concentration of PBR.

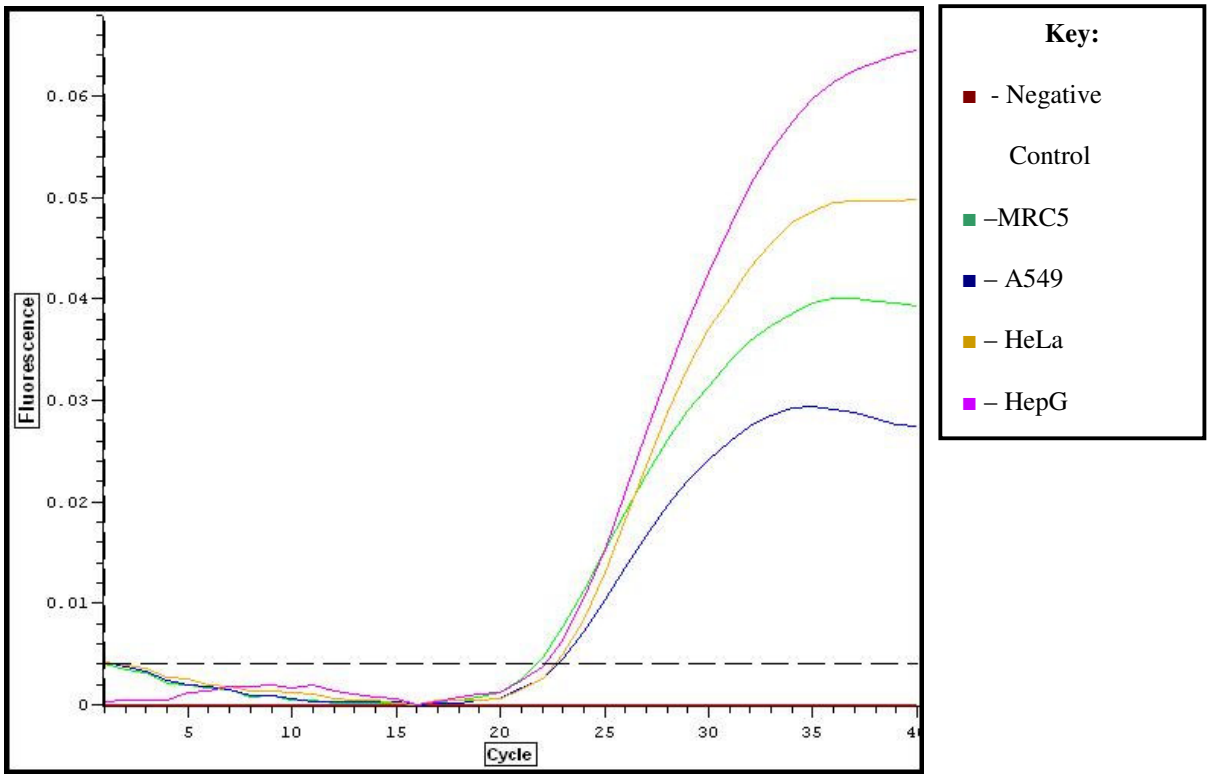



**Figure 3-67: Quantitative Curve of the *Peripheral Benzodiazepine Receptor* Gene in Various Cell Lines**

$C_t$ values and efficiency of PCR was determined in comparison to the negative control containing only $sdH_2O$ (Table 3-5). The efficiency of PCR should lie between 90-100%. However, in this study, only HepG lies in this range, which indicates that the result obtained for this cell line is highly efficient while the other cell lines show efficiency that lies within 72%-78% range. Reasons for low efficiency seen could include the length of the PCR product, secondary structure and primer quality. $C_t$ values should not lie higher than 40 because any value higher than this indicates that no amplification of PCR product occurs. In this study, all the $C_t$ values lie below 40 with MRC5 having a lower $C_t$ value when compared to A549, which indicates that MRC5 had a higher concentration of template PBR than A549. When the cancerous cell lines were compared to each other, it was found that the lowest $C_t$ value was seen in HepG and the highest $C_t$ value was seen in A549, which indicates that

HepG had the highest concentration of template PBR and A549 had the lowest concentration of template PBR.

**Table 3-5: Efficiency and Threshold Cycle Values of PCR Product Synthesised**

| Sample | Efficiency | Threshold Cycle ($C_t$) |
|---|---|---|
| Negative Control | - | - |
| MRC5 | 77.53 | 21.71 |
| A549 | 76.56 | 22.71 |
| HeLa | 99.45 | 22.59 |
| HepG | 72.18 | 22.12 |

In order to determine the relative expression levels of PBR mRNA in absolute terms, the following formula to compare two cell lines were used: Relative Expression Level = $2^{\Delta Ct}$, where $\Delta C_t$ is the difference in the $C_t$ values for the two different cell lines been compared (Table 3-6 and Table 3-7, Figure 3-68 and Figure 3-69). Using this formula, the value 1, which the reference mRNA will have, serves as the base from which increase or decrease expression can be determined, that is any value greater than 1 shows that an increase in expression occurs with regard to the reference mRNA while any value lower than 1 shows that a decrease in expression occurs with regard to the reference mRNA. It was found that A549 had a half-fold decrease in PBR mRNA expression when compared to MRC5. HeLa had a slight increase in PBR mRNA expression when compared to A549 and HepG had a half-fold increase in PBR mRNA when compared to A549 (for calculations refer to Appendix 7 Calculations of the Relative Expression of the Peripheral Benzodiazepine Receptor mRNA in Absolute Terms).

**Table 3-6: Relative Expression Level of the Peripheral Benzodiazepine Receptor mRNA in Lung Adenocarcinoma when Compared Lung Normal in Absolute Terms**

| Cell Line | Threshold Cycle ($C_t$) | Relative Expression Level[1] |
|---|---|---|
| MRC5 | 21.71 | 1 |
| A549 | 22.71 | 0.5 |

1. The relative expression level of PBR mRNA was determined using the following formula: Relative Expression Level = $2^{\Delta Ct}$.
2. The relative expression level of PBR mRNA was determined using the following formula: Relative Expression Level = $2^{\Delta Ct}$.

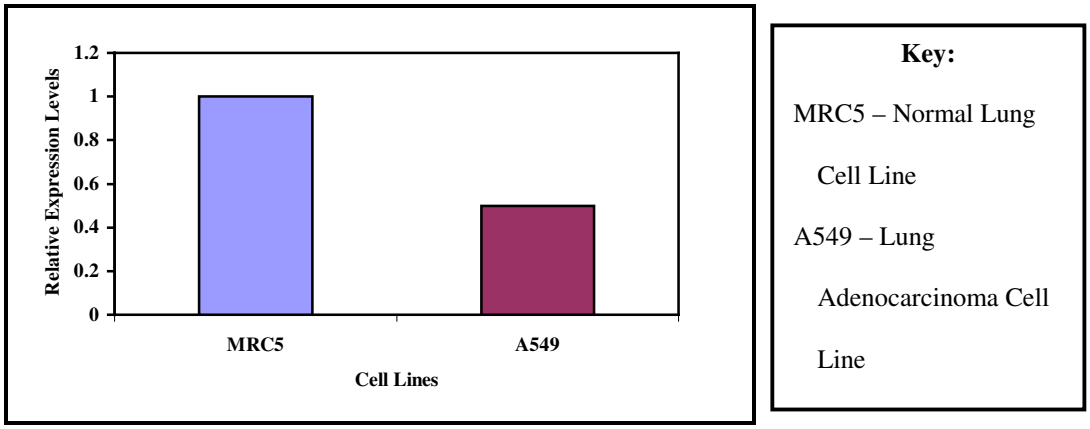



**Figure 3-68: Relative Expression Level of Lung Adenocarcinoma When Compared to its Normal Counterpart**

**Table 3-7: Relative Expression Level of the Peripheral Benzodiazepine Receptor mRNA in Various Cancers in Absolute Terms**

| Cell Line | Threshold Cycle ($C_t$) | Relative Expression Level[1] |
|---|---|---|
| A549 | 22.71 | 1 |
| HeLa | 22.59 | 1.09 |
| HepG | 22.12 | 1.51 |

1. The relative expression level of PBR mRNA was determined using the following formula: Relative Expression Level = $2^{\Delta Ct}$.
2. The relative expression level of PBR mRNA was determined using the following formula: Relative Expression Level = $2^{\Delta Ct}$.

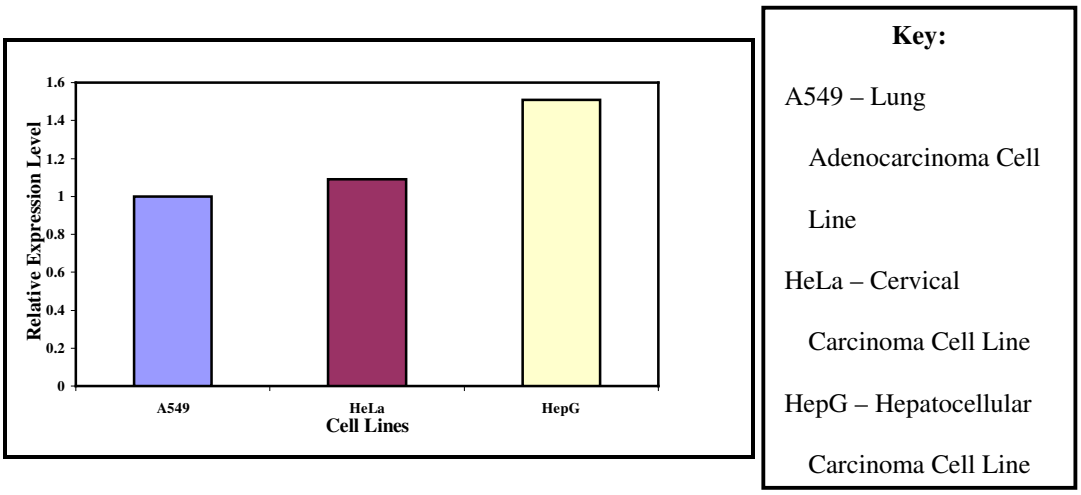



**Figure 3-69: Relative Expression Levels of Peripheral Benzodiazepine Receptor mRNA in Various Cancers**

In order to determine if the *PBR* gene was amplified and not any other product, a melting curve was done. Results are represented as a graph of fluorescence, which is the relative fluorescence units over time ($-dI/dT_{max}$), versus temperature that peaks at the melting temperature ($T_m$) (Figure 3-70) and a table showing the melting temperature for each of the samples (Table 3-8). An additional column is the full width half maximum (FWHM), which

represents the width in ˚C of the $-dI/dT_{max}$ peak and thus describes the sharpness of the peak. In order to reduce background noise, the effect of the blank was subtracted from all four cell lines. It was found that all four cell lines had a major peak at 84 ˚C. However, even after subtracting the blank background noise could still be seen which indicates that the PCR product synthesised is probably not very pure and this could have occurred due to contamination and also due to some DNA degradation.

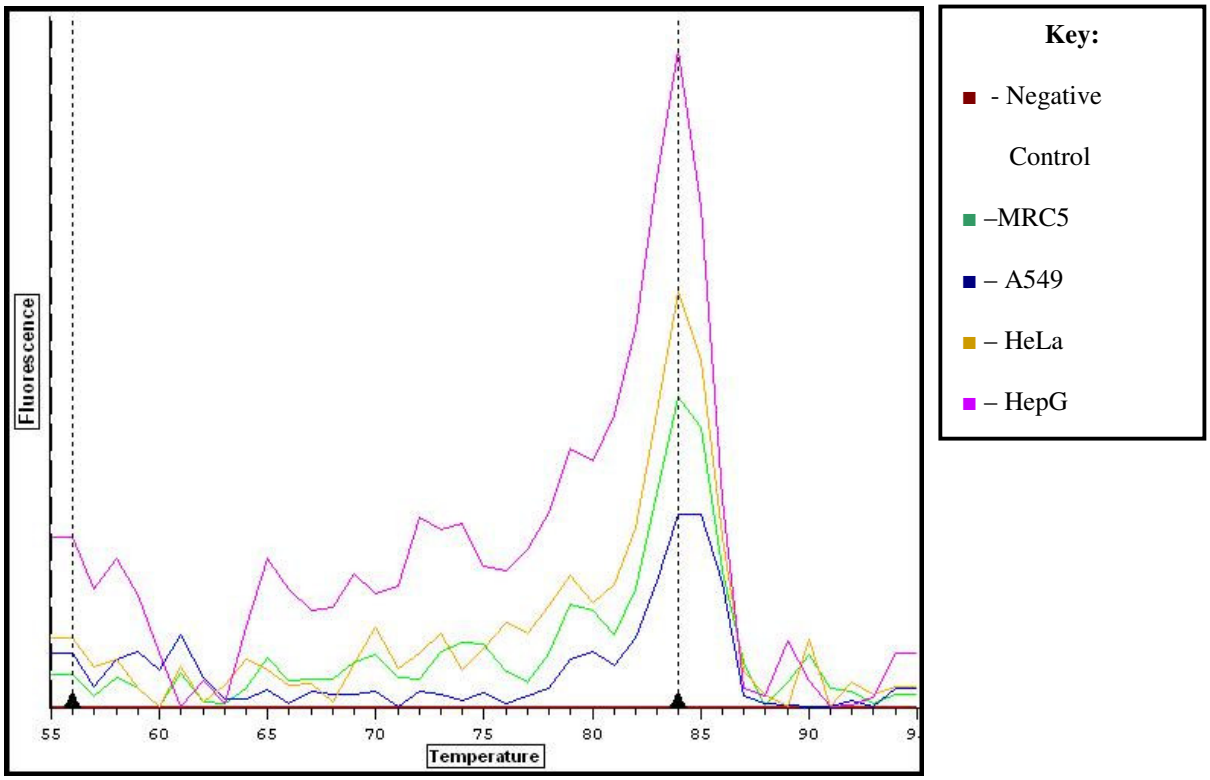
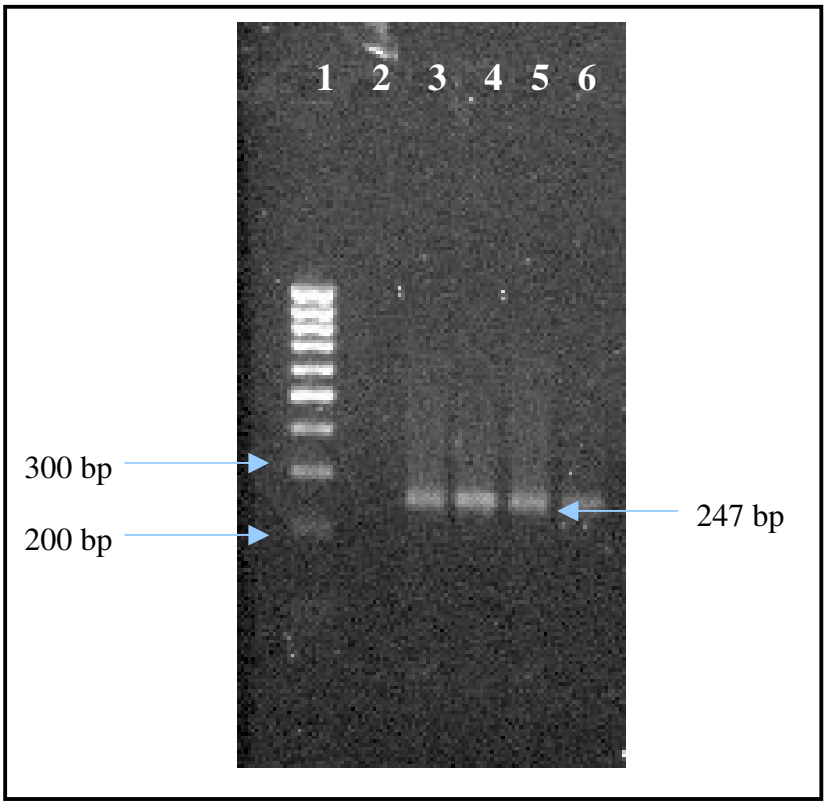



**Figure 3-70: Melting Curve of the Real-Time PCR Products Synthesised**

**Table 3-8: Calculation of Melting Temperatures for the PCR Product Synthesised in each Cell Line**

| Sample | Full Width Half Maximum (FWHM) | Relative Fluorescent Units over Time ($-dI/dT_{max}$) | Melting Temperature ($T_m$) (˚C) |
|---|---|---|---|
| Negative Control | 0.000 | 0.00000 | 56 |
| MRC5 | 3.481 | 0.008731 | 84 |
| A549 | 3.753 | 0.007285 | 84 |
| HepG | 3.535 | 0.011540 | 84 |
| HeLa | 4.156 | 0.015670 | 84 |

Since the efficiency for three of the cell lines were not high enough and the melting curve showed that the PCR product generated was not pure, the PCR product that was generated during real-time PCR for each of the cell lines was run on a 1% agarose gel in order to determine if the PCR product of 247 bp was the only product generated (Figure 3-71). All four cell lines showed the formation of a band of 247 bp (Lanes 3-6), which lies between the 200 bp and 300 bp reference bands of Lane 1. The negative control containing only $sdH_2O$ showed no formation of bands (Lanes 2). However, smearing did occur, which indicates that PCR product may not be pure and contains contaminants or some DNA degradation may have occurred.




**Key:**

Lane 1: GeneRuler$T^M$ 100bp DNA Ladder

Lane 2: Negative Control

Lane 3: MRC5 PCR Product

Lane 4: A549 PCR Product

Lane 5: HeLa PCR Product

Lane 6: HepG PCR Product

**Figure 3-71: Amplification of Real-Time Polymerase Chain Reaction Product**

### *3.3.3. Summary*

Quantitative real-time PCR showed that the expression levels of PBR mRNA varied between lung adenocarcinoma and its normal counterpart and between the different cancer cell lines. It was found that the relative expression of PBR mRNA decreased half-fold in lung adenocarcinoma when compared to it normal counterpart seen by the decrease in concentration of template DNA for the two cell lines. In the case of the cancerous cell lines, the concentration of PBR mRNA increases as follows: liver hepatocellular carcinoma > cervical carcinoma ≥ lung adenocarcinoma, with liver hepatocellular carcinoma showing a half-fold increase compared to lung adenocarcinoma and cervical carcinoma and lung adenocarcinoma showing a similar expression level.

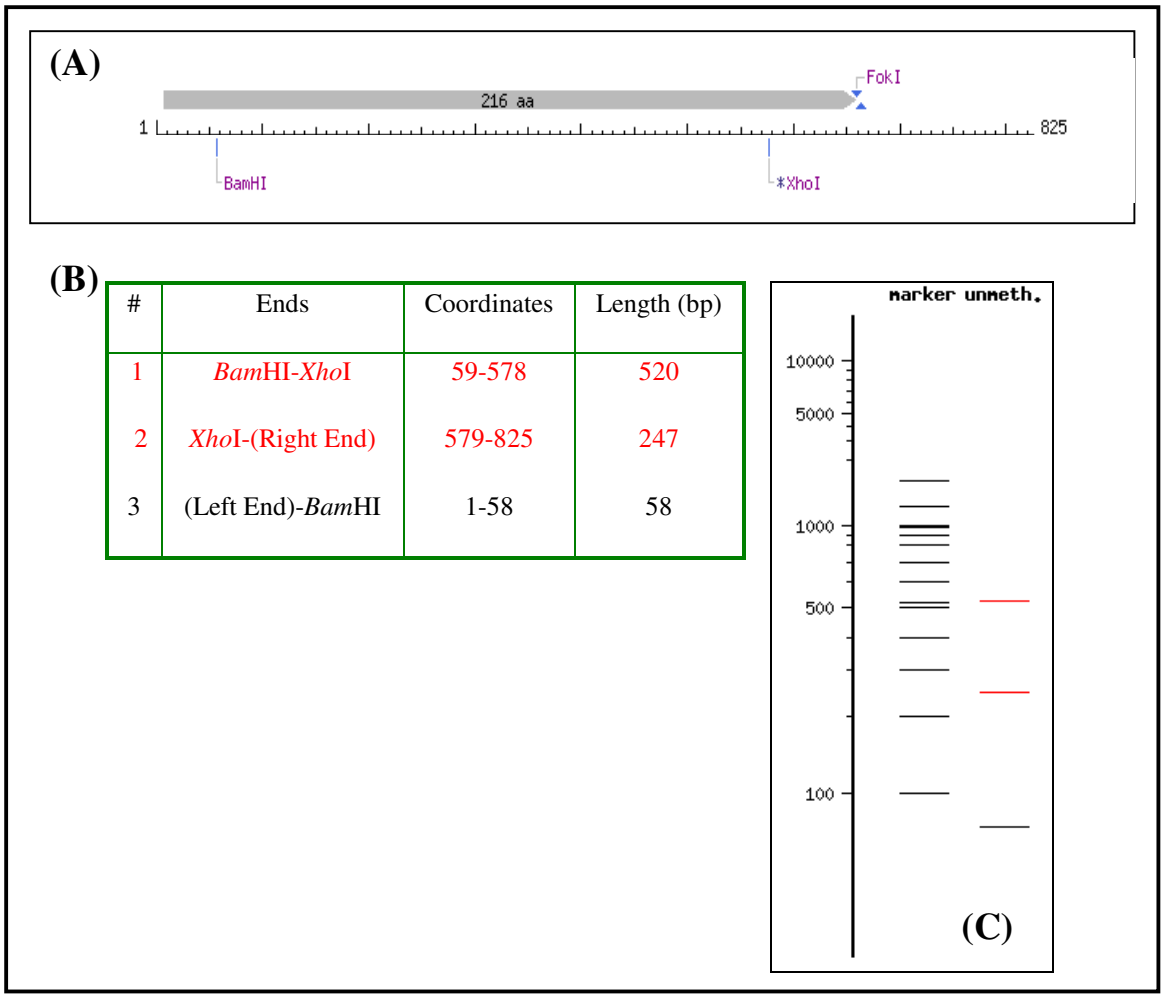
## 3.4. Peripheral Benzodiazepine Receptor Protein Expression

### *3.4.1. Introduction*

Since not many studies have focused on the effect of the Peripheral Benzodiazepine Receptor (PBR) protein specifically in various cancer tissues, it was thought that synthesis of this protein would prove valuable in determining the expression patterns of this protein in various cancer tissues as well as determining its role in cell proliferation and apoptosis. The PBR protein was synthesised by ligating the PBR insert into an expression vector, namely pGEX-6P-2, which contains a GST domain and a *lac* promoter site. Thus, when the pGEX-6P-2 expression vector is induced with IPTG, it results in the expression of a GST-tagged PBR protein, which after purification with gluthathione can be digested with PreScission™ Protease in order to isolate the PBR protein, which can be used for further studies such as immunocytochemistry and TUNEL assays.

### *3.4.2. Restriction Digestion of the Peripheral Benzodiazepine Receptor Insert and pGEX-6P-2 Expression Vector*

In order to ensure that PBR fragment could be digested with *Bam*HI and *Xho*I and to determine the size of the PBR fragment that would be digested from the pGEM-T Easy vector, the sequence of the PBR insert obtained from Inqaba Biotechnical Industries (Pty) Ltd, (Pretoria, Gauteng, South Africa) was digested using NEBCutter (NewEngland, BioLabs, Inc., Beverly, MA, USA) and the results were obtained as seen in Figure 3-72. Using NEBCutter confirmed that *Bam*HI and *Xho*I could digest the PBR fragment and that the fragment size digested by these two enzymes was 520 bp.




| # | Ends | Coordinates | Length (bp) |
|---|---|---|---|
| 1 | *Bam*HI-*Xho*I | 59-578 | 520 |
| 2 | *Xho*I-(Right End) | 579-825 | 247 |
| 3 | (Left End)-*Bam*HI | 1-58 | 58 |

**Figure 3-72: Virtual Results for Peripheral Benzodiazepine Receptor Digested with *Bam*HI and *Xho*I**

(A) is a schematic diagram showing that the PBR insert in the pGEM-T Easy vector can be digested with *Bam*HI and *Xho*I. (B) shows the sizes of the fragments that will result when the PBR fragment in the pGEM-T Easy vector is digested by *Bam*HI and *Xho*I. (C) is the virtual gel showing the relative positions of the bands that would result when the PBR insert in the pGEM-T Easy vector is digested with *Bam*HI and *Xho*I.

Since NEBCutter proved that the PBR insert in pGEM-T Easy vector could be digested with *Bam*HI and *Xho*I, the pGEM-T Easy vector containing PBR and the pGEX-6P-2 expression vector, which has a multiple cloning site for these enzymes, were digested with these enzymes. Results were analysed by agarose gel electrophoresis where the digestions were run on a 1% agarose gel (Figure 3-73). Digestion of the pGEM-T Easy containing PBR with

*Bam*HI and *Xho*I resulted in the formation of two bands (Lane 5) one band forming at a level greater than the 1031 bp reference band (Lane 1) and the other occurring between the 500 bp and 600 bp reference band (Lane 1). This result is different from what was seen using NEBCutter, which showed the resultant of three bands. The two bands seen in the digestion is true as the larger band is the pGEM-T Easy vector while the smaller band is the PBR fragment while NEBCutter only digest with respect to the PBR insert sequence. Digestion of the pGEX-6P-2 expression vector with *Bam*HI and *Xho*I resulted in the formation of a single band (Lane 9) at a level greater than the 1031 bp reference band (Lane 1). Expectant results were to see two bands but the resultant of one band is the indication of a really smaller second band forming that probably ran off the gel. Three controls used for the pGEM-T Easy containing PBR clone and the pGEX-6P-2 expression vector digestion included undigested clone, the clone digested with *Bam*HI only and the clone digested with *Xho*I only. In both the pGEM-T Easy containing PBR clone and the pGEX-6P-2 expression vector case, the undigested clone resulted in the formation of three bands (Lanes 2 and 6), which is indicative of the different states in which the clone exists and digestion with *Bam*HI or *Xho*I only resulted in the linearisation of the clones seen by the occurrence of one band (Lanes 3, 4, 7, and 8) at a level greater than the 1031 bp reference band (Lane 1).

### *3.4.3. Purification of the Peripheral Benzodiazepine Receptor and pGEX-6P-2 Expression Vector*

The released PBR insert and the pGEX-6P-2 expression vector were then purified using the Wizard® SV Gel and PCR Clean-Up System (Promega Corporation, Madison, WI, USA) to remove excess salts and other contaminants. Results were analysed using agarose gel electrophoresis where the purified products were run on a 1% agarose gel (Figure 3-74). It was found that both the PBR insert and the pGEX-6P-2 expression vector were recovered as

is indicated by the formation of one band in each lane (Lanes 2 and 3). In the case of the PBR insert, the band was found between the 500 bp and 600 bp reference bands (Lane 1) while in the case of the pGEX-6P-2 expression vector the band lied at a level greater than the 1031 bp reference band (Lane 1).

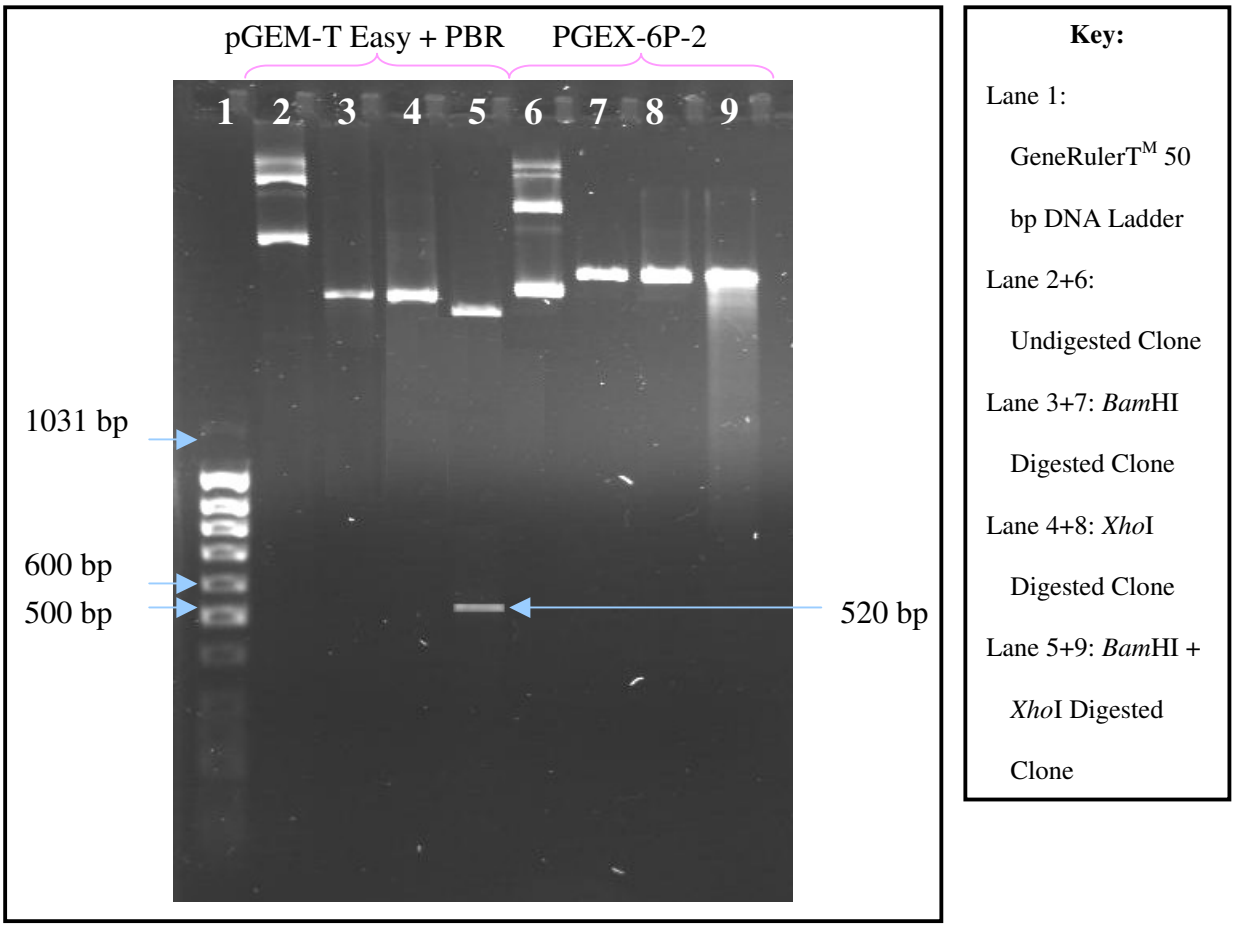



**Figure 3-73: Double Digestion of pGEM-T Easy Containing Peripheral Benzodiazepine Receptor Insert and pGEX-6P-2 Expression Vector**

### *3.4.4. Cloning*

The purified PBR fragment was ligated into the purified pGEX-6P-2 expression vector, which contains a multiple cloning site and an ampicillin resistant domain, using LigaFast™ Rapid Ligation System (Promega Corporation, Madison WI, USA) after which it was transformed into competent MC1061 *Escherichia coli* cells and grown on ampicillin-containing nutrient-

rich agar plates. Thus, only those bacteria containing the ampicillin resistant gene will grow. A negative background control used was to allow the bacteria to grow in the absence of the vector and the insert. This control served the purpose of determining if the bacterial cells contained the ampicillin resistant gene. A positive control used was to grow bacteria in the presence of just the pGEX-6P-2 expression vector only. This control served the purpose of determining if the bacterial cells were competent. It was found that growth occurred on the ampicillin-positive plates where the bacterial cells contained the pGEX-6P-2 expression vector plus the insert or just the pGEX-6P-2 expression vector only while no growth occurred on ampicillin-positive plates where bacterial cells did not contain the pGEX-6P-2 expression vector and insert (Figure 3-75).

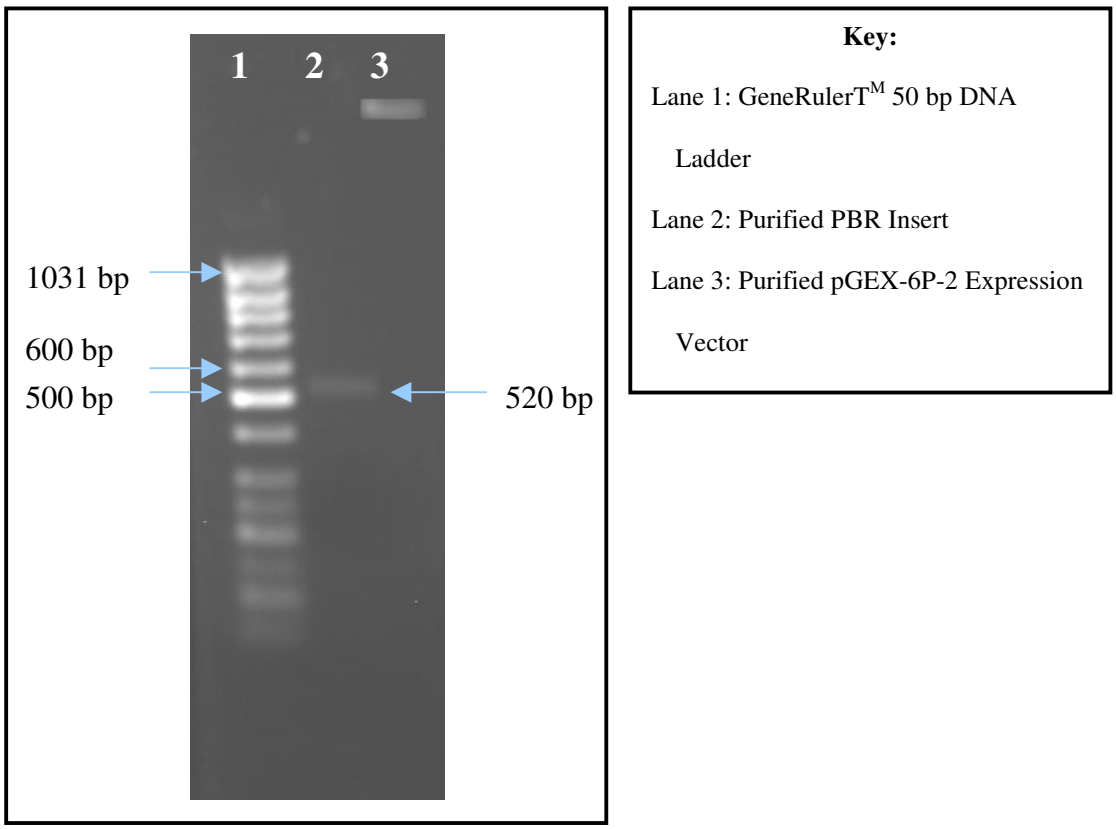



**Figure 3-74: Purification of the Peripheral Benzodiazepine Receptor Insert and pGEX-6P-2 Expression Vector**

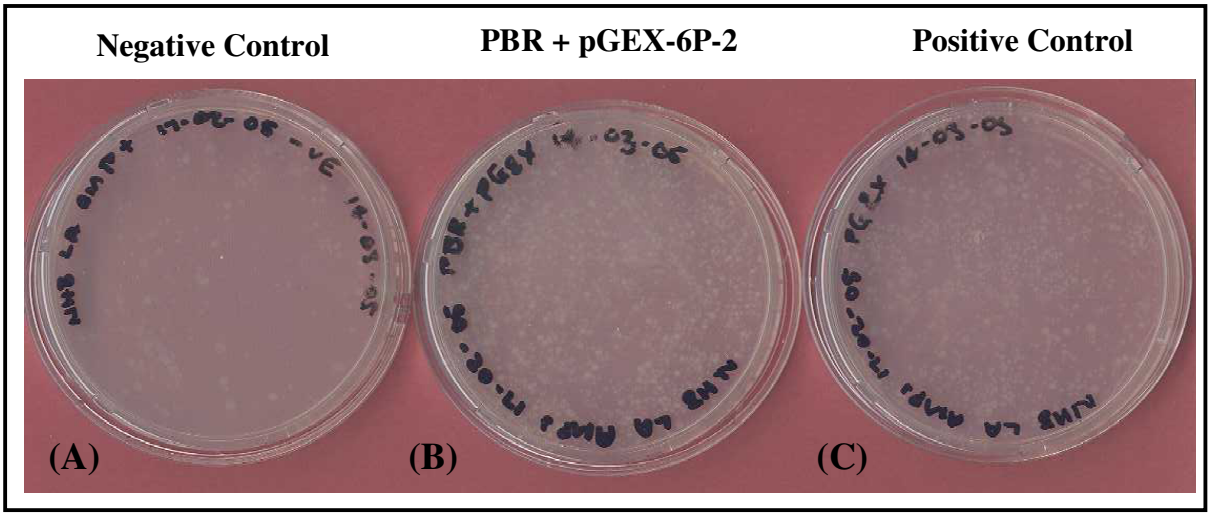



**Figure 3-75: Cloning of the Peripheral Benzodiazepine Receptor Insert into pGEX-6P-2 Expression Vector**

### *3.4.5. Colony Polymerase Chain Reaction*

Colony PCR was done to confirm that the bacterial cells that grew on the ampicillin plates contained the vector plus the insert. Taking the colonies at random that grew on the nutrient-rich agar plates and amplifying the region of interest by PCR using PBR specific primers accomplished this. The results were analysed by agarose gel electrophoresis where the PCR product was run on a 1% agarose gel (Figure 3-76). It was found that the insert was amplified as is indicative by the bands (Lanes 3-10) that lied between 200 bp and 300 bp reference bands (Lane 1). A negative control run with the amplification of the recombinant DNA molecules was to perform PCR in the absence of any recombinant DNA by replacing it with nuclease free $H_2O$, which resulted in no band formation (Lane 2).

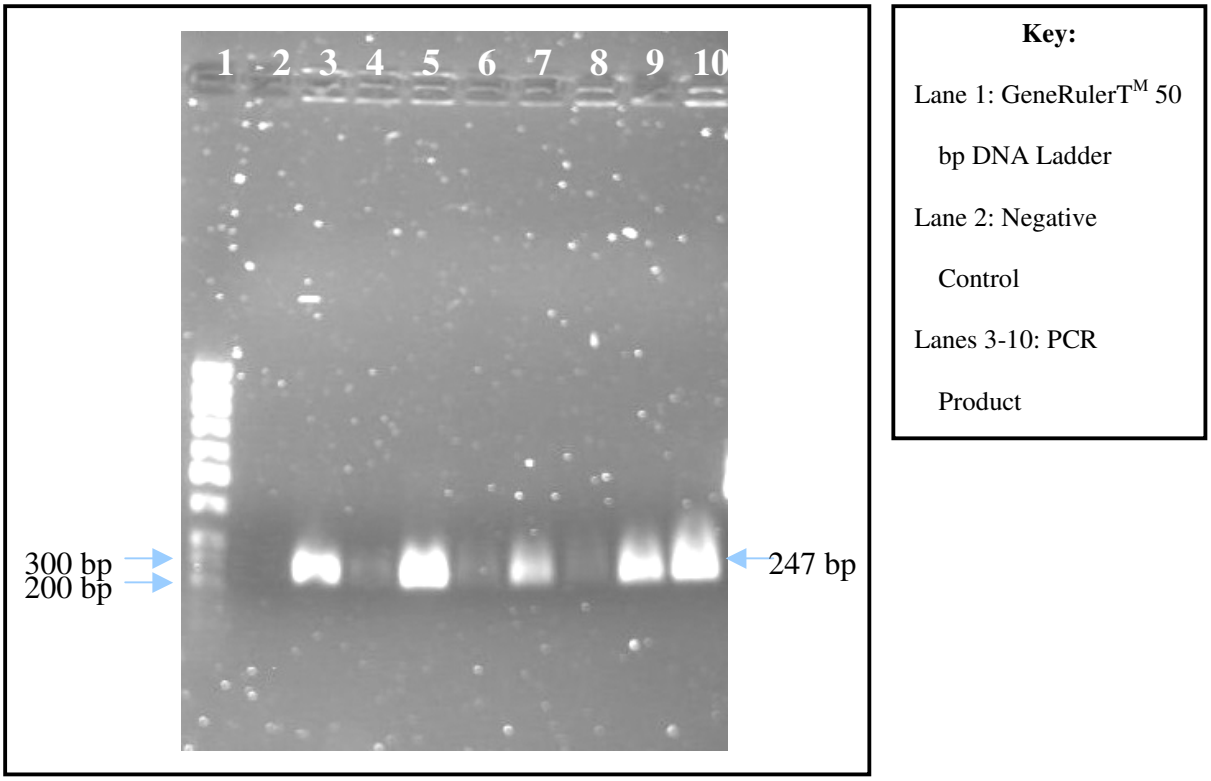



**Figure 3-76: Amplification of the Peripheral Benzodiazepine Receptor via Colony Polymerase Chain Reaction**

### *3.4.6. Miniprep Analysis/Plasmid DNA Extraction*

The pGEX-6P-2 expression vector containing the insert was isolated from the bacterial cells and purified by plasmid DNA extraction using the WizardPlus® SV Miniprep Purification System (Promega Corporation, Madison, WI, USA). To determine if the clones were isolated, the results were analysed by agarose gel electrophoresis where the clones were run on a 1% agarose gel (Figure 3-77). The gel showed the formation of three bands greater than the 1031 bp reference band (Lane 1), which indicates that the pGEX-6P-2 expression vector containing the insert was isolated (Lanes 2-6). The three bands that can be seen are indicative of the different states in which plasmid DNA occurs, namely it may range from supercoiled to completely relaxed. The most tightly supercoiled plasmid DNA will travel furthest in the gel while the most relaxed plasmid will travel the least on the gel.

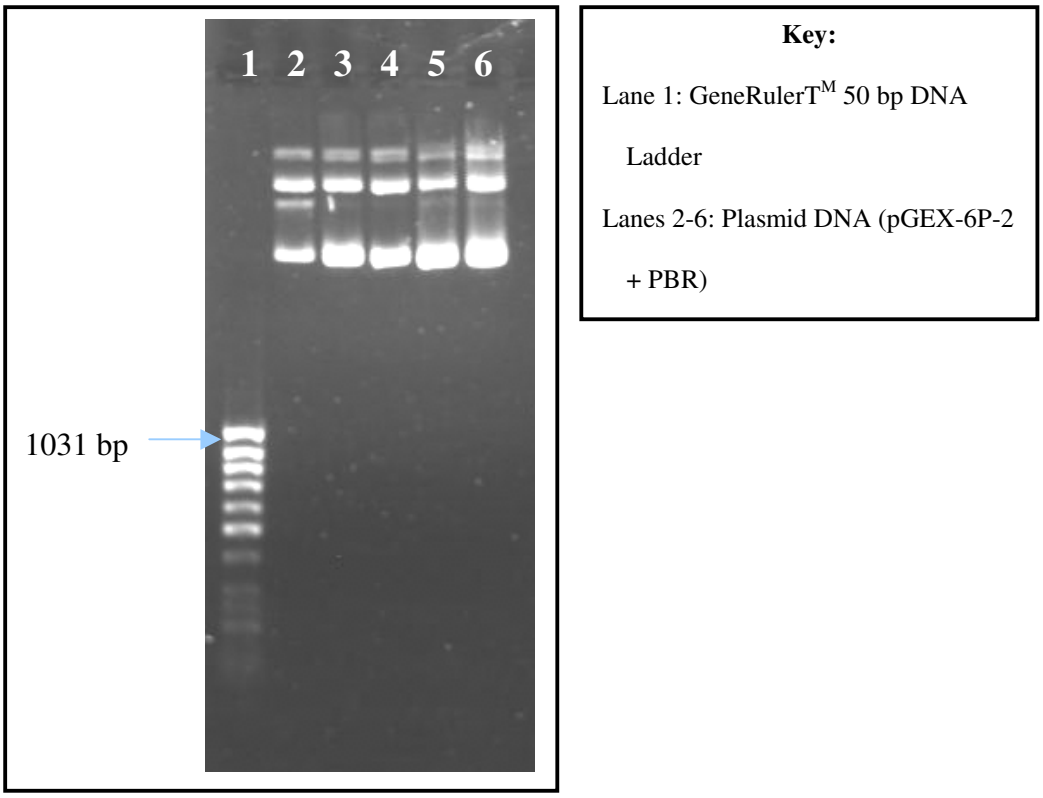



**Figure 3-77: Isolation of Plasmid DNA via Miniprep Analysis**

### *3.4.7. Restriction Digestion*

The purified plasmid DNA was digested with *Bam*HI and *Xho*I to determine the presence of the insert as well as if the correct size of the insert was present in the recombinant plasmid DNA. The results were analysed with agarose gel electrophoresis where the digestions were run on a 1% agarose gel (Figure 3-78). Four controls used in this experiment include the undigested clone (Lane 2), which resulted in the formation of three bands greater than the 1031 bp reference band (Lane 1) that represents the different states of the plasmid DNA, the digestion of the recombinant plasmid DNA with either *Bam*HI or *Xho*I (Lanes 3 and 4), which resulted in the formation of one band greater than the 1031 bp reference band (Lane 1) indicating that the recombinant plasmid DNA was linearised by each enzyme, and the colony PCR product (Lane 6) (used to show if the correct size of the insert is released), which showed the formation of a band between the 200 and 300 bp reference band (Lane 1). When

the recombinant plasmid DNA was double digested with *Bam*HI and *Xho*I, it resulted in the formation of two bands (Lane 5), one band greater than the 1031 bp reference band (Lane 1) and the other band located between the 500 bp and 600 bp reference bands (Lane 1). The size of this fragment varies from the colony PCR product, that is from 247 bp to 520 bp but it is still correct as was indicated by NEBCutter.

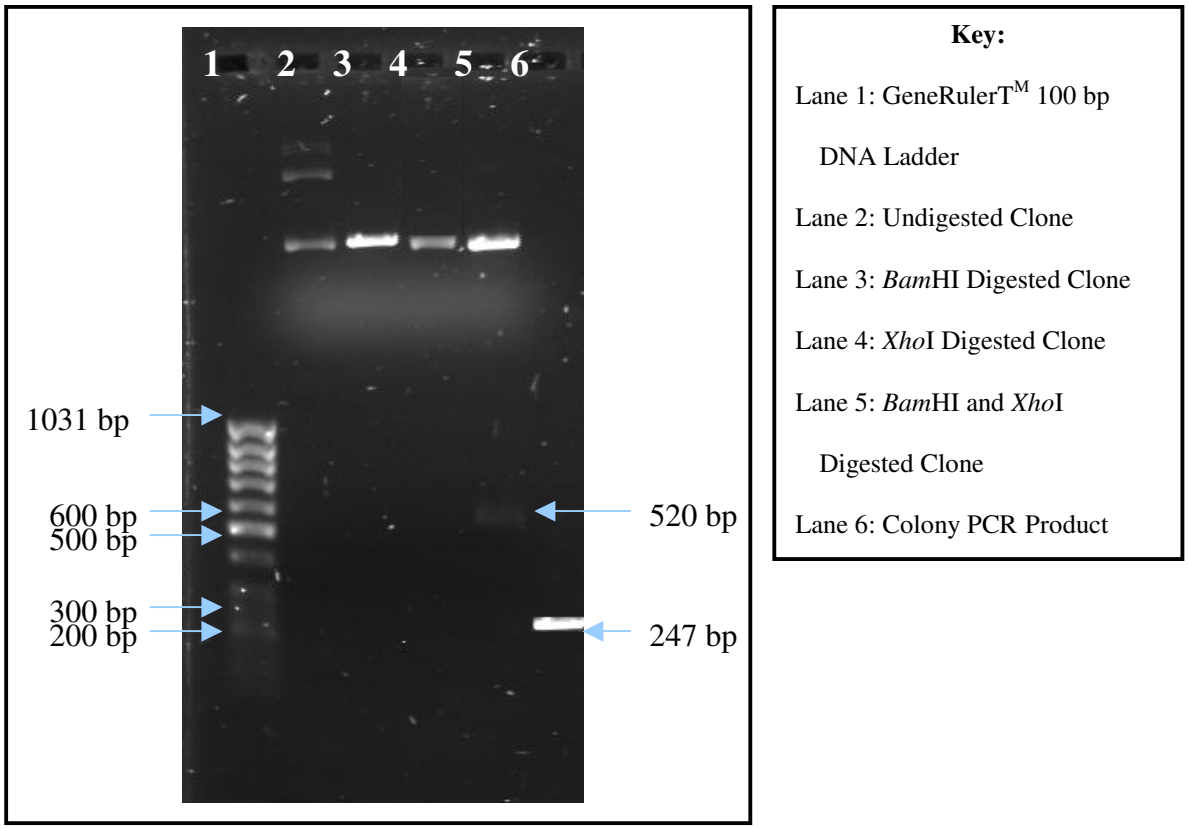
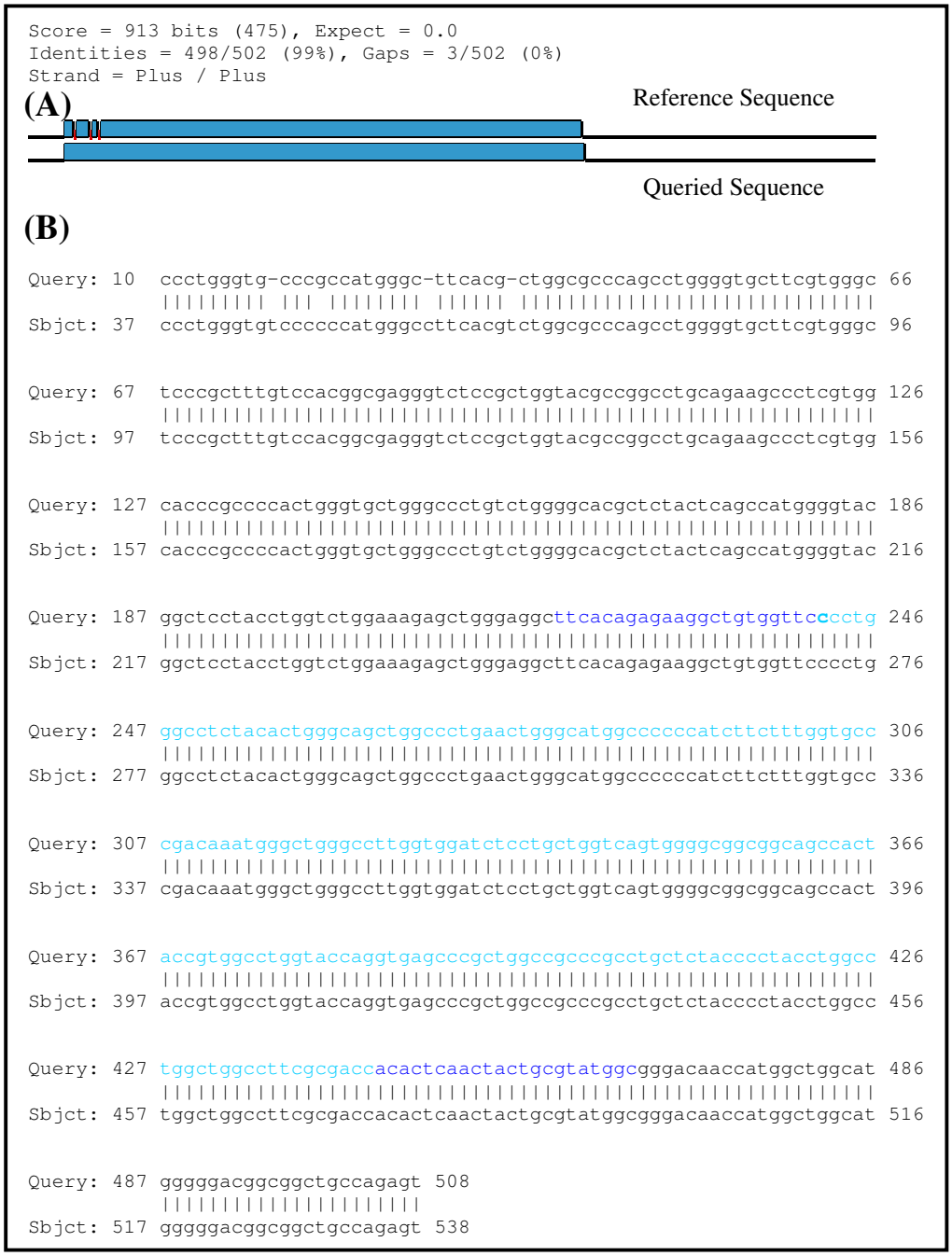



**Figure 3-78: Restriction Digestion of Plasmid DNA containing Peripheral Benzodiazepine Receptor Insert**

### *3.4.8. Sequencing*

The purified recombinant clone containing the region of interest of the *PBR* gene was sent to Inqaba Biotechnical Industries (Pty) Ltd (Pretoria, Gauteng, South Africa) for sequencing to determine if the insert isolated was actually the *PBR* gene. The results were analysed using CHROMAS, version 1.62 and by comparing the PBR sequence obtained to that of the *Homo sapiens* benzodiazepine receptor (peripheral) mRNA reference sequence (Accession Number: BT006949) obtained from Nucleotide database at the NCBI. This was done using BLAST at NCBI where two sequences can be compared to each other (Figure 3-79). It was found that the PBR insert was 502 bp in size and that this size is almost the entire size of the original reference PBR sequence is 99% accurate to the reference sequence and lies in a 5' to 3' orientation.

The sequence of the PBR insert was than processed through DNAMAN, version 6.0 (Lynonn Corporation, Vaudreuil, Quebec, Canada) where the molecular composition of the insert (Table 3-9) and when translated the size of the protein synthesised determined. Further, the amino acid sequence was also determined and it was found that the PBR insert could be translated via three reading frames consisting of 166 or 167 amino acids (Figure 3-80 and Figure 3-81). In addition, Figure 3-80 shows that an additional reading frame exists that can be formed by the translation of the negative strand, that is the complementary strand in the plasmid DNA. Using the number of amino acids, the size of the PBR protein was calculated to be 17 kDa (for calculation see Appendix 7 Calculation of Size of the Peripheral Benzodiazepine Receptor Protein).




| Key: | |
|---|---|
| Query: Reference Sequence (BT006949) | ■ – Binding site for PBR specific primers |
| Subject: Purified Recombinant PBR Sequence | ■ – Original size of the PBR region of interest |

**Figure 3-79: Alignment of the *Peripheral Benzodiazepine Receptor* (*PBR*) Gene**

(A) shows a graphic alignment of the two sequences. (B) shows a detailed alignment of the cloned *PBR* gene to the reference *PBR* gene.

**Table 3-9: Molecular Composition of the Peripheral Benzodiazepine Receptor Insert**

| Nucleotides | Number of Bases | Percentage of Bases (%) |
|---|---|---|
| Adenines (A) | 63 | 12.5 |
| Thymines (T) | 99 | 19.7 |
| Guanines (G) | 168 | 33.5 |
| Cytosines (C) | 172 | 34.3 |

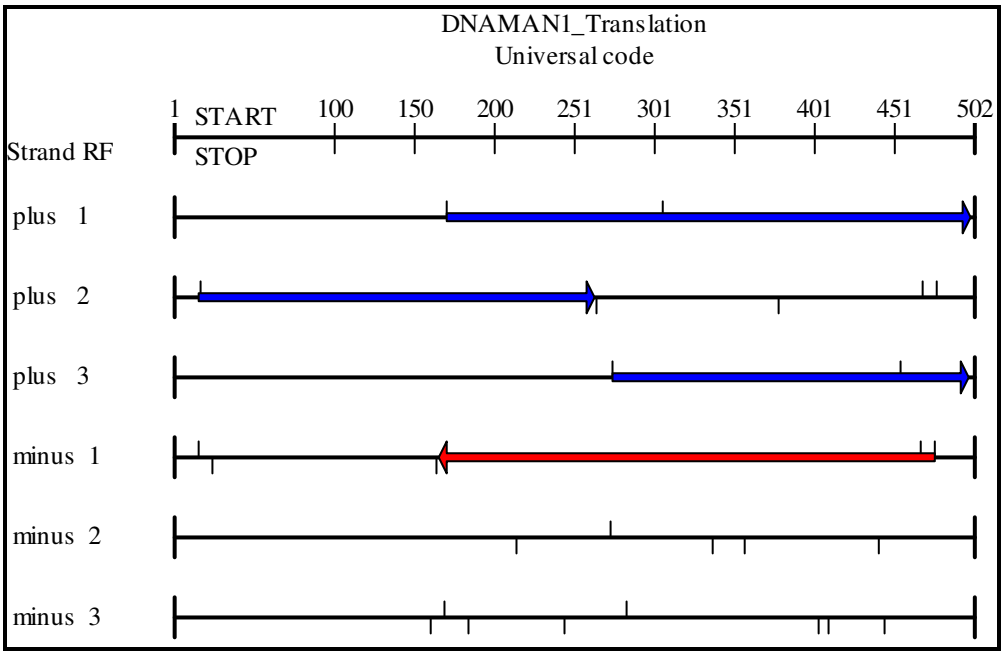
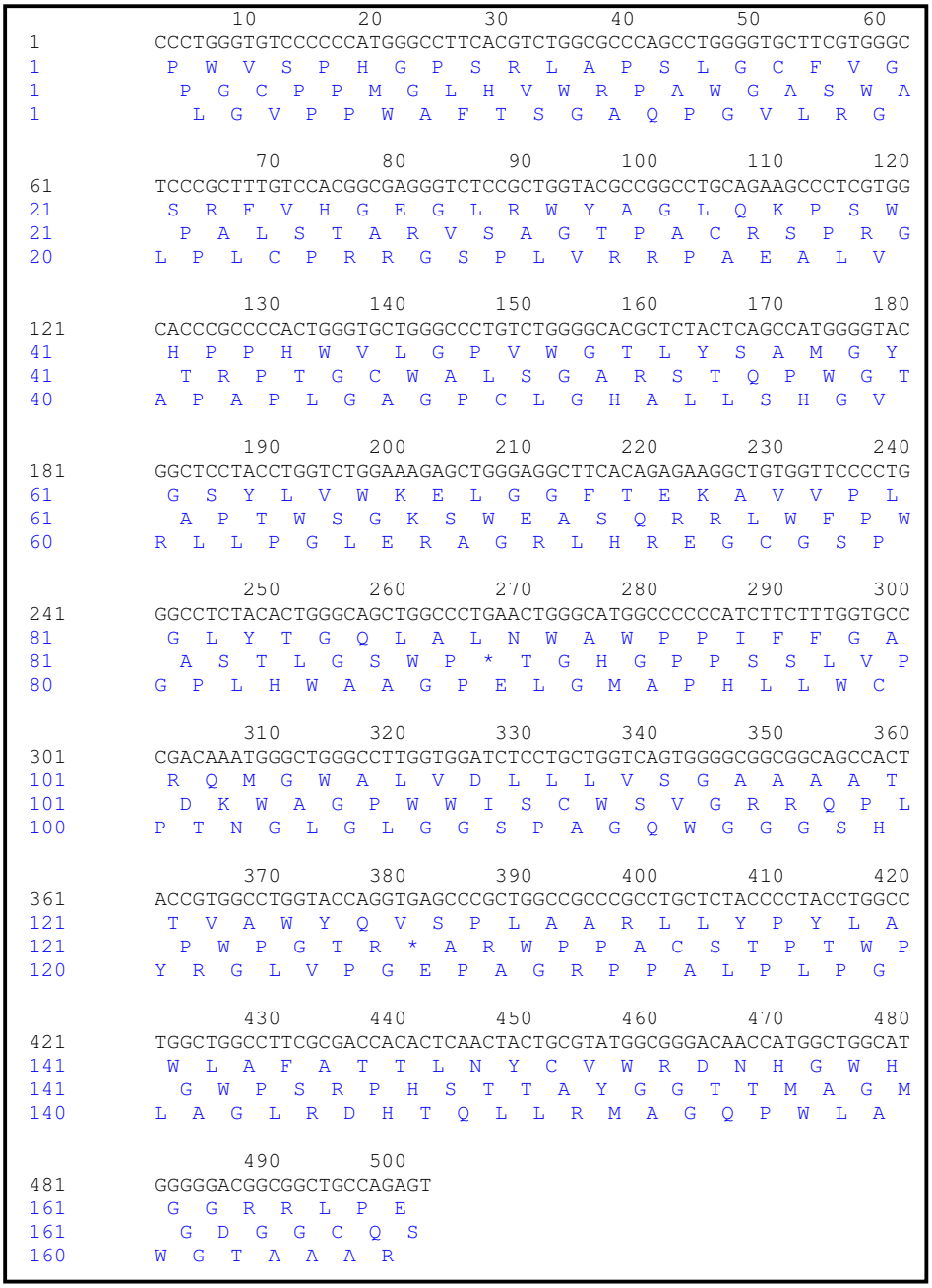



**Figure 3-80: Schematic Representation of the Reading Frames of the Peripheral Benzodiazepine Receptor Protein**

### *3.4.9. Optimisation of Glutathione-S-Transferase Fusion Protein using Isopropyl-β-D-Thiogalactopyranoside*

In order to express the GST fusion protein, that is, GST fused with the PBR protein, the pGEX-6P-2 expression vector containing the PBR insert was transformed into competent BL-2 *Escherichia coli* cells after which it was induced with different concentrations of IPTG. IPTG binds to the *lac* repressor, encoded by the *lac* $I^q$ gene thus allowing for the transcription of all genes downstream of the *tac* promoter in the pGEX-6P-2 expression vector.




Key:

■ – Nucleotide Sequence

■ – Amino Acid Sequence

A – Alanine

C – Cysteine

D – Aspartic Acid

E – Glutamic Acid

F – Phenylalanine

G – Glycine

H – Histidine

I – Isoleucine

L – Leucine

M - Methionine

N - Asparagine

P – Proline

Q – Glutamine

R – Arginine

S – Serine

T - Threonine

V – Valine

W – Tryptophan

Y – Tyrosine

* - Termination

**Figure 3-81: Translation of Peripheral Benzodiazepine Receptor (PBR) Insert**

The transformed *Escherichia coli* cells were plated on ampicillin-containing nutrient-rich agar plates (Figure 3-82). Thus, only those bacteria containing the ampicillin resistant gene will grow. To determine if the BL-2 *Escherichia coli* cells were competent; a background control used was to plate the cloning reactions on nutrient-rich agar plates not containing ampicillin. A negative background control used was to allow the bacteria to grow in the absence of the vector containing the insert. This control served the purpose of determining if the bacterial cells contained the ampicillin resistant gene. It was found that a lawn of growth occurred on ampicillin-negative plates that were plated with bacteria containing no pGEX-6P-2 expression vector or insert or when plated with bacteria containing pGEX-6P-2 expression vector containing the insert. When the bacteria containing no vector or insert were plated on ampicillin-positive plates no growth occurred while bacteria containing the pGEX-6P-2 expression vector containing the insert showed growth in the form of colonies when plated on ampicillin-positive plates.

In order to determine the optimal concentration of IPTG required to induce the GST-fusion protein, different concentrations of IPTG ranging from 0.1 mM to 0.9 mM was used to induce the GST-fusion protein and the results were analysed with SDS-PAGE (Figure 3-83). The negative control was to do protein expression in the absence of IPTG (Lane 7). It was found that these different concentrations of IPTG induced the GST-fusion protein seen by the bold band (Lane 2-6) that lies between the 40 kDa and 55 kDa reference bands (Lane 1). This is correct because it is the molecular weight of the GST protein, which is 26 kDa plus the PBR protein, which is 17 kDa, that is 43 kDa. Further, it was found that 0.7 mM IPTG induced the GST-fusion protein most optimally.

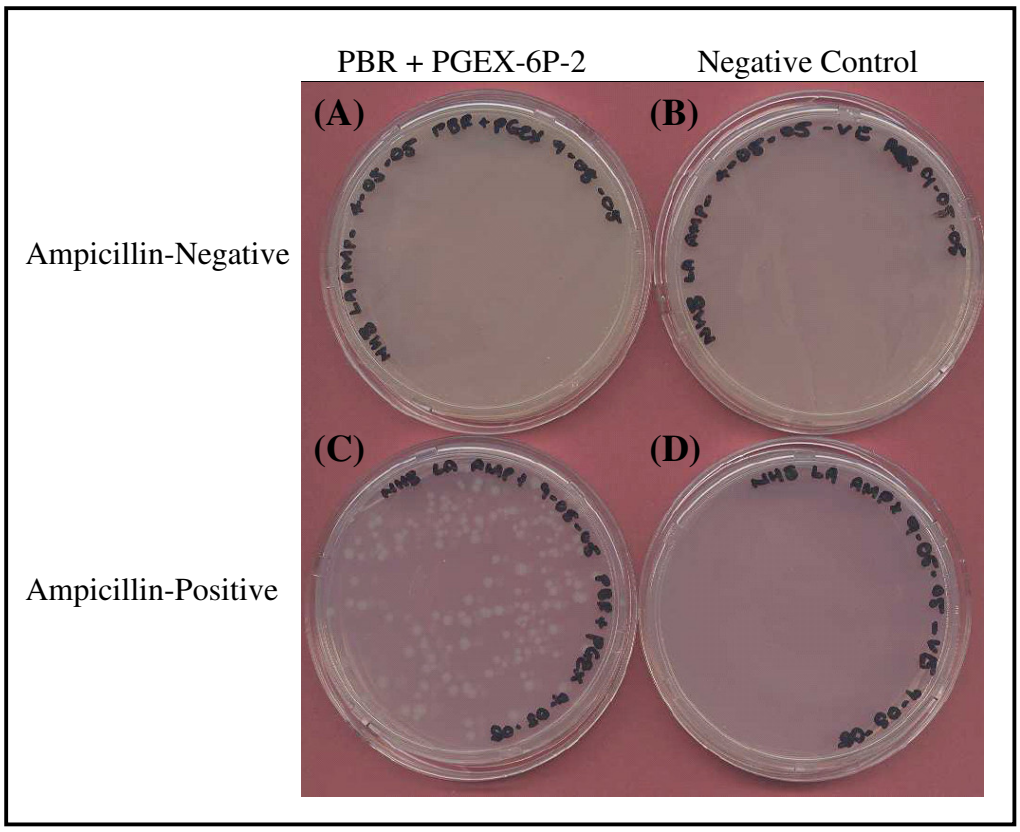



**Figure 3-82: Transformation of the pGEX-6P-2 Expression Vector Containing the Peripheral Benzodiazepine Receptor Insert**

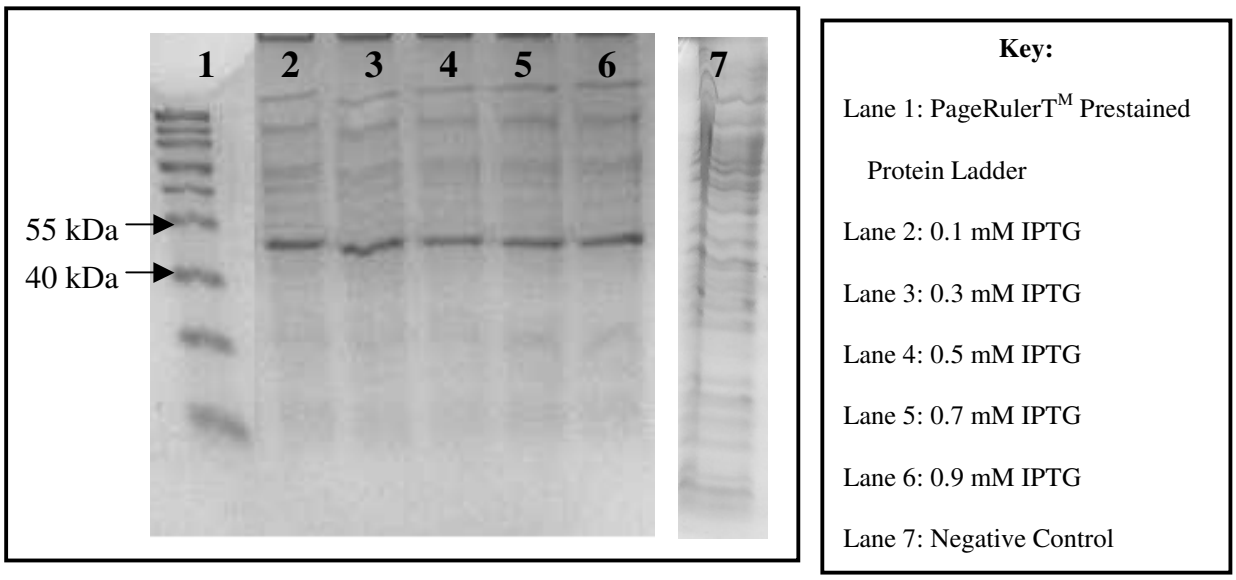



**Figure 3-83: SDS-PAGE of Optimising the Concentration of IPTG Required to Induce Gluthathione-*S*-Transferase Fusion Protein**

### *3.4.10. Summary*

This study only showed preliminary expression of the GST-PBR protein in small concentrations. Thus, future study will have to focus on the expression of the GST-PBR protein with an optimal concentration of IPTG in order to generate a large concentration of the protein after which it can be purified and treated with PreScission™ Protease to isolate the PBR protein.

# APPENDIX 7: Calculations

## Calculations of Concentrations Linearised Clones, Volume Required to Synthesise Probes and Purity of Linearised Clones

- ***Recombinant Plasmid DNA Digested with ApaI***

$A_{260} = 0.070$ $A_{280} = 0.065$

$c = A_{260} \times [A_{260}\text{dsDNA}] \times DF$

$= 0.070 \times 50\ \mu g/ml \times 100$

$= 350\ \mu g/ml$

If there is 350 µg of linearised clone in 1000 µl of DEPC-treated $H_2O$

Then there is 2 µg of linearised clone in x µl of DEPC-treated $H_2O$

$x = 5.7\ \mu l$

Purity of Clone = $A_{260} : A_{280}$

$= 0.070 : 0.065$

$= 1.1$

- ***Recombinant Plasmid DNA Digested with PstI***

$A_{260}$ = 0.082 $A_{280}$ = 0.083

c = $A_{260}$ x [$A_{260}$dsDNA] x DF

= 0.082 x 50 µg/ml x 100

= 410 µg/ml

If there is 410 µg of linearised clone in 1000 µl of DEPC-treated $H_2O$

Then there is 2 µg of linearised clone in x µl of DEPC-treated $H_2O$

x = 4.9 µl

Purity of Clone = $A_{260}$ : $A_{280}$

= 0.082 : 0.083

= 1.0

**Calculations of Concentrations cDNA, Volume Required for Real-Time PCR and Purity of cDNA**

- ***MRC5***

$A_{260}$ = 0.572 $A_{280}$ = 0.347

c = $A_{260}$ x [$A_{260}$dsDNA] x DF

= 0.572 x 50 µg/ml x 100

= 2860 µg/ml

If there is 2860 µg in 1000 µl of sd$H_2O$

Then there is x µg in 1 µl of sd$H_2O$

x = 2.86 µg/µl

When the undiluted sample is diluted 1:10000, the concentration of cDNA is 2.86 x $10^{-4}$ µg/µl = 0.286 ng/µl

Thus, if there is 0.286 ng of cDNA in 1 µl of $sdH_2O$

Then there is 0.216 ng of cDNA in x µl of $sdH_2O$

x = 0.8 µl

Purity of Clone = $A_{260}$ : $A_{280}$

= 0.572 : 0.347

= 1.65

- ***A549***

$A_{260}$ = 0.438

$A_{280}$ = 0.270

c = $A_{260}$ x [$A_{260}$dsDNA] x DF

= 0.438 x 50 µg/ml x 100

= 2190 µg/ml

If there is 2190 µg in 1000 µl of $sdH_2O$

Then there is x µg in 1 µl of $sdH_2O$

x = 2.19 µg/µl

When the undiluted sample is diluted 1:10000, the concentration of cDNA is 2.19 x $10^{-4}$ µg/µl = 0.219 ng/µl

Thus, if there is 0.219 ng of cDNA in 1 µl of $sdH_2O$

Then there is 0.216 ng of cDNA in x µl of $sdH_2O$

x = 1.0 µl

Purity of Clone = $A_{260}$ : $A_{280}$

= 0.438 : 0.270

= 1.62

- ***HeLa***

$A_{260}$ = 1.286 $A_{280}$ = 0.935

c = $A_{260}$ x [$A_{260}$dsDNA] x DF

= 1.286 x 50 µg/ml x 100

= 6430 µg/ml

If there is 6430 µg in 1000 µl of sd$H_2O$

Then there is x µg in 1 µl of sd$H_2O$

x = 6.43 µg/µl

When the undiluted sample is diluted 1:10000, the concentration of cDNA is 6.43 x $10^{-4}$ µg/µl = 0.643 ng/µl

Thus, if there is 0.643 ng of cDNA in 1 µl of sd$H_2O$

Then there is 0.216 ng of cDNA in x µl of sd$H_2O$

x = 0.3 µl

Purity of Clone = $A_{260}$ : $A_{280}$

= 1.286 : 0.935

= 1.38

- ***HepG***

$A_{260}$ = 0.432 $A_{280}$ = 0.266

c = $A_{260}$ x [$A_{260}$dsDNA] x DF

= 0.432 x 50 µg/ml x 100

= 2160 µg/ml

If there is 2160 µg in 1000 µl of sd$H_2O$

Then there is x µg in 1 µl of sd$H_2O$

x = 2.16 µg/µl

When the undiluted sample is diluted 1:10000, the concentration of cDNA is 2.16 x $10^{-4}$ µg/µl = 0.216 ng/µl

Thus, if there is 0.216 ng of cDNA in 1 µl of sd$H_2O$

Then there is 0.216 ng of cDNA in x µl of sd$H_2O$

x = 1.0 µl

Purity of Clone = $A_{260}$ : $A_{280}$

= 0.432 : 0.266

= 1.62

**Calculations of the Relative Expression of the Peripheral Benzodiazepine Receptor mRNA in Relative Terms**

- ***MRC5 and A549***

MRC5: $C_t = 21.71$ A549: $C_t = 22.71$

In order to determine the relative expression of PBR mRNA, A549 was compared to MRC5 as follows:

$$\text{Relative Expression} = 2^{(\text{MRC5 Ct} - \text{A549 Ct})}$$

$$= 2^{(21.71 - 22.71)}$$

$$= 0.5$$

Therefore, A549 shows a half-fold decrease in the level of PBR mRNA expressed when compared to MRC5.

- ***A549 and HeLa***

A549: $C_t = 22.71$ HeLa: $C_t = 22.59$

In order to determine the relative expression of PBR mRNA, HeLa was compared to A549 as follows:

$$\text{Relative Expression} = 2^{(\text{A549 Ct} - \text{HeLa Ct})}$$

$$= 2^{(22.71 - 22.59)}$$

$$= 1.09$$

Therefore, HeLa shows a similar level of PBR mRNA expressed when compared to A549 as it shows only a slight increase.

- ***A549 and HepG***

A549: $C_t = 22.71$ HepG: $C_t = 22.12$

In order to determine the relative expression of PBR mRNA, HepG was compared to A549 as follows:

$$\text{Relative Expression} = 2^{(\text{A549 Ct} - \text{HepG Ct})}$$

$$= 2^{(22.71 - 22.12)}$$

$$= 1.51$$

Therefore, HeLa shows a half-fold increase of PBR mRNA expressed when compared to A549.

**Calculation of Size of the Peripheral Benzodiazepine Receptor Protein**

If 333 amino acids of coding capacity = $3.4 \times 10^4$ Daltons

Then 166 amino acids of coding capacity = x Daltons

x = 16948 Daltons = 17 kDa

# APPENDIX 8: Summary of PBR mRNA Localisation Studies

**Table 1: Expression of the Peripheral Benzodiazepine mRNA in Various Normal Human Tissues**

| Organ | Main Histological Components | Main Cells | Localisation of PBR mRNA | |
|---|---|---|---|---|
| | | | Nuclear | Cytoplasm |
| Liver | Parenchyma | Hepatocytes | No | Yes |
| | Sinusoids | Endothelial Cells | Yes | Yes |
| | | Kupffer Cells | Yes | Yes |
| Colon | Crypts of Lieberkhün | Goblet Cells | No | Yes |
| | | Absorptive Cells | No | Yes |
| | Lamina Propria | Plasma Cells | No | Yes |
| | | Lymphocytes | Yes | Yes |
| Epiploon | Adipose Tissue | Adipose Cells | No | Yes |
| | Stroma | Collagen Fibres | No | Yes |
| | | Fibroblasts | Yes | Yes |
| Stomach | Gastric Glands | Parietal Cells | No | Yes |
| | | Chief Cells | No | Yes |
| | | Surface Mucous Cells | No | Yes |
| | | Neck Mucous Cells | No | Yes |
| | Lamina Propria | Plasma Cells | No | Yes |
| | | Macrophages | No | Yes |
| | | Collagen Fibres | No | Yes |

| | | | | |
|---|---|---|---|---|
| | | Lymphocytes | Yes | Yes |
| Prostate (Hyperplastic Tissue) | Glands | Columnar Epithelial Cells | No | Yes |
| | | Cuboidal Endothelial Cells | Yes | Yes |
| | Stroma | Collagen Fibres | No | Yes |
| | | Elastic Fibres | No | Yes |
| | | Fibroblasts | Yes | Yes |
| Breast | Terminal Ducts and Alveoli | Cuboidal Epithelial Cells | No | Yes |
| | | Myoepithelial Cells | No | Yes |
| | Intralobular Stroma | Collagen Fibres | No | Yes |
| | | Lymphocytes | Yes | Yes |
| | | Endothelial Cells | Yes | No |
| Lung | Stroma | Macrophages | No | Yes |
| | | Plasma Cells | No | Yes |
| | | Fibroblasts | No | Yes |
| | | Lymphocytes | Yes | Yes |
| | Respiratory Bronchiole | Cuboidal Epithelial Cells | No | Yes |
| | Pulmonary Artery | Smooth Muscle Fibres | No | Yes |
| | | Endothelial Cells | Yes | Yes |

| | | | | |
|---|---|---|---|---|
| Kidney | Renal Corpuscle | Flattened Cells in Parietal Layer of Bowman's Capsule | No | Yes |
| | | Endothelial Cells of Glomerulus | No | Yes |
| | Renal Tubules | Proximal Convoluted Tubule | No | Yes |
| | | Vasa Recta | No | Yes |
| | | Thin Ascending and Descending Limbs | No | Yes |
| | | Thick Ascending Limb | No | Yes |
| | | Distal Convoluted Tubule | No | Yes |
| | | Collecting Tubule | No | Yes |
| | | Collecting Duct | No | Yes |
| Brain | Neurones | Pyramidal Cells | No | Yes |
| | | Fusiform Cells | No | Yes |
| | | Stellate Cells | No | Yes |
| | Glial Cells | Oligodendrocytes | No | Yes |
| | | Astrocytes | No | Yes |
| | Fibrillary Network | | No | Yes |

**Table 2: Expression of the Peripheral Benzodiazepine Receptor mRNA in Various Human Cancer Tissues**

| Organ | Cancer | Grade | Cells | Localisation of PBR mRNA | |
|---|---|---|---|---|---|
| | | | | Nuclear | Cytoplasmic |
| Liver | Hepatocellular Carcinoma | II | Tumour Cells | No | Yes |
| | | III | Tumour Cells | Yes | Yes |
| Colon | Adenocarcinoma | I | Tumour Cells | No | Yes |
| | | | Fibromuscular Fibres | No | Yes |
| | | II | Tumour Cells | No | Yes |
| | | III | Tumour Cells | No | Yes |
| Stomach/Epiploon | Squamous Cell Carcinoma | III | Tumour Cells | No | Yes |
| | | | Collagen Fibres | No | Yes |
| Prostate | Adenocarcinoma of the Peripheral Duct and Acini | II | Cuboidal to Columnar Epithelial Cells | No | Yes |
| | | | Collagen Fibres | No | Yes |
| | | | Lymphocytes | Yes | Yes |
| | | | Endothelial Cells | Yes | Yes |
| | | III | Tumour Cells | No | Yes |
| Breast | Invasive Ductal Carcinoma (No Special Type) | III | Tumour Cells | No | Yes |
| | | | Collagen Fibres | No | Yes |
| | | | Lymphocytes | Yes | Yes |

| | | | | | |
|---|---|---|---|---|---|
| Lung | Adenocarcinoma | III | Tumour Cells | Yes | Yes |
| | | | Collagen Fibres | No | Yes |
| | Squamous Cell Carcinoma | III | Tumour Cells | Yes | Yes |
| | Small Cell Carcinoma | | Tumour Cells | Yes | Yes |
| Kidney | Chromophobe Renal Cell Carcinoma | | Tumour Cells | Yes | Yes |
| | Renal Clear Cell Carcinoma | | Tumour Cells | Yes | Yes |
| | | | Branching Vasculature | No | Yes |
| Brain | Diffuse Fibrillary Astrocytoma | II | Tumour Cells | No | Yes |
| | | | Stellate Cells | No | Yes |
| | | | Oligodendrocytes | No | Yes |
| | | | Astrocytic Process | No | Yes |
| | | | Microglia | Yes | No |
| | | | Fusiform Cells | Yes | Yes |
| | Primary Central Nervous System Lymphoma | | Tumour Cells | No | Yes |
| | | | Oligodendrocytes | No | Yes |
| | | | Astrocytes | Yes | Yes |
| | | | Microglia | Yes | Yes |
| | | | Fusiform Cells | Yes | Yes |

| | | | | | |
|---|---|---|---|---|---|
| | Ependymoma | | Tumour Cells | Yes | Yes |
| | | | Fibrillary Processes | No | Yes |
| | | | Lymphocytes | Yes | Yes |

**Table 3: Variation in Expression Levels of PBR mRNA in the Various Normal Tissues of the Human Body**

| Organ | Intensity of Staining[1] |
|---|---|
| Liver | + |
| Colon | ++ |
| Stomach | ++ |
| Epiploon | ++-+++ |
| Prostate (Hyperplastic Tissue) | ++-+++ |
| Breast | +++ |
| Lung | +++ |
| Kidney | + |
| Brain: Grey Matter | + |
| Brain: White Matter | + |

1. 0 – No Staining + - Low Staining ++ - Intermediate Staining +++ - High Staining

**Table 4: Variation in Expression Levels of PBR mRNA in the Various Cancer Tissues**

| Organ | Type of Cancer | Grade | Intensity of Staining[1] |
|---|---|---|---|
| Liver | Hepatocellular Carcinoma | II | ++ |
| | | III | + |
| Colon | Adenocarcinoma | I | ++ |
| | | II | 0-+ |
| | | III | +-++ |
| Stomach/Epiploon | Squamous Cell Carcinoma | III | +++ |
| Prostate | Adenocarcinoma of the Peripheral Duct and Acini | II | ++-+++ |
| | | III | +++ |
| Breast | Invasive Carcinoma (No Specific Type) | III | +++ |
| Lung | Adenocarcinoma | III | ++ |
| | Squamous Cell Carcinoma | III | ++-+++ |
| | Small Cell Carcinoma | - | 0-+ |
| Kidney | Chromophobe Renal Cell Carcinoma | - | +++ |
| | Clear Cell Renal Cell Carcinoma | - | ++-+++ |
| Brain | Diffuse Fibrillary Astrocytoma | II | +-++ |
| | Primary Central Nervous System Lymphoma | - | 0-+ |
| | Ependymoma | - | + |

1. 0 – No Staining + - Low Staining ++ - Intermediate Staining +++ - High Staining

**Table 5: Summary of Expression Pattern of Peripheral Benzodiazepine Receptor mRNA in Various Cancerous Tissues when Compared to its Normal Counterpart**

| Organ | Regions of the Human Body | Intensity of Staining[1] |
|---|---|---|
| ***Liver*** | ▪ *Normal* | + |
| | ▪ *Hepatocellular Carcinoma* | |
| | Grade II | +++ |
| | Grade III | ++ |
| ***Colon*** | ▪ *Normal* | ++ |
| | ▪ *Colonic Adenocarcinoma* | |
| | Grade I | +++ |
| | Grade II | 0-+ |
| | Grade III | + |
| ***Epiploon and Stomach*** | ▪ *Normal Epiploon* | ++-+++ |
| | ▪ *Normal Stomach* | ++ |
| | ▪ *Squamous Cell Carcinoma* | |
| | Grade III | +++ |
| ***Prostate*** | ▪ *Hyperplastic Tissue* | ++ |
| | ▪ *Adenocarcinoma of the Peripheral Duct and Acini* | |
| | Grade II | ++-+++ |
| | Grade III | +++ |

| | | |
|---|---|---|
| ***Breast*** | ▪ *Normal*<br>▪ *Invasive Carcinoma (NST)*<br>Grade III | ++<br><br>+++ |
| ***Lung*** | ▪ *Normal*<br>▪ *Adenocarcinoma*<br>Grade III<br>▪ *Squamous Cell Carcinoma*<br>Grade III<br>▪ *Small Cell Carcinoma* | ++<br><br>+<br><br>+++<br>0-+ |
| ***Kidney*** | ▪ *Normal*<br>▪ *Chromophobe Renal Cell Carcinoma*<br>▪ *Clear Cell Renal Cell Carcinoma* | +-++<br>+++<br>++ |
| ***Brain*** | ▪ *Normal*<br>White Matter<br>Grey Matter<br>▪ *Diffuse Fibrillary Astrocytoma*<br>Grade II<br>▪ *Primary Central Nervous System Lymphoma*<br>▪ *Ependymoma* | <br>+<br>+-++<br><br>+++<br>+-++<br>++ |

1. 0 – No Staining + - Low Staining ++ - Intermediate Staining +++ - High Staining

# 4. DISCUSSION

## 4.1. Cancer

Cancer occurs as a result of an out of control growth of abnormal cells (American Cancer Society, 2006). In a normal body, cells grow, divide and die in an orderly fashion while in cancer, cells continue to grow and divide and instead of dying, outlive normal cells and continue to form new abnormal cells. Cancer cells occurs arise from normal cells that have undergone DNA damage, which is normally repaired in the normal cell, not been repaired (American Cancer Society, 2006).

Cancer is the second leading cause of death in the United States with nearly half of all men and a little over one third of all women in the United States likely to develop cancer during their lifetimes (American Cancer Society, 2006). In South Africa one in six men and one in seven women are likely to develop cancer in their lifetimes (Cancer Association of South Africa, 2006).

Cancer is measured using three factors: incidence, mortality and prevalence. Incidence is the number of new cases occurring that is expressed as an absolute number of cases per year or as a rate per 100000 persons per year. Mortality is the number of deaths occurring and the mortality rate is the number of death occurring per 100000 persons per year. Prevalence is the number of persons alive at a particular point in time with the disease of interest and is presented as the number of persons alive after a given number years following diagnosis (Parkin, *et al.*, 2005).

### *4.1.1. Liver Cancer*

Liver cancer is the sixth most common cancer that occurs worldwide accounting for 5.7 % of all new cancer cases. The rate of incidence and mortality for this cancer can be seen in developing countries such as sub-Saharan Africa, eastern and south eastern Asia and Melanesia while it is low in developed countries, with the exception of southern Europe, Latin America and south central Asia (Parkin, *et al.*, 2005). It is a disease that is more common in men than in women having an overall sex ration of 2.4 (Parkin, *et al.*, 2005).

The prognosis is poor and accounts for almost the same amount of deaths as incidence and thus forms the third most common cause of death from cancer. Cancer registries worldwide have shown that survival rates are between 3 to 5% (Parkin, *et al.*, 2005).

### *4.1.2. Colon Cancer*

Colon cancer is the fourth most common cancer occurring in men and the third most common cancer occurring in women and it occurs at a rate of 1.2:1 when compared between men and women. It is the second most common cancer occurring worldwide (Maaser, *et al.*, 2002) with 1 million new cases been reported in 2002. It has a relatively good prognosis with a mortality rate half that of the incidence rate (Parkin, *et al.*, 2005). The highest rate of incidence has been reported in North America, Australia/New Zealand, Western Europe and Japan, intermediate in South America and low in Africa and Asia. The rate of incidence is still increasing rapidly in geographical regions where the overall risk was formerly low while gradual increase has been seen in countries where incidence was already high with North America the only region showing a decrease (Parkin, *et al.*, 2005).

In South Africa, colon cancer accounts for 3.6% of all female cancers and 3.7% of all male cancers. The highest rate of incidence occurs in the coloured and white population accounting for 4.8% of all female cancers and 4.2% of all male cancers in this population group and is the third leading cause of cancer for this population group in females and the fourth leading cause of cancer for this population group in males. Intermediate rate of incidence occurs in Asians where it accounts for 6% of all colon cancer cases in males and females and is the third leading cause of cancer for this population group in females and the fourth leading cause of cancer for this population group in males while the black population had the lowest rate of incidence (Sitas, *et al.*, 1998).

### *4.1.3. Stomach Cancer*

Stomach cancer is the fourth most common cancer worldwide accounting for an estimated 934000 new cases been reported in 2002. It is the second most common cause of cancer death accounting for 700000 deaths reported in 2002 (American Cancer Society, 2006, Parkin, *et al.*, 2005). A high rate of incidence, that is almost two-thirds of this type of cancer occurs in developing countries with 42% of cases been reported in China alone. Stomach cancer is twice as common in males than in females (American Cancer Society, 2006). A high rate of incidence for men is seen in East Asia such as China and Japan, Eastern Europe and parts of Central and South America while a low rate of incidence for men is seen in Southern Asia, North and East Africa, North America, Australia and New Zealand. The pattern of incidence is similar for women with a slightly increased risk seen in Central Africa and Eastern Europe (Parkin, *et al.*, 2005).

Rate of survival is moderately good in Japan accounting for a 52% survival rate, 40% in North America, 27% in Western Europe and 6% in sub-Saharan Africa. Differences in survival rate is determined by screening for this disease because the earlier this type of cancer is detected the better the prognosis and survival rate (Parkin, *et al.*, 2005).

### *4.1.4. Prostate Cancer*

Prostate cancer is the fifth most common cancer in the world and the second most common cancer in men forming 11.7% of all new cancers reported. In 2002, 679 000 new cases of prostate cancer were reported worldwide. The rate of incidence is 19% in developed countries and 5.3% in developing countries. The rate of incidence is high in the United States, Northern and Western Europe and in Australia/New Zealand (Parkin, *et al.*, 2005). However, the mortality rate is a much better guide in monitoring this cancer as its shows the risk of invasive prostate cancer in different populations. It was found that mortality rates were high in the Caribbean, Southern and Central Africa, North and West Europe, Australia/New Zealand, and North and South America and low in Asia and North Africa and is still thought to be increasing (Parkin, *et al.*, 2005). Prognosis of this cancer is relatively good as the mortality rate through this cancer is 5.8% in men and accounts for 3.3% of all cancer deaths in men (Parkin, *et al.*, 2005).

In South Africa, prostate cancer is the leading cause of cancer in males, which comprised 12.6% of all male cancers. The highest rate of incidence occurs in the coloured and white population group followed by the Asian population group with the lowest rate of incidence seen in the Black population group (Sitas, *et al.*, 1998).

### *4.1.5. Breast Cancer*

Breast cancer is the most common cancer in women forming 23% of all cancers and having an estimated 1.15 million new cases occurring in 2002 and accounts for 3% of women's death. It is ranked the second most common cancer occurring worldwide when both sexes are considered together. Most cases have been observed in industrialised countries such as those found in Europe (27.3% reported cancer cases in women) and North America (31.3% reported cancer cases in women), with North America having the highest rate in the world (American Cancer Society, 2006). The rate of incidence is moderate in Eastern Europe, South America, Southern Africa, except South Africa, and Western Asia while it is low in most of Africa and Asia. However, it is still the most common cancer in women in these geographic regions and is still increasing in most countries (Parkin, *et al.*, 2005). It should be noted that breast cancer also occurs in men (American Cancer Society, 2006).

In South Africa, the incidence of breast cancer occurring in women is 16.4% with breast cancer been the leading form of cancer in Asians, accounting for 6.8% of all female breast cancers, coloureds and whites and been the second most common form of cancer in Black females in 1997 (Sitas, *et al.*, 1998).

Prognosis of breast cancer is good with 73% survival rate recorded in developed countries and 57% reported in developing countries. Breast cancer has been ranked as the fifth most common cause of death from cancer overall, even though it still remains the leading cause of cancer mortality in women (14% of female cancer deaths) (Parkin, *et al.*, 2005). However, because of it high incidence and relatively good prognosis, breast cancer is the most prevalent form of cancer in the world today (Parkin, *et al.*, 2005).

### *4.1.6. Lung Cancer*

Lung cancer is the most common form of cancer worldwide (Hashimoto, *et al.*, 2000) accounting for 12.4% of all new cancers with 1.35 million new cases been reported in 2002. It also forms the most common cause of death by cancer for both men and women accounting for 17.6% of all deaths occurring by cancer worldwide with 1.18 million cases been reported in 2002 as more people die from this form of cancer than those that will die from colon, breast and prostate cancer combined (American Cancer Society, 2006). Nearly 60% of people diagnosed with lung cancer will die within the first year from diagnosis and nearly 75% of people diagnosed with lung cancer will die within two years and this statistic has not improved in the last ten years (American Cancer Society, 2006).

Almost half of the cases of lung cancer occur in developing countries. It is the most common form of cancer in men accounting 35.5% of all new cancers reported in men with the highest rates of incidence seen in North America and Eastern Europe and moderately high rates seen Australia/New Zealand and eastern Asia such as China and Japan. In women the rate of incidence of lung cancer is lower accounting for 12.1% of all new cancers reported in women with the highest rate of incidence seen in North America and Northern Europe (Parkin, *et al.*, 2005). To date, lung cancer still remains a highly lethal disease with the United States reporting a 15% survival rate, Europe reporting a 10% survival rate and developing countries reporting a 8.9% survival rate (Parkin, *et al.*, 2005). The overall rate of incidence and mortality of lung cancer is still on the increase worldwide in both men and women while when looking at certain countries specifically, the rate of incidence has reached its peak and is now declining in both men and women (Parkin, *et al.*, 2005).

In South Africa, lung cancer comprises 2.8% of all female cancers and 6.7% of all male cancers. The highest rate of lung cancer is found in the coloured and white population combined comprising 4% of all male cancers in this population group, thus forming the third leading cause of cancer in this male population group, and 3% of all female cancers in this population group, thus forming the fifth leading cause of cancer in this female population group. Intermediate rates of lung cancer occurs in the Asian population group where it formed the second leading cause of cancer in Asian males comprising 10.6% and the seventh leading cause of cancer in Asian female comprising 2.7%. The black population group showed the lowest rate of incidence for developing lung cancer (Sitas, *et al.*, 1998).

### *4.1.7. Kidney Cancer*

Kidney cancer accounts for 1.9% of the total cancers worldwide with 208000 new cases and 102000 deaths been reported in 2002. The rate of incidence is highest in North America, Australia/New Zealand and western, eastern and northern Europe while it is lowest in Africa, and Asia with the exception of Japanese males and the Pacific Islands (Parkin, *et al.*, 2005).

### *4.1.8. Brain Cancer*

Cancers of the brain accounts for 1.7% of all new cases and 2.1% of all deaths caused by cancer been reported worldwide with 189 000 new cases and 142 000 deaths been reported in 2002. The highest rates of incident occurs in developed countries such as Australia/New Zealand, Europe and North America while it is lowest in Africa and the Pacific Islands. However, the estimates are thought to be underdeveloped in many countries because of the poor availability of diagnostic facilities. Furthermore, the mortality rates tend to be unreliable because of the confusion that exists between primary and metastatic cancers (Parkin, *et al.*, 2005).

### *4.1.9. Cervical Cancer*

Cervical cancer is the second most common cancer in women with an estimated 493000 new cases reported and 274000 deaths occurring in 2002. It is the seventh most common cancer worldwide when both sexes are considered together. It is much more common in developing countries accounting for 15% of all female cancers while in developed countries it accounts for 3.6% of all new female cancers reported. The highest rates of incidence have been reported in sub-Saharan Africa, Melanesia, Latin America and the Caribbean, south central Asia and south east Asia while the rate of incidence is generally low in developed countries today such as the United States due to the introduction of screening programs, China and Western Asia. Incidence of cervical cancer occurring has declined in developed countries, however developing countries have also showed decline such as seen in China and now only sub-Saharan Africa, central America, south central Asia and Melanesia show a high rate of incidence (Parkin, *et al.*, 2005). The ratio of mortality to incidence is 55% and survival rate vary between regions with quite good prognosis seen in low risk regions (Parkin, *et al.*, 2005).

Cervical cancer is the leading cause of cancer among South African women accounting for 18.2% of all cancers reported. It is the leading cause of cancer amongst black females accounting for 85% of all cancers reported followed by 14% seen in coloured and white females combined with the least rate of incidence seen in Asians. This may be in part due to the lower socio-economic status that has been associated with a higher risk of developing cervical cancer and is in part due to lack of access to good health care and Papanicolaou (Papsmear) tests. However, the rate of incidence can be decreased with the implementation of screening programmes (Sitas, *et al.*, 1998).

## 4.2. Expression of the Peripheral Benzodiazepine Receptor mRNA in Various Normal and Cancer Tissues

### *4.2.1. Tissue Microarrays*

The use of tissue microarrays is a powerful technology that efficiently and economically assesses the expression of proteins or genes across large sets of tissue specimens assembled onto a single microscope slide (Chen, *et al.*, 2004). Advantages of using tissue microarrays include: (i) allows for the amplification of limited tissue resources by providing the means by which a large number of small core biopsies rather than a single section, (ii) each tissue specimen on the microarray is treated in an identical manner such that reagent concentrations, incubation times, temperatures and washing conditions are consistent across discs on each tissue microarray slide (Chen, *et al.*, 2004).

As mentioned above, the use of tissue arrays in this study provided an efficient way in analysing multiple cancers. However, the disadvantage that arose through the use of this particular tissue array was that many cancers had only one disc (dot), that is one specimen of a particular type of cancer and so generalization and trends in a particular expression pattern were difficult to make. To compensate for this colorimetric and fluorescent *in situ* hybridisation was done on 3 tissue array slides respectively. Thus, future studies should be done using tissue arrays that are specific for a particular type of cancer, which will allow for more generalised results to be obtained for a particular type of cancer and not specific results as was obtained in this study.

### *4.2.2. In Situ Hybridisation*

The expression pattern of PBR mRNA in normal human tissues and cancerous human tissues was determined by *in situ* hybridisation. It looked at the expression of PBR mRNA in some tissues for which current information on expression of PBR mRNA is still sparse. Further, it should be noted that very few to no studies have used *in situ* hybridisation to determine the expression pattern of PBR mRNA in various tissues.

*In situ* hybridisation is a qualitative or semi-quantitative technique by which mRNA of interest in the cytoplasm or DNA of interest in the nucleus can be localised through the hybridisation of the sequence of interest to the complimentary strand of a nucleotide probe. The sensitivity of this technique is such that the threshold levels of detection in the region of 10 to 20 copies of mRNA or DNA per cell. This technique provides considerable information regarding the structure and function of the cell within pathological means (Lanlani, *et al.*, 1997).

In order to conduct *in situ* hybridisation anti-sense probes complementary to the PBR mRNA had to be synthesised. This was done by the isolation of the PBR region of interest from mRNA in normal kidney tissue. The use of mRNA is advantageous as it contains only the functional regions known as the exons, which are required for translation to synthesise the protein. The PBR region of interest was isolated and multiple copies generated using gene-specific primers during PCR after which the PBR fragments were ligated into pGEM-T Easy cloning vector and transformed into *Escherichia coli* in order to generate stable complexes. After cloning, the recombinant DNA was purified and linearised in preparation for probe synthesis. Both sense- and anti-sense RNA probes were generated by *in vitro* transcription. The use of RNA probes in *in situ* hybridisation is advantageous because RNA probes are

already single-stranded and thus there is no need for the denaturation step and RNA-RNA hybrids are very thermostable and resistant to digestion by RNases. However, the disadvantage of using RNA probes includes their instability and the difficulty that exists to inactivate RNases.

The reason for the use of both the colorimetric and fluorescent detection methods for *in situ* hybridisation was because fluorescent detection offers several advantages. These include the fact that it is simple, far more accurate than colorimetric detection as it reduces a lot of the background staining and thus is more reliable and requires a shorter time period for performing the technique before which results can be viewed (Lanlani, *et al.*, 1997). However, several disadvantages for the use of fluorescent detection also occur including the fact that it is far more expensive and have a short time period in which results can be viewed, in this case approximately three days. The advantage of using colorimetric detection is that it is cheaper while the disadvantage of using colorimetric detection is the higher background staining making it more difficult to determine if localisation occurred. High background staining occurs as a result of the intermediates that form during the NBT/BCIP reaction, which is relatively slow, diffusing away into the medium making it difficult to localise the site of hybridisation and reducing the hybridisation signal.

It was found that the expression pattern of PBR mRNA was uniform in most tissues studied with the exception been epiploon normal tissue, which showed intermediate expression in 50% of cases and high expression in 50% of cases and lung small cell carcinoma, which showed low expression in 50% of cases and no expression in 50% of cases.

#### *4.2.2.1. Localisation of the Peripheral Benzodiazepine Receptor mRNA in Various Normal Tissues*

This study focused on determining the expression pattern of PBR mRNA in liver, colon, epiploon, stomach, prostate, breast, lung, kidney and brain. To my knowledge, this is the first time that the expression pattern of PBR mRNA has been determined in epiploon.

The PBR mRNA was expressed in all normal human tissues studied. From the results obtained it is clear that the PBR mRNA is expressed mainly in the cytoplasm. This is understandable since the PBR protein is synthesised in the ribosomes and is located mainly in the outer mitochondrial membrane (Hans, *et al.*, 2005, Kletsas, *et al.*, 2004, Lacapère, *et al.*, 2003). However, nuclear localisation of PBR mRNA were observed, which further suggest as previous studies that the PBR protein is involved in the transport of cholesterol from the cytoplasm into the nucleus where it affects genes involved in the cell cycle (Corsi, *et al.*, 2005) or it could be as a result of the PBR mRNA been just transcribed in the nucleus and still having not been transferred to the cytoplasm for translation or as a result of PBR anti-sense probe binding with DNA in the nucleus.

The results obtained in this study are similar to those obtained by Bribes *et al.*, who looked at the expression pattern of the PBR protein through the use of a monoclonal antibody specific for PBR. However this study looked at additional tissues including kidney, brain and epiploon and showed expression in some cells, which Bribes, *et al.* did not show (Bribes, *et al.*, 2004). Previous studies have also shown that PBR is expressed mainly in the glial cells (Jordà, *et al.*, 2005, Kassiou, *et al.*, 2004, Veenman, *et al.*, 2004), however, this study clearly showed that PBR is expressed in neurones and in the fibrillary network.

The level of expression within a given organ varies. In normal tissue, high expression levels of PBR mRNA were seen in epiploon, prostate, breast and lung, intermediate expression levels were seen in colon and stomach and low expression levels were seen in liver, kidney and brain with white matter showing a higher level of expression than grey matter. The level of expression seen in this study for PBR mRNA is similar to those seen previously for the PBR protein, with the exception been lung, which previously was reported to show intermediate expression and in this study shows high expression. These results have mainly been confirmed in other species but not in human (Bribes, *et al.*, 2004, Casellas, *et al.*, 2002).

#### *4.2.2.2. Localisation of the Peripheral Benzodiazepine Receptor mRNA in Various Human Cancer Tissues*

In order to determine if the level of expression of PBR mRNA increased or decreased in the cancerous state, cancerous tissues were compared to its normal counterpart. It was found that that expression of PBR mRNA increased in Grade II and Grade III liver hepatocellular carcinoma, Grade I colonic adenocarcinoma, Grade III stomach squamous cell carcinoma, Grade II and Grade III prostate adenocarcinoma of the peripheral duct and acini, Grade III breast invasive ductal carcinoma (NST), Grade III lung squamous cell carcinoma, kidney chromophobe renal cell carcinoma, kidney clear cell carcinoma, Grade II brain diffuse fibrillary astrocytoma, brain PCNSL and brain ependymoma while the expression of PBR mRNA decreased in Grade II and Grade III colonic adenocarcinoma, Grade III lung adenocarcinoma and lung small cell carcinoma. Similar patterns have been observed in previous studies for some cancers including hepatocellular carcinoma, colonic adenocarcinoma, breast invasive ductal carcinoma (NST), prostate adenocarcinoma, diffuse fibrillary astrocytoma and ependymoma (Allenfall, *et al.*, 1995, Gavish, *et al.*, 1999, Hardwick, *et al.*, 2002, Miettinen, *et al.*, 1995, Venturini, *et al.*, 1998), however a previous

study conducted in renal clear cell carcinoma showed an absence of PBR binding sites, which appears contradictory to those obtained in this study (Katz, *et al.*, 1989). It should be noted that they were looking at the PBR protein while this study focused on the PBR mRNA. To my knowledge it was the first time that stomach Grade III squamous cell carcinoma, lung Grade III adenocarcinoma, lung Grade III squamous cell carcinoma, lung small cell carcinoma, chromophobe renal carcinoma and brain PCNSL were studied.

The level of PBR mRNA varies also with tumour malignancy grade. In hepatocellular carcinoma the level of PBR mRNA decreased as tumour invasion increased while in prostate adenocarcinoma of the peripheral duct and acini PBR mRNA level increased as tumour invasion increased. This suggests that PBR may serve as a prognostic marker in these diseases. A previous study has shown that the expression of PBR varies with tumour malignancy grade for hepatocellular carcinoma (Venturini, *et al.*, 1998). In colon adenocarcinoma expression of PBR mRNA decreased from Grade I to Grade II and Grade III colonic adenocarcinoma. However, Grade III colonic adenocarcinoma had a higher PBR mRNA expression level than Grade II colonic adenocarcinoma. However, this is not the same as what was found in a previous study where the expression of PBR mRNA decreased as tumour malignancy increased (Maaser, *et al.*, 2002).

The level of expression of PBR mRNA varies for the different cancers, which was determined by comparing the different tissues. High expression levels were seen in epiploon Grade III squamous cell carcinoma, Grade II and Grade III prostate adenocarcinoma of the peripheral duct and acini, with Grade II showing a lower expression than Grade III, breast Grade III invasive ductal carcinoma (NST), lung Grade III squamous cell carcinoma, chromophobe renal cell carcinoma and renal clear cell carcinoma with chromophobe renal cell carcinoma

showing the highest expression level, intermediate expression levels were seen in Grade II hepatocellular carcinoma, Grade I and Grade III colon adenocarcinoma, lung Grade III adenocarcinoma, brain Grade II diffuse fibrillary astrocytoma and low expression levels were seen in Grade III hepatocellular carcinoma, Grade II colonic adenocarcinoma, lung small cell carcinoma, brain PCNSL and brain ependymoma with highest expression level seen in ependymoma and lowest expression level seen in PCNSL.

The expression of PBR mRNA was clearly seen in all cancerous tissues studied. From the results obtained it is clear that the PBR mRNA is expressed mainly in the cytoplasm with some nuclear localisation also seen. The expression of PBR mRNA in the nucleus is thought to be essential in the regulation of cell proliferation and thus ultimately may function in the development and progression of the disease (Galiègue, *et al.*, 2004).

From this study, it can be concluded that the PBR may serve as a prognostic marker in cancer tissues where the expression level of PBR mRNA varies with tumour malignancy grade and that this receptor may play an important role in the development of cancer. It should be noted that this study provided specific results for the different cancer types and further studies will have to be done to determine generalized trends for the expression of PBR mRNA in the various types of cancers focused on in this study. This may be achieved by getting a higher number of patients for each type of cancer that is by using tissue microarrays having only one type of cancer. Also future studies should focus on looking at the different grades for a specific type of cancer, which will allow one to see if the expression of PBR mRNA is uniform as tumour malignancy increases.

### *4.2.3. Expression Levels of Peripheral Benzodiazepine Receptor mRNA in Human Normal and Various Cancer Cell Lines*

#### *4.2.3.1. Quantitative Real-Time Reverse-Transcriptase Polymerase Chain Reaction*

The relative expression levels of the PBR mRNA in normal lung and various human cancer cell lines were determined in absolute terms by quantitative real-time RT-PCR. Quantitative real-time RT-PCR is a technique used to rapidly measure the quantity of PCR product synthesised and thus indirectly functions in quantitatively determining the amounts of DNA, cDNA or RNA. The amount of RNA or more specifically mRNA used as the starting material correlates with the amount of protein that will be synthesised by the cell eventually. Thus, it is a commonly used molecular biology tool to determine quantification of gene expression levels in a particular cell or tissue as only minute amounts of sample is required. Very few to no studies have focused on determining the expression level of PBR mRNA in this manner.

#### *4.2.3.2. Relative Expression Levels of the Peripheral Benzodiazepine Receptor mRNA in Normal and Various Cancer Cell Lines*

The normal cell line studied was the lung normal (MRC5) and cancers studied include lung adenocarcinoma (A549), cervical carcinoma (HeLa) and liver hepatocellular carcinoma (HepG). RNA was extracted from each of the confluent cell lines after which they were reverse transcribed using reverse transcriptase and oligo-$(dT)_{15}$ primers to synthesise cDNA after which real-time PCR was performed using PBR-specific primers and SYBR Green 1. In order to determine the relative expression levels of the lung normal and cancers, the same concentration (216 ng/µl) of each of the cDNA were used. Thus, any variation that occurred in the amount of PCR product synthesised would indicate the difference in expression levels for the normal cell line and each of the cancer cell lines and thus ultimately which cell line had the most starting product as each cell line was subjected to the same starting conditions.

#### *4.2.3.2.1. Quantitative Real RT-PCR Versus Conventional PCR*

The use of quantitative real-time PCR offers several advantages including: (i) conventional PCR is measured at the end-point while real-time PCR is measured during the exponential growth phase, (ii) the increase in reporter fluorescence signal is directly proportional to the number of PCR products generated, (iii) the cleaved probe provides a permanent record of amplification of the PCR product, (iv) the increased dynamic range of detection, (v) the need for a thousand-fold less RNA than that is required in conventional PCR, (vi) no post-PCR processing due to its closed system, thus no need for electrophoresis, (vii) the PCR product is detected down to a two-fold change and (viii) small PCR products result in increase amplification efficiency. One major disadvantage of quantitative real-time PCR is because of its sensitivity; the introduction of any contaminants to the samples dramatically affects the final results.

Conventional PCR requires the use of agarose gel electrophoresis in order to analyse results. The results analysed by agarose gel electrophoresis is measured at the end-point of the PCR reaction, based on size discrimination, which is not very precise and is time consuming. In addition, the resolution of the agarose gel is very poor at around ten-fold. Thus, the disadvantages of end-point detection include poor precision, low sensitivity, a short dynamic range of less than two logs, low resolution, non-automated processing, PCR products are discriminated by size only, results via ethidium bromide staining is not very quantitative and post-PCR processing.

*4.2.3.2.2. Expression Levels of Peripheral Benzodiazepine Receptor mRNA*

Efficiency of the reactions should lie within 90% to 100%. However, in this study the efficiency was lower than this for three cell lines, which could have occurred as a result of secondary structure and primer quality. Thus, in order to increase this efficiency, primers more sensitive than the ones used should be designed.

The most important value to determine the success of the reaction was to determine the $C_t$ values for each of the reactions. The $C_t$ value is the threshold cycle at which the system begins to detect the increase in signal associated with an exponential growth of the PCR products during the log-linear phase of PCR. $C_t$ values should not lie higher than 40 because any value higher than this indicates that no amplification of PCR product occurs. In this study, all the $C_t$ values lie below 40 with MRC5 having a lower $C_t$ value when compared to A549, which indicates that MRC5 had a higher concentration of template PBR than A549. When the cancerous cell lines were compared to each other, it was found that the lowest $C_t$ value was seen in HepG and the highest $C_t$ value was seen in A549, which indicates that HepG had the highest concentration of template PBR and A549 had the lowest concentration of template PBR.

The expression levels of PBR mRNA varied between lung adenocarcinoma and its normal counterpart and between the different cancer cell lines. It was found that the relative expression of PBR mRNA decreased half-fold in lung adenocarcinoma when compared to it normal counterpart seen by the decrease in concentration of template DNA for the two cell lines. The results serve to confirm the results via *in situ* hybridisation, which showed a decrease in PBR mRNA expression in Grade III lung adenocarcinoma when compared to its normal counterpart. In the case of the cancerous cell lines, the concentration of PBR mRNA

increases as follows: liver hepatocellular carcinoma > cervical carcinoma ≥ lung adenocarcinoma, with liver hepatocellular carcinoma showing a half-fold increase compared to lung adenocarcinoma and cervical carcinoma and lung adenocarcinoma showing a similar expression level.

This study shows preliminary results of expression levels in human normal and various cancer cell lines. In order to obtain much better efficiency future studies should focus on designing primers that are more sensitive and specific for the PBR mRNA. Future studies should also include a reference or standard gene such as glyceraldehydes-3-phospahte-dehydrogenase mRNA or β-actin mRNA, which serves as an internal standard to which experimental variables may be compared to allow for a more efficient and accurate result to be obtained. In addition, future studies will have to focus on determining the changes in expression levels between various normal and cancerous cell lines.

Expression of PBR mRNA in the different cancers suggests that PBR may play a role in cancer progression probably through the induction of cell proliferation. However, in the case of lung adenocarcinoma where a decrease in expression of PBR mRNA is seen, it could further play a role in suppressing apoptosis.

### *4.2.4. In Situ Hybridisation Versus Quantitative Reverse Transcriptase Real-Time Polymerase Chain Reaction*

*In situ* hybridisation is the technique by which nucleic acids are fixed *in situ* instead of being extracted thus permitting the localisation of the hybridising probe within a cell or tissue (Harvey, 2002). It has the advantage of requiring only small amounts of tissues and tolerates the degradation of target nucleic acids due to formalin fixation (Biedermann, *et al.*, 2004).

Disadvantages of this technique include: (i) maintaining the morphology and structure of the cells introduces more potentially inhibitory elements and thus in order to make the nucleic acids accessible for hybridisation, protease pre-treatment has to be performed, (ii) it cannot quantify mRNA or DNA in a prognostic-diagnostic significant manner and (iii) the chance of false-positives increases during RNA analysis because of the spliced nature and abundance of RNA (Biedermann, *et al.*, 2004, Harvey, 2002).

Real-time quantitative PCR is a timesaving high throughput analysis technique by which mRNA or DNA can be detected and quantified in a prognostic-diagnostic significant manner. This technique is more sensitive in detecting the sequence of interest than *in situ* hybridisation. Disadvantages of real-time PCR include: (i) the detection of false-positives due to unspecific signals and (ii) it is an expensive technique to conduct. The detection of false-positives increases through the use of SYBR Green, which has the disadvantage of binding to double-stranded DNA of any sequence, thus making accurate product detection more difficult. Further, it is difficult to decipher specific peaks from unspecific peaks during melting curve analysis. Thus, the more accurate the probe is the better because it will overcome the problem of non-specificity and thus permit more accurate quantification (Biedermann, *et al.*, 2004).

### 4.3. Peripheral Benzodiazepine Receptor Protein Expression

This study focused on the preliminary steps required to isolate the PBR protein. PBR protein isolation involves a number of steps including, (i) cloning, where the protein sequence of interest (PBR) is ligated into an expression vector such as pGEX-6P-2, which contains a *lac* repressor gene and a *GST* gene that functions as an affinity tag when transformed into *Escherichia coli* cells, (ii) bacterial colonies containing the expression vector are selected and

grown, (iii) *Escherichia coli* cells are induced by IPTG in the case of pGEX-6P-2 to express the recombinant protein and harvested, (iv) the recombinant protein is purified using gluthathione in the case of GST via affinity chromatography and (v) digestion with a proteases such as PreScission™ protease in the case of GST allows for the isolation of the protein of interest.

The PBR protein was isolated via the expression of recombinant proteins in *Escherichia coli* (in this case GST fused to the PBR protein (GST-PBR)), which enables the production of large amounts of proteins from relatively small amounts of biomass and later simplifies its purification and detailed characterisation. Producing recombinant proteins is advantageous because purifying protein from native sources requires large amounts of starting material to yield small amounts of protein. Furthermore, the purifying step for non-recombinant proteins is a multi-step process where at each step a proportion of the target protein is lost. However, in the case of recombinant proteins, a standardised affinity chromatography procedure (in this case GST-PBR can be purified and isolated in the presence of gluthathione) is only required in order to purify the protein obtained at a high level of purity eliminating the need to develop a protein-specific purification procedure for each new target protein.

The efficient and controlled expression of the GST-PBR in *Escherichia coli* cells is regulated by the presence of the *lac* repressor protein. The *lac* repressor protein binds to the operator sequences on the pGEX-6P-2 expression vector during normal cell growth and prevents GST-PBR expression. However, when the *Escherichia coli* cells are treated with IPTG, it induces GST-PBR expression as it binds to the *lac* repressor protein and inactivates it, thus allowing the host cell's RNA polymerase to transcribe the sequences downstream from the promoter, which are then translated to form the recombinant protein. This tightly controlled expression

of recombinant protein is advantageous as it allows for the almost exclusive production of the recombinant protein and proteins that may have adverse effects on the growing cells are not expressed.

This study only showed preliminary expression of the GST-PBR protein in small concentrations. Thus, future study requires the expression of the GST-PBR protein with an optimal concentration of IPTG in order to generate a large concentration of the protein after which it can be purified and treated with PreScission$^{TM}$ Protease to isolate the PBR protein. The isolation of the PBR protein will allow for antibodies to be raised, which can be used in future studies that will determine the expression pattern of the PBR protein in different types of human normal and cancerous tissues.

# 5. CONCLUSION

Localisation of PBR mRNA was determined by *in situ* hybridisation. It was found that PBR mRNA is expressed in both normal and cancerous human tissues studied. Subcellularly, it was found that PBR mRNA was expressed in the cytoplasm of most cells, however, nuclear localisation have been seen in some cells. Cytoplasmic localisation is conclusive of what previous studies have suggested that PBR is located mainly on the outer mitochondrial membrane and that the PBR protein is synthesised in the ribosomes that are also located in the cytoplasm. The nuclear localisation of PBR is thought to function in the transport of cholesterol into the nucleus it affects genes involved in the cell cycle and in promoting aberrant mitogenic activity and thus malignancy. Thus, expression of PBR mRNA in the nucleus is thought to be essential in the regulation of cell proliferation and thus ultimately may function in the development and progression of the disease.

PBR mRNA expression determined by *in situ* hybridisation showed that the expression levels vary between the normal and the cancerous state, with an increase expression of PBR mRNA seen in most cases. Increase levels of PBR mRNA were seen in Grade II and Grade III liver hepatocellular carcinoma, Grade I colonic adenocarcinoma, Grade III stomach squamous cell carcinoma, Grade II and Grade III prostate adenocarcinoma of the peripheral duct and acini, Grade III breast invasive ductal carcinoma (NST), Grade III lung squamous cell carcinoma, kidney chromophobe renal cell carcinoma, kidney clear cell carcinoma, Grade II brain diffuse fibrillary astrocytoma, brain primary central nervous system lymphoma and brain ependymoma while the expression of PBR mRNA decreased in Grade II and Grade III colonic adenocarcinoma, Grade III lung adenocarcinoma and lung small cell carcinoma.

The level of PBR mRNA varies also with tumour malignancy grade. In hepatocellular carcinoma the level of PBR mRNA decreased as tumour invasion increased while in prostate adenocarcinoma of the peripheral duct and acini PBR mRNA level increased as tumour invasion increased. This suggests that PBR may serve as a prognostic marker in these diseases. In colon adenocarcinoma expression of PBR mRNA decreased from Grade I to Grade II and Grade III colonic adenocarcinoma. However, Grade III colonic adenocarcinoma had a higher PBR mRNA expression level than Grade II colonic adenocarcinoma.

*In situ* hybridisation studies showed that the level of expression of PBR mRNA varies for the different cancers. High expression levels were seen in epiploon Grade III squamous cell carcinoma, Grade II and Grade III prostate adenocarcinoma of the peripheral duct and acini, with Grade II showing a lower expression than Grade III, breast Grade III invasive ductal carcinoma (NST), lung Grade III squamous cell carcinoma, chromophobe renal cell carcinoma and renal clear cell carcinoma with chromophobe renal cell carcinoma showing the highest expression level, intermediate expression levels were seen in Grade II hepatocellular carcinoma, Grade I and Grade III colon adenocarcinoma, lung Grade III adenocarcinoma, brain Grade II diffuse fibrillary astrocytoma and low expression levels were seen in Grade III hepatocellular carcinoma, Grade II colonic adenocarcinoma, lung small cell carcinoma, brain PCNSL and brain ependymoma with highest expression level seen in ependymoma and lowest expression level seen in PCNSL.

*In situ* hybridisation studies showed that the level of expression of PBR mRNA varies for the different normal tissues. High expression levels of PBR mRNA were seen in epiploon, prostate, breast and lung, intermediate expression levels were seen in colon and stomach and low expression levels were seen in liver, kidney and brain with white matter showing a higher level of expression than grey matter.

Relative quantitative real-time PCR was done to determine the expression levels of PBR mRNA in human normal and various cancer cell lines. The expression levels of PBR mRNA varied between lung adenocarcinoma and its normal counterpart and between the different cancer cell lines. It was found that the relative expression of PBR mRNA decreased one-fold in lung adenocarcinoma when compared to it normal counterpart seen by the decrease in concentration of template DNA for the two cell lines. In the case of the cancerous cell lines, the concentration of PBR mRNA increases as follows: liver hepatocellular carcinoma > cervical carcinoma ≥ lung adenocarcinoma, with liver hepatocellular carcinoma showing a half-fold increase compared to lung adenocarcinoma and cervical carcinoma and lung adenocarcinoma showing a similar expression level.

The steps involving the isolation of the PBR protein was only obtained in the preliminary stages, that is only small concentrations of the GST-PBR protein was isolated using various concentrations of IPTG. Thus, future studies requires the expression of the GST-PBR protein with an optimal concentration of IPTG in order to generate a large concentration of the GST-PBR protein after which it can be purified and treated with PreScission$^{TM}$ Protease to isolate the PBR protein. The isolation of the PBR protein will allow for antibodies to be raised, which can be used in future studies that will determine the expression pattern of the PBR protein in different types of human normal and cancerous tissues.

Determination of the PBR mRNA expression in many cancer tissues is still in the preliminary stages and further studies will have to be done to determine and confirm its expression. However, from previous studies and this one, it is clear that PBR may play a role in cancer progression, serves as a biochemical marker or prognostic factor in the development of cancer and correlates with tumour malignancy. Determining the role of PBR in cancer may lead to the discovery of new therapies for the treatment of cancer.

# 6. REFERENCES


- Ackrell BAC, (2002), Chapter 2: Cytopathies Involving Mitochondrial Complex II, *Mol Aspects Med*, **23**(5): 369-384

- Akech J, Roy SS, Das SK, (2005), Modulation of Cholinephosphotransferase Activity in Breast Cancer Cell Lines by Ro5-4864, a Peripheral Benzodiazepine Receptor Agonist, *Biochem Biophys Res Commun*, **333**(1): 35-41

- Allenfall J, Batra S, (1995), Modulation of the Peripheral Benzodiazepine Receptor by Testosterone in Dunning G Prostatic Adenocarcinoma, *Life Sci*, **56**(22): 1897-1902

- URL: www.cancer.org/docroot/LRN/LRN_0.asp

  American Cancer Society, (2006), Cancer Reference Information:

  What is Cancer?, Liver Cancer, Colorectal Cancer, Stomach Cancer, Prostate Cancer, Breast Cancer, Lung Cancer, Brain and Spinal Cord Tumours in Adults, Cervical Cancer

- Barbatis C, (1995), The Histopathology of Colorectal Adenocarcinoma, *Hellenic Archives of Pathology*, **3**(1): 1-9

- Biedermann K, Dandachi N, Trattner M, *et al.*, (2004), Comparison of Real-time PCR Signal-Amplified In Situ Hybridization and Conventional PCR for Detection and Quantification of Human Papillomavirus in Archival Cervical Cancer Tissue, *J Clin Microbiol*, **42**(8), 3758-3756

- Bribes E, Carrière D, Goubet C, *et al.*, (2004), Immunohistochemical Assessment of the Peripheral Benzodiazepine Receptor in Human Tissues, *J Histochem Cytochem*, **52**(1): 19-28

- Bribes E, Bourrie B, Casellas P, (2003), Ligands of the Peripheral Benzodiazepine Receptor have Therapeutic Effects in Pneumopathies *In Vivo*, *Immunol Lett*, **88**(3): 241-247

- Brown HS, (2002), Hematoxylin and Eosin: The Routine Stain, *Sigma-Aldrich Corporation*: 1-3

- Brown RC, Degenhardt B, Kotoula M, *et al.*, (2000), Location-Dependent Role of the Human Glioma Cell Peripheral-Type Benzodiazepine Receptor in Proliferation and Steroid Biosynthesis, *Cancer Lett*, **156**(2): 125-132

- URL: www.health24.com/Man/Medical/748-766,18188.asp

  Cancer Association of South Africa, (2006), Cancer in South Africa – What are the Stats

- Carmel I, Fares FA, Leschiner S, (1999), Peripheral-Type Benzodiazepine Receptors in the Regulation of Proliferation of MCF-7 Human Breast Carcinoma Cell Line, *Biochem Pharmacol*, **58**(2): 273-278

- Casellas P, Galiègue S, Basile AS, (2002), Peripheral Benzodiazepine Receptors and Mitochondrial Function, *Neurochem Int*, **40**(6): 475-486

- Chen W, Reiss M, Foran DJ, (2004), A Prototype for Unsupervised Analysis of Tissue Microarrays for Cancer Research and Diagnostics, *IEEE Trans Inf Technol Biomed*, **8**(2): 89-96

- Collins K, Jacks T, Pavletich NP, (1997), The Cell Cycle and Cancer, *Proc Natl Acad Sci*, **94**: 2776-2778

- Coltran RS, Kumar VD, Collin T, (1999), Robbins Pathologic Basis of Diseases, 6th ed., Philadelphia: WB Saunders Company

- Corsi L, Geminiani E, Avallone R, *et al.*, (2005), Nuclear Location-Dependent Role of Peripheral Benzodiazepine Receptor (PBR) in Hepatic Tumoral Cell Lines Proliferation, *Life Sci*, **76**(22): 2523-2533

- Corsi L, Avallone R, Geminiani E, *et al.*, (2004), Peripheral Benzodiazepine Receptors in Potatoes (*Solanum tuberosum*), *Biochem Biophys Res Commun*, **313**(1): 62-66

- Deane NG, Parker MA, Beauchamp RD, (2005), Cell Proliferation: a Matter of Time and Place, *Surgery*, **138**(1): 1-7

- Debatin KM, (2004), Apoptosis Pathways in Cancer and Cancer Therapy, *Cancer Immunol Immunother*, **53**(3): 153-159

- Decaudin D, Castedo M, Nemati F, (2002), Peripheral Benzodiazepine Receptor Ligands Reverse Apoptosis Resistance of Cancer Cells *In Vitro* and *In Vivo*, *Cancer Res*, **62**(5): 1388-1393

- Eroschenko VP, (2000), DiFore's Atlas of Histology with Functional Correlations, 9th ed., Philadelphia: Lippincott Williams and Wilkins

- Fang JY, Richardson BC, (2005), The MAPK Signalling Pathways and Colorectal Cancer, *Lancet Oncol*, **6**: 322-327

- Ferzaz B, Brault E, Bourliaud G, (2002), SSR180575 (7-Chloro-*N*, *N*, 5-Trimethyl-4-Oxo-3-Phenyl-3,5-Dihydro-4*H*-Pyridazino[4,5-*b*]Indole-1-Acetamide), a Peripheral Benzodiazepine Receptor Ligand, Promotes Neuronal Survival and Repair, *J Pharmacol Exp Ther*, **301**(3): 1067-1078

- Fine HA, Mayer RJ, (1993), Primary Central Nervous System Lymphoma, *Ann Int Med*, **119**(11): 1093-1104

- Galiègue S, Casellas P, Kramar A, *et al.*, (2004), Immunohistochmical Assessment of the Peripheral Benzodiazepine Receptor in Breast Cancer and Its Relationship with Survival, *Clin Cancer Res*, **10**(6): 2058-2064

- Gavish M, Bachman I, Shoukrun R, *et al.*, (1999), Enigma of the Peripheral Benzodiazepine Receptor, *Pharmacol Rev*, **51**(4): 629-650

- Green DR, Kroemer G, (2004), The Pathophysiology of Mitochondrial Cell Death, *Science*, **305**(5684): 626-629

- Guo P, Ma J, Li S, *et al.*, (2001), Targeted Delivery of a Peripheral Benzodiazepine Receptor Ligand-Gemcitabine Conjugate to Brain Tumors in a Xenograft Model, *Cancer Chemother Pharmacol*, **48**(2): 169-176

- Hanahan D, Weinberg RA, (2000), The Hallmarks of Cancer, *Cell*, **100**(1): 57-70

- Hans G, Wislet-Gendebien S, Lallemend F, *et al.*, (2005), Peripheral Benzodiazepine Receptor (PBR) Ligand Cytotoxicity Unrelated to PBR Expression, *Biochem Pharmacol*, **69**(5): 819-830

- Hardwick M, Cavalli LR, Barlow KD, *et al.*, (2002), Peripheral-Type Benzodiazepine Receptor (*PBR*) Gene Amplification in MDA-MB-231 Aggressive Breast Cancer Cells, *Cancer Genet Cytogenet*, **139**(1): 48-51

- Harvey, (2002), *In Situ* Hybridisation, *Sigma-Aldrich Corporation*: 41-43

- Hashimoto T, Tokuchi Y, Hayashi M, *et al.*, (2000), Different Subtypes of Human Lung Adenocarcinoma Caused by Different Etiological Factors: Evidence From p53 Mutational Spectra, *Am J Pathol*, **157**(6): 2133-2141

- Herzig M, Christofori G, (2002), Recent Advances in Cancer Research: Mouse Models of Tumorigenesis, *Biochim Biophys Acta*, **1602**(2): 97-113

- Hsu S, Singh B, Schuster G, (2004), Induction of Apoptosis in Oral Cancer Cells, *Oral Oncol*, **40**(5): 461-473

- Huang YC, Guh JH, Teng CM, (2004), Induction of Mitotic Arrest and Apoptosis by Evodiamine in Human Leukemic T-Lymphocytes, *Life Sci*, **75**(1): 35-49

- Jordà EG, Jiménez A, Verdaguer E, *et al.*, (2005), Evidence in Favour of a Role for Peripheral-Type Benzodiazepine Receptor Ligands in Amplification of Neuronal Apoptosis, *Apoptosis*, **10**(1): 91-104

- Joseph-Liauzun E, Delmas P, Shire D, *et al.*, (1998), Topological Analysis of the Peripheral Benzodiazepine Receptor in Yeast mitochondrial Membranes Supports a Five-Transmembrane Structure, *J Biol Chem*, **273**(4): 2146-2152

- Karpinets TV, Foy BD, (2004), Model of the Developing Tumorigenic Phenotype in Mammalian Cells and the Roles of Sustained Stress and Replicative Senescence, *J Theor Biol*, **227**(2): 253-264

- Kassiou M, Meikle SR, Banati RB, (2004), Ligands for Peripheral Benzodiazepine Binding Sites in Glial Cells, *Brain Res Rev*, **48**(2): 207-210

- Kastan MB, Bartek J, (2004), Cell-Cycle Checkpoints and Cancer, *Nature*, **432**: 316-323

- Katz Y, Moskovitz B, Levin DR, *et al.*, (1989), Absence of Peripheral-Type Benzodiazepine Binding Sites in Renal Carcinoma: a Potential Biochemical Marker, *Br J Urol*, **63**(2): 124-127

- Kletsas D, Li W, Han Z, *et al.*, (2004), Peripheral-Type Benzodiazepine Receptor (PBR) and PBR Drug Ligands in Fibroblast and Fibrosarcoma Cell Proliferation: Role of ERK, c-Jun and Ligand-Activated PBR-Independent Pathways, *Biochem Pharmacol*, **67**(10): 1927-1932

- Lacapère JJ, Papadopoulos V, (2003), Peripheral-Type Benzodiazepine Receptor: Structure and Function of a Cholesterol-Binding Proteins in Steroid and Bile Acid Biosynthesis, *Steroids*, **68**(7-8): 569-585

- Lanlani EN, Stubbs A, Stamp GWH, (1997), Prostate Cancer: the Interface Between Pathology and Basic Scientific Research, *Semin Cancer Biol*, **8**(1): 53-59

- Leducq N, Bono F, Sulpice T, (2003), Role of Peripheral Benzodiazepine Receptors in Mitochondrial, Cellular, and Cardiac Damage Induced by Oxidative Stress and Ischemia Reperfusion, *J Pharmacol Exp Ther*, **306**(3): 828-837

- Lokitnov A, (2004), Common Gene Polymorphisms, Cancer Progression and Prognosis, *Cancer Lett*, **208**(1): 1-33

- Maaser K, Sutter AP, Scherübl H, (2005), Mechanisms of Mitochondrial Apoptosis Induced by Peripheral Benzodiazepine Receptor Ligands in Human Colorectal Cancer Cells, *Biochem Biophys Res Commun*, **332**(3): 646-652

- Maaser K, Sutter AP, Krahn A, *et al.*, (2004), Cell Cycle-Related Signaling Pathways Modulated by Peripheral Benzodiazepine Receptor Ligands in Colorectal Cancer Cells, *Biochem Biophys Res Commun*, **324**(2): 878-886

- Maaser K, Grabowski P, Sutter AP, *et al.*, (2002), Overexpression of the Peripheral Benzodiazepine Receptor is a Relevant Prognostic Factor in Stage III Colorectal Cancer, *Clin Cancer Res*, **8**(10): 3205-3209

- Miettinen H, Kononen J, Haapasalo H, *et al.*, (1995), Expression of Peripheral-Type Benzodiazepine Receptor and Diazepam Binding Inhibitor in Human Astrocytomas: Relationship to Cell Proliferation, *Cancer Res*, **55**(12): 2691-2695

- Olson JM, Hallahan AR, (2004), p38 MAP Kinase: a Convergence Point in Cancer Therapy, *Trends Mol Med*, **10**(3): 125-129

- Parkin DM, Bray F, Ferlay J, *et al.*, (2005), Global Cancer Statistics, 2002, *CA Cancer J Clin*, **55**(2): 74-108

- Pulido MD, Parrish AR, (2003), Metal-Induced Apoptosis: Mechanisms, *Mutat Res*, **533**(1-2): 227-241

- Reynolds RJ, Schecker JA, (1995), Radiation, Cell Cycle and Cancer, *Los Alamos Science*, **23**: 51-89

- Riond J, Mattei MG, Kaghad M, *et al.*, (1991), Molecular Cloning and Chromosomal Localization of a Human Peripheral-Type Benzodiazepine Receptor, *J Biochem*, **195**(2): 305-311

- Rosai J, (2004), Rosai and Ackerman's Surgical Pathology, 9th ed. Edinburgh: Mosby

- Samuel T, Weber HO, Funk JO, (2002), Linking DNA Damage to Cell Cycle Checkpoints, *Cell Cycle*: **1**(3): 162-168

- Sänger N, Strohmeier R, Kaufmann M, (2000), Cell Cycle-Related Expression and Ligand Binding of Peripheral Benzodiazepine Receptor in Human Breast Cancer Cell Lines, *Eur J Cancer*, **36**(16): 2157-2163

- Schmidt C, Schmid A, Lüttges JE, (2001), Primary Squamous Cell Carcinoma of the Stomach. Report of a Case and Review of Literature, *Hepato-Gastroenterology*, **48**: 1033-1036

- Scoltock AB, Cidlowski JA, (2004), Activation of Intrinsic and Extrinsic Pathways in Apoptotic Signaling during UV-C-Induced Death of Jurkat Cells: the Role of Caspase Inhibition, *Exp Cell Res*, **297**(1): 212-223

- Sitas F, Madhoo J, Wessie J, (1998), Incidence of Histologically Diagnosed Cancer in South Africa, 1993-1995, *National Cancer Registry of South Africa*, *SA Institute for Medical Research*, Johannesburg, South Africa

- Stewart ZA, Westfall MD, Pietenpol JA, (2003), Cell-Cycle Dysregulation and Anticancer Therapy, *TRENDS Pharmacol Sci*, **24**(3): 139-145

- Strohmeier R, Roller M, Sänger N, *et al.*, (2002), Modulation of Tamoxifen-Induced Apoptosis by Peripheral Benzodiazepine Receptor Ligands in Breast Cancer Cells, *Biochem Pharmacol*, **64**(1): 99-107

- Sutter AP, Maaser K, Höpfner M, *et al.*, (2005), Cell Cycle Arrest and Apoptosis Induction in Hepatocellular Carcinoma Cells by HMG-CoA Reductase Inhibitors. Synergistic Anti-Proliferative Action with Ligands of the Peripheral Benzodiazepine Receptor, *J Hepatol*, **43**(5): 808-816

- Sutter AP, Maaser K, Gerst B, *et al.*, (2004). Enhancement of the Peripheral Benzodiazepine Receptor Ligand-Induced Apoptosis and Cell Cycle Arrest of Esophageal Cancer Cells by Simultaneous Inhibition of MAPK/ERK Kinase, *Biochem Pharmacol*, **67**(9): 1701-1710

- Sutter AP, Maaser K, Grabowski P, *et al.*, (2004), Peripheral Benzodiazepine Receptor Ligands Induce Apoptosis and Cell Cycle Arrest in Human Hepatocellular Carcinoma Cells and Enhance Chemosensitivity to Paclitaxel, Docetaxel, Doxorubicin and the Bcl-2 Inhibitor HA14-1, *J Hepatol*, **41**(5): 799-807

- Sutter AP, Maaser K, Barthel B, *et al.*, (2003), Ligands of the Peripheral Benzodiazepine Receptor Induce Apoptosis and Cell Cycle Arrest in Oesophageal Cancer Cells: Involvement of the p38 MAPK Signalling Pathway, *Br J Cancer*, **89**(3): 564-572

- Torii S, Nakayama K, Yamamoto T, *et al.*, (2004), Functions of the MAP Kinase Cascades: Regulatory Mechanisms and Function of ERK MAP Kinases, *J Biochem*, **136**(5): 557-561

- Veenman L, Levin E, Weisinger G, *et al.*, (2004), Peripheral-Type Benzodiazepine Receptor Density and *In Vitro* Tumorigenicity of Glioma Cell Lines, *Biochem Pharmacol*, **68**(4): 689-698

- Venturini I, Zeneroli ML, Corsi L, *et al.*, (1998), Up-Regulation of Peripheral Benzodiazepine Receptor System in Hepatocellular Carcinoma, *Life Sci*, **63**(14): 1269-1280

- Vin V, Leducq N, Bono F, *et al.*, (2003), Binding Characteristics of SSR180575, a Potent and Selective Peripheral Benzodiazepine Ligand, *Biochem Biophys Res Commun*, **310**(3): 785-790

- Vineis, P, (2003), Cancer as an Evolutionary Process at the Cell Level: an Epidemiological Perspective, *Carcinogenesis*: **24**(1): 1-6

- Weisinger G, Kelly-Hershkovitz E, Veenman L, *et al.*, (2004), Peripheral Benzodiazepine Receptor Antisense Knockout Increases Tumorigenicity of MA-10 Leydig Cells *In Vivo* and *In Vitro*, *Biochemistry*, **43**(38): 12315-12321

- Woods MJ, Williams C, (1996), Multiple Forms and Locations for the Peripheral-Type Benzodiazepine Receptor, *Biochem Pharmacol*, **52**(12): 1805-1814

- Yeliseev AA, Kaplan S, (2000), TspO of *Rhodobacter sphaeroides*: a Structural and Functional Model for the Mammalian Peripheral Benzodiazepine Receptor, *J Biol Chem*, **275**(8): 5657-5667

- Yildirim Y, Akcali Z, Bilezikci B, *et al.*, (2005), Primary Squamous Cell Carcinoma of the Stomach: A Case Report, *Tumori*, **91**(5): 440-442

- Young B, Heath JW, (2000), Wheater's Functional Histology: A Text and Colour Atlas, 4th ed., Edinburgh: Churchill Livingstone

- Zambrano NR, Lubensky IA, Merino MJ, *et al.*, (1999), Histopathology and Molecular Genetics of Renal Tumours: Towards Unification of a Classification System, *J Urol*, **162**(4): 1246-1258